NASA CR-159545
R79AEG288

DESIGN STUDY AND PERFORMANCE ANALYSIS OF A HIGH-SPEED MULTISTAGE VARIABLE-GEOMETRY FAN FOR A VARIABLE CYCLE ENGINE

FINAL REPORT

MARCH 1979

by

T. J. Sullivan, D. E. Parker

GENERAL ELECTRIC COMPANY
AIRCRAFT ENGINE GROUP
CINCINNATI, OHIO 45215

Prepared For

National Aeronautics and Space Administration

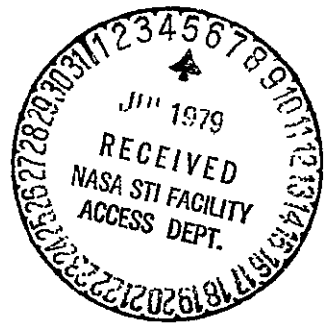

NASA Lewis Research Center
Contract NAS3-20041

1. Report No.	2. Government Accession No.	3. Recipient's Catalog No.
NASA CR-159545		

4. Title and Subtitle	5. Report Date
Design Study and Performance Analysis of a High-Speed Multistage Variable Geometry Fan for a Variable Cycle Engine	March 1979
	6. Performing Organization Code
7. Author(s)	8. Performing Organization Report No.
T. J. Sullivan, D. E. Parker	R79AEG288
	10. Work Unit No.
9. Performing Organization Name and Address General Electric Company Aircraft Engine Group Cincinnati, Ohio 45215	11. Contract or Grant No. NAS3-20041
	13. Type of Report and Period Covered
12. Sponsoring Agency Name and Address National Aeronautics and Space Administration Washington, D. C. 20548	Final June 1976 - July 1977
	14. Sponsoring Agency Code

15. Supplementary Notes
Project Manager, L. Joseph Herrig
NASA-Lewis Research Center
Cleveland, Ohio 44135

16. Abstract

A design technology study was performed to identify a high speed, multistage, variable-geometry fan configuration capable of achieving wide flow modulation with near optimum efficiency at the important operating conditions. A parametric screening study of the front and rear block fans was conducted in which the influence of major fan design features on weight and efficiency was determined. Key design parameters were varied systematically to determine the fan configuration most suited for a double bypass, variable cycle engine. Two- and three-stage fans were considered for the front block. A single stage, core-driven fan was studied for the rear block. Variable geometry concepts were evaluated to provide near-optimum off-design performance. A detailed aerodynamic design and a preliminary mechanical design were carried out for the selected fan configuration. Performance predictions were made for the front and rear block fans.

17. Key Words (Suggested by Author(s))	18. Distribution Statement
Fan Aerodynamic Design Study High Speed, Multistage Variable-Geometry Fan Variable Cycle Engines	Unclassified - Unlimited

19. Security Classif. (of this report)	20. Security Classif. (of this page)	21. No. of Pages	22. Price*
Unclassified	Unclassified	224	

* For sale by the National Technical Information Service, Springfield, Virginia 22151

FOREWORD

This report was prepared by the Aircraft Engine Group of the General Electric Company, Cincinnati, Ohio, to document the results of a design study performed to identify a high speed, multistage, variable geometry fan configuration most suited for the double bypass, variable cycle engine. Mr. L. Joseph Herrig, NASA-Lewis Research Center, Fluid System Components Division, was Project Manager.

The authors wish to acknowledge the valuable contributions made to this program by various supporting organizations within the General Electric Company. In particular, appreciation is extended to Mr. R. G. Giffin, III for his continuous support in identifying the variable cycle engine requirements, and to Mr. F. W. Teagarden and the many contributors in his organization for their efforts in performing the preliminary mechanical design and associated studies.

TABLE OF CONTENTS

TABLE OF CONTENTS (Concluded)

LIST OF ILLUSTRATIONS

LIST OF ILLUSTRATIONS (Continued)

LIST OF ILLUSTRATIONS (Continued)

LIST OF ILLUSTRATIONS (Continued)

LIST OF ILLUSTRATIONS (Concluded)

LIST OF TABLES

SECTION I

SUMMARY

A design technology study was performed to identify a high speed, multi-stage, variable geometry fan configuration capable of achieving a wide flow range modulation with near optimum efficiency at the important operating conditions. The initial phase of this study involved defining fan operating requirements and conducting a parametric screening study of several fan configurations. In order to achieve the fan requirements that were identified, a front block fan with 3.17 design pressure ratio and a rear block single-stage, core-driven fan of a 1.48 design pressure ratio are required. A parametric screening study of the front and rear block fan configurations was conducted in which the influence of major fan design features on weight and efficiency was determined. Key design parameters were varied systematically to determine an optimized fan design. Two-stage and three-stage fans were considered for the front block fan. A single-stage rear block fan was studied. It was assumed that composite blade technology advancements would permit use of composite blading.

The selected front block fan has a design point inlet specific flow rate of 205 kg/sec m^2 (42 lbm/sec ft^2) operating at a corrected tip speed of 467 m/sec (1532 ft/sec). The fan flowpath is characterized by a nearly constant tip diameter and a large increase in hub radius through the first rotor with an inlet radius ratio of 0.40 and a design exit Mach number of 0.48. The rear block fan configuration is a single stage rotor driven by a high pressure rotor shaft. The design point inlet specific flow is 187.9 kg/sec m^2 (38.5 lbm/sec ft^2) with a pressure ratio of 1.48. This front and rear block fan configuration offered the best combination of fan efficiency, engine weight and turbine performance.

Variable geometry concepts were evaluated by investigating the effect of the level and the radial distribution of the swirl ahead of the front fan rotors on key aerodynamic parameters at the aerodynamic design point and at the supersonic cruise condition. An articulated inlet guide vane was selected, imparting no swirl at the fan design point.

A detailed aerodynamic design of both the front and the rear block fans and their interconnecting ducts was performed at their respective design point conditions. Blade and vane airfoil coordinates were defined and a preliminary mechanical design analysis was made to assure mechanical feasibility. Performance maps were generated for each fan block covering a wide range of flow modulation. Velocity distributions were calculated at the extremes of the bypass ratio swings.

SECTION II

INTRODUCTION

Under NASA-sponsored Supersonic Cruise Airplane Research (SCAR) studies, the General Electric Company has shown that the double bypass, variable cycle engine concept is a viable propulsion system for an advanced supersonic transport aircraft. These studies have shown that appreciable gains in cycle efficiency and reductions in fuel consumption can be achieved by use of high pressure ratio cycles combined with features which allow variation of the cycle characteristics to provide near-optimum performance in each significant regime of the flight spectrum. The studies have also shown that an attractive variable cycle engine (VCE) can be developed if fan technology can be extended to provide a suitable variable-bypass-ratio fan. The fan requirements include a high unit flow capacity at takeoff with a moderate efficiency penalty to permit an optimum trade-off between takeoff fan efficiency and nacelle size. An effective variable-bypass-ratio system requires that the fan stages be separated into two blocks with a bypass-flow splitter between the blocks. In the selected arrangement, the rear block fan rotor is part of the core spool in a dual-rotor engine.

A design technology study was conducted under NASA Contract NAS3-20041 aimed at identifying the most suitable fan configuration. The front and rear block fan configurations were selected from a parametric screening study and were each examined in a detailed aerodynamic design. A preliminary mechanical design analysis was conducted to assure a feasible and structurally-sound mechanical arrangement. Performance map predictions were calculated for each fan block. The results of this study are described in this report.

SECTION III

AERODYNAMIC STUDIES

A. Engine System Studies

Cycle Definition

The fan design requirements were defined at the outset of the present study consistent with current General Electric Advanced Supersonic Technology (AST) engine studies. A flow size of 382.4 kg/sec (843 lbm/sec) at takeoff was adopted as a likely size for the ultimate engine. The fan cycle requirements for both the front and rear fan blocks at several important operating conditions are given in Table I. The key operating conditions are supersonic cruise, subsonic cruise, takeoff and hold.

The takeoff condition sets the airflow size and hence, the diameter of the front block fan. A high airflow is desired at takeoff to reduce jet noise. Since this is the front block sizing point, a fairly high specific flow rate is desirable to minimize the fan diameter. Some sacrifice in efficiency is acceptable here to achieve the high specific flow since a relatively small percent of the total mission fuel is used during takeoff. The primary aerodynamic design point of the front block fan was selected at the condition of 2.8% less flow than at takeoff with an airflow of 372 kg/sec (820 lbm/sec) and a design pressure ratio of 3.17. The maximum physical speed of the front block is 108.6% of the aerodynamic design speed which occurs at takeoff on a hot day. Table I shows that a substantial part of the front block airflow bypasses the rear block at takeoff and therefore, it is necessary to close the rear block inlet guide vanes (IGV2) in order to reduce the rear block pumping capacity at the relatively high core spool corrected speed.

It is anticipated that the aircraft inlet would be sized for the supersonic cruise airflow to minimize spillage drag. Auxiliary inlet doors would be used at takeoff to permit passing the desired flow at this condition. During the climb/acceleration and supersonic cruise phases of the mission, it is desirable to maintain a high engine specific thrust. In order to accomplish this, the front block flow is reduced by closing the inlet guide vanes (IGV) and the outer bypass stream is closed off forcing all of the airflow through the rear fan block. This is the sizing condition for the rear block fan. The corrected flow into the rear block is 139.7 kg/sec (308.0 lbm/sec) at a design pressure ratio of 1.48.

At supersonic cruise and other high specific thrust operating conditions it is desirable to close off the outer bypass stream and force all the air through the rear block. This requires a relatively high front block pressure ratio at the supersonic cruise airflow. The physical speed is kept at a maximum (approximately 100 percent) to maximize pressure ratio capability and the IGV is closed to match the corrected airflow. For the supersonic cruise conditions, as shown in Table I, the front block corrected speed is 78.7 percent and the IGVs are closed 39 degrees.

Table I. AST Front and Rear Block Fan Performance Parameters.

AST Front Block Fan Performance Parameters

Operating Conditions	Pct Corr. Speed	Corr. Flow	P/P	Outer Bypass Ratio
Front Block Design	100	820	3.17	0.550
Takeoff	105	843	3.20	0.647
Hold	81	492	1.90	0.537
Supersonic Cruise	79	472	1.80	0.041
Subsonic Cruise	93	671	2.60	0.552

AST Rear Block Fan Performance Parameters

Operating Condition	Pct Corr. Speed	Corr. Flow	P.P	Inner Bypass Ratio
Rear Block Design	100	308	1.48	0.340
Takeoff	94	200	1.18	0.087
Hold	88	190	1.15	0.160
Supersonic Cruise	90	281	1.33	0.513
Subsonic Cruise	93	199	1.17	0.093

When diverting to an alternate airfield or for holding patterns, the variable bypass features of the engine allow operation at subsonic speeds and intermediate power settings with relatively high bypass ratios (see Table I), which improves the propulsive efficiency. The front fan block operates around 90 percent corrected speed with the IGV closed somewhat. At this condition, the fan efficiency should be near its peak value.

Stall Margin Requirements

A stability margin study was conducted to define the front and rear block stall margin requirements. Stackups were performed at SLS takeoff, 0.3 M_o/0 K altitude rotation, 0.5 M_o/15K hold, 0.95 M_o/35K subsonic cruise and 2.32 M_o/53.5K supersonic cruise flight conditions. For this study, the front block distortion sensitivity and distortion transfer characteristics were assumed to be similar to those of General Electric's YJ101 fan, while the rear block characteristics were assumed to be similar to the NASA Task II Stage with IGV/stator schedules of 0°/0° and 40°/8°.

The objective of the stability stackup was to insure that the installed fan stall line is higher than the engine operating requirements at all flight conditions. The approach to obtaining the stackup called for establishing the limiting stability rating points by identifying all the destabilizing influences and then summing the items to define the required margin. The destabilizing influences can be separated into external and internal categories The external destabilizing influences are those that are attributable to the distortion (nonuniformity) of the inlet flow field. The internal destabilizing influences are those that are attributable to items such as quality variations, deterioration, thermal or power transients, control tracking (steady-state and transient) and installation bleed/power extraction. Summing the stall margins required for external and internal destabilizing influences determines the minimum separation between the fan stall and nominal performance operating lines. An itemized tabulation of the stability stackup margins are shown in Table IIa and IIb for both the front and the rear block fans. The primary operating conditions which set the required design point stall margins are the hold (front block fan) and takeoff (rear block fan) points. The amount of stall margin required at the important operating points is shown schematically on the typical front and rear block fan performance maps in Figures 1 and 2, respectively.

The required stall margin at the design point of the front block fan is approximately 20 percent based on an extrapolation of the required low speed stall line. To assure meeting the engine rquirements, a stall margin of 22 percent was used to determine the required fan corrected tip speed. In order to achieve the required stall margin on the rear block fan at all operating conditions, a value of 22 percent was assumed.

Noise Considerations

A brief and limited acoustical study was conducted early in the program to determine whether or not fan noise was a problem to be addressed in the design phase of the fan. The results of the study showed that at takeoff

Table IIa. AST Front Block Fan Stability Margin Stack-Up.

Operating Condition	Δ Stall Margin at Constant Airflow (%)				
	Deterior-ation	Quality & Control	Transients	Distor-tion	Total
Takeoff	1.5	3.0	2.0	6.5	13.0
Hold	2.0	4.0	4.0	7.1	17.1
Subsonic Cruise	1.5	3.0	3.0	3.2	10.7
Supersonic Cruise	2.0	4.0	4.0	5.6	15.6

Table II b. AST Rear Block Fan Stability Margin Stack-Up.

Operating Condition	Δ Stall Margin at Constant Flow (%)				
	Deterior-ation	Quality & Control	Transients	Distor-tion	Total
Takeoff	1.0	3.0	1.0	7.3	12.3
Hold	1.0	3.0	1.0	6.1	11.1
Subsonic Cruise	1.0	3.0	1.0	4.3	9.3
Supersonic Cruise	1.5	2.0	1.0	4.1	8.6

the jet noise predominates and the fan noise is insignificant. At the approach point, fan noise would be predominant if no inlet suppression were used. The use of a hybrid inlet (a variable geometry inlet which has a throat Mach number of about 0.80 combined with acoustic panels on the duct walls) will reduce the noise to acceptable levels. It was therefore concluded that no special fan design features need be included for acoustic reasons.

B. Parametric Screening Studies

Parameters and Range of Parameters Studied

A series of preliminary designs were carried out for both the front and rear block fans to determine the optimum combination of design parameters for each fan block. Both two- and three-stage front block fans were investigated. Only single-stage fans were investigated for the rear block because of its low design pressure ratio.

A nominal two-stage front block configuration was defined which had the following characteristics:

Inlet Radius Ratio	0.438
Flow/Annulus Area, kg/sec m^2 (lbm/sec ft^2)	210 (43)
Exit Mach Number	0.48
Rotor Inlet Swirl Angle, degrees	5
Rotor Aspect Ratio (average)	1.6
Stator Aspect Ratio (average)	2.6
Rotor Pitchline Solidity (average)	1.7
Stator Pitchline Solidity (average)	2.0
Flowpath Shape	Tapered Casing

The flowpath for this nominal configuration is shown in Figure 3.

The corrected tip speed required to achieve 22 percent stall margin and fan efficiency potential were calculated for this nominal configuration. Each of the above parameters (except for flowpath shape) were individually varied to both a higher and lower value than the nominal case. The required tip speed and efficiency potential were calculated for each configuration. Preliminary weight estimates were made for many of the configurations. In addition, estimates were made of the low pressure turbine efficiency, weight, and cooling flow requirements. The combined effect of the fan efficiency and weight, and the turbine efficiency, weight and cooling flow requirements were used to obtain a differential aircraft range through the use of derivatives.

A similar approach was followed for the three-stage front block fans, except that two nominal flowpath shapes were investigated; one, with a constant pitch diameter and the other with a near-constant tip diameter.

The nominal three-stage fan configurations employed higher aspect ratio blading and it was assumed that they would require rotor tip shrouds for adequate aero-mechanical stability. The integral tip shrouded fan blades were assumed to be titanium for the estimted weight calculations. The flowpaths for the two nominal three-stage fans are shown in Figures 4 and 5.

Table III lists the parameters investigated and the range of variables for the three nominal front block fan configurations.

Table IV lists the parameters and range of variables considered for the rear block fan configuration. The overall engine configuration places many more constraints on the core-driven fan stage than on the front block. Since it is driven from the high-pressure core spool, its RPM must be compatible with achieving the required core compressor pressure ratio and stall margin in a relatively few number of stages. Furthermore, the high pressure turbine efficiency, weight, stress levels, and cooling flow requirements must be considered.

The inlet specific flow of the rear block should be such that no large diffusion or accelerations are required between the front and the rear fan blocks. Similarly, its exit Mach number must be compatible with the core compressor inlet conditions. Considering these constraints, the design parameters were investigated over a smaller range than for the front block.

Efficiency Prediction and Stall Correlation Model

Preliminary design studies of advanced fans and compressors at the General Electric Company rely on a computerized procedure, identified as the Compressor Unification Study, to estimate both efficiency potential and stall pressure ratio potential. This model was the principal tool used in selecting the front and rear block fan configurations. The efficiency prediction model is intended to indicate the potential peak efficiency of a well-designed compressor. It is intended to account for all known sources of loss except for those due to off-design operation, blading unsuited for the aerodynamic environment or poor hardware quality. The potential peak efficiency at the design point is dependent upon the magnitude of loss from four sources: (1) end-wall boundary layer and end-wall region secondary flows and leakage flows; (2) blade surface profile drag; (3) blade passage shocks; and (4) part-span shrouds. These losses are correlated with aspect ratio, solidity, stagger, tip clearance, blade row axial spacing, and aerodynamic loading level. Blade surface profile losses are related to suction surface diffusion, blade maximum thickness and trailing edge thickness, Reynolds number, surface finish, Mach number and streamtube contraction. The shock loss model relates passage shock losses to inlet Mach number and relates leading edge bow shock losses to Mach number and edge thickness. The model for part-span shroud losses is based on measured shroud drag coefficients.

A detailed description of this efficiency model and some comparisons showing the capability of the model to predict efficiency is given in Reference 1.

Table III. Front Block Fan Nominal Design and Range of Parameters.

	Two Stage Tapered Casing*			Three Stage NCT*			Three Stage CP*		
	Nominal	High	Low	Nominal	High	Low	Nominal	High	Low
Flow/Annulus									
kg/sec m^2	210	215	205	210	215	205	210	215	205
(lbm/sec ft^2)	43	44	42	43	44	42	43	44	42
Inlet Radius Ratio	0.438	0.50	0.38	0.438	0.50	0.38	0.438	0.50	0.38
Exit Mach Number	0.48	0.55	0.45	0.48	0.55	0.45	0.48	0.55	0.45
Swirl Angle (deg.)	5	20	0	5	20	0	5	20	0
Aspect Ratio									
Rotor Avg	1.6	1.8	1.2	3.0	3.5	2.0	3.0	3.5	2.0
Stator Avg	2.6	2.8	2.0	3.2	3.5	2.5	3.2	3.5	2.5
Solidity (Pitchline)									
Rotor Avg	1.7	1.9	1.5	1.65	1.80	1.50	1.65	1.80	1.50
Stator Avg	2.0	2.2	1.8	1.80	2.00	1.60	1.80	2.00	1.60

* Tapered - Tapered Casing Flowpath

* NCT - Near-Constant Tip Flowpath

* CP - Constant Pitch Flowpath

Table IV. Rear Block Single Stage Fan Nominal Design Parameters and Range of Parameters.

Parameter	Nominal	High	Low
Flow/Unit Annulus Area ~kg/sec m^2 (lbm/sec ft^2)	188(38.5)	195(40)	175(36)
Inlet Radius Ratio	0.65	0.70	0.60
Exit Mach Number	0.52	0.55	0.45
Swirl Angle~degrees	0°	20°	0°
Aspect Ratio (Rotor Average)	1.5	2.0	1.2
Solidity (Rotor Average)	1.66	1.90	1.40

The stall pressure ratio prediction model relies upon two basic groups of background data. The first group of data describes the measured stall pressure rise capabilities of a large number of low speed repeating stages covering a wide range of stage geometries. These data have been expressed in the form of a pressure rise coefficient, which is related by a correlation to stage geometry parameters such as aspect ratio and solidity. The second collection of background data is from high speed multispeed compressors. These data are presented in the form of a ratio, called effectivity, of an individual stage pressure rise coefficient measured at design speed stall to that predicted by data correlation.

In applying the stall prediction model to a new design, certain features of its stage geometry and an appropriate value of effectivity are specified, and the correlation is used to deduce the pressure rise coefficient for each stage. Other input quantities are the distributions of axial velocity and stator exit flow angle at the design speed stall point, the airflow, pitchline radii and an estimated wheel speed. The computer program calculates the stage pressure ratios, stacks the stages to give an overall pressure ratio, and adjusts the speed until the desired overall pressure ratio is obtained. Hub and tip radii consistent with these results and other quantities of interest are then calculated.

Weight Estimates and Low Pressure Turbine Considerations

As part of the parametric screening study to define the optimum low pressure system for the AST engine, the total full-size fan weight was estimated for several of the two- and three-stage fan configurations.

Several assumptions were made that will affect the rotor absolute weight, but should still result in acceptable relative weights. Some of the pertinent assumptions are:

- Life required is 20000 start/stop cycles
- Minimum blade $t_m/c = 0.025$
- Blade root Stress Concentration Factor, $K_t = 2.0$
- Blade dovetail orientation angle = 15°
- Disk width = 0.85 x projected blade chord
- Disk temperature constant @ 200° F
- Disk bore radius: 15 cm on Stages 1 and 2; 20 cm on Stage 3

Actual weight estimation was done by predicting a design, based on given data and past experience, then processing the design parameters through a series of preliminary design computer programs. These programs all have provisions to adjust key parameters in the design until an acceptable compromise design is arrived at which meets the design criteria. In this case, programs which handle the blade airfoil, blade and disk dovetail and non-rigid disk as individual components were used.

The cantilevered rotor blades for the two-stage fans were assumed to be made of 1985 state-of-the-art boron/aluminum material. The three-stage fan blades were assumed to be titanium (Ti 6-4) with integral tip shrouds. The stator vanes were also assumed to be titanium (Ti 6-4). Other rotor and static component part materials would be 1985 state-of-the-art nickel and titanium alloy materials. The items covered in the rotor weight estimate include the blades, disks, shaft, spacers and other miscellaneous parts. The stator weight includes the vanes, casing, lever arms, shroud, and inlet guide vane ring, shroud, frame and centerbody. The nominal two stage fan rotor weight was estimated to be 446.8 Kg (985 lb) and the stator weight was estimated at 423.7 Kg (934 lb) for a total fan weight of 870.5 Kg (1919 lb) or for the nominal constant pitch fan 899.0 Kg (1982 lb).

Further evaluation of the low pressure system for the variable cycle AST engine was made by estimating the low pressure turbine weights, efficiencies, and cooling flows. A preliminary mechanical layout of the turbine components for the AST engine was done and is shown in Figure 6. The flowpath for the various turbines studied remained essentially unchanged so that the low pressure turbine (LPT) weight and cooling flow changes are due primarily to changes in RPM and the number of blades. Of these two variables, RPM has the largest effect. Stator variations were found to have a negligible effect on cooling/weight sensitivities as did variations in turbine casings for the small flowpath changes.

Each turbine was analyzed by the following procedure:

1. Sizing the tip shroud to adequately span the distance between adjacent blades.

2. Applying the shroud load to the airfoil and sizing the blade taper to minimize blade stress (up to an area ratio limit of 2.0).

3. Analyzing and sizing the disk to provide satisfactory steady-state life and overspeed margin.

4. Cooling flows are sized by considering the stress in each blade and the allowable metal temperatures required to give equivalent life in each design.

Figure 7 shows the trends of weight, cooling flow and LPT efficiency as a function of RPM. Since the range of RPM covered by the data from eight fan configurations covers the range of RPM for all fan configurations, the weights, cooling flows and efficiencies were noted for all the various two- and three-stage fan configurations. The nominal, full-size engine, LPT weight is 591.9 Kg (1305 lb) which includes the shaft (104.3 Kg), the stator (337.9 Kg), and the LPT rotor (149.7 Kg). Only the LPT rotor weight changes with RPM for the various fan configurations. The nominal stage 1 turbine bucket cooling flow is 4.2 percent of the total inlet flow.

The combined effect of the fan weight and efficiency and the turbine weight, efficiency and cooling flow were considered in the selection of the optimized low pressure system for the AST engine.

Results of Front Block Fan Parametric Screening Studies

A summary of the aerodynamic design data from the front block fan screening studies is given in Tables V and VI. Table V presents a comparison of the efficiencies, speeds, approximate lengths and inlet tip diameters for the various two stage configurations. Tables VIa and VIb present the same data for the three stage, near-constant-tip (NCT) and three stage, constant pitch (CP) fan configurations, respectively. Since the bulk of the fuel is burned at the supersonic cruise operating condition, it is intended to favor the lower corrected speed operation during the detailed design of the rotor and stator airfoils. This would introduce some compromise to the efficiency at the aerodynamic design point. Therefore, the efficiencies listed are one point lower than those calculated by the efficiency potential model. It should be noted that the high Reynolds number associated with the large size of these fans has a beneficial effect on the calculated efficiency.

The corrected speeds listed in the Tables V and VI result from the stall prediction model assuming 22 percent stall margin above the 3.17 operating line pressure ratio. All fans are sized for a design corrected flow of 372 kg/sec (820 lb/sec).

The results of varying aspect ratio (Figures 8 and 9 for the two-stage and three-stage fans, respectively) show an increase in efficiency as the aspect ratio is reduced from the nominal case value. The reduced aspect ratio permits a lower tip speed for the same stall margin, which results in lower Mach numbers and lower shock losses. The higher blade chord Reynolds number of the low aspect ratio blades also contributes to reduced profile losses. There is an increase in the end-wall losses, but not of sufficient magnitude to offset the reduction in profile and shock losses. An additional small gain occurs as a result of the assumption that the blade root tm/c could be somewhat lower for the lower aspect ratio cases. This, however, comes at the expense of a sizeable length increase and consequently, as will be shown later, a sizeable increase in fan weight.

The solidity variation results are shown in Figures 10 and 11, for the two- and three-stage fans, respectively. For the two-stage fan, a small gain in efficiency results from increasing the solidity from the nominal case Changing the solidity had essentially no effect on the efficiency of the three stage fans.

The effects of varying flow per unit annulus area, shown in Figures 12 and 13, indicate that the lower level of inlet specific flow is beneficial from a fan efficiency standpoint. The fan exit Mach number was held constant as the inlet specific flow was varied so that by dropping the inlet Mach number (specific flow) less diffusion across the fan is required. Two additional considerations also contribute to the improved efficiency. First, the average blade Mach number is reduced and, secondly, the lower flow coefficient leads to higher staggered blading which reduces the end-wall losses as a result of increased passage aspect ratio.*

*Passage aspect ratio is defined as the blade height divided by the pitchline staggered spacing between blades.

Table V. AST Front Block Fan Screening Study, Summary of Two Stage Fan Aerodynamic Design Data.

Two-Stage Fans ~ Tapered Casing Flowpath

	Adiabatic Efficiency	Tip Speed m/sec (fps)	Corrected Speed rpm	Length RI Inlet To S2 Exit, m (in.)	Inlet Tip Diameter m (in.)
Nominal	0.858	493 (1619)	5641	0.60 (23.6)	1.67 (65.78)
Low Aspect Ratio (Rotor/Stator Avg. = 1.2/2.0)	0.864	471 (1546)	5387	0.78 (30.8)	1.67 (65.78)
High Aspect Ratio (Rotor/Stator Avg. = 1.8/2.9)	0.852	503 (1651)	5753	0.54 (21.2)	1.67 (65.78)
Low Solidity (Rotor/Stator Avg. = 1.5/1.8)	0.855	500 (1642)	5721	0.59 (23.4)	1.67 (65.78)
High Solidity (Rotor/Stator Avg. = 1.9/2.2)	0.860	490 (1607)	5599	0.60 (23.6)	1.67 (65.78)
Low Flow/Annulus Area [205 (42)]	0.862	496 (1627)	5603	0.60 (23.6)	1.69 (66.55)
High Flow/Annulus Area [215 (44)]	0.855	491 (1611)	5678	0.60 (23.6)	1.65 (65.02)
Low Inlet Radius Ratio 0.38 (r/r exit = 0.755)	0.865	479 (1571)	5632	0.62 (24.6)	1.62 (63.93)
High Inlet Radius Ratio 0.50 (r/r exit = 0.755)	0.850	508 (1668)	5598	0.57 (22.4)	1.73 (68.28)
Low Inlet Radius Ratio 0.38 (r/r exit = 0.746)	0.863	487 (1598)	5729	0.63 (24.8)	1.62 (63.93)
High Inlet Radius Ratio 0.50 (r/r exit = 0.767)	0.854	496 (1627)	5461	0.56 (22.2)	1.73 (68.28)
Low Exit Mach No. (0.45)	0.856	501 (1645)	5732	0.60 (23.6)	1.67 (65.78)
High Exit Mach No. (0.55)	0.859	469 (1538)	5359	0.59 (23.2)	1.67 (65.78)
IGV/S1 Exit Swirl = 0°	0.846	494 (1620)	5645	0.59 (23.2)	1.67 (65.78)
IGV/S1 Exit Swirl = 10°	0.866	496 (1627)	5669	0.61 (23.9)	1.67 (65.78)
IGV/S1 Exit Swirl = 15°	0.870	500 (1642)	5721	0.62 (24.3)	1.67 (65.78)
IGV/S1 Exit Swirl = 20°	0.870	507 (1664)	5798	0.63 (24.7)	1.67 (65.78)

Table VI. AST Front Block Fan Screening Study Summary of Three-Stage Fan Aerodynamic Design Data.

a. Three-Stage Fans ~ Near-Constant Tip Flowpath

Configuration	Adiabatic Efficiency	Tip Speed m/sec (fps)	Corrected Speed rpm	Length R1 Inlet To S3 Exit, m (in.)	Inlet Tip Diameter m (in.)
Nominal	0.872	420 (1378)	4801	0.66 (25.8)	1.67 (65.78)
Low Aspect Ratio (Rotor/Stator Avg. = 2.0/2.5)	0.884	392 (1285)	4477	0.85 (33.6)	1.67 (65.78)
High Aspect Ratio (Rotor/Stator Avg. = 3.5/3/5)	0.865	429 (1408)	4906	0.60 (23.6)	1.67 (65.78)
Low Solidity (Rotor/Stator Avg. = 1.5/1.6)	0.873	427 (1400)	4878	0.65 (25.7)	1.67 (65.78)
High Solidity (Rotor/Stator Avg. = 1.8/2.0)	0.870	415 (1360)	4739	0.66 (25.9)	1.67 (65.78)
Low Flow./Annulus Area [205 (42)]	0.875	424 (1390)	4787	0.65 (25.7)	1.69 (66.55)
High Flow/Annulus Area [215 (44)]	0.863	420 (1378)	4857	0.65 (25.7)	1.65 (65.02)
Low Inlet Radius Ratio (0.38)	0.873	417 (1368)	4904	0.68 (26.7)	1.62 (63.93)
High Inlet Radius Ratio (0.50)	0.866	436 (1432)	4807	0.63 (24.9)	1.73 (68.28)
Low Exit Mach No. (0.45)	0.871	432 (1416)	4934	0.67 (26.2)	1.67 (65.78)
High Exit Mach No. (0.55)	0.872	399 (1310)	4564	0.65 (25.4)	1.67 (65.78)
IGV/S1/S2 Exit Swirl = 0°	0.861	421 (1382)	4815	0.65 (25.6)	1.67 (65.78)
IGV/S1/S2 Exit Swirl = 10°	0.880	420 (1380)	4808	0.66 (26.1)	1.67 (65.78)
IGV/S1/S2 Exit Swirl = 15°	0.881	423 (1387)	4833	0.67 (26.3)	1.67 (65.78)
IGV/S1/S2 Exit Swirl = 20°	0.862	427 (1402)	4885	0.68 (26.6)	1.67 (65.78)

Table VI. AST Front Block Fan Screening Study, Summary of Three-Stage Fan Aerodynamic Design Data. (Concluded)

b. Three-Stage Fans ~ Constant Pitch Flowpath

Configuration	Adiabatic Efficiency	Tip Speed m/sec (fps)	Corrected Speed rpm	Length Rl Inlet To S3 Exit, m (in.)	Inlet Tip Diameter m (in.)
Nominal	0.856	485 (1592)	5547	0.70 (27.4)	1.67 (65.78)
Low Aspect Ratio (Rotor/Stator Avg. = 2.0/2.5)	0.868	458 (1501)	5230	0.90 (35.6)	1.67 (65.78)
High Aspect Ratio (Rotor/Stator Avg. = 3.5/3.5)	0.850	496 (1627)	5669	0.63 (24.9)	1.67 (65.78)
Low Solidity (Rotor/Stator Avg. = 1.5/1.6)	0.854	496 (1627)	5669	0.69 (27.2)	1.67 (65.78)
High Solidity (Rotor/Stator Avg. = 1.8/2.0)	0.855	479 (1570)	5470	0.70 (27.5)	1.67 (65.78)
Low Flow/Annulus Area [205 (42)]	0.860	485 (1590)	5476	0.69 (27.3)	1.69 (66.55)
High Flow/Annulus Area [215 (44)]	0.850	485 (1592)	5611	0.70 (27.4)	1.65 (65.02)
Low Inlet Radius Ratio (0.38)	0.852	504 (1655)	5933	0.73 (28.9)	1.62 (63.93)
High Inlet Radius Ratio (0.50)	0.858	468 (1536)	5156	0.65 (25.7)	1.73 (68.28)
Low Exit Mach No. (0.45)	0.854	494 (1620)	5645	0.70 (27.6)	1.67 (65.78)
High Exit Mach No. (0.55)	0.860	465 (1527)	5321	0.69 (27.1)	1.67 (65.78)
IGV/S1/S2 Exit Swirl = 0°	0.843	485 (1592)	5547	0.69 (27.1)	1.67 (65.78)
IGV/S1/S2 Exit Swirl = 10°	0.865	488 (1600)	5575	0.70 (27.6)	1.67 (65.78)
IGV/S1/S2 Exit Swirl = 15°	0.871	491 (1611)	5613	0.71 (27.9)	1.67 (65.78)
IGV/S1/S2 Exit Swirl = 20°	0.872	498 (1635)	5697	0.71 (28.1)	1.67 (65.78)

The effects of the radius ratio variations on fan efficiency and tip speed are shown in Figures 14 and 15. For the two stage fan configurations where the inlet radius ratios were varied, the inlet-to-exit flowpath shapes were specified in two different manners. The first method (open symbols on Figure 14) held the exit radii constant and moved the inlet radii about the nominal values. This resulted in a flowpath that had a steeper hub slope for the low (0.38) radius ratio and a shallower hub slope for the high (0.50) radius ratio case. The second method (shaded symbols on Figure 14) kept the hub and tip slopes approximately the same and moved the inlet and exit flowpath dimensions. Here, the ratio of the exit hub radius to the inlet tip radius was held constant. The first method of flowpath variation was employed on the three stage near-constant-tip fans and the second method was used when varying radius ratio on the three stage constant pitch fans.

Figure 14 shows the two-stage fan results for both methods of flowpath variation. The low radius ratio case where the exit radii are the same as the nominal case shows the lowest required tip speed and, also, a correspondingly higher efficiency potential. The steeper hub slope causes a greater change in the average radii across a blade row, especially through the first rotor, thereby producing a centrifugal effect on the work input of the stage. The net result is a lower tip speed and only a slightly lower RPM since the diameter has been reduced. The overall length is slightly longer than the nominal case since the blade heights are larger. The increased efficiency is primarily due to a cascade efficiency improvement resulting from the lower tip speed and lower rotor Mach numbers. The variation of inlet and exit radius ratios coming from the second method shows the same trends of efficiency and tip speed, but to a lesser extent. The lower inlet and exit radius ratio case appears beneficial from the standpoint of engine size and core transition duct severity. Although there is a modest increase in fan length, this is compensated for by a lesser amount of radius change in the transition duct and thus, a shorter duct length.

The three-stage fan results from varying inlet radius ratio are listed in Tables VIa and VIb and shown graphically in Figure 15. The near-constant tip flowpath fan shows little gain from the lower inlet radius ratio in both efficiency and reduced tip speed. In this case, the hub slope is not as steep as for the two-stage fan since the overall fan length is greater. For near-constant tip flowpaths, the high inlet radius ratio is less attractive since the engine diameter is increased and efficiency is poorer due to the larger required tip speed.

The three-stage constant pitch flowpath fans show a reversed trend of efficiency and tip speed relative to the other fan configurations. Here, the higher radius ratio fan requires less tip speed and has a greater efficiency potential since the higher pitchline radius means a higher average blade speed. The magnitude of the efficiency change over the range of radius ratios studied is not significant.

The results of varying the exit Mach number are shown in Figures 16 and 17 and indicate only a slight advantage in choosing a higher design exit Mach number. Furthermore, the higher exit Mach number will necessitate larger diffusion rates to the rear block fan and result in higher duct losses.

Stator exit swirl angle variations were evaluated for the three fan configurations and the results are shown in Figures 18 and 19. The trends show a distinct increase in efficiency with swirl angle increases up to 20 degrees. The additional swirl (lower reaction) is applied at each rotor inlet station and the model assumes it to be radially constant. The corrected tip speed is lightly higher for the higher swirl cases and there are small increases in overall length. For the high swirl angle cases, the last stator row loadings become extremely high. This suggests a design with less swirl would be more acceptable. Furthermore, large degrees of rotor inlet swirl and a large radial variation would present a more severe radial mismatch problem at off-design conditions. This facet of the design will be discussed in more detail in Section III C.

In general, the results of the front block fan screening study show that the best efficiencies calculated by the model occur for the lower tip speed fans, fans with large through-blade radius changes, fans with lower through-flow Mach numbers, and also for fans with large degrees of stator exit swirl. The three-stage (NCT) fan appears distinctly better, at least from an efficiency standpoint (+ 1.4 points), than the other nominal fan configurations. Other considerations of the total low pressure system will be discussed in the expanded screening study.

Expanded Screening Study

It became apparent from the initial screening study that, in general, there was a net gain in the low pressure system (including the front block fan and the LP turbine) for two-stage fan configurations which had low design RPM's. Lower fan design tip speeds generally resulted in improved fan efficiency and an overall improved low pressure system, provided the fan blade aspect ratios were not too low. Reducing the aspect ratio from the nominal case, however, resulted in a significant weight increase in the fan which offset the fan efficiency gain and the weight reduction in the LP turbine. Lowering the RPM caused a small penalty in turbine efficiency, but this was more than offset by the lower turbine cooling flow requirements. Primarily as a result of this trend, the screening study was expanded to include two-stage fan configurations with constant tip diameter flowpaths.

The constant tip designs provided a larger increase in hub radius through the first stage rotor and an increased blade speed of the second stage relative to the first. These features permitted achieving the required stall margin with lower first stage design tip speeds and with reduced RPM.

It was previously noted that decreasing the inlet specific flow was beneficial to the fan efficiency. This, however, would increase the diameter and, hence, the frontal area if the inlet radius ratio remained at the nominal value. By decreasing the inlet radius ratio as the specific flow is reduced, the tip diameter can be held essentially the same as the nominal case.

Three two-stage, constant-tip configurations were investigated as part of the additional screening study work. The first configuration maintained the

nominal values of inlet radius ratio (0.438) and inlet specific flow of 210 kg/sec m^2 (43 lbm/sec ft^2) but utilized a constant-tip diameter flowpath. The second configuration reduced the inlet specific flow to 205 kg/sec m^2 (42 lbm/sec ft^2) and the inlet radius ratio to 0.40. The fan diameter for this case is 165.81 cm (65.28 in.) compared to the nominal case value of 167.07 cm (65.78 in.). The third fan configuration further reduced inlet radius ratio and specific flow to 0.35 and 195.3 kg/sec m^2 (40 lbm/sec ft^2), respectively. The constant tip diameter for this case is 166.23 cm (65.45 in.). Other design parameters, with the exception of the first rotor inlet swirl, were kept the same as the nominal configuration. Zero degrees of preswirl were specified for these cases instead of the nominal five degrees to help minimize the radial mismatch which occurs when the inlet guide vane is closed from the design setting. The selection of the design swirl angle will be discussed in more detail in a later section. Flowpath sketches of the three constant-tip configurations are shown in Figures 20, 21 and 22.

The more promising fan configurations of the front block fan screening study, including the constant tip configurations, were evaluated in terms of fan and low pressure turbine weights, efficiencies and LPT cooling flows and their net effect on the aircraft range. Table VII presents a summary of low pressure system data for each of the fans. The delta efficiencies, weights, cooling flows and range are shown relative to the nominal two-stage fan. For comparison, all three of the nominal fan configurations were included in this summary along with the two-stage tapered casing types where aspect ratio, radius ratio and swirl variations occur.

The data shown in Table VII indicates that the constant tip fans generally run at lower tip speeds, are lighter weight in both the fan and the turbine, and have better fan efficiency. The low aspect ratio fans, although attractive from a fan efficiency standpoint, are extremely heavy and have a net disadvantage in aircraft range. The low inlet radius ratio case shows up as fairly attractive relative to the nominal fan but the tapered casing flowpath does not have the additional stage 2 blade speed provided by the constant-tip type fans and therefore is not as attractive. The high stator exit swirl case has a high fan efficiency but requires a higher RPM, has higher exit-stator aerodynamic loadings, has a weight penalty, and would present more severe radial mismatch problems at off-design conditions. The net effect is only slightly better than the nominal case.

The three-stage fan information presented in Table VII shows the near-constant-tip (NCT) fan to have a positive effect on the overall aircraft range where the constant-pitch (CP) fan shows a distinctly negative effect. The biggest difference between the two fans is the fan efficiency (2.6 points). However, the NCT fan's higher efficiency potential, essentially due to its lower speed, is largely negated by the lower LPT efficiency. The required cooling flow and turbine weight are less. Only the low radius ratio, constant tip, two-stage configurations show better aircraft range than the three-stage NCT fan. Although no attempt was made to determine the cost of the various fan configurations, the three-stage, high aspect ratio fans have almost twice as many airfoils as the two-stage constant-tip fans, and are probably more expensive.

Table VII. Summary of Low Pressure System Data from Refined Front Blocking Fan Screening Study.

Configuration	Inlet Radius Ratio	Corrected Tip Speed m/sec (fps)	Corrected Speed rpm	Δ Fan Eff. %	Δ LPT Eff. %	Δ Fan Weight kg (lbs)	Δ LPT Weight kg (lbs)	Δ LPT Cooling Flow, %	Δ Aircraft Range, %
Two-Stage Tapered Casing Fans									
- Nominal	0.438	493 (1619)	5641	0	0	0	0	0	0
- Low Aspect Ratio	0.438	471 (1546)	5387	+ 0.6	- 0.4	+158 (+349)	- 5.4 (-12)	- 0.3	- 0.38
- High Aspect Ratio	0.438	503 (1651)	5753	- 0.6	+ 0.1	- 47 (-104)	+ 0.9 (+ 2)	+ 0.2	+ 0.13
- Low Inlet Radius Ratio (Exit r/r = 0.755)	0.380	479 (1571)	5632	+ 0.7	0	- 12 (- 27)	- 1.4 (- 3)	0	+ 0.24
- High Inlet Radius Ratio (Exit r/r = 0.755)	0.500	508 (1668)	5598	- 0.8	- 0.1	+ 30 (+ 65)	- 2.3 (- 5)	- 0.1	- 0.21
- High Swirl (20°)	0.438	507 (1664)	5798	+ 1.2	+ 0.2	+ 22 (+ 48)	+ 1.8 (+ 4)	+ 0.3	+ 0.09
Three-Stage Fans									
- Nominal Near-Constant Tip	0.438	420 (1378)	4801	+ 1.4	- 1.3	+ 29 (+ 64)	- 19.0 (- 42)	- 0.7	+ 0.28
- Nominal Constant Pitch	0.438	485 (1592)	5547	- 1.2	- 0.4	+ 29 (+ 63)	- 0.9 (- 2)	- 0.1	- 0.36
Two-Stage Constant Tip Fans									
- Case 1	0.438	467 (1533)	5341	+ 0.2	- 0.5	- 20 (- 45)	- 6.8 (- 15)	- 0.3	+ 0.20
- Case 2	0.400	463 (1520)	5336	+ 0.9	+ 0.5	- 44 (- 97)	- 7.3 (- 16)	- 0.4	+ 0.48
- Case 3	0.350	454 (1489)	5214	+ 1.9	- 0.6	- 76 (-168)	- 9.5 (- 21)	- 0.4	+ 0.79

In summary, the evaluation of the various fan configurations in terms of the total low pressure system leads to the conclusion that the two-stage, constant-tip fans are distinctly more attractive.

Results of Rear Block Fan Parametric Screening Study

The rear block fan parametric screening study was conducted for a nominal single stage fan as shown in Figure 23. The results of the parametric investigation are listed in Table VIII and displayed graphically in Figures 24-29. The trends are generally similar to those seen in the front block screening study. Aspect ratio and solidity variations reflect only a change in the rotor level since the stage, as currently conceived, does not employ a stator vane row immediately downstream of the core-driven fan rotor. Instead, the core inlet guide vane will serve as the stator for the core flow portion and a fixed vane row in the inner bypass duct will remove the swirl in the outer portion. The nominal fan rotor is assumed to have titanium blades and no shrouds. The fan efficiency and tip speed results plotted in Figures 24-29 show that the low aspect ratio and the high IGV exit swirl cases have the best efficiency potential. The variations in rotor solidity and stage exit Mach number were of little consequence to the stage performance. The level of flow per unit annulus area is restricted by the amount of diffusion required between the front and the rear block fans and between the rear block fan and the core. The inlet radius ratio was also somewhat constrained due to the size of the core compressor and the minimum length desired between the overhung core-driven rear block rotor and the core compressor rotor.

A cursory look at the core compressor design for the AST engine was necessary since the rear block fan RPM would have to be compatible with the speed required by the core. A preliminary design study was conducted using a 5-stage compressor operating at the cycle design pressure ratio of 4.44. Two flowpaths were evaluated and are compared in Figure 23 along with the nominal rear block fan flowpath. One has a constant-hub radius, the other a slight hub convergence. The constant-hub radius flowpath configuration would require a core design physical speed of approximately 7690 RPM. The modified hub flowpath compressor would require about 4% less speed (7366 RPM) which would ultimately mean a lighter weight high pressure turbine. For this reason, it was desirable to choose a rear block fan configuration close to the lower RPM value. The selected rear block fan has a physical RPM of 7225, giving a corrected tip speed of 413 m/sec (1355 ft/sec).

C. Study of Variable Geometry Concepts for Optimum Off-Design Performance

An investigation of the effect of the level and the radial distribution of swirl ahead of the front fan rotors on key aerodynamic parameters was carried out at the aerodynamic design point and at the supersonic cruise condition. These studies were conducted to assist in the selection of the design swirl and also to provide information on the location and type of variable geometry that is desirable from an aerodynamic standpoint.

Table VIII. AST Rear Block Fan Screening Study, Summary of Core-Driven Fan Stage Aerodynamic Design Data.

Configuration	Adiabatic Efficiency	Corrected Tip Speed m/sec (fps)	Physical Speed rpm	Rotor Tip Diameter m (in.)
Nominal	0.860	413 (1355)	7225	1.28 (50.4)
Low Aspect Ratio (ARR = 1.2)	0.873	394 (1294)	6900	1.28 (50.4)
High Aspect Ratio (ARR = 2.0)	0.836	439 (1439)	7673	1.28 (50.4)
Low Solidity (Rotor Sol. = 1.4)	0.858	418 (1370)	7305	1.28 (50.4)
High Solidity (Rotor Sol. = 1.9)	0.861	406 (1331)	7097	1.28 (50.4)
Low Flow/Annulus Area [175.8 (36)]	0.854	436 (1431)	7378	1.32 (52.1)
High Flow/Annulus Area [195.3 (40)]	0.858	402 (1320)	7174	1.25 (49.4)
Low Inlet Radius Ratio (0.60)	0.864	417 (1368)	7679	1.22 (47.9)
High Inlet Radius Ratio (0.70)	0.859	406 (1332)	6674	1.36 (53.6)
Low Exit Mach No. (0.45)	0.857	422 (1383)	7374	1.28 (50.4)
High Exit Mach No. (0.55)	0.863	405 (1328)	7081	1.28 (50.4)
IGV Exit Swirl = 8°	0.875	418 (1370)	7305	1.28 (50.4)
IGV Exit Swirl = 12°	0.880	422 (1386)	7390	1.28 (50.4)
IGV Exit Swirl = 20°	0.882	445 (1459)	7779	1.28 (50.4)

For the variable cycle engine, flow modulation through the use of variable geometry inlet guide vanes (IGV) is required to achieve the best compromise of design and off-design aerodynamic performance. At off-design conditions, the IGV's are closed from the design angle settings and introduce a radial gradient of streamline axial velocities and therefore create an undesirable incidence angle distribution on the downstream rotor. The study was intended to identify the type and location of variable geometry which would significantly alleviate this radial mismatch of the flow.

The variable stagger stator, which is widely used and relatively simple, served as a bench mark for evaluating the aerodynamic desirability, mechanical complexity and reliability of other forms of variable geometry. Off-design calculations were made using stator exit flow angles and stator leading edge metal angles which would result from the use of variable stagger stators. The resulting incidence angles and aerodynamic loadings served as a basis for comparison with the other variable geometry concepts investigated.

Some of the other variable geometry concepts which were considered in this screening study are: (1) Tandem cascades, including flap-type guide vanes and stators to achieve the effect of variable camber, and (2) configurations which achieve some radial variation of effective closure by having a radial variation of solidity of the movable portion, and (3) a circumferentially-leaned inlet guide vane.

Off-Design Analysis Model

The Axisymmetric Data Analysis program (ADA) is the analysis version of General Electric's primary aerodynamic tool, the Circumferential Average Flow Determination (CAFD) program. A numerical solution of the exact radial equilibrium equation, continuity equation, and energy equation is found which yields circumferentially-averaged velocity and thermodynamic property distributions throughout the annulus. The total-pressure loss coefficients and deviation angles can either be obtained by an optional correlation built into the program or be separately specified.

The built-in correlation which varies the design values of loss coefficient and deviation angle with incidence angle, Mach number and aerodynamic loading was used for evaluating variable geometry swirl distributions at off-design conditions. The efficiency prediction model of the Compressor Unification Study (CUS) was also employed to help select the endwall boundary layer displacement thickness, which is an input to ADA, and also served as a check on the loss coefficients obtained from the cascade option of ADA.

Variable Geometry Concepts Study

Axisymmetric Data Analysis (ADA) program calculations were made at the design point and at the supersonic cruise condition of the front block fan for several different levels and radial distributions of design swirl. The supersonic cruise condition is a representative off-design case where the corrected speed is 79 percent of the aerodynamic design speed. The inlet

guide vanes are closed approximately 39 degrees at this condition to match the inlet requirements and to obtain good stall margin. The off-design swirl level was varied radially to evaluate the radial shift in incidence angle and aerodynamic loading. The nominal two stage fan with an inlet radius ratio of 0.438 and a tapered casing flowpath was used as the basic fan configuration for most of the off-design calculations.

As one means of evaluating the off-design incidence angle distributions, the flow angle leaving the IGV is increased from the design by the same amount at all radii, simulating the use of a conventional variable stagger guide vane. Cases where the amount of flow angle closure varied radially at the off-design condition were also studied. A combined strut and flap type inlet guide vane with a fixed leading edge portion (strut) and a variable trailing edge portion (flap) of varying chord lengths were used to simulate these flow angles.

An inlet guide vane configuration that was leaned in the circumferential direction was investigated in an attempt to reduce the large rotor tip incidence angles at the supersonic cruise condition. The IGV was envisioned as a strut/flap type configuration that imparted no swirl at the design condition. At the supersonic cruise condition, the flap was closed to effect about 40 degrees of pre-swirl at the pitchline. The flap tapered off to zero chord at the outer diameter, and added no swirl to the flow in either the closed or nominal position. The hub swirl was 10 degrees in the closed position. The pressure side of the closed vane was leaned downward 40 degrees at the mean radius so that a radially inward blade force was directed on the flow. Relative to a radial vane, the leaned vane will tend to increase the static pressure in the hub region and decrease it at the tip. The reduced static pressure in the outer portion of the flowpath will increase the meridional Mach number and tend to reduce the tip incidence angle.

Results of Off-Design Analysis

The off-design analysis program (ADA) was run for the nominal two-stage fan with three different levels of rotor 1 inlet design swirl. The design swirl distributions included: (1) a radially constant zero degrees, (2) a linear variation from 10 degrees of preswirl at the tip to 10 degrees of counterswirl at the hub, and (3) a linear variation with 10 degrees of counterswirl at the tip to 10 degrees of pre-swirl at the hub. Other more radical distributions of swirl were studied but did not show a positive gain in alleviating the off-design incidence angle problem. The design point parameters of inlet Mach number and diffusion factor are shown in Figure 30 and 31 for rotor one and stator one, respectively. Each of these design swirl distributions was run at the supersonic cruise off-design speed. In order to match the supersonic cruise airflow required by the cycle, the inlet guide vanes had to be closed approximately 38 degrees. The off-design incidence angles and diffusion factors for the design zero degrees swirl case are shown relative to the design values in Figures 32 and 33 for the first rotor and stator, respectively. The data shown represent three radial distributions of IGV turning angle, presupposing an IGV configuration which had some radial

variation of solidity. Each radial distribution is identified by a symbol representing a different radial variation of turning angle. At the O.D., all three types show approximately 10 degrees of rotor 1 incidence or a 7 degrees shift from the design point. If the flow angle leaving the IGV is increased from the design by the same amount at all radii (as is approximately done for a conventional variable stagger guide vane), the hub incidence angle gets smaller than design and moves toward choke. Less closure of the IGV at the hub than at the pitch helps to keep the hub incidence angle nearer to the design value. The configuration which produces more IGV turning at the tip and less at the hub relative to the pitch results in the least incidence angle swing on stator one. The first rotor D-factors are less than design when the guide vanes are closed and stator one D-factors shift from design largely in the pitch region.

The off-design rotor incidence angles were also calculated for other design IGV swirl angle distributions, including the linear distribution of 10 degrees pre-swirl at the tip to 10 degrees counterswirl at the hub. The resulting off-design incidence angles on the first rotor at the supersonic cruise speed condition are shown in Figure 34. Three radial variations of IGV closure were investigated. The large positive incidence angle swing from design at the tip is still prevalent and no indication of a significant reduction in the radial mis-match problem is apparent. Figure 35 shows the rotor incidence angle comparison between design and supersonic cruise when the fan is designed for an IGV swirl distribution that has 10 degrees counterswirl at the tip, 0 degrees at the pitch and 10 degrees pre-swirl at the hub. This design combination has the favorable effect of reducing the rotor tip incidence angle at the cruise condition by approximately two degrees. However, this improvement is at the expense of an increase of approximately 0.10 rotor tip relative Mach number at the design condition, which would have an adverse effect on the high speed efficiency. It was judged that the reduction in high speed efficiency made the choise of this combination undesirable.

The effect of the circumferential lean added to the IGV hub was insignificant in reducing the off-design rotor 1 tip incidence angle.

Summary of Off-Design Swirl Investigation

- No swirl distribution was found that had a marked effect on lowering the rotor incidence angle at the supersonic cruise condition with the IGV closed.

- The design swirl distribution which had 10 degrees counterswirl at the tip, 0 degrees at the pitch, and 10 degrees preswirl at the hub had the lowest calculated tip incidence angle at the supersonic cruise condition, but also had a higher rotor tip relative Mach number at the design condition which would have an adverse effect on the high speed efficiency. Because of the latter, this combination was judged undesirable.

- Comparisons of the low inlet radius ratio designs with the 0.438 nominal case indicated that there was not any significant difference in the off-design incidence angle at the rotor tip but the low radius ratio fans had a more negative incidence angle (hence, less favorable) at the hub.

- Circumferential lean added to the IGV at the I.D. had no significant effect on reducing the rotor tip incidence angle.

D. Recommended Fan Configuration

The 0.35 and 0.40 inlet radius ratio, constant-tip fans gave the best aircraft range and would probably be less expensive than the three-stage fans. While these low radius ratio designs had a somewhat larger radial gradient of rotor incidence angle at the supersonic cruise condition than the nominal fan, it is believed that the superior design point efficiency favored a radius ratio lower than 0.438. However, there was concern that the 0.35 inlet radius ratio configuration might involve mechanical design constraints that were not revealed in the very preliminary study used to determine the fan weight. Therefore, the 0.40 inlet radius ratio configuration was believed to be the best all around choice considering the design point performance, the off-design operation, and the degree of mechanical design risk.

The fan configuration recommended for the AST variable cycle engine as a result of this study program consists of a two-stage front block fan and a single stage rear block driven by the high pressure turbine. The flowpath of both fan blocks, the interconnecting duct and a portion of the bypass duct is shown in Figure 36. The important aerodynamic design parameters are:

Recommended Fan Configuration

Aerodynamic Design Point Parameters.

Parameter	Front Block	Rear Block
No. of Stages	2	1
Corrected Flow, Kg/sec (lbm/sec)	372.0 (820)	139.7 (308)
Flow per Annulus Area, Kg/sec m^2 (lbm/sec ft^2)	205.0 (42.0)	187.9 (38.5)
Inlet Radius Ratio	0.40	0.65
Corrected Tip Speed, m/sec (ft/sec)	467 (1532)	413 (1355)
Total-Pressure Ratio	3.17	1.48
Adiabatic Efficiency Objective	0.865	0.860
Stall Margin Objective %	22	22
Exit Mach No.	0.48	0.52

The front block fan flowpath has a constant tip diameter of 165.8 cm (65.3 in.) through the first stage and a slight casing taper (2.5° slope) through the second stage to help reduce the large radius drop in the transition duct to the rear block. The inlet guide vane (IGV) configuration is the variable camber type with a fixed leading edge portion and a variable trailing edge flap. At the aerodynamic design point, the guide vane imparts no swirl at the rotor leading edge. The off-design calculations indicated some advantage for using a lower IGV flap solidity at the hub so that less flow-turning is accomplished at the I.D. when the IGV is closed from the design setting. However, this is contrary to some test experience within the General Electric Company. Consequently, the selected IGV flap solidity will result in approximately a constant radial distribution of swirl when closed from the design setting. The first stage stator vane will be a conventional, variable stagger type stator. The design swirl ahead of rotor 2 will be a radially constant 5 degrees. At off-design, the stator will be closed a maximum of 20 degrees to help the off-design performance. Stator 2 will be a circumferentially-leaned vane fixed at both ends with the trailing edge angles designed to turn the flow back to the axial direction.

The rear block fan will also employ a variable camber type inlet guide vane with no swirl ahead of the core-driven rotor at the design point.

The recommended fan configuration was selected primarily from the results of the parametric screening studies. The constant-tip flowpath fans provided for the best low pressure system, utilizing the attractive features of low speed, low inlet radius ratio and low inlet specific flow. The only issue to be decided was how low the inlet radius ratio should be. Based on the variable geometry study at off-design conditions, the very low radius ratios did not show good off-design performance because of a more severe radially mismatch of the flow. An inlet radius ratio of 0.40 was chosen. The rear block fan was limited somewhat by the restrictions imposed upon it by the high pressure (HP) system. The primary concern was choosing a stage which would be compatible in speed with the HP compressor and be positioned to avoid large flowpath slopes and curvatures.

SECTION IV

AERODYNAMIC DESIGN

A. Design Calculation Procedure

The General Electric Circumferential Average Flow Determination (CAFD) computer program was used to determine the circumferential-average flow properties for the front and rear block fans at their respective aerodynamic design points. The CAFD calculation procedure is outlined in Reference 2. In addition to calculation stations at the blade row edges and in the ducts upstream and downstream of the fan blocks, calculation stations interior to the rotor and stator blades were included to improve the overall accuracy of the solution by taking into account the effects of blade thickness blockage, lean angle and energy (rV_θ) addition on the streamline slopes and curvatures. The intra-blade calculation stations also aid in the determination of the rotor blade meanline shapes.

The chordwise energy addition assumed for the front block rotors is linear from leading to trailing edge for the tip streamline. For the streamlines where the inlet relative Mach number is sonic or less than sonic, a chordwise rV_θ distribution approximating the first quarter cycle of a sine wave was assumed. The radial variation is linear from the tip streamline to the location where the quarter sine wave is used. The selection of the linear work input distribution in the tip region is generally consistent with measured static pressure data from other high Mach number rotor blade tip sections. The quarter sine wave distribution was assumed for all the streamlines of the rear block fan.

In applying the CAFD procedure to these fan designs, an effective area coefficient that accounts for the displacement thickness of the wall boundary layer and the wakes from the upstream blade rows was used. Values of effective area coefficients were selected from past experience and from the values indicated by the Compressor Unification Study. A radially constant value was used in the axial space between blade rows and varied linearly from leading to trailing edge through the blades. Upstream of the front block fan, a value of 0.985 was assumed. At the inlet to the first rotor, the coefficient is 0.975 and is then reduced to 0.950 at the front block exit. For the rear block fan design point, the effective area coefficients were assumed to vary from 0.945 at the guide vane inlet, to 0.940 at the rotor inlet and 0.93 at the rotor exit.

The axisymmetric flow calculation for the front block fan included stations far upstream and and also, downstream in the outer bypass duct and the transition duct to the rear block fan. Fourteen (14) streamlines including a double, splitter-stagnation streamline were used for the design calculation. The rear block design point calculation included stations from the front block fan exit through the core compressor first stage and also through the inner bypass duct. An inlet profile of total pressure and total temperature were

used at the initial calculation station simulating the front block exit conditions at the rear block design point. To represent the flow through the rear block, eleven (11) streamlines, including a double streamline for the inner flow splitter, were used.

A list of the axisymmetric flow calculation results for the front and rear block fan design points is included in Appendix B.

B. Flowpath

The front block fan inlet hub/tip radius of 0.40 and the inlet specific flow rate of 205 kg/sec m^2 (42 lbm/sec ft^2) were selected to minimize the required fan size and nacelle diameter. The tip flowpath contour through the first stage is a constant diameter of 165.81 cm (65.28 in.) in the full AST engine size of 376.95 kg/sec (820 lbm/sec). A large increase in the hub radius across the first rotor enhances the pressure rise capability of the fan at a moderate level of inlet corrected tip speed, 467 m/sec (1532 ft/sec). The flowpath for both the front and rear block fans and the bypass and transition ducts is shown in Figure 35.

The flow is split downstream of the front block and at the front block fan design point 35.5 percent of the total flow is bypassed through the outer duct. The remaining flow passes through the rear block fan operating off-design at a high corrected speed with the inlet guide vanes (IGV2) closed approximately 45 degrees. The flowpath of the transition duct undergoes a considerable change in hub radius from the exit of the front block to the inlet of the rear block fan rotor where the hub/tip radius ratio is 0.65. A slight increase in hub radius is made through the core-driven rotor to a cylindrical hub section just ahead of the core compressor. The flow is split again downstream of the rear block fan with 93.5 percent passing through the core compressor.

At the aerodynamic design point of the rear block fan, the front fan is low-flowed and nearly the entire amount of inlet flow is directed into the rear block. The rear block fan and duct flowpaths are shown in greater detail in Figure 37. For calculation purposes, it was assumed that 2 percent of the inlet flow was bypassed through the outer duct. The remaining flow of 139.7 kg/sec (308 lbm/sec) represents the maximum flow that passes through the rear block fan anytime during the AST engine cycle. The flow is split downstream of the fan such that 25 percent is bypassed through the inner duct and 75 percent is passed through the core. At the aerodynamic design point, the specific flow rate is 188 kg/sec m^2 (38.5 lbm/sec ft^2). The design pressure ratio is 1.48 at a corrected tip speed of 413 m/sec (1355 ft/sec). The maximum physical speed of this stage is 518.2 m/sec (1700 ft/sec) occurring at the supersonic cruise condition.

The flowpath coordinates of the front and rear block fans, the bypass ducts and the connecting transition duct are tabulated in Appendix A. The selection of the design parameters for each fan is discussed below.

C. Design Parameters

1. Front Block Fan

The radial variation of design total-pressure ratio at the exit of the front block fan rotors is shown in Figure 38. The total-pressure leaving the hub of the first rotor was specified to be about 5 percent higher than the tip value to increase the meridional velocity entering the second stage and hence reduce the hub loading of that stage. Past experience with fans of this type indicates that this is the region which usually initiates stall at the higher corrected speeds. The profile is radially constant behind the second rotor to minimize the radial gradient of total pressure into the rear block fan. The adiabatic efficiency profiles at the stage exit stations are shown in Figure 39.

The total-pressure loss coefficients for the front block rotors and stators are shown in Figure 40. The values in the pitchline region are consistent with the free stream profile losses calculated by the efficiency model used in the screening studies and reported in Reference 1. The end-wall loss coefficients shown in Figure 40 are comparable to other, recently-tested, high Mach number fan designs. The rather large loss coefficient at the hub of the first rotor was assumed because of the concern for the higher than normal through-flow velocity in the hub region where the blade blockage is the greatest.

The design rotor and stator inlet Mach numbers and diffusion factors resulting from the design point axisymmetric flow calculation are shown in Figures 41 and 42. The calculation procedure was carried out with the rotor inlet design swirl levels of zero degrees at rotor 1 and 5 degrees at rotor 2 inlet, both being constant values from tip to hub. Figure 41 shows the first rotor inlet tip Mach number at a level of 1.64 and remaining greater than sonic for the outer 85 percent flow region. The second rotor has Mach numbers greater than 1.0 over the entire span. The stator inlet Mach numbers, also shown in Figure 41, indicate a rather high value (0.97) at the first stator inlet. The level of Mach number shown for stator 2 reflects a considerable reduction due to the addition of circumferential lean in the hub region. The discussion of stator 2 lean will be taken up in the Airfoil Design Section.

The design point diffusion factors are shown in Figure 42. The first stage rotor is slightly more heavily-loaded over most of the span than the second stage, with the loading dropping off rapidly at the hub due to the high local flowpath curvatures. The highest loading on stator 1 occurs in the hub region where the inlet Mach numbers are the largest. Over most of the stator span however, the loadings are moderate at levels less than 0.40. The second stage stator loadings are slightly larger than stage 1 since the vanes turn the flow back to the axial direction whereas stator 1 leaves a radially constant 5 degrees of swirl.

2. Rear Block Fan

The total-pressure ratio and adiabatic efficiency profiles for the rear block fan at its design point are shown in Figure 43. The tip total-pressure for this stage is also specified lower than the average so that the pressure of the bypassed flow is kept to a minimum and can be matched with the outer duct pressure more easily. Also, to achieve a high specific thrust, the core flow is supercharged to a greater degree by having a higher than average hub total-pressure. The average stage total-pressure ratio at design is 1.48 at an adiabatic efficiency of 86 percent.

At the aerodynamic design corrected inlet flow of 139.7 kg/sec (308 lbm/sec), the velocity diagrams were calculated using the CAFD program. The design point inlet relative Mach numbers, loss coefficients and diffusion factors are shown in Figure 44.

D. Airfoil Design

Rotors

The front block fan rotor blade airfoil sections were specifically tailored for each streamline section. In the outer portion of the blades, where the inlet mach numbers are supersonic, the airfoils were shaped in an attempt to minimize shock losses. In the hub region where the relative Mach numbers are approximately 1.00 or less, airfoils similar to a double-circular arc were used. The design relative Mach numbers introduced in the previous section are shown in Figure 41. The design of the rotor blade sections was performed along axisymmetric stream surfaces with the surfaces viewed along a radial blade axis using the General Electric Streamsurface Blade Section program.

The rotor blade incidence angles are shown in Figure 45. With supersonic relative Mach numbers, the blade inlet region sets the amount of flow the cascade can pass, provided the throat area is not limiting. The blade suction surface upstream of the Mach wave which intersects the leading edge of the adjacent blade was offset a small amount from the "free-flow" streamline to account for the effects of leading edge thickness, bow wave losses and boundary layer build-up. The "free-flow" streamline is the direction of the flow if there were no disturbances or blade forces. Figure 46 shows the location of the free flow streamline for a rotor 1 streamline airfoil section near the tip. Figure 47 shows the rotor 1 streamline airfoil section near the hub. Other information on Figures 46 and 47 will be discussed later. After establishing the suction surface of the airfoil for the outer portion of the blades in this manner, relatively little freedom remains for the incidence angle selection. The incidence angles in the extreme hub region were selected large enough to permit sufficient passage throat areas.

The trailing edge angles were established by calculating Carter's Rule deviation angles using the camber of an equivalent two-dimensional cascade and applying an adjustment factor derived from past experience. The rotor deviation angles are shown in Figure 45 (including adjustment), along with the empirical adjustments to Carter's Rule which were utilized.

The passage throat areas were set such that the effective throat-to-capture area ratio exceeded the critical area ratio by approximately 6 percent at all streamlines after allowances for losses of a normal shock at the upstream Mach number. The throat areas represent a compromise of the desire to have a small throat for the best design point efficiency but sufficiently large to permit good off-design performance. The throat-to-capture area ratios for each rotor streamline are shown in Figure 48.

For operation with an oblique leading edge shock, the ratio of the contraction from the cascade mouth to the throat (see Figures 46 and 47 for mouth and throat locations) must not exceed the critical contraction ratio including normal shock losses at the mouth Mach number. The amount by which the passage area exceeds the limiting contraction ratio is referred to as starting margin. The calculated internal contraction ratios and margins for each rotor streamline are plotted versus mouth Mach number in Figure 49.

The airfoil shape for each streamline section is dependent upon the chordwise thickness distribution and meanline blade angles. For the front block fan rotors, the maximum thickness-to-chord (Tm/c) ratios and their radial distributions are primarily dependent upon mechanical and aeromechanical considerations. The rotor blade chord and tm/c distributions are shown in Figure 50. Briefly, the Tm/c for both rotor tip sections is 0.025 and at the hub is 0.090 for rotor 1 and 0.070 for rotor 2. The location of the maximum chordwise thickness for both rotors was specified at 60 percent at the tip. The maximum thickness location moves forward at lower radii until the hub streamline is reached where it occurs at 48 percent chord. The thickness varies from leading edge to the point of maximum thickness for all streamlines according to a quarter sine wave distribution and then reverses the distribution from the maximum thickness point to the trailing edge.

The throat-to-exit area ratio parameter was used as a guide in determining the passage area distribution in the trailing edge region. Assuming that sonic velocity exists at the passage throat, then the increase in area from the throat to the passage exit (see Figures 46 and 47) should be compatible with the diffusion required to reduce the relative Mach number from 1.00 to the value calculated by the axisymmetric flow solution at the passage exit. The front block fan rotors were designed intentionally to have smaller throat-to-exit area ratios than the diffusion rate would require so that adequate blade camber would exist. The values of the throat-to-exit area ratios are shown in Figure 48 plotted versus the exit Mach number.

The meanline blade angles are a result of the axisymmetric calculated flow angles and the specified angles of departure from the flow direction. The incidence and deviation angles are the departure angles at the leading and trailing edges, respectively. Between the two edge values, the departure angles were specified for each streamline considering the throat margins, internal contraction ratios, suction surface Mach numbers and throat-to-exit area ratios. In the outer portion of the blade where shocks are present in the cascade, slightly negative departure angles can result. In the inner portion, where the Mach numbers are subsonic or only slightly supersonic, the flow is assumed to follow a path of near-perfect guidance with the airfoil shape so departure angles near zero were used as a design guideline.

The rear block fan rotor blade design was conducted in a similar manner to the front block rotors. The airfoils were specifically shaped for each of the ten (10) streamlines using the Streamsurface Blade Section (SBS) program. The tip and hub streamline airfoil sections generated by the SBS program are shown in Figures 51 and 52. The incidence angles for the supersonic inlet Mach number streamlines were selected after establishing the suction surface of the airfoil relative to the "free-flow" streamline, as was described earlier. The hub incidence angles were chosen compatible with the required throat margins. The deviation angles were calculated from Carter's Rule using the camber of an equivalent two-dimensional cascade with an empirical adjustment. The incidence, deviation and adjustment angles are plotted versus streamfunction in Figure 53.

The rear block fan airfoil sections were defined on streamlines by specifying the thickness and blade angle along the meanline of the streamsurface. The maximum thickness-to-chord ratio varied linearly from 0.025 at the tip to 0.070 at the hub as shown in Figure 54. The thickness was applied to each streamline from leading to trailing edge according to the first quarter cycle of the sine wave. The blade angles resulted from the difference between the calculated flow angles and the departure angles. The departure angles are compatible with the considerations of throat margin, internal contraction ratio, suction surface Mach number and throat-to-exit area ratios. The throat margins were specified at approximately 5 percent for all streamlines. Figures 55 and 56 show the throat margins and area ratio parameters for each streamline.

The manufacturing section coordinates for the front block and rear block rotor blades are tabulated in Appendix C. Five sections from tip to hub are listed for the front block rotor and three sections for the rear block rotor.

Stators

The first stage stator vane sections are double circular-arc airfoils. The stage 2 vanes are NACA 65-series thickness distributions on circular-arc meanlines. The stage 2 vanes were leaned circumferentially with the pressure side down to reduce the stator hub exit Mach number. Both vane rows have moderate levels of aspect ratio (2.6 on stage 1 and 1.9 on stage 2) and have pitchline solidities of 2.0. A correlation of the NASA low speed cascade data was used as a guide in selecting vane incidence angles at design. The stage 1 incidence angles were set identical to the low speed data values and provided throat margins of approximately 10 percent at the outer dimeter (O.D.) decreasing to 4 percent at the inner diameter (I.D.). Stator 2 incidence angles were set less than a degree more negative than the NASA data since ample throat margins of 14 percent at the O.D. and 9 percent at the I.D. were calculated. The deviation angles were obtained from Carter's Rule as described for the rotors; however, no empirical adjustment was made for either vane row. The incidence and deviation angles for both stators are shown in Figure 57.

The Streamsurface Blade Section (SBS) program was employed for the stator vane design as well as for the rotors. Figures 58-61 show the tip and hub streamline sections for stator 1 and stator 2. The passage area distribution is shown as well as the throat, mouth and exit locations. The vane maximum thickness-to-chord ratios and chord distributions for both stators are shown in Figure 62.

While the circumferential lean of stator 2 was primarily used to lower the stator hub exit Mach number and hence reduce the amount of diffusion required in the downstream duct, there was also a beneficial reduction in the Mach number entering the stator. The downward radial force on the flow imposed by the leaned vane increases the static pressure and thereby, reduces the Mach number. The amount of lean selected for the final vane configuration varied from 0 degrees at the tip to 25 degrees at the hub. No lean was specified at the O.D. to avoid an undesirable acute angle between the vane suction surface and the casing flowpath. The lean affected the level of Mach numbers at the tip and hub streamlines for both the second stage rotor and stator. Although there is no lean locally at the tip, the radial gradient of lean produces a slight increase in the tip Mach numbers. In the hub region, however, the absolute Mach number at the leading edge of stator 2 was reduced from 0.82 to 0.74. The effect on the stator aerodynamic loadings is minimal at the tip and causes only a slight increase in the hub region.

Stator vane airfoil manufacturing sections were defined on flat plane surfaces stacked on a radial vane axis through the 50 percent meanline chord location. The manufacturing section coordinates for four sections at the tip, near tip, pitch and hub for both stators are listed in Appendix C.

Inlet Guide Vanes

The inlet guide vane configurations for both fan blocks employ variable camber geometry with the leading edge portion (strut) fixed and the trailing edge portion (flap) variable. The blading setting or design point for each IGV was chosen at a condition for which the flap is closed 5 degrees relative to its position at the aerodynamic design points. It was felt that designing the IGV at this condition would provide a more nearly optimum IGV airfoil over the anticipated range of operation.

The inlet guide vane meanlines were made continuous as though the fixed strut and flap portions were a single airfoil. At the vane design setting point, the section meanlines are close approximations of the A_4K_6 meanline.

The thickness distribution over the first 70 percent of the strut chord was scaled to correspond to the first 35 percent of the chord of a NACA 63-series thickness distribution, while the remaining 30 percent of strut chord was held at a constant thickness. The flaps employ the NACA 0010 basic thickness distribution. The manufacturing section airfoil coordinates for both fan inlet guide vanes, specified separately as strut and flap sections, are listed in Appendix C.

SECTION V

PRELIMINARY MECHANICAL DESIGN

A. Rotor Design

Preliminary design of the front block fan rotor was conducted to achieve a mechanical configuration meeting the typical engine hardware objectives of high reliability, durability, safety, ease of maintenance and ease of assembly. These objectives insure the mechanical integrity and operational life of the rotor. Design techniques and procedures were concentrated on the following goals to achieve the above objectives.

- Assure the absence of low integral order first flexural and first torsional resonances in the high speed range.
- A minimum first flexural frequency margin of 15 percent with respect to two/rev excitation at maximum operating speed.
- Assure the absence of responsive airfoil panel mode resonances with known or anticipated sources of excitation, such as airfoil row passing frequency, two/rev inlet distortion, struts, probes, rotating stalls, etc., in the operating speed range.
- Avoid prohibitive levels of self-excited airfoil vibration of an aeromechanical nature (in the unstalled operating range); specifically, instability vibration and separated flow vibration.
- Insure the critical regions of the airfoil and supporting rotating structure have adequate strength to withstand normal operating and stall induced stresses.
- Blade airfoil foreign object impact tolerance.
- 4000 hours operating life
  50000 cycles low cycle fatigue life
  10^7 cycles high cycle fatigue life
- 122 percent burst speed margin over maximum operating speed.

Consideration of these goals during the rotor preliminary design strongly influences design parameters, such as airfoil spanwise chord and tm/c distributions, the support pattern of the rotating structure under the airfoil, and airfoil attachment to the rotating supporting structure. The rotor mechanical design point was the hot day, takeoff condition of 5841 physical rpm (108.9 percent of the aerodynamic design point) which results in a blade tip speed of 508.5 m/sec (1668 ft/sec).

The preliminary design of the front block, two stage fan rotor meeting the above goals is shown in Figure 63 with the material specified. The design is mounted off a forward thrust ball bearing. The blades are constructed out of 5.6 mil diameter boron/1100 aluminum composite. The rotor structure is manufactured from beta forged Ti 17.

In the initial preliminary design phase, both boron/aluminum and titanium blade designs were considered. The titanium designs did not meet the first flex frequency margin over 2 per rev excitation and were flexurally unstable. The long, flexible blade shank resulting from the high hub flowpath angle and blade airfoil geometry was the main cause of the titanium designs' deficiencies. The long, flexible shank did not pose a problem to the boron/aluminum composite with its higher strength-to-weight ratio. Workable titanium designs would involve either a part-span shroud, increased tm/c distribution, or an integral blade and disk configuration (blisk). The first two were unacceptable from an aerodynamic viewpoint. The latter was unacceptable from its reduced maintainability standpoint not having individually replaceable blades and from its increased manufacturing difficulty resulting from the physical size of the first stage rotor.

The airfoils stress, deflection, and vibration analyses were accomplished through the use of the General Electric computer program, TWISTED BLADE (TWBL), which models the airfoil as a tapered, twisted, cambered, cantilevered beam undergoing coupled torsion-bending deformation. Several iterations involving chord and tm/c spanwise distributions and shank thickness were conducted to achieve a reasonable balance between aerodynamic and mechanical design requirements.

A summary of the selected blades' geometry is presented in Table IX. Figures 64 and 65 are the Campbell Diagrams for the stage 1 and stage 2 blade designs, respectively. Stage 1 has a 16 percent first flex frequency margin over 2 per rev excitation. Stage 2 has a 16 percent first flex frequency margin over 3 per rev excitation. Both stages have a possible first torsion frequency resonance with the 16 per rev excitation of the inlet guide vanes near idle speed. This may dictate a change in the number of inlet guide vanes which has only tentatively been set at 16 or produce minor airfoil geometry changes. Stability plots for the stage 1 and 2 blades are presented in Figures 66 and 67. Both blade designs are stable in the unstalled operating range.

Blade/disk dovetails for stage 1 and 2 are of different configurations. Stage 1 dovetail is of the keyhole design which allows the blade to rotate tangentially in the dovetail slot during foreign object impact thus absorbing energy which might otherwise damage the blade. Stage 2 has a conventional dovetail design with 55° pressure face angles and an orientation angle of 20° which makes the transition from the moderately staggered root airfoil section to the shank easier.

As can be seen from Figure 63, the stage 1 disk is a ring configuration. This design results from the low first stage inlet radius ratio and long blade shank to accommodate the high hub flowpath angle. Stage 2 is a conventional T-disk design. Wherever possible, disks and shafts are integrally joined by inertia welding to minimize material envelopes and eliminate heavy, multiflange bolt joints.

Table IX. Fan Blade Geometry Summary.

		Stage 1	Stage 2
Number of Blades		28	42
L.E. Tip Diameter	cm (in.)	165.81 (65.28)	165.58 (65.19)
T.E. Tip Diameter	cm (in.)	165.81 (65.28)	164.77 (64.87)
L.E. Hub Diameter	cm (in.)	66.32 (26.11)	111.56 (43.92)
T.E. Hub Diameter	cm (in.)	98.27 (38.69)	122.15 (48.09)
Inlet Radius Ratio		0.400	0.674
Aspect Ratio (Pitch)		1.63	1.41
Airfoil Type		Arbitrary	Arbitrary
Chord, Root	cm (in.)	25.24 (9.94)	17.00 (6.69)
Tip	cm (in.)	27.99 (11.02)	17.46 (6.87)
Solidity, Root		2.500	1.953
Tip		1.504	1.406
Tm/c, Root		0.088	0.069
Tip		0.025	0.025
Camber, Root		98.86°	47.00°
Tip		-0.03°	5.68°
Stagger, Root		3.14°	36.18°
Tip		61.15°	62.09°
Dovetail		Keyhole	Single Tang
Shroud		None	None

The rotor structure design is based on relating operating stresses and temperatures to require fatigue, creep and rupture life for -3σ material properties.

Stress Analysis was accomplished using General Electric's "CLASS-MASS" computer program which analyzes shells of revolution for either axisymmetric or non-axisymmetric loading. Resultant rotor structure stress and assumed temperatures for 5841 rpm are shown in Figure 68.

B. Structure Design

The major portion of the stators and structures design effort was concentrated on the stator 1 and 2 preliminary frequency and stress analysis. Vane analysis was accomplished using the General Electric twisted blade program. In terms of vibration, it is impractical to keep all vane frequencies out of the operating range with this high speed fan design. Therefore, the frequencies remaining in the operating range are those which are typically hard to excite as opposed to the first fundamental modes.

The frequency analysis of the original aero design vane coordinates with an average 0.068 tm/c for both stator 1 and stator 2 resulted in the vanes having a two-stripe frequency mode (chordwise bending) in the fan operating range. The Campbell diagrams for these stators are shown in Figures 69 and 70. Based on previous engine test data, the two-stripe mode is a very detrimental and easily excitable mode of vibration. Therefore, it is imperative that this mode of vibration be driven out of the operating range on new engine vane designs. Based on empirical equations derived from previous engine test data, a recommended parameter for these vanes required that thickness be increased 75% on stator 1 and 44% on stator 2. These large increases in airfoil thicknesses are undesirable from an aerodynamic design viewpoint because of the high airflow velocities associated with this fan.

Analysis was then conducted on various airfoil configurations in an attempt to minimize the additional thickness increases yet still ensure mechanical integrity in terms of airfoil vibration. The configuration chosen which is most suitable for the aero design vane configuration and the mechanical requirements is a hollow vane design. Both stator 1 and stator 2 were analyzed using an approximate wall thickness of 0.060 in. with solid leading and trailing edges and solid base sections. The material chosen for the vanes is titanium (Ti) 6-4.

The resulting vane frequencies are displayed in Figures 71 and 72. For both vanes the two-stripe mode is out of the operating range. These configurations essentially meet the original aerodynamic requirements for pitchline maximum thicknesses of 0.932 cm (0.367 in.) for stator 1 and 0.665 cm (0.262 in.) for stator 2. As seen in the Campbell diagram for stator 1, the second flex and second torsional modes are in the operating range at the rotor 1 excitation crossover points. These rotor 1 crossover points are the prime source of stator vane excitation and it is desirable, but not necessary,

to keep all frequencies out of this operating range. Based on previous experience, these two frequencies are difficult to excite and should present little if no vibratory problems. The other stator 1 frequency in the operating range is the third torsional mode which would be excited by the rotor 2 crossover. This mode is also difficult to excite and the rotor 2 excitation force should be minimal since it is downstream of stator 1. For stator 2, the prime source of excitation is the rotor 2 crossovers. The frequency in this range is the third torsional mode which requires a high driving force to cause excitation. Since this mode is in the operating range, the point of crossover should be kept at as low a fan speed as possible. No problems are anticipated with either the stator 1 or stator 2 configurations.

Steady state stress results are shown in Figures 73 and 74 for the stator 1 and stator 2, respectively. The stresses are a resultant of aerodynamic loading at 100% aero design speed. The maximum stress on the stator 1 is 6 ksi at the hub section and on the stator 2, 7 ksi, also at the hub section. The Goodman diagram for the stators is shown in Figure 75. Both stators have roughly 43 ksi allowable alternating stress for the design load steady state stresses. If unexpected vibration problems are encountered, the stators will have good margin in terms of allowable alternating stress for the material selected for the design. The torsional stabilities for the stators are shown in Figure 76. No stability margin problems are anticipated with these stator configurations.

Although all above data is preliminary-design oriented, no problems are expected with this stator configuration in terms of airfoil vibration and stress.

C. Scale Model Test Rig Design

Preliminary design of the scaled front block fan rotor was conducted to achieve the same objectives and goals established for the full scale fan rotor preliminary design. Attainment of these objectives and goals would allow aeromechanically and mechanically trouble-free aerodynamic component testing to be accomplished. Difficulties arose in meeting these objectives and goals, especially frequency margin over 2 per rev and stability margin while duplicating the boron-aluminum blading's aerodynamic design using a current state-of-the-art blading alloy, titanium (Ti) 6-4. The switch to Ti 6-4 was made to avoid costly boron-aluminum blade manufacturing process development for a component test fan rotor. Stage 1 in Ti 6-4 requires an integral blade and disk design (blisk) with its increased stiffness to meet the frequency margins. The fan rotor maintainability decrease using the blisk is acceptable for a fan rotor component test. A conventional blade and disk design was achieved on stage 2. Figure 77 is a cross section of the fan rotor in the scaled test rig. Figures 78 through 81 are the Campbell and stability diagrams of the stage 1 and 2 airfoils, respectively.

The scale model stators 1 and 2 Campbell diagrams are shown in Figures 82 and 83. The frequencies are arrived at by assuming that the scaled stators would have corresponding scaled flexibilities of the full size stators. If the scaled stators could not be made hollow, other mechanical methods, such

as unidirectional stiffening patches, would be employed to adjust the frequency response of the stators. The aerodynamic stator configuration of the full size stator would not be changed by utilizing stiffening methods in the scaled vehicle. The torsional stabilities are shown in Figure 84. More detailed analysis of the scaled stator vanes will be performed during the final mechanical design phase.

SECTION VI

PERFORMANCE ANALYSIS

A. Off-Design Calculation Procedure

Performance map predictions were generated for the front block and rear block fans using a bladerow, pitchline calculation procedure. The procedure uses as input the design point average velocity diagram information for each blade row along with the inlet flow and applies an incidence angle-loss coefficient correlation to predict the off-design performance. The total loss coefficient is a summation of the losses attributed to off-design incidence angles, shock and Mach number effects and the two dimensional cascade diffusion. Inlet guide vanes are treated separately with the loss coefficient being a function of the amount of cascade turning. The procedure solves the continuity and energy equations and then stacks the performance of each blade row to give an overall fan performance. Performance data calculations were specified at several points along the speedline from near stall to near choke. Speedlines at 60, 70, 80, 85, 90, 95, 100 and 105 percent of design speed were selected to adequately define the performance map.

B. Flowpath Mach Number Distribution

The AST fan flowpath wall contours, as reflected in the fan cross-sections (Figures 36 and 37), were chosen after careful study of the duct Mach number distributions. The circumferential-average flow calculations were carried out at cycle conditions which included the extremes of bypass flow operation. The front block fan design point was selected at a flow and speed slightly less than the take-off condition. At this cycle point, a substantial part of the front block airflow (35.5%) bypasses the rear block fan and hence, it is necessary to close the rear block inlet guide vanes (IGV2) to reduce its pumping capacity at the relatively high core corrected speed. The meridional Mach numbers along the flowpath wall for the design point of the front block fan are shown in Figure 85 plotted versus the axial stations of the fan cross-section, as shown. The Mach number distributions are labeled, referring to the numbered flowpath contours.

The design point of the rear block fan corresponds to a high engine specific thrust condition such as the climb/acceleration and supersonic cruise phases of the mission. This point was chosen to represent the other extreme of bypass operation where no flow passes through the outer bypass duct. At this condition, the front block airflow is reduced by closing the front block, inlet guide vanes (IGV1) and the outer bypass duct thus forcing all of the airflow through the rear block fan. Here, the outer bypass ratio is virtually zero (0.005) and the inner bypass ratio is 0.340. The inlet total fan flow is 312 kg/sec (687 lbm/sec); the rear block corrected airflow is 139.7 kg/sec (308 lbm/sec). The meridional Mach number distribution, along the flowpath walls, at this condition is shown in Figure 86. The outer duct Mach number

is approximately zero as nearly all the flow enters the rear block fan. A small amount of flow in the outer bypass duct was necessary for an accurate, numerical solution to the circumferential-average flow calculation. Part of the rear block flow is then bypassed out the inner duct with the remaining flow satisfying the core corrected speed-flow requirements.

C. Front Block Fan Maps

The predicted performance maps for the front block fan are shown in Figures 87 and 88. The maps represent two differenct speed-flow relationships which are compared in Figure 89. The predicted performance with the inlet guide vane (IGV) and stator 1 fixed at their design settings is shown in Figure 87. The variable stator performance is shown in Figure 88. The IGV and Stator 1 settings shown in Figure 90 as a function of speed were selected to match the AST engine cycle data provided at the beginning of this program.

The stall line at design speed is consistent with the 20 percent margin required by the stability margin stack-up. At part speed, the stall line occurring with the variable stator schedule is consistent with test experience of fans with well-matched stages. The predicted stall lines on the two maps differ significantly at part speed conditions where the influence of the closed guide vane relieves the loading on the first stage and delays the point of stall. At 55 percent design flow, the variable geometry map indicates an increase of approximately 14 percentage points in stall margin.

The peak efficiency on the map is also affected by the stator schedule and shows that a higher efficiency potential can be achieved when the stages are optimally matched at their peak performance.

D. Rear Block Fan Maps

Performance maps were generated for the rear block fan with the inlet guide vane fixed at its design setting and also closed 15, 30 and 45 degrees from design. The design IGV setting performance map is shown in Figure 91. The maps where the IGV is closed the same amount at all speeds is shown in Figures 92-94.

The stall line with the IGV at the design setting takes into account the requirements of the stability margin stack-up at all speeds. At 100 percent corrected speed, the stall margin is 22 percent.

The efficiency contours on the maps in Figures 92-94 reflect the additional losses encountered when the IGV is closed a marked amount from design. For the closed-down IGV operating conditions, such as take-off and subsonic cruise, the fan rotor is aerodynamically unloaded and the stall margin is increased.

SECTION VII

CONCLUSIONS AND RECOMMENDATIONS

The parametric screening study effort identified a number of factors leading to a near optimum AST fan configuration. The factors which show a higher fan efficiency potential are:

1. Lower tip speeds resulting in lower Mach numbers and lower shock losses.

2. Lower inlet specific flow rates which reduce the through-flow Mach numbers.

3. Low inlet radius ratios providing a larger increase in radius across the first rotor hub.

4. The constant tip flowpath designs provided a larger increase in hub radius through the first rotor and an increased blade speed of the second stage relative to the first. These features permitted achieving the required stall margin with lower first stage design tip speeds and with reduced RPM.

The impact of the low pressure turbine and engine weight considerations led to the following conclusions:

1. The lower rpm cases showed lower LP turbine efficiencies, but also indicated less cooling flow required and lower LPT weight.

2. The lowest fan blading aspect ratio case indicated a considerable increase in fan weight.

3. The lower radius ratio cases with constant tip flowpaths showed a trend of improved fan efficiency, reduced weight and subsequently an increased engine aircraft range.

A two-stage constant tip, front block fan with an inlet radius ratio of 0.40 and an inlet specific flow rate of 205 kg/sec m^2 (42 lbm/sec ft^2) was identified from the screening study and recommended for further development.

The detailed aerodynamic design of this front block fan as well as a single stage rear block fan was carried out in the full engine size. A preliminary mechanical design of the front block fan was also carried out. The mechanical design analysis identified the first stage rotor of the scaled component fan as a titanium BLISK (integral blade and disk) configuration. The full size fan would have boron-aluminum blading and hollow titanium stator vanes.

It is recommended that a follow-on program be conducted for the detailed mechanical design, assembly and rig test of a scale model of the front block fan.

APPENDIX A

FAN FLOWPATH COORDINATES

APPENDIX A.

AST FRONT AND REAR BLOCK FAN

FLOWPATH COORDINATES (CENTIMETERS)

Radius Outer	Radius Inner	Axial Dist. Outer	Axial Dist. Inner	Station Description
84.836	0	-88.9	-88.9	
84.836	18.857	-50.8	-50.8	
84.788	24.602	-38.11	-30.254	
84.384	26.937	-25.989	-17.782	
83.977	27.91	-17.793	-13.459	
83.505	29.141	- 9.624	- 8.893	
83.035	30.752	- 2.070	- 4.559	
82.906	33.162	6.579	0	Rotor 1 L.E.
82.906	34.714	7.948	2.619	
82.906	36.213	9.317	5.235	
82.906	37.767	10.686	7.849	
82.906	39.411	12.055	10.465	
82.906	41.115	13.424	13.081	
82.906	42.837	14.793	15.70	
82.906	44.534	16.162	18.316	
82.906	46.17	17.531	20.932	
82.906	47.711	18.90	23.548	
82.906	49.139	20.269	26.165	Rotor 1 T.E.
82.906	50.391	26.965	28.9	Stator 1 L.E.
82.906	51.171	29.53	30.691	
82.906	51.976	32.095	32.482	
82.906	52.804	34.661	34.272	
82.906	53.619	37.226	36.065	
82.906	54.399	39.792	37.856	Stator 1 T.E.
82.784	55.781	44.097	41.456	Rotor 2 L.E.
82.735	56.264	44.922	42.824	
82.69	56.744	45.748	44.186	
82.644	57.272	46.573	45.545	
82.601	57.798	47.399	48.265	
82.56	58.334	48.224	48.265	
82.52	58.898	49.05	49.627	

Radius Outer	Radius Inner	Axial Dist. Outer	Axial Dist. Inner	Station Description
82.484	59.472	49.182	50.985	
82.448	60.061	50.701	52.347	
82.413	60.665	51.526	53.708	
82.38	61.267	52.352	55.067	Rotor 2 T.E.
82.266	61.770	55.578	56.416	Stator 2 L.E.
82.202	62.260	57.569	58.072	
82.139	62.624	59.560	59.728	
82.075	62.865	61.552	61.382	
82.004	62.964	63.541	63.038	
81.912	62.997	65.532	64.694	Stator 2 T.E.
81.694	62.588	68.58	68.58	
80.963	61.308	73.66	73.66	
80.091	59.24	78.74	78.74	
80.091	56.482	83.82	83.82	
73.182	52.134	91.44	91.44	
70.16	49.362	96.52	96.52	
68.583	47.335	100.33	100.33	IGV2 Strut L.E.
67.485	45.712	103.505	103.505	
66.515	45.832	106.68	106.68	
65.606	42.931	109.982	109.982	
64.320	41.976	115.301	113.543	IGV2 Flap T.E.
63.607	41.686	118.816	117.858	Core Driven Fan L.E.
63.348	41.905	120.305	119.85	
63.119	42.263	121.951	121.841	
62.926	42.682	123.284	123.833	
62.776	43.076	124.772	125.824	
62.677	43.383	126.71	127.815	Core Driven Fan T.E.
63.388	43.561	134.62	134.62	
58.169	43.561	141.1	141.778	IGV L.E.
57.125	43.561	146.558	145.928	IGV T.E.
56.878	43.561	148.333	147.323	R1 L.E.
56.385	43.823	152.781	153.957	R1 T.E.
65.202	60.688	139.819	141.074	Inner Bypass Duct
67.61	63.109	144.490	145.687	
71.598	66.098	151.089	152.613	
81.136	75.024	90.223	91.45	Outer Bypass Duct
82.316	75.613	93.271	94.242	
82.857	75.618	99.06	99.06	
83.124	74.61	116.84	116.84	
82.794	73.066	149.86	149.86	

APPENDIX A.

AST FRONT AND REAR BLOCK FAN

FLOWPATH COORDINATES (INCHES)

Radius Outer	Radius Inner	Axial Dist. Outer	Axial Dist. Inner	Station Description
33.40	0.00	-35.0	-35.0	
33.40	7.424	-20.0	-20.0	
33.381	9.686	-15.004	-11.911	IGV Strut L.E.
33.222	10.605	-10.323	- 7.001	
33.062	10.988	- 7.005	- 5.299	
32.876	11.473	- 3.789	- 3.501	
32.691	12.107	- 0.815	- 1.795	IGV Flap T.E.
32.64	13.056	2.59	0.00	Rotor 1 L.E.
32.64	13.667	3.129	1.031	
32.64	14.257	3.668	2.061	
32.64	14.869	4.207	3.090	
32.64	15.516	4.746	4.120	
32.64	16.187	5.285	5.150	
32.64	16.865	5.824	6.181	
32.64	17.533	6.363	7.211	
32.64	18.177	6.902	8.241	
32.64	18.784	7.441	9.271	
32.64	19.346	7.980	10.301	Rotor 1 T.E.
32.64	19.839	10.616	11.378	Stator 1 L.E.
32.64	20.146	11.626	12.083	
32.64	20.463	12.636	12.788	
32.64	20.789	13.646	13.493	
32.64	21.111	14.656	14.199	
32.64	21.417	15.666	14.904	Stator 1 T.E.
32.592	21.961	17.361	16.325	Rotor 2 L.E.
32.573	22.151	17.686	16.860	
32.555	22.346	18.011	17.396	
32.537	22.548	18.336	17.931	
32.52	22.755	18.661	18.467	
32.504	22.966	18.986	19.002	
32.488	23.188	19.311	19.538	
32.474	23.414	19.363	20.073	

Radius Outer	Radius Inner	Axial Dist. Outer	Axial Dist. Inner	Station Description
32.46	23.646	19.961	20.609	
32.446	23.884	20.286	21.145	
32.433	24.121	20.611	21.680	Rotor 2 T.E.
32.388	24.319	21.881	22.211	Stator 2 L.E.
32.363	24.512	22.665	22.863	
32.338	24.655	23.449	23.515	
32.313	24.750	24.233	24.166	
32.285	24.789	25.016	24.818	
32.249	24.802	25.80	25.47	Stator 2 T.E.
32.163	24.641	27.0	27.0	
31.875	24.137	29.0	29.0	
31.532	23.323	31.0	31.0	
31.532	22.237	33.0	33.0	
28.812	20.525	36.0	36.0	
27.622	19.434	38.0	38.0	
27.001	18.636	39.5	39.5	IGV2 Strut L.E.
26.569	17.997	40.75	40.75	
26.187	18.044	42.0	42.0	
25.829	16.902	43.3	43.3	
25.323	16.526	45.394	44.702	IGV2 Flap T.E.
25.042	16.412	46.778	46.401	Core Driven Fan L.E.
24.94	16.498	47.364	47.185	
24.85	16.639	47.951	47.969	
24.774	16.804	48.537	48.753	
24.715	16.959	49.123	49.537	
24.676	17.080	49.710	50.321	Core Driven Fan T.E.
24.956	17.150	53.0	53.0	
22.901	17.150	55.551	55.818	Core IGV L.E.
22.49	17.150	57.7	57.452	Core IGV T.E.
22.393	17.150	58.399	58.001	Core R1 L.E.
22.199	17.261	60.150	60.613	Core R1 T.E.
25.67	23.893	55.047	55.541	
25.618	24.846	56.886	57.357	Inner Bypass Duct
28.188	26.023	59.484	60.084	
32.136	29.537	35.521	36.004	
32.408	29.769	36.721	37.103	
32.621	29.771	39.0	39.0	Outer Bypass Duct
32.726	29.374	46.0	46.0	
32.596	28.766	59.0	59.0	

APPENDIX B 1

CIRCUMFERENTIAL - AVERAGE FLOW SOLUTION FOR FRONT BLOCK FAN DESIGN POINT

NOMENCLATURE FOR APPENDIX B

PCT IMM	Percent Immersion from O.D.
RADIUS	Inlet and Exit Radii ~ cm(in.)
MERID ANGLE	Inlet and Exit Slope ~ degrees
STREAM FUNCT	Inlet and Exit Streamline Percent Flow from O.D.
ABS ANGLE	Inlet and Exit Absolute Air Angle ~ degrees
REL ANGLE	Inlet and Exit Relative Air Angle ~ degrees
ABS VEL	Inlet and Exit Absolute Velocity ~ m/sec (ft/sec)
REL VEL	Inlet and Exit Relative Velocity ~ m/sec (ft/sec)
MERID VEL	Inlet and Exit Meridional Velocity ~ m/sec (ft/sec)
TANG VEL	Inlet and Exit Tangential Velocity ~ m/sec (ft/sec)
BLADE SPEED	Inlet and Exit Blade Speed ~ m/sec (ft/sec)
ABS MACH NO	Inlet and Exit Absolute Mach Number
REL MACH NO	Inlet and Exit Relative Mach Number
AXIAL VEL R	Inlet and Exit Axial Velocity Ratio ~ Exit/Inlet
CH'	Static Pressure-Rise Coefficient
ACC PT RATIO	Accumulative Total Pressure Ratio
ACC TT RATIO	Accumulative Total Temperature Ratio
EFFICIENCY ADIA	Accumulative Adiabatic Efficiency
EFFICIENCY POLY	Accumulative Polytropic Efficiency
RBAR	Average Radius ~ cm (in.)
INC	Incidence Angle - degrees
DEV (C-R)	Carter's Rule Deviation Angle ~ degrees
XFACT	Empirical Adjustment Factor ~ degrees
TMC	Max Thickness-To-Chord Ratio
CAM	Camber Angle - degrees
STGR	Stagger Angle - degrees
TURN	Turning Angle - degrees
D-FACT	Diffusion Factor
SOL	Solidity
LOSS COEFF	Total-Pressure Loss Coefficient
INLET CORR	Fan Inlet Corrected Weight Flow ~ kg/sec (lbm/sec)
PRESS RATIO	Accumulative Average Total-Pressure Ratio
TEMP RATIO	Accumulative Average Total Temperature Ratio
ADIA EFF	Accumulative Average Adiabatic Efficiency
INLET CORR RPM	Fan Inlet Corrected Revolutions per Minute

BLADE ROW PRINTOUT (METRIC)

IGVF

PCT IMM	RADIUS IN	RADIUS OUT	MERID ANGLE IN	MERID ANGLE OUT	STREAM FUNCT IN	STREAM FUNCT OUT	ABS ANGLE IN	ABS ANGLE OUT	REL ANGLE IN	REL ANGLE OUT
0.	84.384	83.035	-2.6	-3.6	0.	0.	0.	0.		
3.5	82.317	81.303	-2.0	-1.6	0.050	0.050	0.	0.		
6.9	80.250	79.553	-1.4	-0.9	0.100	0.100	0.	0.		
14.0	76.066	75.958	-0.4	0.6	0.200	0.200	0.	0.		
21.4	71.767	72.206	0.7	2.1	0.300	0.300	0.	0.		
25.5	69.329	70.060	1.4	3.0	0.355	0.355	0.	0.		
25.5	69.329	70.060	1.4	3.0	0.355	0.355	0.	0.		
29.1	67.283	68.252	1.9	3.8	0.400	0.400	0.	0.		
37.3	62.513	64.018	3.2	5.7	0.500	0.500	0.	0.		
46.2	57.346	59.409	4.7	8.0	0.600	0.600	0.	0.		
56.1	51.635	54.276	6.4	10.8	0.700	0.700	0.	0.		
73.9	41.424	44.955	9.4	16.1	0.850	0.850	0.	0.		
89.6	32.597	36.552	11.3	21.7	0.950	0.950	0.	0.		
100.0	26.937	30.752	12.3	23.8	1.000	1.000	0.	0.		

PCT IMM	ABS VEL IN	ABS VEL OUT	REL VEL IN	REL VEL OUT	MERID VEL IN	MERID VEL OUT	TANG VEL IN	TANG VEL OUT	BLADE SPEED IN	BLADE SPEED OUT
0.	162.1	227.7			162.1	227.7	0.	0.		
3.5	166.2	229.8			166.2	229.8	0.	0.		
6.9	169.7	229.8			169.7	229.8	0.	0.		
14.0	174.8	229.4			174.8	229.4	0.	0.		
21.4	178.5	228.6			178.5	228.6	0.	0.		
25.5	179.8	227.8			179.8	227.8	0.	0.		
25.5	179.8	227.8			179.8	227.8	0.	0.		
29.1	180.4	226.8			180.4	226.8	0.	0.		
37.3	180.3	223.0			180.3	223.0	0.	0.		
46.2	179.1	217.7			179.1	217.7	0.	0.		
56.1	176.9	209.8			176.9	209.8	0.	0.		
73.9	170.2	192.8			170.2	192.8	0.	0.		
89.6	162.9	169.0			162.9	169.0	0.	0.		
100.0	157.4	146.4			157.4	146.4	0.	0.		

PCT IMM	ABS MACH NO IN	ABS MACH NO OUT	REL MACH NO IN	REL MACH NO OUT	AXIAL VEL R	CHI	ACC PT RATIO	ACC TT RATIO	EFFICIENCY ADIA	EFFICIENCY POLY
0.	0.487	0.701			1.403	-1.072	0.9827	1.0000		
3.5	0.500	0.708			1.383	-0.983	0.9869	1.0000		
6.9	0.511	0.708			1.354	-0.895	0.9884	1.0000		
14.0	0.528	0.707			1.312	-0.770	0.9901	1.0000		
21.4	0.539	0.704			1.280	-0.684	0.9908	1.0000		
25.5	0.543	0.701			1.266	-0.646	0.9913	1.0000		
25.5	0.543	0.701			1.266	-0.646	0.9913	1.0000		
29.1	0.545	0.698			1.255	-0.620	0.9918	1.0000		
37.3	0.545	0.685			1.233	-0.568	0.9919	1.0000		
46.2	0.541	0.667			1.208	-0.513	0.9924	1.0000		
56.1	0.534	0.641			1.173	-0.443	0.9928	1.0000		
73.9	0.513	0.585			1.103	-0.317	0.9936	1.0000		
89.6	0.490	0.509			0.983	-0.119	0.9929	1.0000		
100.0	0.472	0.438			0.871	0.085	0.9922	1.0000		

RBAR	INC (INPUT	DEV (C-R)	X-FACT	CAM	STGR	TURN	D-FACT	SOL	LOSS COEFF
83.710	0.	0.	0.	0.	0.	0.	-0.405	0.728	0.115
81.810	0.	0.	0.	0.	0.	0.	-0.383	0.742	0.083
79.901	0.	0.	0.	0.	0.	0.	-0.354	0.756	0.071
76.012	0.	0.	0.	0.	0.	0.	-0.312	0.782	0.057
71.986	0.	0.	0.	0.	0.	0.	-0.281	0.814	0.051
69.695	0.	0.	0.	0.	0.	0.	-0.267	0.830	0.048
69.695	0.	0.	0.	0.	0.	0.	-0.267	0.830	0.048
67.767	0.	0.	0.	0.	0.	0.	-0.257	0.843	0.045
63.265	0.	0.	0.	0.	0.	0.	-0.237	0.877	0.044
58.377	0.	0.	0.	0.	0.	0.	-0.215	0.909	0.042
52.956	0.	0.	0.	0.	0.	0.	-0.186	0.947	0.041
43.190	0.	0.	0.	0.	0.	0.	-0.133	1.016	0.039
34.574	0.	0.	0.	0.	0.	0.	-0.038	1.078	0.047
28.844	0.	0.	0.	0.	0.	0.	0.070	1.120	0.055

INLET CORR WTFLOW	PRESS RATIO	TEMP RATIO	ADIA EFF	INLET CORR RPM
371.83	0.9914	1.0000		5378.5

BLADE ROW PRINTOUT (ENGLISH)

IGVF

PCT IMM	RADIUS IN	RADIUS OUT	MERID ANGLE IN	MERID ANGLE OUT	STREAM FUNCT IN	STREAM FUNCT OUT	ABS ANGLE IN	ABS ANGLE OUT	REL ANGLE IN	REL ANGLE OUT
0.	33.222	32.691	-2.6	-3.6	0.	0.	0.	0.		
3.5	32.408	32.009	-2.0	-1.6	0.050	0.050	0.	0.		
6.9	31.594	31.320	-1.4	-0.9	0.100	0.100	0.	0.		
14.0	29.947	29.905	-0.4	0.6	0.200	0.200	0.	0.		
21.4	28.255	28.428	0.7	2.1	0.300	0.300	0.	0.		
25.5	27.295	27.583	1.4	3.0	0.355	0.355	0.	0.		
25.5	27.295	27.583	1.4	3.0	0.355	0.355	0.	0.		
29.1	26.489	26.871	1.9	3.8	0.400	0.400	0.	0.		
37.3	24.611	25.204	3.2	5.7	0.500	0.500	0.	0.		
46.2	22.577	23.389	4.7	8.0	0.600	0.600	0.	0.		
56.1	20.329	21.368	6.4	10.8	0.700	0.700	0.	0.		
73.9	16.309	17.699	9.4	16.1	0.850	0.850	0.	0.		
89.6	12.833	14.391	11.3	21.7	0.950	0.950	0.	0.		
100.0	10.605	12.107	12.3	23.8	1.000	1.000	0.	0.		

PCT IMM	ABS VEL IN	ABS VEL OUT	REL VEL IN	REL VEL OUT	MERID VEL IN	MERID VEL OUT	TANG VEL IN	TANG VEL OUT	BLADE SPEED IN	BLADE SPEED OUT
0.	531.9	747.1			531.9	747.1	0.	0.		
3.5	545.4	754.1			545.4	754.1	0.	0.		
6.9	556.7	753.8			556.7	753.8	0.	0.		
14.0	573.6	752.7			573.6	752.7	0.	0.		
21.4	585.6	749.9			585.6	749.9	0.	0.		
25.5	589.8	747.4			589.8	747.4	0.	0.		
25.5	589.8	747.4			589.8	747.4	0.	0.		
29.1	591.7	744.1			591.7	744.1	0.	0.		
37.3	591.4	731.6			591.4	731.6	0.	0.		
46.2	587.7	714.3			587.7	714.3	0.	0.		
56.1	580.3	688.4			580.3	688.4	0.	0.		
73.9	558.5	632.6			558.5	632.6	0.	0.		
89.6	534.4	554.5			534.4	554.5	0.	0.		
100.0	516.4	480.3			516.4	480.3	0.	0.		

PCT IMM	ABS MACH NO IN	ABS MACH NO OUT	REL MACH NO IN	REL MACH NO OUT	AXIAL VEL R	CH'	ACC PT RATIO	ACC TT RATIO	EFFICIENCY ADIA	EFFICIENCY POLY
0.	0.487	0.701			1.403	-1.072	0.9827	1.0000		
3.5	0.500	0.708			1.383	-0.983	0.9869	1.0000		
6.9	0.511	0.708			1.354	-0.895	0.9884	1.0000		
14.0	0.528	0.707			1.312	-0.770	0.9901	1.0000		
21.4	0.539	0.704			1.280	-0.684	0.9908	1.0000		
25.5	0.543	0.701			1.266	-0.646	0.9913	1.0000		
25.5	0.543	0.701			1.266	-0.646	0.9913	1.0000		
29.1	0.545	0.698			1.255	-0.620	0.9918	1.0000		
37.3	0.545	0.685			1.233	-0.568	0.9919	1.0000		
46.2	0.541	0.667			1.208	-0.513	0.9924	1.0000		
56.1	0.534	0.641			1.173	-0.443	0.9928	1.0000		
73.9	0.513	0.585			1.103	-0.317	0.9936	1.0000		
89.6	0.490	0.509			0.983	-0.119	0.9929	1.0000		
100.0	0.472	0.438			0.871	0.085	0.9922	1.0000		

RBAR	INC (INPUT	DEV (C-R)	X-FACT	CAM	STGR	TURN	D-FACT	SOL	LOSS COEFF
32.956	0.	0.	0.	0.	0.	0.	-0.405	0.728	0.115
32.209	0.	0.	0.	0.	0.	0.	-0.383	0.742	0.083
31.457	0.	0.	0.	0.	0.	0.	-0.354	0.756	0.071
29.926	0.	0.	0.	0.	0.	0.	-0.312	0.782	0.057
28.341	0.	0.	0.	0.	0.	0.	-0.281	0.814	0.051
27.439	0.	0.	0.	0.	0.	0.	-0.267	0.830	0.048
27.439	0.	0.	0.	0.	0.	0.	-0.267	0.830	0.048
26.680	0.	0.	0.	0.	0.	0.	-0.257	0.843	0.045
24.908	0.	0.	0.	0.	0.	0.	-0.237	0.877	0.044
22.983	0.	0.	0.	0.	0.	0.	-0.215	0.909	0.042
20.849	0.	0.	0.	0.	0.	0.	-0.186	0.947	0.041
17.004	0.	0.	0.	0.	0.	0.	-0.133	1.016	0.039
13.612	0.	0.	0.	0.	0.	0.	-0.038	1.078	0.047
11.356	0.	0.	0.	0.	0.	0.	0.070	1.120	0.055

INLET CORR WTFLOW	PRESS RATIO	TEMP RATIO	ADIA EFF	INLET CORR RPM
	0.9914	1.0000		5378.5

BLADE ROW PRINTOUT (METRIC)

R1

PCT IMM	RADIUS IN	RADIUS OUT	MERID ANGLE IN	MERID ANGLE OUT	STREAM FUNCT IN	STREAM FUNCT OUT	ABS ANGLE IN	ABS ANGLE OUT	REL ANGLE IN	REL ANGLE OUT
0.	82.906	82.906	0.	0.	0.	0.	0.	49.1	62.1	63.0
3.9	81.236	81.318	0.1	0.7	0.050	0.050	0.	46.6	61.2	61.6
7.8	79.555	79.779	0.5	1.5	0.100	0.100	0.	45.0	60.4	60.4
15.5	76.128	76.760	1.7	3.3	0.200	0.200	0.	43.1	58.8	58.1
23.3	72.575	73.758	3.4	5.0	0.300	0.300	0.	42.1	57.3	55.7
27.7	70.552	72.092	4.6	5.9	0.355	0.355	0.	42.0	56.5	54.2
27.7	70.552	72.092	4.6	5.9	0.355	0.355	0.	42.0	56.5	54.2
31.4	68.852	70.710	5.6	6.7	0.400	0.400	0.	42.2	55.9	52.9
40.0	64.883	67.545	7.9	8.6	0.500	0.500	0.	43.2	54.9	49.7
49.1	60.575	64.268	10.5	10.9	0.600	0.600	0.	44.7	54.1	44.6
58.8	55.782	60.887	13.5	13.6	0.700	0.700	0.	46.3	53.2	38.4
76.0	46.969	55.370	19.9	18.6	0.850	0.850	0.	49.2	52.7	25.4
90.5	38.945	51.296	25.4	23.4	0.950	0.950	0.	51.2	51.9	13.2
100.0	33.162	49.140	31.9	26.7	1.000	1.000	0.	51.7	54.5	6.2

PCT IMM	ABS VEL IN	ABS VEL OUT	REL VEL IN	REL VEL OUT	MERID VEL IN	MERID VEL OUT	TANG VEL IN	TANG VEL OUT	BLADE SPEED IN	BLADE SPEED OUT
0.	246.8	228.6	528.1	330.0	246.8	149.6	0.	172.9	467.0	467.0
3.9	251.6	229.5	522.2	331.1	251.6	157.6	0.	166.8	457.5	458.0
7.8	254.7	230.5	515.4	329.4	254.7	162.9	0.	163.1	448.1	449.3
15.5	259.6	233.1	501.2	322.1	259.6	170.5	0.	159.0	428.8	432.3
23.3	263.0	236.7	486.1	311.7	263.0	176.0	0.	158.2	408.8	415.4
27.7	263.9	239.4	477.0	304.2	263.9	178.5	0.	159.7	397.4	406.0
27.7	263.9	239.4	477.0	304.2	263.9	178.5	0.	159.7	397.4	406.0
31.4	263.6	242.2	468.9	297.1	263.6	180.1	0.	161.9	387.8	398.3
40.0	259.2	247.9	448.0	278.9	259.2	181.6	0.	168.8	365.4	380.4
49.1	251.2	260.3	423.7	259.7	251.2	186.7	0.	181.4	341.2	362.0
58.8	241.6	273.6	396.3	242.2	241.6	191.9	0.	195.1	314.2	342.9
76.0	214.7	299.2	340.7	221.0	214.7	201.5	0.	221.1	264.5	311.9
90.5	190.6	323.1	290.6	217.6	190.6	212.7	0.	243.2	219.4	288.9
100.0	157.3	340.6	244.2	226.8	157.3	225.8	0.	255.0	186.8	276.8

PCT IMM	ABS MACH NO IN	ABS MACH NO OUT	REL MACH NO IN	REL MACH NO OUT	AXIAL VEL R	CH'	ACC PT RATIO	ACC TT RATIO	EFFICIENCY ADIA	EFFICIENCY POLY
0.	0.766	0.616	1.640	0.890	0.606	0.496	1.9703	1.2788	0.767	0.788
3.9	0.783	0.623	1.625	0.898	0.626	0.504	1.9574	1.2640	0.802	0.819
7.8	0.794	0.629	1.607	0.898	0.640	0.512	1.9467	1.2532	0.828	0.844
15.5	0.811	0.641	1.566	0.885	0.656	0.529	1.9313	1.2376	0.871	0.883
23.3	0.823	0.654	1.522	0.861	0.668	0.546	1.9210	1.2272	0.903	0.912
27.7	0.826	0.663	1.494	0.843	0.675	0.555	1.9188	1.2241	0.914	0.922
27.7	0.826	0.663	1.494	0.843	0.675	0.555	1.9188	1.2241	0.914	0.922
31.4	0.826	0.672	1.468	0.824	0.682	0.562	1.9194	1.2229	0.919	0.926
40.0	0.810	0.690	1.400	0.776	0.699	0.574	1.9176	1.2220	0.922	0.929
49.1	0.782	0.726	1.318	0.724	0.742	0.578	1.9397	1.2270	0.919	0.926
58.8	0.748	0.766	1.228	0.678	0.794	0.569	1.9548	1.2312	0.914	0.921
76.0	0.657	0.844	1.043	0.624	0.946	0.491	1.9809	1.2384	0.905	0.914
90.5	0.578	0.921	0.882	0.620	1.134	0.317	2.0021	1.2428	0.904	0.913
100.0	0.472	0.979	0.733	0.652	1.511	-0.025	2.0122	1.2440	0.907	0.916

RBAR	INC (INPUT)	DEV (C-A)	X-FACT	TMC	CAM	STGR	TURN	D-FACT	SOL	LOSS COEFF.
82.906	3.00	3.72	0.20	0.0250	-0.17	59.23	-0.89	0.484	1.500	0.195
81.277	3.14	3.63	0.25	0.0253	0.11	58.00	-0.38	0.471	1.521	0.163
79.667	3.20	3.78	0.40	0.0259	0.61	56.89	0.02	0.464	1.541	0.139
76.444	3.52	3.80	0.45	0.0274	1.01	54.79	0.73	0.459	1.582	0.100
73.167	3.98	1.98	1.00	0.0304	2.27	52.27	1.37	0.460	1.628	0.073
71.322	4.20	4.64	1.00	0.0333	2.71	50.94	2.26	0.464	1.657	0.065
71.322	4.20	4.64	1.00	0.0333	2.71	50.94	2.26	0.464	1.657	0.065
69.741	4.47	4.98	1.10	0.0370	3.14	49.73	3.03	0.470	1.682	0.062
66.264	5.42	5.40	1.30	0.0509	5.20	46.80	5.22	0.488	1.745	0.063
62.421	6.03	6.64	1.70	0.0447	10.13	42.99	9.54	0.508	1.822	0.073
58.335	6.32	9.74	2.50	0.0771	17.22	34.23	11.80	0.532	1.914	0.089
51.170	6.68	12.11	2.50	0.0794	32.93	22.64	27.21	0.515	2.146	0.130
45.121	5.29	14.61	1.20	0.0858	47.80	22.32	38.09	0.448	2.411	0.175
41.151	5.90	16.72	1.10	0.0900	60.03	19.44	44.30	0.397	2.643	0.230

INLET CORR MFLOW	PRESS RATIO	T-TP RATIO	ADIA EFF	INLET CORR RPM
371.43	1.2481	1.2356	0.921	5378.5

BLADE ROW PRINTOUT (ENGLISH)

R1

PCT IMM	RADIUS IN	RADIUS OUT	MERID ANGLE IN	MERID ANGLE OUT	STREAM FUNCT IN	STREAM FUNCT OUT	ABS ANGLE IN	ABS ANGLE OUT	REL ANGLE IN	REL ANGLE OUT
0.	32.640	32.640	0.	0.	0.	0.	0.	49.1	62.1	63.0
3.9	31.982	32.015	0.1	0.7	0.050	0.050	0.	46.6	61.2	61.6
7.8	31.321	31.409	0.5	1.5	0.100	0.100	0.	45.0	60.4	60.4
15.5	29.971	30.221	1.7	3.3	0.200	0.200	0.	43.1	58.8	58.1
23.3	28.573	29.038	3.4	5.0	0.300	0.300	0.	42.1	57.3	55.7
27.7	27.776	28.383	4.6	5.9	0.355	0.355	0.	42.0	56.5	54.2
27.7	27.776	28.383	4.6	5.9	0.355	0.355	0.	42.0	56.5	54.2
31.4	27.107	27.838	5.6	6.7	0.400	0.400	0.	42.2	55.9	52.9
40.0	25.544	26.593	7.9	8.6	0.500	0.500	0.	43.2	54.9	49.7
49.1	23.848	25.302	10.5	10.9	0.600	0.600	0.	44.7	54.1	44.6
58.8	21.962	23.971	13.5	13.6	0.700	0.700	0.	46.3	53.2	38.4
76.0	18.492	21.799	19.9	18.6	0.850	0.850	0.	49.2	52.7	25.4
90.5	15.333	20.195	25.4	23.4	0.950	0.950	0.	51.2	51.9	13.2
100.0	13.056	19.346	31.9	26.7	1.000	1.000	0.	51.7	54.5	6.2

PCT IMM	ABS VEL IN	ABS VEL OUT	REL VEL IN	REL VEL OUT	MERID VEL IN	MERID VEL OUT	TANG VEL IN	TANG VEL OUT	BLADE SPEED IN	BLADE SPEED OUT
0.	809.6	750.1	1732.8	1082.6	809.6	490.9	0.	567.1	1532.0	1532.0
3.9	825.4	753.0	1713.1	1086.3	825.4	517.1	0.	547.3	1501.1	1502.7
7.8	835.5	756.2	1690.9	1080.7	835.5	534.5	0.	535.0	1470.1	1474.2
15.5	851.7	764.8	1644.5	1056.9	851.7	559.3	0.	521.6	1406.7	1418.4
23.3	863.0	776.5	1594.8	1022.7	863.0	577.6	0.	519.0	1341.1	1363.0
27.7	865.8	785.6	1565.0	998.1	865.8	585.5	0.	523.8	1303.7	1332.2
27.7	865.8	785.6	1565.0	998.1	865.8	585.5	0.	523.8	1303.7	1332.2
31.4	865.0	794.5	1538.5	974.8	865.0	590.8	0.	531.3	1272.3	1306.6
40.0	850.4	813.4	1469.9	915.0	850.4	595.8	0.	553.7	1199.0	1248.2
49.1	824.0	853.9	1389.9	852.1	824.0	612.4	0.	595.2	1119.3	1187.6
58.8	792.5	897.6	1300.2	794.7	792.5	629.4	0.	640.0	1030.8	1125.1
76.0	704.3	981.5	1117.7	725.0	704.3	661.0	0.	725.5	867.9	1023.2
90.5	625.2	1059.9	953.3	713.9	625.2	697.9	0.	797.7	719.7	947.9
100.0	515.9	1117.5	801.1	744.1	515.9	740.7	0.	836.7	612.8	908.0

PCT IMM	ABS MACH NO IN	ABS MACH NO OUT	REL MACH NO IN	REL MACH NO OUT	AXIAL VEL R	CH*	ACC PT RATIO	ACC TT RATIO	EFFICIENCY ADIA	EFFICIENCY POLY
0.	0.766	0.616	1.640	0.890	0.606	0.496	1.9703	1.2788	0.767	0.788
3.9	0.783	0.623	1.625	0.898	0.626	0.504	1.9574	1.2640	0.802	0.819
7.8	0.794	0.629	1.607	0.898	0.640	0.512	1.9467	1.2532	0.828	0.844
15.5	0.811	0.641	1.566	0.885	0.656	0.529	1.9313	1.2376	0.871	0.883
23.3	0.823	0.654	1.522	0.861	0.668	0.546	1.9210	1.2272	0.903	0.912
27.7	0.826	0.663	1.494	0.843	0.675	0.555	1.9188	1.2241	0.914	0.922
27.7	0.826	0.663	1.494	0.843	0.675	0.555	1.9188	1.2241	0.914	0.922
31.4	0.826	0.672	1.468	0.824	0.682	0.562	1.9194	1.2229	0.919	0.926
40.0	0.810	0.690	1.400	0.776	0.699	0.574	1.9176	1.2220	0.922	0.929
49.1	0.782	0.726	1.318	0.724	0.742	0.578	1.9397	1.2270	0.919	0.926
58.8	0.748	0.766	1.228	0.678	0.794	0.569	1.9548	1.2312	0.914	0.921
76.0	0.657	0.844	1.043	0.624	0.946	0.491	1.9809	1.2384	0.905	0.914
90.5	0.578	0.921	0.882	0.620	1.134	0.317	2.0021	1.2428	0.904	0.913
100.0	0.432	0.975	0.753	0.632	1.271	0.225	2.0122	1.2446	0.907	0.916

RBAR	INC (INPUT	DEV (C-R)	X-FACT	DFC	CAM	STGR	TURN	D-FACT	SOL	LOSS COEFF
32.640	3.00	3.72	0.20	0.0250	-0.17	59.23	-0.89	0.484	1.500	0.195
31.999	3.14	3.63	0.20	0.0253	0.11	58.00	-0.38	0.471	1.521	0.163
31.365	3.20	3.78	0.40	0.0259	0.61	56.69	0.02	0.464	1.541	0.139
30.096	3.52	3.80	0.45	0.0274	1.31	54.79	0.73	0.453	1.582	0.100
28.806	3.88	4.59	1.00	0.0304	2.27	52.27	1.57	0.460	1.628	0.073
28.079	4.20	4.54	1.00	0.0333	2.71	50.94	2.26	0.464	1.657	0.065
28.079	4.20	4.64	1.00	0.0333	2.71	50.94	2.26	0.464	1.657	0.065
27.473	4.47	4.73	1.10	0.0347	3.44	49.73	3.03	0.470	1.682	0.062
26.069	5.42	5.40	1.30	0.0409	5.20	46.39	5.22	0.488	1.745	0.063
24.575	6.05	6.54	1.70	0.0447	10.13	42.99	9.54	0.509	1.812	0.073
22.960	6.30	7.71	2.50	0.0718	17.22	33.23	14.40	0.522	1.934	0.039
20.143	6.64	12.11	3.20	0.0794	42.68	22.54	27.25	0.515	2.146	0.130
17.744	5.62	14.61	1.20	0.0438	47.60	22.39	38.05	0.448	2.414	0.175
16.201	5.00	16.72	1.10	0.0400	50.03	17.44	45.30	0.307	2.643	0.230

FILE CODE	PRESS RATIO	TEMP RATIO	ADIA EFF	INLET CORR RPM
21475	1.9481	1.2356	0.891	5378.5

BLADE ROW PRINTOUT (METRIC)

SI

PCT IMM	RADIUS IN	RADIUS OUT	MERID ANGLE IN	MERID ANGLE OUT	STREAM FUNCT IN	STREAM FUNCT OUT	ABS ANGLE IN	ABS ANGLE OUT	REL ANGLE IN	REL ANGLE OUT
0.	82.906	82.906	0.	0.	0.	0.	46.4	5.0		
4.5	81.430	81.640	1.3	0.1	0.050	0.050	44.2	5.0		
8.9	79.985	80.374	2.2	0.9	0.100	0.100	42.8	5.0		
17.8	77.121	77.828	3.7	2.7	0.200	0.200	41.2	5.0		
26.7	74.247	75.247	4.9	4.8	0.300	0.300	40.3	5.0		
31.7	72.647	73.806	5.6	6.0	0.355	0.355	40.2	5.0		
31.7	72.647	73.806	5.6	6.0	0.355	0.355	40.2	5.0		
35.9	71.322	72.613	6.2	7.0	0.400	0.400	40.4	5.0		
45.3	68.293	69.898	7.7	9.3	0.500	0.500	41.3	5.0		
55.1	65.136	67.069	9.6	11.7	0.600	0.600	42.6	5.0		
65.3	61.833	64.151	11.8	14.3	0.700	0.700	44.2	5.0		
81.7	56.467	59.500	16.7	18.2	0.850	0.850	46.9	5.0		
93.6	52.514	56.167	21.2	20.9	0.950	0.950	49.0	5.0		
100.0	50.391	54.399	23.4	22.7	1.000	1.000	49.7	5.0		

PCT IMM	ABS VEL IN	ABS VEL OUT	REL VEL IN	REL VEL OUT	MERID VEL IN	MERID VEL OUT	TANG VEL IN	TANG VEL OUT	BLADE SPEED IN	BLADE SPEED OUT
0.	238.8	184.5			164.7	183.8	172.9	16.1		
4.5	239.0	185.3			171.4	184.6	166.6	16.2		
8.9	239.3	186.7			175.5	186.0	162.6	16.3		
17.8	240.8	189.6			181.4	188.9	158.3	16.5		
26.7	243.5	192.2			185.9	191.4	157.2	16.7		
31.7	245.9	193.8			188.1	193.1	158.4	16.8		
31.7	245.9	193.8			188.1	193.1	158.4	16.8		
35.9	248.5	195.2			189.7	194.5	160.5	16.9		
45.3	254.2	196.4			191.8	195.6	166.9	16.9		
55.1	266.3	202.2			197.2	201.5	179.0	17.3		
65.3	278.7	205.7			201.9	205.0	192.1	17.4		
81.7	302.9	212.5			211.5	211.7	216.8	17.6		
93.6	325.0	219.3			221.8	218.6	237.5	17.9		
100.0	338.4	222.2			229.5	221.4	248.7	17.9		

PCT IMM	ABS MACH NO IN	ABS MACH NO OUT	REL MACH NO IN	REL MACH NO OUT	AXIAL VEL R	CH'	ACC PT RATIO	ACC TT RATIO	EFFICIENCY ADIA	EFFICIENCY POLY
0.	0.646	0.491			1.115	0.323	1.9261	1.2788	0.739	0.762
4.5	0.651	0.496			1.078	0.326	1.9169	1.2640	0.774	0.794
8.9	0.655	0.503			1.060	0.324	1.9093	1.2532	0.802	0.819
17.8	0.663	0.514			1.042	0.326	1.9004	1.2376	0.848	0.861
26.7	0.674	0.524			1.030	0.333	1.8951	1.2272	0.883	0.893
31.7	0.683	0.529			1.026	0.339	1.8948	1.2241	0.895	0.904
31.7	0.683	0.529			1.026	0.339	1.8948	1.2241	0.895	0.904
35.9	0.691	0.533			1.024	0.346	1.8967	1.2229	0.901	0.909
45.3	0.709	0.537			1.016	0.372	1.8971	1.2220	0.905	0.913
55.1	0.744	0.553			1.014	0.393	1.9178	1.2270	0.902	0.910
65.3	0.782	0.562			1.005	0.424	1.9300	1.2312	0.894	0.904
81.7	0.856	0.580			0.993	0.467	1.9419	1.2384	0.877	0.888
93.6	0.927	0.599			0.988	0.483	1.9350	1.2428	0.855	0.868
100.0	0.972	0.607			0.970	0.490	1.9184	1.2440	0.839	0.853

RBAR	INC (INPUT	DEV (C-R)	X-FACT	TMC	CAM	STGR	TURN	D-FACT	SOL	LOSS COEFF
82.906	0.35	8.82	0.	0.1000	49.85	21.10	41.38	0.400	1.900	0.092
81.535	0.60	8.22	0.	0.0990	46.82	20.19	39.20	0.389	1.911	0.084
80.179	0.90	7.80	0.	0.0975	44.74	19.57	37.84	0.378	1.922	0.077
77.475	1.25	7.28	0.	0.0951	42.18	18.81	36.15	0.363	1.943	0.063
74.747	1.55	6.97	0.	0.0921	40.73	18.39	35.31	0.356	1.964	0.051
73.227	1.70	6.90	0.	0.0902	40.45	18.32	35.25	0.356	1.975	0.047
73.227	1.70	6.90	0.	0.0902	40.45	18.32	35.25	0.356	1.975	0.047
71.967	1.80	6.90	0.	0.0883	40.50	18.35	35.41	0.358	1.985	0.043
69.091	1.80	7.06	0.	0.0841	41.56	18.72	36.29	0.373	2.005	0.038
66.103	1.80	7.32	0.	0.0807	43.15	19.25	37.63	0.388	2.025	0.037
62.992	1.80	7.65	0.	0.0755	45.03	19.87	39.18	0.412	2.045	0.038
57.984	1.80	8.23	0.	0.0664	48.37	20.96	41.94	0.452	2.074	0.052
54.340	1.60	8.70	0.	0.0575	51.07	21.83	43.97	0.480	2.093	0.079
52.395	1.10	8.99	0.	0.0543	52.64	22.32	44.74	0.499	2.102	0.103

INLET CORR WFLOW	PRESS RATIO	TEMP RATIO	ADIA EFF	INLET CORR RPM
371.83	1.9153	1.2356	0.867	5378.5

BLADE ROW PRINTOUT (ENGLISH)

S1

PCT IMM	RADIUS IN	RADIUS OUT	MERID ANGLE IN	MERID ANGLE OUT	STREAM FUNCT IN	STREAM FUNCT OUT	ABS ANGLE IN	ABS ANGLE OUT	REL ANGLE IN	REL ANGLE OUT
0.	32.640	32.640	0.	0.	0.	0.	46.4	5.0		
4.5	32.059	32.142	1.3	0.1	0.050	0.050	44.2	5.0		
8.9	31.490	31.643	2.2	0.9	0.100	0.100	42.8	5.0		
17.8	30.363	30.641	3.7	2.7	0.200	0.200	41.2	5.0		
26.7	29.231	29.625	4.9	4.8	0.300	0.300	40.3	5.0		
31.7	28.601	29.057	5.6	6.0	0.355	0.355	40.2	5.0		
31.7	28.601	29.057	5.6	6.0	0.355	0.355	40.2	5.0		
35.9	28.079	28.588	6.2	7.0	0.400	0.400	40.4	5.0		
45.3	26.887	27.515	7.7	9.3	0.500	0.500	41.3	5.0		
55.1	25.644	26.405	9.6	11.7	0.600	0.600	42.6	5.0		
65.3	24.344	25.256	11.8	14.3	0.700	0.700	44.2	5.0		
81.7	22.231	23.425	16.7	18.2	0.850	0.850	46.9	5.0		
93.6	20.675	22.113	21.2	20.9	0.950	0.950	49.0	5.0		
100.0	19.839	21.417	23.4	22.7	1.000	1.000	49.7	5.0		

PCT IMM	ABS VEL IN	ABS VEL OUT	REL VEL IN	REL VEL OUT	MERID VEL IN	MERID VEL OUT	TANG VEL IN	TANG VEL OUT	BLADE SPEED IN	BLADE SPEED OUT
0.	783.4	605.2			540.5	602.9	567.1	52.7		
4.5	784.1	608.0			562.2	605.7	546.6	53.0		
8.9	785.1	612.7			575.9	610.4	533.6	53.4		
17.8	789.9	622.0			595.2	619.6	519.2	54.2		
26.7	798.7	630.5			610.0	628.1	515.6	54.8		
31.7	806.8	635.8			617.0	633.4	519.8	55.1		
31.7	806.8	635.8			617.0	633.4	519.8	55.1		
35.9	815.3	640.6			622.4	638.1	526.7	55.4		
45.3	834.1	644.2			629.2	641.9	547.7	55.4		
55.1	873.7	663.4			646.9	661.0	587.2	56.6		
65.3	914.2	674.8			662.3	672.4	630.2	57.0		
81.7	993.8	697.0			693.9	694.7	711.4	57.7		
93.6	1066.2	719.6			727.7	717.2	779.2	58.6		
100.0	1110.2	728.9			752.8	726.5	815.9	58.6		

PCT IMM	ABS MACH NO IN	ABS MACH NO OUT	REL MACH NO IN	REL MACH NO OUT	AXIAL VEL R	CH	ACC PT RATIO	ACC TT RATIO	EFFICIENCY ADIA	EFFICIENCY POLY
0.	0.646	0.491			1.115	0.323	1.9261	1.2788	0.739	0.762
4.5	0.651	0.496			1.078	0.326	1.9169	1.2640	0.774	0.794
8.9	0.655	0.503			1.060	0.324	1.9093	1.2532	0.802	0.819
17.8	0.663	0.514			1.042	0.326	1.9004	1.2376	0.848	0.861
26.7	0.674	0.524			1.030	0.333	1.8951	1.2272	0.863	0.893
31.7	0.683	0.529			1.026	0.339	1.8948	1.2241	0.895	0.904
31.7	0.683	0.529			1.026	0.339	1.8948	1.2241	0.895	0.904
35.9	0.691	0.533			1.024	0.346	1.8967	1.2229	0.901	0.909
45.3	0.709	0.537			1.016	0.372	1.8971	1.2220	0.905	0.913
55.1	0.744	0.553			1.014	0.393	1.9178	1.2270	0.902	0.910
65.3	0.782	0.562			1.005	0.424	1.9300	1.2312	0.894	0.904
81.7	0.856	0.580			0.993	0.467	1.9419	1.2384	0.877	0.888
93.6	0.927	0.599			0.988	0.483	1.9350	1.2428	0.855	0.868
100.0	0.972	0.607			0.970	0.490	1.9184	1.2440	0.839	0.853

RBAR	INC (INPUT	DEV (C-R)	X-FACT	TMC	CAM	STGR	TURN	D-FACT	SOL	LOSS COEFF
32.640	0.35	8.82	0.	0.1000	49.85	21.10	41.38	0.400	1.900	0.092
32.100	0.60	8.22	0.	0.0990	46.82	20.19	39.20	0.389	1.911	0.084
31.567	0.90	7.80	0.	0.0975	44.74	19.57	37.84	0.378	1.922	0.077
30.502	1.25	7.28	0.	0.0951	42.18	18.81	36.15	0.363	1.943	0.062
29.428	1.55	6.97	0.	0.0921	40.73	18.39	35.31	0.356	1.964	0.051
28.829	1.70	6.90	0.	0.0902	40.45	18.32	35.25	0.356	1.975	0.047
28.829	1.70	6.90	0.	0.0902	40.45	18.32	35.25	0.356	1.975	0.047
28.334	1.80	6.90	0.	0.0883	40.50	18.35	35.41	0.358	1.985	0.043
27.201	1.80	7.06	0.	0.0841	41.56	18.72	36.29	0.373	2.005	0.038
26.025	1.80	7.32	0.	0.0807	43.15	19.25	37.63	0.388	2.025	0.037
24.800	1.80	7.65	0.	0.0755	45.03	19.87	39.18	0.412	2.045	0.038
22.828	1.80	8.23	0.	0.0664	48.37	20.96	41.94	0.452	2.074	0.052
21.394	1.60	8.70	0.	0.0575	51.07	21.83	43.97	0.480	2.093	0.079
20.628	1.10	8.99	0.	0.0543	52.64	22.32	44.74	0.499	2.102	0.103

INLET CORR WTFLOW	PRESS RATIO	TEMP RATIO	ADIA EFF	INLET CORR RPM
	1.9153	1.2356	0.867	5378.5

BLADE ROW PRINTOUT (METRIC)

R2

PCT IMM	RADIUS IN	RADIUS OUT	MERID ANGLE IN	MERID ANGLE OUT	STREAM FUNCT IN	STREAM FUNCT OUT	ABS ANGLE IN	ABS ANGLE OUT	REL ANGLE IN	REL ANGLE OUT
0.	82.784	82.381	-3.4	-2.2	0.	0.	4.7	48.4	66.4	60.1
4.7	81.586	81.308	-1.8	-1.4	0.050	0.050	4.7	46.7	65.9	59.5
9.4	80.389	80.263	-0.6	-0.4	0.100	0.100	4.6	45.4	65.3	58.8
18.6	77.987	78.222	1.6	1.9	0.200	0.200	4.6	43.4	64.2	57.6
27.8	75.557	76.219	4.0	4.2	0.300	0.300	4.6	42.4	63.1	56.3
32.9	74.201	75.122	5.3	5.5	0.355	0.355	4.6	42.2	62.5	55.4
32.9	74.201	75.122	5.3	5.5	0.355	0.355	4.6	42.2	62.5	55.4
37.1	73.080	74.221	6.5	6.6	0.400	0.400	4.6	42.2	62.0	54.6
46.7	70.522	72.195	9.1	8.9	0.500	0.500	4.6	42.4	61.1	52.7
56.4	67.871	70.143	11.7	11.2	0.600	0.600	4.6	42.1	59.7	50.4
66.5	65.115	68.054	14.3	13.6	0.700	0.700	4.6	42.8	58.6	47.8
82.5	60.691	64.777	17.9	17.4	0.850	0.850	4.7	44.5	57.0	43.0
94.0	57.476	62.477	19.6	20.5	0.950	0.950	4.8	46.3	55.9	38.7
100.0	55.781	61.268	19.2	22.3	1.000	1.000	4.7	47.3	54.6	35.6

PCT IMM	ABS VEL IN	ABS VEL OUT	REL VEL IN	REL VEL OUT	MERID VEL IN	MERID VEL OUT	TANG VEL IN	TANG VEL OUT	BLADE SPEED IN	BLADE SPEED OUT
0.	198.0	243.6	491.5	325.2	197.4	161.9	16.1	182.0	466.3	464.0
4.7	199.2	242.2	485.8	327.2	198.6	166.3	16.2	176.1	459.5	458.0
9.4	201.4	241.3	480.5	327.6	200.7	169.5	16.3	171.7	452.8	452.1
18.6	205.2	240.5	469.7	326.0	204.6	174.6	16.5	165.3	439.3	440.6
27.8	208.5	241.4	458.7	321.0	207.9	178.5	16.6	162.5	425.6	429.3
32.9	210.5	242.9	452.8	316.8	209.9	180.4	16.7	162.7	417.9	423.1
32.9	210.5	242.9	452.8	316.8	209.9	180.4	16.7	162.7	417.9	423.1
37.1	212.3	244.6	448.0	312.7	211.6	181.8	16.8	163.6	411.6	418.0
46.7	213.4	249.2	435.9	302.8	212.7	185.1	16.7	166.9	397.2	406.6
56.4	218.6	254.9	425.3	295.6	217.9	190.6	17.1	169.2	382.3	395.1
66.5	221.1	261.5	413.3	285.1	220.4	194.5	17.1	174.8	366.8	383.3
82.5	221.9	273.8	392.8	267.4	221.2	199.8	17.3	187.2	341.8	364.8
94.0	221.1	284.7	377.3	254.2	220.4	203.4	17.5	199.3	323.7	351.9
100.0	224.1	293.7	371.5	248.9	223.4	207.6	17.4	207.8	314.2	345.1

PCT IMM	ABS MACH NO IN	ABS MACH NO OUT	REL MACH NO IN	REL MACH NO OUT	AXIAL VEL R	CH'	ACC PT RATIO	ACC TT RATIO	EFFICIENCY ADIA	EFFICIENCY POLY
0.	0.529	0.598	1.313	0.798	0.821	0.441	3.2922	1.5424	0.745	0.783
4.7	0.536	0.600	1.306	0.810	0.838	0.444	3.2707	1.5150	0.780	0.813
9.4	0.544	0.601	1.298	0.816	0.844	0.449	3.2528	1.4942	0.808	0.837
18.6	0.559	0.606	1.279	0.821	0.854	0.458	3.2262	1.4628	0.857	0.878
27.8	0.571	0.613	1.256	0.815	0.859	0.465	3.2065	1.4425	0.891	0.907
32.9	0.578	0.618	1.242	0.807	0.859	0.468	3.1990	1.4366	0.901	0.915
32.9	0.578	0.618	1.242	0.807	0.859	0.468	3.1990	1.4366	0.901	0.915
37.1	0.583	0.624	1.230	0.797	0.859	0.470	3.1955	1.4342	0.905	0.919
46.7	0.586	0.637	1.198	0.774	0.870	0.474	3.1941	1.4323	0.908	0.922
56.4	0.600	0.652	1.168	0.756	0.876	0.470	3.1941	1.4342	0.904	0.918
66.5	0.607	0.669	1.134	0.729	0.885	0.464	3.1941	1.4398	0.893	0.909
82.5	0.607	0.700	1.075	0.684	0.905	0.446	3.1941	1.4526	0.867	0.887
94.0	0.604	0.728	1.030	0.650	0.918	0.430	3.1941	1.4641	0.846	0.868
100.0	0.612	0.751	1.015	0.636	0.910	0.423	3.1941	1.4713	0.833	0.857

RBAR	INC (INPUT)	DEV (C-R)	X-FACT	TMC	CAM	STGR	TURN	D-FACT	SOL	LOSS COEFF
82.583	3.00	3.42	0.	0.0253	6.63	60.05	6.22	0.459	1.399	0.181
81.447	3.00	2.90	-0.30	0.0264	6.32	59.72	6.42	0.444	1.402	0.154
80.326	3.10	2.39	-0.60	0.0276	5.75	59.33	6.46	0.433	1.412	0.130
78.105	3.40	1.68	-1.00	0.0301	4.85	58.37	6.57	0.416	1.444	0.097
75.888	3.90	1.57	-1.00	0.0326	4.50	56.96	6.83	0.407	1.494	0.069
74.662	4.20	1.60	-0.98	0.0339	4.47	56.05	7.07	0.407	1.525	0.065
74.662	4.20	1.60	-0.98	0.0339	4.47	56.05	7.07	0.407	1.525	0.065
73.651	4.50	1.66	-0.95	0.0351	4.49	55.22	7.34	0.409	1.553	0.065
71.358	5.25	2.20	-0.60	0.0382	5.38	53.15	8.43	0.413	1.620	0.065
69.007	6.00	2.73	-0.25	0.0419	6.06	50.68	9.33	0.413	1.694	0.070
66.585	6.60	3.63	0.20	0.0460	7.80	48.07	10.77	0.421	1.772	0.088
62.734	7.40	5.58	1.10	0.0539	12.22	43.52	14.04	0.438	1.888	0.129
59.976	7.80	7.16	1.65	0.0612	16.54	39.80	17.18	0.455	1.966	0.162
58.525	8.00	8.13	2.00	0.0657	19.15	37.01	19.02	0.465	2.006	0.177

INLET CORR WTFLOW	PRESS RATIO	TEMP RATIO	ADIA EFF	INLET CORR RPM
371.83	3.2107	1.4546	0.868	5378.5

BLADE ROW PRINTOUT (ENGLISH)

R2

PCT IMM	RADIUS IN	RADIUS OUT	MERID ANGLE IN	MERID ANGLE OUT	STREAM FUNCT IN	STREAM FUNCT OUT	ABS ANGLE IN	ABS ANGLE OUT	REL ANGLE IN	REL ANGLE OUT
0.	32.592	32.433	-3.4	-2.2	0.	0.	4.7	48.4	66.4	60.1
4.7	32.120	32.011	-1.8	-1.4	0.050	0.050	4.7	46.7	65.9	59.5
9.4	31.649	31.599	-0.6	-0.4	0.100	0.100	4.6	45.4	65.3	58.8
18.6	30.703	30.796	1.6	1.9	0.200	0.200	4.6	43.4	64.2	57.6
27.8	29.747	30.007	4.0	4.2	0.300	0.300	4.6	42.4	63.1	56.3
32.9	29.213	29.576	5.3	5.5	0.355	0.355	4.6	42.2	62.5	55.4
32.9	29.213	29.576	5.3	5.5	0.355	0.355	4.6	42.2	62.5	55.4
37.1	28.772	29.221	6.5	6.6	0.400	0.400	4.6	42.2	62.0	54.6
46.7	27.765	28.423	9.1	8.9	0.500	0.500	4.6	42.4	61.1	52.7
56.4	26.721	27.615	11.7	11.2	0.600	0.600	4.6	42.1	59.7	50.4
66.5	25.636	26.793	14.3	13.6	0.700	0.700	4.6	42.8	58.6	47.8
82.5	23.894	25.503	17.9	17.4	0.850	0.850	4.7	44.5	57.0	43.0
94.0	22.628	24.597	19.6	20.5	0.950	0.950	4.8	46.3	55.9	38.7
100.0	21.961	24.121	19.2	22.3	1.000	1.000	4.7	47.3	54.6	35.6

PCT IMM	ABS VEL IN	ABS VEL OUT	REL VEL IN	REL VEL OUT	MERID VEL IN	MERID VEL OUT	TANG VEL IN	TANG VEL OUT	BLADE SPEED IN	BLADE SPEED OUT
0.	649.7	799.3	1612.6	1066.8	647.5	531.3	52.8	597.2	1529.8	1522.3
4.7	653.7	794.8	1593.8	1073.6	651.5	545.6	53.0	577.9	1507.6	1502.5
9.4	660.7	791.5	1576.3	1074.7	658.6	556.0	53.4	563.4	1485.5	1483.2
18.6	673.3	788.9	1540.9	1069.5	671.1	572.9	54.0	542.4	1441.1	1445.5
27.8	684.2	792.1	1505.1	1053.2	682.0	585.8	54.5	533.2	1396.2	1408.4
32.9	690.7	797.0	1485.5	1039.5	688.5	591.9	54.8	533.7	1371.2	1388.2
32.9	690.7	797.0	1485.5	1039.5	688.5	591.9	54.8	533.7	1371.2	1388.2
37.1	696.4	802.5	1469.7	1025.8	694.2	596.4	55.1	536.9	1350.4	1371.5
46.7	700.1	817.6	1430.1	993.6	698.0	607.1	54.9	547.6	1303.2	1334.1
56.4	717.1	836.2	1395.3	969.7	714.9	625.4	55.9	555.1	1254.2	1296.2
66.5	725.4	858.0	1356.0	935.4	723.2	638.1	56.2	573.6	1203.3	1257.6
82.5	727.9	898.2	1288.7	877.2	725.7	655.5	56.6	614.0	1121.5	1197.0
94.0	725.2	934.2	1237.9	834.1	723.0	667.2	57.3	653.9	1062.1	1154.5
100.0	735.3	963.7	1218.7	816.5	733.1	681.1	57.2	681.8	1030.8	1132.2

PCT IMM	ABS MACH NO IN	ABS MACH NO OUT	REL MACH NO IN	REL MACH NO OUT	AXIAL VEL R	CH'	ACC PT RATIO	ACC TT RATIO	EFFICIENCY ADIA	EFFICIENCY POLY
0.	0.529	0.598	1.313	0.798	0.821	0.441	3.2922	1.5424	0.745	0.783
4.7	0.536	0.600	1.306	0.810	0.838	0.444	3.2707	1.5150	0.780	0.813
9.4	0.544	0.601	1.298	0.816	0.844	0.449	3.2528	1.4942	0.808	0.837
18.6	0.559	0.606	1.279	0.821	0.854	0.458	3.2262	1.4Y8	0.857	0.878
27.8	0.571	0.613	1.256	0.815	0.859	0.465	3.2065	1.4425	0.891	0.907
32.9	0.578	0.618	1.242	0.807	0.859	0.468	3.1990	1.4366	0.901	0.915
32.9	0.578	0.618	1.242	0.807	0.859	0.468	3.1990	1.4366	0.901	0.915
37.1	0.583	0.624	1.230	0.797	0.859	0.470	3.1955	1.4342	0.905	0.919
46.7	0.586	0.637	1.198	0.774	0.870	0.474	3.1941	1.4323	0.908	0.922
56.4	0.600	0.652	1.168	0.756	0.876	0.470	3.1941	1.4342	0.904	0.918
66.5	0.607	0.669	1.134	0.729	0.885	0.464	3.1941	1.4398	0.893	0.909
82.5	0.607	0.700	1.075	0.684	0.905	0.446	3.1941	1.4526	0.867	0.887
94.0	0.604	0.728	1.030	0.650	0.918	0.430	3.1941	1.4641	0.846	0.868
100.0	0.612	0.751	1.015	0.636	0.910	0.423	3.1941	1.4713	0.833	0.857

RBAR	INC (INPUT	DEV (C-R)	X-FACT	TMC	CAM	STGR	TURN	D-FACT	SOL	LOSS COEFF
32.513	3.00	3.42	0.	0.0253	6.63	60.05	6.22	0.459	1.399	0.181
32.066	3.00	2.90	-0.30	0.0264	6.32	59.72	6.47	0.444	1.402	0.154
31.624	3.10	2.39	-0.60	0.0276	5.75	59.33	6.46	0.433	1.412	0.130
30.750	3.40	1.68	-1.00	0.0301	4.85	58.37	6.57	0.416	1.444	0.092
29.877	3.90	1.57	-1.00	0.0326	4.50	56.96	6.83	0.407	1.494	0.069
29.394	4.20	1.60	-0.98	0.0339	4.47	56.05	7.07	0.407	1.525	0.065
29.394	4.20	1.60	-0.98	0.0339	4.47	56.05	7.07	0.407	1.525	0.065
28.996	4.50	1.66	-0.95	0.0351	4.49	55.22	7.34	0.409	1.553	0.065
28.094	5.25	2.20	-0.60	0.0382	5.38	53.15	8.43	0.413	1.620	0.065
27.168	6.00	2.73	-0.25	0.0419	6.06	50.68	9.33	0.413	1.694	0.070
26.214	6.60	3.63	0.20	0.0460	7.80	48.07	10.77	0.421	1.772	0.088
24.698	7.40	5.58	1.10	0.0539	12.22	43.52	14.04	0.438	1.888	0.179
23.613	7.80	7.16	1.65	0.0612	16.54	39.80	17.18	0.455	1.966	0.162
23.041	8.00	8.13	2.00	0.0657	19.15	37.01	19.02	0.465	2.006	0.177

' BLADE ROW PRINTOUT (METRIC)

S2 NACA 65 FOIL

PCT	RADIUS		MERID ANGLE		STREAM FUNCT		ABS ANGLE		REL ANGLE	
IMM	IN	OUT	IN	OUT	IN	OUT	IN	OUT	IN	OUT
0.	82.265	81.912	-1.9	-3.1	0.	0.	46.5	0.		
5.0	81.252	80.974	-0.7	-3.5	0.050	0.050	44.7	0.		
9.8	80.263	80.044	0.2	-3.8	0.100	0.100	43.5	0.		
19.4	78.324	78.202	1.9	-4.1	0.200	0.200	41.6	0.		
28.9	76.409	76.373	3.6	-4.3	0.300	0.300	40.6	0.		
34.1	75.355	75.369	4.5	-4.4	0.355	0.355	40.4	0.		
34.1	75.355	75.369	4.5	-4.4	0.355	0.355	40.4	0.		
38.4	74.488	74.547	5.2	-4.4	0.400	0.400	40.5	0.		
48.1	72.533	72.707	7.1	-4.5	0.500	0.500	40.7	0.		
57.8	70.538	70.845	9.1	-4.4	0.600	0.600	40.6	0.		
67.8	68.494	68.951	11.2	-4.2	0.700	0.700	41.3	0.		
83.4	65.274	66.033	14.7	-3.5	0.850	0.850	43.1	0.		
94.3	62.982	64.025	17.5	-2.4	0.950	0.950	45.2	0.		
100.0	61.771	62.996	18.6	-1.7	1.000	1.000	46.8	0.		

PCT	ABS VEL		REL VEL		MERID VEL		TANG VEL		BLADE SPEED	
IMM	IN	OUT	IN	OUT	IN	OUT	IN	OUT	IN	OUT
0.	251.5	176.5			173.3	176.5	182.3	0.		
5.0	250.4	177.1			177.8	177.1	176.3	0.		
9.8	249.5	178.5			181.0	178.5	171.7	0.		
19.4	248.6	181.2			185.8	181.2	165.1	0.		
28.9	249.2	184.1			189.2	184.1	162.1	0.		
34.1	250.4	185.9			190.8	185.9	162.2	0.		
34.1	250.4	185.9			190.8	185.9	162.2	0.		
38.4	251.8	187.4			191.9	187.4	163.1	0.		
48.1	255.7	190.6			194.4	190.6	166.1	0.		
57.8	260.4	193.6			198.7	193.6	168.3	0.		
67.8	266.2	196.8			201.7	196.8	173.7	0.		
83.4	276.7	202.3			205.1	202.3	185.7	0.		
94.3	285.4	206.9			205.9	206.9	197.7	0.		
100.0	290.0	209.8			204.0	209.8	206.1	0.		

PCT	ABS MACH NO		REL MACH NO		AXIAL	CH'	ACC PT	ACC TT	EFFICIENCY	
IMM	IN	OUT	IN	OUT	VEL R		RATIO	RATIO	ADIA	POLY
0.	0.618	0.426			1.017	0.433	3.2297	1.5424	0.731	0.771
5.0	0.621	0.431			0.994	0.431	3.2125	1.5150	0.766	0.800
9.8	0.623	0.438			0.984	0.426	3.2004	1.4942	0.795	0.826
19.4	0.628	0.450			0.973	0.417	3.1823	1.4628	0.845	0.868
28.9	0.634	0.461			0.972	0.411	3.1696	1.4425	0.880	0.898
34.1	0.639	0.466			0.974	0.410	3.1651	1.4366	0.891	0.907
34.1	0.639	0.466			0.974	0.410	3.1651	1.4366	0.891	0.907
38.4	0.644	0.470			0.977	0.411	3.1635	1.4342	0.895	0.911
48.1	0.655	0.479			0.985	0.413	3.1650	1.4323	0.900	0.915
57.8	0.667	0.487			0.984	0.416	3.1644	1.4342	0.896	0.911
67.8	0.682	0.494			0.992	0.420	3.1609	1.4398	0.883	0.900
83.4	0.708	0.506			1.018	0.420	3.1456	1.4526	0.854	0.875
94.3	0.730	0.516			1.053	0.408	3.1191	1.4641	0.825	0.851
100.0	0.741	0.523			1.085	0.392	3.0973	1.4713	0.807	0.835

RBAR	INC (INPUT	DEV (C-R)	X-FACT	TMC	CAM	STGR	TURN	D-FACT	SOL	LOSS COEFF
82.089	-0.60	9.96	0.	0.0800	57.02	18.55	46.46	0.489	1.909	0.084
81.113	-0.45	9.47	0.	0.0785	54.67	17.86	44.75	0.476	1.919	0.078
80.154	-0.30	9.10	0.	0.0771	52.90	17.35	43.50	0.463	1.930	0.070
78.263	0.	8.54	0.	0.0744	50.18	16.55	41.64	0.442	1.950	0.058
76.391	0.30	8.19	0.	0.0717	48.53	16.08	40.64	0.426	1.970	0.049
75.362	0.40	8.10	0.	0.0704	48.14	15.98	40.45	0.421	1.981	0.044
75.362	0.40	8.10	0.	0.0704	48.14	15.98	40.45	0.421	1.981	0.044
74.517	0.50	8.06	0.	0.0694	48.03	15.96	40.47	0.419	1.990	0.041
72.620	0.60	8.05	0.	0.0673	48.18	16.04	40.74	0.416	2.010	0.036
70.692	0.70	7.95	0.	0.0654	47.87	15.98	40.62	0.415	2.030	0.036
68.722	0.78	8.04	0.	0.0634	48.54	16.23	41.28	0.419	2.050	0.039
65.653	0.88	8.36	0.	0.0600	50.59	16.94	43.12	0.429	2.081	0.054
63.503	0.96	8.76	0.	0.0569	53.00	17.74	45.20	0.439	2.103	0.079
62.384	1.00	9.11	0.	0.0553	54.93	18.36	46.83	0.443	2.112	0.099

INLET CORR WTFLOW	PRESS RATIO	TEMP RATIO	ADIA EFF	INLET CORR RPM
371.83	3.1674	1.4546	0.856	5378.5

BLADE ROW PRINTOUT (ENGLISH)

S2 NACA 65 FOIL

PCT IMM	RADIUS IN	RADIUS OUT	MERID ANGLE IN	MERID ANGLE OUT	STREAM FUNCT IN	STREAM FUNCT OUT	ABS ANGLE IN	ABS ANGLE OUT	REL ANGLE IN	REL ANGLE OUT
0.	32.388	32.249	-1.9	-3.1	0.	0.	46.5	0.		
5.0	31.989	31.879	-0.7	-3.5	0.050	0.050	44.7	0.		
9.8	31.600	31.513	0.2	-3.8	0.100	0.100	43.5	0.		
19.4	30.836	30.788	1.9	-4.1	0.200	0.200	41.6	0.		
28.9	30.082	30.068	3.6	-4.3	0.300	0.300	40.6	0.		
34.1	29.667	29.673	4.5	-4.4	0.355	0.355	40.4	0.		
34.1	29.667	29.673	4.5	-4.4	0.355	0.355	40.4	0.		
38.4	29.326	29.349	5.2	-4.4	0.400	0.400	40.5	0.		
48.1	28.556	28.625	7.1	-4.5	0.500	0.500	40.7	0.		
57.8	27.771	27.892	9.1	-4.4	0.600	0.600	40.6	0.		
67.8	26.966	27.146	11.2	-4.2	0.700	0.700	41.3	0.		
83.4	25.698	25.997	14.7	-3.5	0.850	0.850	43.1	0.		
94.3	24.796	25.206	17.5	-2.4	0.950	0.950	45.2	0.		
100.0	24.319	24.802	18.6	-1.7	1.000	1.000	46.8	0.		

PCT IMM	ABS VEL IN	ABS VEL OUT	REL VEL IN	REL VEL OUT	MERID VEL IN	MERID VEL OUT	TANG VEL IN	TANG VEL OUT	BLADE SPEED IN	BLADE SPEED OUT
0.	825.2	578.9			568.6	578.9	598.1	0.		
5.0	821.4	581.1			583.4	581.1	578.3	0.		
9.8	818.5	585.6			593.8	585.6	563.4	0.		
19.4	815.5	594.3			609.7	594.3	541.6	0.		
28.9	817.6	604.1			620.9	604.1	531.9	0.		
34.1	821.5	609.8			626.0	609.8	532.0	0.		
34.1	821.5	609.8			626.0	609.8	532.0	0.		
38.4	826.3	614.7			629.7	614.7	535.0	0.		
48.1	839.0	625.4			637.8	625.4	545.0	0.		
57.8	854.2	635.2			651.8	635.2	552.0	0.		
67.8	873.3	645.5			661.8	645.5	569.9	0.		
83.4	907.8	663.7			672.9	663.7	609.3	0.		
94.3	936.4	678.7			675.4	678.7	648.6	0.		
100.0	951.5	688.5			669.4	688.5	676.2	0.		

PCT IMM	ABS MACH NO IN	ABS MACH NO OUT	REL MACH NO IN	REL MACH NO OUT	AXIAL VEL R	CH	ACC PT RATIO	ACC TT RATIO	EFFICIENCY ADIA	EFFICIENCY POLY
0.	0.618	0.426			1.017	0.433	3.2297	1.5424	0.731	0.771
5.0	0.621	0.431			0.994	0.431	3.2125	1.5150	0.766	0.800
9.8	0.623	0.438			0.984	0.426	3.2004	1.4942	0.795	0.826
19.4	0.628	0.450			0.973	0.417	3.1823	1.4628	0.845	0.868
28.9	0.634	0.461			0.972	0.411	3.1696	1.4425	0.880	0.898
34.1	0.639	0.466			0.974	0.410	3.1651	1.4366	0.891	0.907
34.1	0.639	0.466			0.974	0.410	3.1651	1.4366	0.891	0.907
38.4	0.644	0.470			0.977	0.411	3.1635	1.4342	0.895	0.911
48.1	0.655	0.479			0.985	0.413	3.1650	1.4323	0.900	0.915
57.8	0.667	0.487			0.984	0.416	3.1644	1.4342	0.896	0.911
67.8	0.682	0.494			0.992	0.420	3.1609	1.4398	0.883	0.900
83.4	0.708	0.506			1.018	0.420	3.1456	1.4526	0.854	0.875
94.3	0.730	0.516			1.053	0.408	3.1191	1.4641	0.825	0.851
100.0	0.741	0.523			1.085	0.392	3.0973	1.4713	0.807	0.835

RBAR	INC (INPUT	DEV (C-R)	X-FACT	TMC	CAM	STGR	TURN	D-FACT	SOL	LOSS COEFF
32.318	-0.60	9.96	0.	0.0800	57.02	18.55	46.46	0.489	1.909	0.084
31.934	-0.45	9.47	0.	0.0785	54.67	17.86	44.75	0.476	1.919	0.078
31.556	-0.30	9.10	0.	0.0771	52.90	17.35	43.50	0.463	1.930	0.070
30.812	0.	8.54	0.	0.0744	50.18	16.55	41.64	0.442	1.950	0.058
30.075	0.30	8.19	0.	0.0717	48.53	16.08	40.64	0.426	1.970	0.049
29.670	0.40	8.10	0.	0.0704	48.14	15.98	40.45	0.421	1.981	0.044
29.670	0.40	8.10	0.	0.0704	48.14	15.98	40.45	0.421	1.981	0.044
29.337	0.50	8.06	0.	0.0694	48.03	15.96	40.47	0.419	1.990	0.041
28.590	0.60	8.05	0.	0.0673	48.18	16.04	40.74	0.416	2.010	0.036
27.831	0.70	7.95	0.	0.0654	47.87	15.98	40.62	0.415	2.030	0.036
27.056	0.78	8.04	0.	0.0634	48.54	16.23	41.28	0.419	2.050	0.039
25.848	0.88	8.36	0.	0.0600	50.59	16.94	43.12	0.429	2.081	0.054
25.001	0.96	8.76	0.	0.0569	53.00	17.74	45.20	0.439	2.103	0.079
24.560	1.00	9.11	0.	0.0553	54.93	18.36	46.83	0.443	2.112	0.099

INLET CORR WTFLOW	PRESS RATIO	TEMP RATIO	ADIA EFF	INLET CORR RPM
	3.1674	1.4546	0.856	5378.5

APPENDIX B 2

CIRCUMFERENTIAL - AVERAGE FLOW SOLUTION FOR REAR BLOCK FAN DESIGN POINT

BLADE ROW PRINTOUT (METRIC)

IGV2

PCT IMM	RADIUS IN	RADIUS OUT	MERID ANGLE IN	MERID ANGLE OUT	STREAM FUNCT IN	STREAM FUNCT OUT	ABS ANGLE IN	ABS ANGLE OUT	REL ANGLE IN	REL ANGLE OUT
0.	68.582	64.320	-20.3	-12.4	0.	0.	0.	0.		
6.7	67.121	62.868	-20.8	-12.1	0.082	0.082	0.	0.		
15.2	65.256	61.022	-21.0	-11.8	0.184	0.184	0.	0.		
20.1	64.171	59.949	-21.2	-11.6	0.242	0.242	0.	0.		
20.1	64.171	59.949	-21.2	-11.6	0.242	0.242	0.	0.		
28.4	62.359	58.152	-21.4	-11.3	0.337	0.337	0.	0.		
42.4	59.304	55.099	-21.9	-10.8	0.490	0.490	0.	0.		
62.8	54.913	50.599	-23.1	-10.1	0.694	0.694	0.	0.		
80.0	51.311	46.712	-24.7	-9.8	0.847	0.847	0.	0.		
92.9	48.710	43.694	-26.4	-9.9	0.949	0.949	0.	0.		
100.0	47.334	41.977	-27.6	-10.6	1.000	1.000	0.	0.		

PCT IMM	ABS VEL IN	ABS VEL OUT	REL VEL IN	REL VEL OUT	MERID VEL IN	MERID VEL OUT	TANG VEL IN	TANG VEL OUT	BLADE SPEED IN	BLADE SPEED OUT
0.	258.3	273.2			258.3	273.2	0.	0.		
6.7	252.9	269.2			252.9	269.2	0.	0.		
15.2	247.0	263.2			247.0	263.2	0.	0.		
20.1	244.6	259.8			244.6	259.8	0.	0.		
20.1	244.6	259.8			244.6	259.8	0.	0.		
28.4	241.2	254.1			241.2	254.1	0.	0.		
42.4	237.1	243.6			237.1	243.6	0.	0.		
62.8	232.5	223.9			232.5	223.9	0.	0.		
80.0	230.5	202.5			230.5	202.5	0.	0.		
92.9	231.2	182.6			231.2	182.6	0.	0.		
100.0	232.4	170.0			232.4	170.0	0.	0.		

PCT IMM	ABS MACH NO IN	ABS MACH NO OUT	REL MACH NO IN	REL MACH NO OUT	AXIAL VEL R	CH*	ACC PT RATIO	ACC TT RATIO	EFFICIENCY ADIA	EFFICIENCY POLY
0.	0.665	0.707			1.102	-0.167	0.9850	1.0000		
6.7	0.656	0.702			1.113	-0.183	0.9850	1.0000		
15.2	0.645	0.691			1.117	-0.186	0.9850	1.0000		
20.1	0.640	0.684			1.116	-0.181	0.9850	1.0000		
20.1	0.640	0.684			1.116	-0.181	0.9850	1.0000		
28.4	0.632	0.669			1.109	-0.163	0.9850	1.0000		
42.4	0.620	0.639			1.088	-0.111	0.9850	1.0000		
62.8	0.606	0.582			1.031	0.013	0.9850	1.0000		
80.0	0.598	0.521			0.953	0.167	0.9850	1.0000		
92.9	0.595	0.464			0.869	0.314	0.9850	1.0000		
100.0	0.596	0.429			0.811	0.402	0.9850	1.0000		

RBAR	INC (INPUT	DEV (C-R)	X-FACT	TMC	CAM	STGR	TURN	D-FACT	SOL	LOSS COEFF
66.451	0.	0.	0.	0.0806	0.	0.	0.	-0.058	1.000	0.059
64.995	0.	0.	0.	0.0785	0.	0.	0.	-0.064	1.000	0.060
63.139	0.	0.	0.	0.0759	0.	0.	0.	-0.065	1.000	0.061
62.060	0.	0.	0.	0.0745	0.	0.	0.	-0.062	1.000	0.062
62.060	0.	0.	0.	0.0745	0.	0.	0.	-0.062	1.000	0.062
60.255	0.	0.	0.	0.0721	0.	0.	0.	-0.053	1.000	0.064
57.202	0.	0.	0.	0.0682	0.	0.	0.	-0.027	1.000	0.066
52.756	0.	0.	0.	0.0625	0.	0.	0.	0.037	1.000	0.068
49.011	0.	0.	0.	0.0578	0.	0.	0.	0.122	1.000	0.070
46.202	0.	0.	0.	0.0539	0.	0.	0.	0.210	1.000	0.071
44.656	0.	0.	0.	0.0518	0.	0.	0.	0.269	1.000	0.070

INLET CORR WTFLOW	PRESS RATIO	TEMP RATIO	ADIA EFF	INLET CORR RPM
139.72	0.9854			6161.5

BLADE ROW PRINTOUT (ENGLISH)

IGV2

PCT IMM	RADIUS IN	RADIUS OUT	MERID ANGLE IN	MERID ANGLE OUT	STREAM FUNCT IN	STREAM FUNCT OUT	ABS ANGLE IN	ABS ANGLE OUT	REL ANGLE IN	REL ANGLE OUT
0.	27.001	25.323	-20.3	-12.4	0.	0.	0.	0.		
6.7	26.426	24.751	-20.8	-12.1	0.082	0.082	0.	0.		
15.2	25.691	24.024	-21.0	-11.8	0.184	0.184	0.	0.		
20.1	25.264	23.602	-21.2	-11.6	0.242	0.242	0.	0.		
20.1	25.264	23.602	-21.2	-11.6	0.242	0.242	0.	0.		
28.4	24.551	22.894	-21.4	-11.3	0.337	0.337	0.	0.		
42.4	23.348	21.693	-21.9	-10.8	0.490	0.490	0.	0.		
62.8	21.619	19.921	-23.1	-10.1	0.694	0.694	0.	0.		
80.0	20.201	18.391	-24.7	-9.8	0.847	0.847	0.	0.		
92.9	19.177	17.202	-26.4	-9.9	0.949	0.949	0.	0.		
100.0	18.636	16.526	-27.6	-10.6	1.000	1.000	0.	0.		

PCT IMM	ABS VEL IN	ABS VEL OUT	REL VEL IN	REL VEL OUT	MERID VEL IN	MERID VEL OUT	TANG VEL IN	TANG VEL OUT	BLADE SPEED IN	BLADE SPEED OUT
0.	847.5	896.3			847.5	896.3	0.	0.		
6.7	829.7	883.1			829.7	883.1	0.	0.		
15.2	810.4	863.4			810.4	863.4	0.	0.		
20.1	802.4	852.4			802.4	852.4	0.	0.		
20.1	802.4	852.4			802.4	852.4	0.	0.		
28.4	791.5	833.8			791.5	833.8	0.	0.		
42.4	777.9	799.2			777.9	799.2	0.	0.		
62.8	762.7	734.6			762.7	734.6	0.	0.		
80.0	756.3	664.2			756.3	664.2	0.	0.		
92.9	758.6	599.0			758.6	599.0	0.	0.		
100.0	762.6	557.8			762.6	557.8	0.	0.		

PCT IMM	ABS MACH NO IN	ABS MACH NO OUT	REL MACH NO IN	REL MACH NO OUT	AXIAL VEL R	CH'	ACC PT RATIO	ACC TT RATIO	EFFICIENCY ADIA	EFFICIENCY POLY
0.	0.665	0.707			1.102	-0.167	0.9850	1.0000		
6.7	0.656	0.702			1.113	-0.183	0.9850	1.0000		
15.2	0.645	0.691			1.117	-0.186	0.9850	1.0000		
20.1	0.640	0.684			1.116	-0.181	0.9850	1.0000		
20.1	0.640	0.684			1.116	-0.181	0.9850	1.0000		
28.4	0.632	0.669			1.109	-0.163	0.9850	1.0000		
42.4	0.620	0.639			1.088	-0.111	0.9850	1.0000		
62.8	0.606	0.582			1.031	0.013	0.9850	1.0000		
80.0	0.598	0.521			0.953	0.167	0.9850	1.0000		
92.9	0.595	0.464			0.869	0.314	0.9850	1.0000		
100.0	0.596	0.429			0.811	0.402	0.9850	1.0000		

RBAR	INC (INPUT	DEV (C-R)	X-FACT	TMC	CAM	STGR	TURN	D-FACT	SOL	LOSS COEFF
26.162	0.	0.	0.	0.0806	0.	0.	0.	-0.058	1.000	0.059
25.588	0.	0.	0.	0.0785	0.	0.	0.	-0.064	1.000	0.060
24.858	0.	0.	0.	0.0759	0.	0.	0.	-0.065	1.000	0.061
24.433	0.	0.	0.	0.0745	0.	0.	0.	-0.062	1.000	0.062
24.433	0.	0.	0.	0.0745	0.	0.	0.	-0.062	1.000	0.062
23.723	0.	0.	0.	0.0721	0.	0.	0.	-0.053	1.000	0.064
22.520	0.	0.	0.	0.0682	0.	0.	0.	-0.027	1.000	0.066
20.770	0.	0.	0.	0.0625	0.	0.	0.	0.037	1.000	0.068
19.296	0.	0.	0.	0.0578	0.	0.	0.	0.122	1.000	0.070
18.190	0.	0.	0.	0.0539	0.	0.	0.	0.210	1.000	0.071
17.581	0.	0.	0.	0.0518	0.	0.	0.	0.269	1.000	0.070

INLET CORR WTFLOW	PRESS RATIO	TEMP RATIO	ADIA EFF	INLET CORR RPM
308.03	0.9854			6161.5

BLADE ROW PRINTOUT (METRIC)

CDFS

PCT IMM	RADIUS IN	RADIUS OUT	MERID ANGLE IN	MERID ANGLE OUT	STREAM FUNCT IN	STREAM FUNCT OUT	ABS ANGLE IN	ABS ANGLE OUT	REL ANGLE IN	REL ANGLE OUT
0.	63.601	62.676	-10.4	-2.8	0.	0.	0.	31.9	59.4	59.5
7.0	62.171	61.238	-9.8	-3.4	0.082	0.082	0.	31.1	59.3	58.0
15.7	60.352	59.477	-8.9	-3.6	0.184	0.184	0.	30.7	59.1	57.1
20.7	59.294	58.471	-8.4	-3.3	0.242	0.242	0.	30.6	59.0	56.6
20.7	59.294	58.471	-8.4	-3.3	0.242	0.242	0.	30.6	59.0	56.6
29.0	57.525	56.807	-7.6	-2.8	0.337	0.337	0.	30.9	58.8	55.9
43.1	54.520	54.015	-6.0	-2.0	0.490	0.490	0.	32.2	58.4	54.0
63.4	50.108	50.047	-3.5	0.1	0.694	0.694	0.	34.1	58.3	49.6
80.3	46.314	46.865	-0.8	2.8	0.847	0.847	0.	35.5	58.9	44.7
93.0	43.367	44.592	1.7	5.4	0.949	0.949	0.	37.6	60.0	39.8
100.0	41.688	43.384	3.5	7.2	1.000	1.000	0.	39.2	60.9	36.3

PCT IMM	ABS VEL IN	ABS VEL OUT	REL VEL IN	REL VEL OUT	MERID VEL IN	MERID VEL OUT	TANG VEL IN	TANG VEL OUT	BLADE SPEED IN	BLADE SPEED OUT
0.	288.9	241.3	561.3	402.9	288.9	204.9	0.	127.4	481.2	474.2
7.0	283.7	246.2	549.3	397.1	283.7	211.0	0.	126.9	470.4	463.3
15.7	276.9	244.9	534.0	387.3	276.9	210.6	0.	125.0	456.6	450.0
20.7	272.9	243.9	525.1	381.4	272.9	210.1	0.	124.0	448.6	442.4
20.7	272.9	243.9	525.1	381.4	272.9	210.1	0.	124.0	448.6	442.4
29.0	266.4	241.8	510.3	369.7	266.4	207.6	0.	123.9	435.2	429.8
43.1	254.9	241.1	484.9	346.5	254.9	203.9	0.	128.6	412.5	408.7
63.4	234.5	247.0	445.8	315.5	234.5	204.6	0.	138.4	379.1	378.7
80.3	211.8	256.0	409.4	293.1	211.8	208.5	0.	148.6	350.4	354.6
93.0	189.8	266.2	379.0	274.6	189.8	211.3	0.	162.0	328.1	337.4
100.0	175.8	274.6	361.1	264.0	175.8	213.4	0.	172.9	315.4	328.2

PCT IMM	ABS MACH NO IN	ABS MACH NO OUT	REL MACH NO IN	REL MACH NO OUT	AXIAL VEL R	CH'	ACC PT RATIO	ACC TT RATIO	EFFICIENCY ADIA	EFFICIENCY POLY
0.	0.752	0.575	1.460	0.960	0.720	0.393	1.4167	1.1449	0.712	0.726
7.0	0.744	0.593	1.440	0.957	0.753	0.404	1.4465	1.1436	0.765	0.777
15.7	0.731	0.597	1.410	0.943	0.769	0.416	1.4612	1.1401	0.808	0.818
20.7	0.721	0.596	1.388	0.932	0.777	0.422	1.4651	1.1374	0.830	0.839
20.7	0.721	0.596	1.388	0.932	0.777	0.422	1.4651	1.1374	0.830	0.839
29.0	0.704	0.593	1.349	0.907	0.785	0.435	1.4695	1.1340	0.858	0.866
43.1	0.671	0.592	1.276	0.850	0.804	0.452	1.4725	1.1322	0.875	0.882
63.4	0.612	0.606	1.163	0.774	0.874	0.459	1.4732	1.1312	0.882	0.889
80.3	0.546	0.627	1.056	0.718	0.983	0.433	1.4634	1.1306	0.870	0.877
93.0	0.483	0.648	0.965	0.668	1.109	0.375	1.4457	1.1334	0.822	0.831
100.0	0.444	0.667	0.913	0.641	1.206	0.321	1.4379	1.1375	0.785	0.795

RBAR	INC (INPUT	DEV (C-R)	X-FACT	TMC	CAM	STGR	TURN	D-FACT	SOL	LOSS COEFF
63.139	2.00	2.55	0.	0.0300	0.53	57.17	-0.02	0.369	1.294	0.151
61.704	2.25	2.44	0.	0.0317	1.51	56.27	1.32	0.362	1.348	0.121
59.914	2.55	2.28	0.	0.0351	1.70	55.67	1.98	0.356	1.435	0.095
58.883	2.72	2.20	0.	0.0372	1.81	55.34	2.33	0.352	1.487	0.081
58.883	2.72	2.20	0.	0.0372	1.81	55.34	2.33	0.352	1.487	0.081
57.166	3.01	2.12	0.	0.0406	1.99	54.74	2.88	0.352	1.574	0.065
54.268	3.47	2.69	0.35	0.0462	3.68	53.11	4.46	0.364	1.680	0.057
50.078	4.09	4.17	1.15	0.0544	8.81	49.81	8.73	0.380	1.756	0.058
46.590	4.54	5.26	1.50	0.0612	14.88	46.88	14.16	0.385	1.815	0.076
43.980	4.85	6.47	1.72	0.0664	21.76	44.23	20.14	0.391	1.873	0.132
42.536	5.00	7.68	2.00	0.0700	27.32	42.25	24.64	0.398	1.900	0.187

INLET CORR WTFLOW	PRESS RATIO	TEMP RATIO	ADIA EFF	INLET CORR RPM
139.72	1.4635	1.1340	0.848	6161.5

BLADE ROW PRINTOUT (ENGLISH)

CDFS

PCT IMM	RADIUS IN	RADIUS OUT	MERID ANGLE IN	MERID ANGLE OUT	STREAM FUNCT IN	STREAM FUNCT OUT	ABS ANGLE IN	ABS ANGLE OUT	REL ANGLE IN	REL ANGLE OUT
0.	25.040	24.676	-10.4	-2.8	0.	0.	0.	31.9	59.4	59.5
7.0	24.477	24.109	-9.8	-3.4	0.082	0.082	0.	31.1	59.3	58.0
15.7	23.761	23.416	-8.9	-3.6	0.184	0.184	0.	30.7	59.1	57.1
20.7	23.344	23.020	-8.4	-3.3	0.242	0.242	0.	30.6	59.0	56.6
20.7	23.344	23.020	-8.4	-3.3	0.242	0.242	0.	30.6	59.0	56.6
29.0	22.648	22.365	-7.6	-2.8	0.337	0.337	0.	30.9	58.8	55.9
43.1	21.465	21.266	-6.0	-2.0	0.490	0.490	0.	32.2	58.4	54.0
63.4	19.728	19.704	-3.5	0.1	0.694	0.694	0.	34.1	58.3	49.6
80.3	18.234	18.451	-0.8	2.8	0.847	0.847	0.	35.5	58.9	44.7
93.0	17.074	17.556	1.7	5.4	0.949	0.949	0.	37.6	60.0	39.8
100.0	16.412	17.080	3.5	7.2	1.000	1.000	0.	39.2	60.9	36.3

PCT IMM	ABS VEL IN	ABS VEL OUT	REL VEL IN	REL VEL OUT	MERID VEL IN	MERID VEL OUT	TANG VEL IN	TANG VEL OUT	BLADE SPEED IN	BLADE SPEED OUT
0.	948.0	791.6	1841.5	1321.7	948.0	672.4	0.	417.9	1578.7	1555.8
7.0	930.9	807.7	1802.2	1302.9	930.9	692.2	0.	416.2	1543.2	1520.1
15.7	908.4	803.6	1751.9	1270.6	908.4	691.1	0.	410.2	1498.1	1476.3
20.7	895.3	800.3	1722.7	1251.4	895.3	689.2	0.	406.8	1471.8	1451.4
20.7	895.3	800.3	1722.7	1251.4	895.3	689.2	0.	406.8	1471.8	1451.4
29.0	874.0	793.2	1674.1	1212.9	874.0	681.1	0.	406.5	1427.9	1410.1
43.1	836.4	790.9	1590.9	1136.7	836.4	669.0	0.	421.8	1353.3	1340.8
63.4	769.3	810.5	1462.5	1035.2	769.3	671.2	0.	454.2	1243.8	1242.3
80.3	694.8	839.9	1343.3	961.6	694.8	684.1	0.	487.4	1149.6	1163.3
93.0	622.7	873.4	1243.6	900.9	622.7	693.2	0.	531.4	1076.5	1106.9
100.0	576.7	901.1	1184.6	866.0	576.7	700.1	0.	567.2	1034.8	1076.9

PCT IMM	ABS MACH NO IN	ABS MACH NO OUT	REL MACH NO IN	REL MACH NO OUT	AXIAL VEL R	CH*	ACC PT RATIO	ACC TT RATIO	EFFICIENCY ADIA	EFFICIENCY POLY
0.	0.752	0.575	1.460	0.960	0.720	0.393	1.4167	1.1449	0.712	0.726
7.0	0.744	0.593	1.440	0.957	0.753	0.404	1.4465	1.1436	0.765	0.777
15.7	0.731	0.597	1.410	0.943	0.769	0.416	1.4612	1.1401	0.808	0.818
20.7	0.721	0.596	1.388	0.932	0.777	0.422	1.4651	1.1374	0.830	0.839
20.7	0.721	0.596	1.388	0.932	0.777	0.422	1.4651	1.1374	0.830	0.839
29.0	0.704	0.593	1.349	0.907	0.785	0.435	1.4695	1.1340	0.858	0.866
43.1	0.671	0.592	1.276	0.850	0.804	0.452	1.4725	1.1322	0.875	0.882
63.4	0.612	0.606	1.163	0.774	0.874	0.459	1.4732	1.1312	0.882	0.889
80.3	0.546	0.627	1.056	0.718	0.983	0.433	1.4634	1.1306	0.870	0.877
93.0	0.483	0.648	0.965	0.668	1.109	0.375	1.4457	1.1334	0.822	0.831
100.0	0.444	0.667	0.913	0.641	1.206	0.321	1.4379	1.1375	0.785	0.795

RBAR	INC (INPUT	DEV (C-R)	X-FACT	TMC	CAM	STGR	TURN	D-FACT	SOL	LOSS COEFF
24.858	2.00	2.55	0.	0.0300	0.53	57.17	-0.02	0.369	1.294	0.151
24.293	2.25	2.44	0.	0.0317	1.51	56.27	1.32	0.362	1.348	0.121
23.588	2.55	2.28	0.	0.0351	1.70	55.67	1.98	0.356	1.435	0.095
23.182	2.72	2.20	0.	0.0372	1.81	55.34	2.33	0.352	1.487	0.081
23.182	2.72	2.20	0.	0.0372	1.81	55.34	2.33	0.352	1.487	0.081
22.506	3.01	2.12	0.	0.0406	1.99	54.74	2.88	0.352	1.574	0.065
21.365	3.47	2.69	0.35	0.0462	3.68	53.11	4.46	0.364	1.680	0.057
19.716	4.09	4.17	1.15	0.0544	8.81	49.81	8.73	0.380	1.756	0.058
18.342	4.54	5.26	1.50	0.0612	14.88	46.88	14.16	0.385	1.815	0.076
17.315	4.85	6.47	1.72	0.0664	21.76	44.23	20.14	0.391	1.873	0.132
16.746	5.00	7.68	2.00	0.0700	27.32	42.25	24.64	0.398	1.900	0.187

INLET CORR WTFLOW	PRESS RATIO	TEMP RATIO	ADIA EFF	INLET CORR RPM
308.03	1.4635	1.1340	0.848	6161.5

APPENDIX C

BLADE AND VANE AIRFOIL
MANUFACTURING SECTION
COORDINATES

1. Front Block Fan Rotor 1 ·

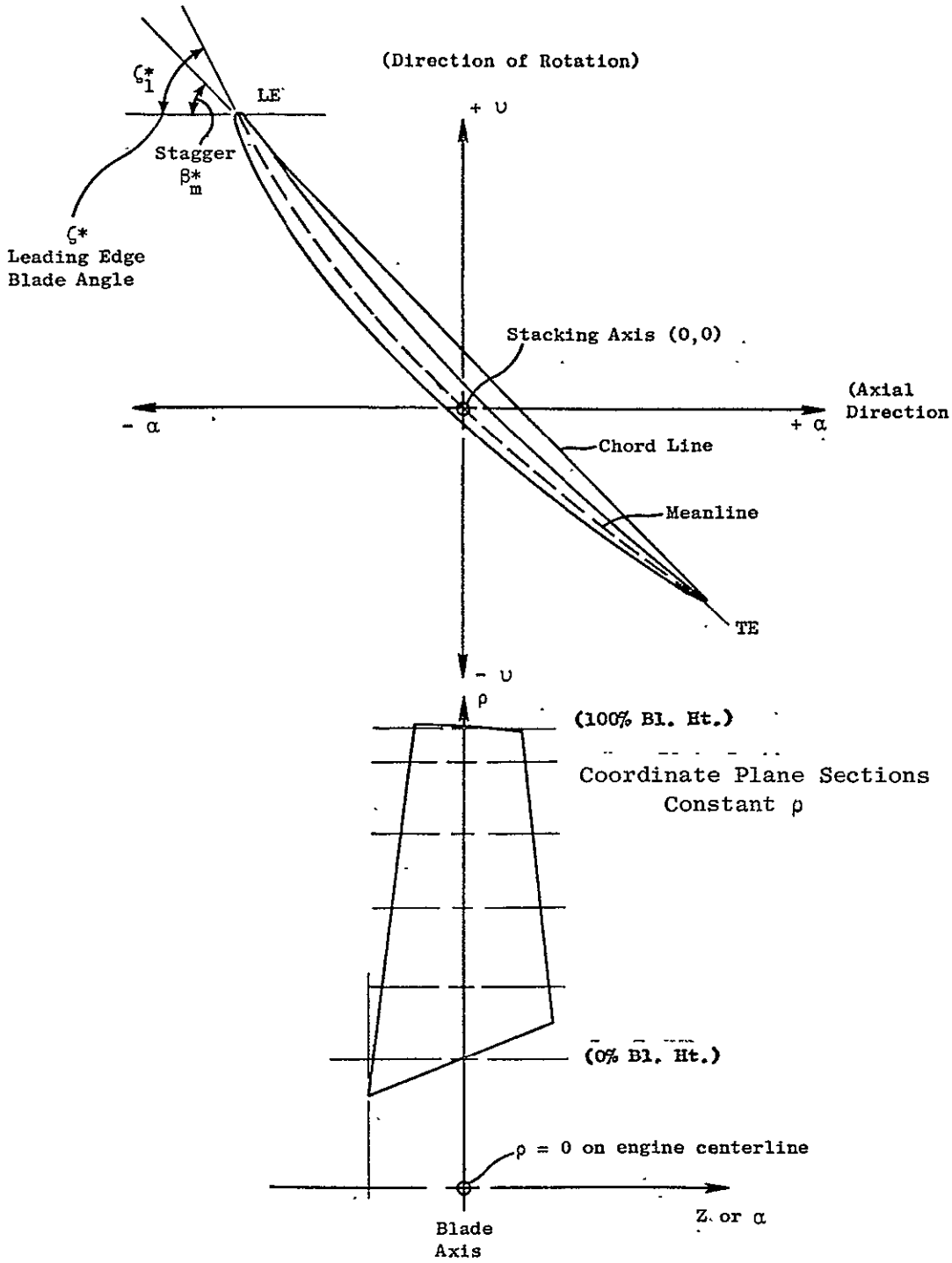

Rotor Blade Coordinate Orientation

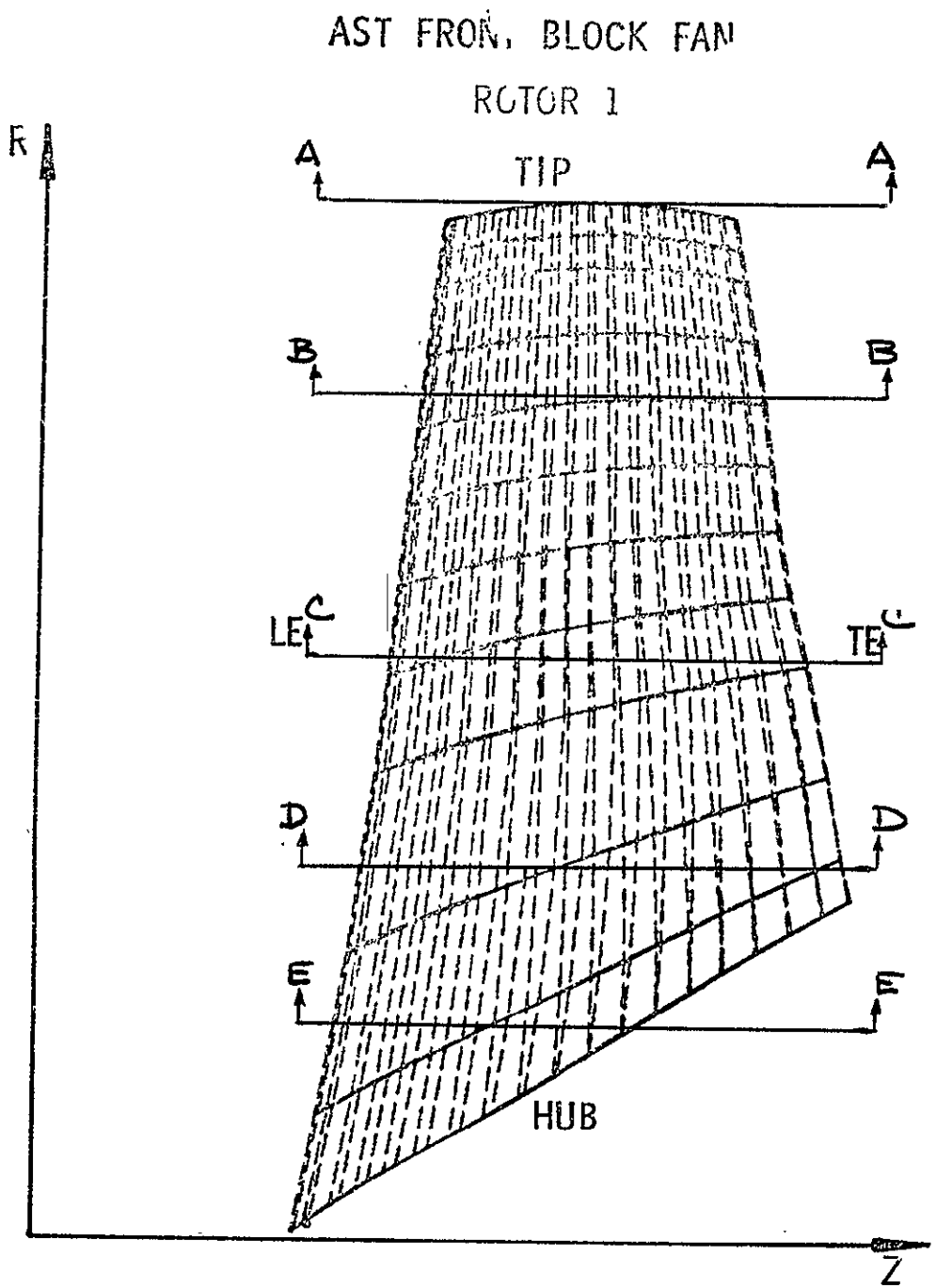
AST FRON. BLOCK FAN
ROTOR 1
R
A
TIP
A
B
B
LE
C
C
TE
D
D
E
E
HUB
Z

AST FRONT ROTOR FAN R1 (STACKED ON ZETAPL, C, 6.34218477

STAGE 1. ROTOR NB 28.

COORD SYSTEM ORIGIN Z 13.71219 R 0. MU 0. ETA 0.

SECTION NO 1 SECTION AA RHO 82.9056

MEANLINE INPUT DATA

PT	ALPHA	ZETA*	THICKNESS	UPSILON
1	-0.99597	60.981	0.13918	12.76131
2	-0.67292	60.731	0.17607	12.18353
3	-0.02065	60.362	0.24904	11.03264
4	-0.36223	60.210	0.32009	9.88041
5	-1.69777	60.320	0.38778	8.71961
6	-3.96134	60.449	0.45715	7.42411
7	-3.15183	60.637	0.52516	5.99145
8	-2.33726	61.020	0.58368	4.53433
9	-1.51926	61.835	0.63122	3.03465
10	-0.69859	62.922	0.66663	1.48549
11	0.12268	63.469	0.68914	-0.16580
12	0.94324	63.290	0.69838	-1.80550
13	1.76110	62.664	0.68851	-3.41095
14	2.57445	61.802	0.64915	-4.95801
15	3.38265	60.933	0.58180	-6.43699
16	4.18428	60.420	0.48961	-7.86222
17	4.97764	60.420	0.37725	-9.25990
18	5.76212	60.715	0.25033	-10.64912
19	6.40742	61.080	0.13823	-11.81010

SURFACE COORDINATES WITH ORIGIN AT SECTION AXIS

PT	T/C	UPPER ALPHA	UPPER UPSILON	LOWER ALPHA	LOWER UPSILON
1	0.00497	-6.99597	12.76131	-6.99597	12.76131
2	0.00497	-7.00822	12.74341	-6.97439	12.76228
3	0.00497	-7.01048	12.70894	-6.94395	12.74606
4	0.00497	-7.00149	12.65862	-6.90592	12.71194
5	0.00497	-6.97969	12.59330	-6.86183	12.65906
6	0.00497	-6.94415	12.51352	-6.81258	12.58693
7	0.00497	-6.89574	12.41878	-6.75725	12.49605
8	0.00634	-6.73824	12.11865	-6.58353	12.20556
9	0.00769	-6.41939	11.51577	-6.23221	11.62200
10	0.00902	-6.10034	10.91764	-5.88110	11.04267
11	0.01032	-5.78102	10.32164	-5.53024	10.46499
12	0.01159	-5.46134	9.72699	-5.17975	9.88819
13	0.01283	-5.14127	9.13312	-4.82966	9.31144
14	0.01402	-4.82081	8.53872	-4.47995	8.73320
15	0.01517	-4.49986	7.94265	-4.13073	8.15253
16	0.01629	-4.17892	7.22541	-3.71246	7.45293
17	0.01773	-3.72707	6.50655	-3.29511	6.75056
18	0.01888	-3.33929	5.78576	-2.87868	6.04489
19	0.01995	-2.95061	5.06223	-2.46316	5.33469
20	0.02093	-2.56105	4.33385	-2.04852	4.61750
21	0.02181	-2.17062	3.59797	-1.63474	3.89024
22	0.02259	-1.77934	2.85071	-1.22183	3.14874
23	0.02326	-1.38693	2.08825	-0.81003	2.38981
24	0.02382	-0.99319	1.30943	-0.39956	1.61291
25	0.02427	-0.59775	0.51471	0.00919	0.81980
26	0.02461	-0.20932	-0.28991	0.41597	0.0178I
27	0.02484	0.19895	-1.09674	0.82091	-0.78585
28	0.02495	0.60012	-1.90041	1.22394	-1.58657
29	0.02490	1.00349	-2.69662	1.62477	-2.38065
30	0.02464	1.40971	-3.48209	2.02276	-3.16595
31	0.02412	1.81944	-4.25419	2.41723	-3.94072
32	0.02332	2.23263	-5.01696	2.80824	-4.70325
33	0.02227	2.64847	-5.75094	3.19621	-5.45245
34	0.02099	3.06777	-6.47506	3.58151	-6.19003
35	0.01948	3.48915	-7.16573	3.96433	-6.91857
36	0.01775	3.91273	-7.86476	4.34496	-7.64197
37	0.01582	4.33841	-8.58261	4.72348	-8.36397
38	0.01372	4.76606	-9.27615	5.10003	-9.08654
39	0.01147	5.19541	-9.96964	5.47489	-9.81158
40	0.00909	5.62621	-10.66690	5.84829	-10.54251
41	0.00704	5.98627	-11.25354	6.15840	-11.15792
42	0.00494	6.31094	-11.78459	6.43701	-11.71480
43	0.00494	6.35920	-11.81560	6.44252	-11.76424
44	0.00494	6.40742	-11.81010	6.40742	-11.81010

LE RAD 0.01941 CENTER AT ALPHA -6.98651 UPSILON 12.74436

TE RAD 0.00711 CENTER AT ALPHA 6.37249 UPSILON -11.74701

ZPC

AST FRONT BLOCK FAN R1 (STACKED ON ZETAPL, C, G,)4/18/77

STAGE 1, ROTOR NB 20

COORD SYSTEM ORIGIN Z 13,71219 R 0, MU 0, ETA 0,

SECTION NO 2 SECTION BR RHO 73,6600

MEANLINE INPUT DATA

PT	ALPHA	ZETA*	THICKNESS	UPSILON
1	-8,09109	55,480	0,16322	11,24199
2	-7,70465	55,023	0,20649	10,68561
3	-6,92733	54,201	0,29282	9,59342
4	-6,14452	53,779	0,37733	8,51999
5	-5,35670	53,945	0,45829	7,44446
6	-4,48489	54,843	0,54124	6,23140
7	-3,52424	56,055	0,62192	4,84100
8	-2,56595	56,329	0,68972	3,39951
9	-1,59905	55,515	0,74249	1,96729
10	-0,62872	54,146	0,77840	0,58960
11	0,34005	52,868	0,79624	-0,72368
12	1,31774	51,955	0,79359	-1,98758
13	2,29184	51,344	0,76417	-3,21776
14	3,26561	51,029	0,70875	-4,42767
15	4,23821	50,976	0,62963	-5,62766
16	5,20916	51,004	0,53014	-6,82586
17	6,17709	51,072	0,41442	-8,02248
18	7,14115	51,292	0,28746	-9,21984
19	7,94072	51,594	0,17705	-10,22285

SURFACE COORDINATES WITH ORIGIN AT SECTION AXIS

PT	T/C	UPPER ALPHA	UPPER UPSILON	LOWER ALPHA	LOWER UPSILON
1	0,00609	-8,09109	11,24199	-8,09109	11,24199
2	0,00609	-8,10349	11,21970	-8,06582	11,24561
3	0,00609	-8,10242	11,17917	-8,02831	11,23013
4	0,00609	-8,08648	11,12136	-7,97992	11,19462
5	0,00609	-8,05393	11,04745	-7,92227	11,13797
6	0,00609	-8,00374	10,95816	-7,85629	11,05954
7	0,00609	-7,93684	10,85285	-7,78091	10,96006
8	0,00777	-7,77548	10,60539	-7,60511	10,72489
9	0,00944	-7,39242	10,02511	-7,18658	10,17186
10	0,01109	-7,00907	9,45334	-6,76834	9,62739
11	0,01272	-6,62546	8,88861	-6,35035	9,08952
12	0,01431	-6,24168	8,32834	-5,93254	8,55510
13	0,01586	-5,85773	7,76968	-5,51490	8,02089
14	0,01737	-5,47363	7,20982	-5,09741	7,48370
15	0,01882	-5,08944	6,64582	-4,68001	6,94005
16	0,02047	-4,62830	5,95852	-4,17925	6,27356
17	0,02203	-4,14625	5,25519	-3,67939	5,58866
18	0,02346	-3,70274	4,53736	-3,18099	4,88793
19	0,02477	-3,23713	3,80888	-2,68469	4,17662
20	0,02594	-2,76898	3,07765	-2,19093	3,46362
21	0,02697	-2,29833	2,35195	-1,69967	2,75668
22	0,02785	-1,82512	1,63778	-1,21097	2,06153
23	0,02857	-1,34960	0,93999	-0,72459	1,38188
24	0,02913	-0,87193	0,26621	-0,24035	0,71856
25	0,02952	-0,39248	-0,40107	0,24212	0,07084
26	0,02974	0,08845	-1,04595	0,72309	-0,56427
27	0,02978	0,57103	-1,67700	1,20242	-1,18942
28	0,02959	1,05568	-2,29584	1,67968	-1,80686
29	0,02915	1,54269	-2,90394	2,15458	-2,41870
30	0,02846	2,03191	-3,50314	2,62726	-3,02676
31	0,02754	2,52326	-4,09533	3,09782	-3,63257
32	0,02639	3,01669	-4,68199	3,56630	-4,23737
33	0,02502	3,51212	-5,26451	4,03278	-4,84234
34	0,02345	4,00944	-5,84427	4,49737	-5,44854
35	0,02169	4,50861	-6,42259	4,96011	-6,05672
36	0,01976	5,00956	-7,00002	5,42107	-6,66690
37	0,01768	5,51210	-7,57685	5,88043	-7,27901
38	0,01547	6,01604	-8,15324	6,33841	-7,89285
39	0,01315	6,52105	-8,72954	6,79531	-8,50854
40	0,01074	7,02688	-9,30731	7,25138	-9,12734
41	0,00869	7,44895	-9,79122	7,63090	-9,64617
42	0,00661	7,81343	-10,21095	7,95811	-10,09617
43	0,00661	7,86958	-10,28184	7,97545	-10,15749
44	0,00661	7,94072	-10,22285	7,94072	-10,22285

LE RAD 0,02314 CENTER AT ALPHA -8,07798 UPSILON 11,22292

TE RAD 0,09243 CENTER AT ALPHA 7,88329 UPSILON -10,15043

AST FRONT BLOCK FAN R1 (STACKED ON ZETAPL, C, G.)4/18/77

STAGE 1, ROTOR NB 28

COORD SYSTEM ORIGIN Z 13.71219 R 0, MU 0, ETA 0,

SECTION NO 3 SECTION CC RHO -60.9600

MEANLINE INPUT DATA

PT	ALPHA	ZETA*	THICKNESS	UPSILON
1	-9.42102	50.041	0.19618	9.35792
2	-8.97089	49.360	0.30400	8.82516
3	-8.06365	48.195	0.52152	7.78894
4	-7.10805	47.786	0.73635	6.77331
5	-6.22377	48.090	0.94233	5.75012
6	-5.19704	46.436	1.15191	4.59808
7	-4.06528	47.794	1.35236	3.33101
8	-2.92241	45.184	1.51571	2.12250
9	-1.76887	41.961	1.63514	1.02858
10	-0.60550	40.019	1.70470	0.02256
11	0.56718	38.556	1.72089	-0.93735
12	1.74882	36.884	1.68319	-1.85205
13	2.94809	35.202	1.59312	-2.71950
14	4.14064	33.625	1.45336	-3.54237
15	5.35091	32.124	1.26810	-4.32557
16	6.57163	30.506	1.04231	-5.06970
17	7.80330	28.754	0.78205	-5.77101
18	9.04550	27.081	0.49449	-6.43006
19	10.08942	25.722	0.23995	-6.94813

SURFACE COORDINATES WITH ORIGIN AT SECTION AXIS

PT	T/C	UPPER ALPHA	UPPER UPSILON	LOWER ALPHA	LOWER UPSILON
1	0.00772	-9.42102	9.35792	-9.42102	9.35792
2	0.00772	-9.43492	9.32850	-9.38980	9.36630
3	0.00772	-9.43074	9.27868	-9.34164	9.35334
4	0.00772	-9.40717	9.20956	-9.27777	9.31799
5	0.00772	-9.36266	9.12244	-9.19961	9.25906
6	0.00772	-9.29635	9.01804	-9.10783	9.17599
7	0.00772	-9.20935	8.89542	-9.00104	9.06996
8	0.01231	-9.05213	8.67936	-8.81440	8.88301
9	0.01692	-8.80699	8.37759	-8.58401	8.56170
10	0.02150	-8.16138	7.48812	-7.75410	7.85288
11	0.02603	-7.71539	6.90695	-7.22457	7.35080
12	0.03045	-7.26915	6.33037	-6.69528	6.85016
13	0.03474	-6.82247	5.75499	-6.16644	6.34671
14	0.03888	-6.37509	5.17837	-5.63830	5.83741
15	0.04282	-5.92582	4.59906	-5.11205	5.32236
16	0.04726	-5.38313	3.90227	-4.48411	4.69964
17	0.05135	-4.83395	3.20804	-3.86266	4.08052
18	0.05504	-4.27664	2.52606	-3.24935	3.47667
19	0.05832	-3.71001	1.86633	-2.64535	2.89859
20	0.06115	-3.13366	1.23873	-2.05108	2.35067
21	0.06349	-2.55275	0.65601	-1.46136	1.83971
22	0.06534	-1.96909	0.09575	-0.87439	1.34550
23	0.06666	-1.38408	-0.42976	-0.28878	0.86395
24	0.06746	-0.79767	-0.93350	0.29544	0.38840
25	0.06772	-0.20615	-1.42090	0.87454	-0.08025
26	0.06746	0.39061	-1.89091	1.44841	-0.54070
27	0.06667	0.99171	-2.34235	2.01794	-0.99295
28	0.06539	1.59665	-2.77505	2.58362	-1.43712
29	0.06361	2.20477	-3.18904	3.14613	-1.87373
30	0.06137	2.81563	-3.58484	3.70590	-2.30333
31	0.05867	3.42869	-3.96317	4.26346	-2.72663
32	0.05556	4.04365	-4.32504	4.81914	-3.14422
33	0.05205	4.66049	-4.67138	5.37292	-3.55615
34	0.04816	5.27897	-5.00265	5.92507	-3.96233
35	0.04394	5.89907	-5.31909	6.47559	-4.36214
36	0.03940	6.52038	-5.62032	7.02491	-4.75478
37	0.03459	7.14202	-5.90612	7.57390	-5.14006
38	0.02953	7.76354	-6.17721	8.12300	-5.51810
39	0.02426	8.38475	-6.43435	8.67242	-5.88880
40	0.01880	9.00549	-6.67796	9.22240	-6.25199
41	0.01414	9.52186	-6.87109	9.68145	-6.58877
42	0.00948	9.92393	-7.01609	10.08015	-6.77642
43	0.00944	10.01096	-7.01700	10.09549	-6.88626
44	0.00944	10.08942	-6.94813	10.08942	-6.94813

LE RAD 0.03166 CENTER AT ALPHA -9.40069 UPSILON 9.33365,
TE RAD 0.13399 CENTER AT ALPHA 9.96878 UPSILON -6.88983

AST FRONT BLOCK FAN R1 (STACKED ON ZETAPL, C, 6,)4/18/77

STAGE 1. ROTOR NB 28

COORD SYSTEM ORIGIN Z 13.71219 R 0. HU 0. ETA 0.

SECTION NO 4 SECTION DD RHO 50.8000

MEANLINE INPUT DATA

PT	ALPHA	ZETA*	THICKNESS	UPSILON
1	=10.63702	48.222	0.22253	7.81608
2	=10.13582	47.279	0.35676	7.26361
3	=9.12310	45.511	0.62287	6.19944
4	=8.09781	44.338	0.87978	5.17618
5	=7.06999	43.437	1.12067	4.17387
6	=5.90397	41.320	1.36160	3.10969
7	=4.62577	37.573	1.58881	2.05156
8	=3.33050	34.184	1.76794	1.11361
9	=2.01895	31.379	1.89051	0.26714
10	=0.69036	28.241	1.95355	=0.49675
11	0.65590	24.779	1.95767	=1.17000
12	2.02090	20.951	1.90771	=1.74650
13	3.40636	16.646	1.80410	=2.22170
14	4.81449	11.799	1.64714	=2.58532
15	6.24868	6.422	1.43765	=2.82831
16	7.71390	0.403	1.17848	=2.93422
17	9.21744	=6.329	0.87597	=2.87814
18	10.76745	=13.456	0.54350	=2.62651
19	12.10677	=19.511	0.25790	=2.22508

SURFACE COORDINATES WITH ORIGIN AT SECTION AXIS

PT	T/C	UPPER ALPHA	UPPER UPSILON	LOWER ALPHA	LOWER UPSILON
1	0.00895	=10.63702	7.81608	=10.63702	7.81608
2	0.00895	=10.65213	7.78186	=10.60138	7.82720
3	0.00895	=10.66603	7.72514	=10.54571	7.81477
4	0.00895	=10.61734	7.64716	=10.47125	7.77768
5	0.00895	=10.56440	7.54940	=10.37942	7.71466
6	0.00895	=10.48630	7.43266	=10.27079	7.62520
7	0.00895	=10.38425	7.29588	=10.14373	7.51077
8	0.01507	=10.20589	7.06336	=9.93096	7.31800
9	0.02112	=9.68921	6.80607	=9.31045	6.76959
10	0.02703	=9.17613	5.76825	=8.69234	6.24094
11	0.03278	=8.64904	5.14488	=8.07624	5.72665
12	0.03831	=8.12604	4.53813	=7.46205	5.22104
13	0.04359	=7.59973	3.93963	=6.85117	4.72330
14	0.04860	=7.06885	3.35245	=6.24486	4.23601
15	0.05331	=6.53058	2.78018	=5.64594	3.76697
16	0.05854	=5.87399	2.12369	=4.93791	3.23621
17	0.06327	=5.20807	1.50801	=4.23920	2.74731
18	0.06743	=4.53426	0.93549	=3.54838	2.29146
19	0.07098	=3.85659	0.40445	=2.86143	1.86167
20	0.07387	=3.17458	=0.09157	=2.17881	1.45163
21	0.07611	=2.48659	=0.55584	=1.50217	1.06016
22	0.07769	=1.79218	=0.98924	=0.83195	0.68681
23	0.07863	=1.09086	=1.39117	=0.16864	0.33262
24	0.07895	=0.38363	=1.76022	0.48876	=0.00196
25	0.07868	0.32836	=2.09590	1.14139	=0.31664
26	0.07788	1.04398	=2.39799	1.79040	=0.61136
27	0.07655	1.76232	=2.66634	2.43669	=0.88658
28	0.07470	2.48351	=2.90094	3.08013	=1.14214
29	0.07235	3.20730	=3.10089	3.72096	=1.37713
30	0.06950	3.93216	=3.26498	4.36073	=1.59108
31	0.06618	4.65665	=3.39282	5.00087	=1.78393
32	0.06240	5.38032	=3.48435	5.64182	=1.95523
33	0.05819	6.10254	=3.53898	6.28423	=2.10384
34	0.05357	6.82246	=3.55588	6.92894	=2.22834
35	0.04859	7.53920	=3.53394	7.57683	=2.32658
36	0.04328	8.25199	=3.47207	8.22957	=2.39620
37	0.03771	8.95636	=3.37031	8.88892	=2.43520
38	0.03193	9.65471	=3.22912	9.55520	=2.44159
39	0.02603	10.34715	=3.04640	10.22739	=2.41054
40	0.02012	11.03202	=2.81862	10.90715	=2.33434
41	0.01523	11.59433	=2.59535	11.48203	=2.23364
42	0.01037	12.03192	=2.40156	11.93947	=2.13342
43	0.01037	12.09742	=2.34027	12.03741	=2.14537
44	0.01037	12.10677	=2.22508	12.10677	=2.22508

LE RAD 0.03751 CENTER AT ALPHA =10.61203 UPSILON 7.78811

TE RAD 0.14253 CENTER AT ALPHA 11.97223 UPSILON =2.27213

/PL

AST FRONT BLOCK FAN R1 (STACKED ON /FTAPL, C, 6,)4/18/77

STAGE 1, ROTOR NB 28

COORD SYSTEM ORIGIN Z 13,71219 R 0, MU 0, ETA 0,

SECTION NO 5, SECTION EF RHO 43,1800

MEANLINE INPUT DATA

PT	ALPHA	ZETA*	THICKNESS	UPSILON
1	-11,84581	48,297	0,24160	6,84099
2	-11,31257	47,591	0,38590	6,24843
3	-10,23301	46,240	0,66895	5,09651
4	-9,13748	44,594	0,93849	3,99996
5	-8,02680	42,040	1,19075	2,94844
6	-6,78412	38,136	1,44473	1,91346
7	-5,41678	33,536	1,68512	0,93441
8	-4,02613	29,127	1,87902	0,09500
9	-2,61621	24,246	2,02443	-0,61354
10	-1,18547	18,386	2,11693	-1,17827
11	0,26913	11,937	2,14958	-1,58041
12	1,75432	4,563	2,11759	-1,80060
13	3,28054	-3,585	2,00988	-1,81544
14	4,86005	-12,169	1,82068	-1,60148
15	6,50576	-20,859	1,55453	-1,13014
16	8,23307	-29,326	1,22644	-0,36927
17	10,05549	-37,167	0,86254	0,72181
18	11,98913	-43,913	0,49747	2,19553
19	13,70379	-48,724	0,21343	3,78375

SURFACE COORDINATES WITH ORIGIN AT SECTION AXIS

PT	T/C	UPPER ALPHA	UPPER UPSILON	LOWER ALPHA	LOWER UPSILON
1	0,00939	-11,84581	6,84099	-11,84581	6,84099
2	0,00939	-11,84234	6,80379	-11,80708	6,85302
3	0,00939	-11,85539	6,74212	-11,74666	6,83945
4	0,00939	-11,82497	6,65731	-11,66590	6,79905
5	0,00939	-11,76784	6,55092	-11,56638	6,73042
6	0,00939	-11,68354	6,42379	-11,44878	6,63297
7	0,00939	-11,57341	6,27473	-11,31136	6,50823
8	0,01610	-11,35974	5,99326	-11,05439	6,27313
9	0,02264	-10,77986	5,24742	-10,35679	5,64808
10	0,02897	-10,19629	4,52301	-9,66289	5,04390
11	0,03505	-9,60774	3,81982	-8,97395	4,46156
12	0,04086	-9,01302	3,14101	-8,29119	3,90549
13	0,04639	-8,41054	2,49097	-7,61619	3,38195
14	0,05162	-7,79971	1,87522	-6,94955	2,89593
15	0,05653	-7,18018	1,29714	-6,29160	2,44894
16	0,06108	-6,42695	0,65667	-5,51185	1,96171
17	0,06678	-5,66571	0,07208	-4,74011	1,51973
18	0,07100	-4,89613	-0,46152	-3,97672	1,11735
19	0,07464	-4,11835	-0,94677	-3,22153	0,75162
20	0,07769	-3,33016	-1,38489	-2,47674	0,42283
21	0,08013	-2,53100	-1,77329	-1,74292	0,13200
22	0,08193	-1,72097	-2,10661	-1,01998	-0,12028
23	0,08307	-0,90076	-2,38717	-0,30721	-0,33376
24	0,08353	-0,07199	-2,60581	0,39700	-0,50831
25	0,08332	0,76372	-2,76181	1,09426	-0,64359
26	0,08240	1,60444	-2,85187	1,78652	-0,73950
27	0,08073	2,44647	-2,87295	2,47747	-0,79597
28	0,07830	3,28534	-2,82431	3,17157	-0,81271
29	0,07514	4,11799	-2,70656	3,87190	-0,78880
30	0,07130	4,94172	-2,52110	4,58114	-0,72230
31	0,06684	5,75386	-2,27019	5,30198	-0,61069
32	0,06186	6,55251	-1,95754	6,03630	-0,45170
33	0,05647	7,33786	-1,58683	6,78393	-0,24356
34	0,05076	8,11104	-1,16070	7,54373	0,01593
35	0,04487	8,87276	-0,68157	8,31498	0,32945
36	0,03891	9,62346	-0,15301	9,09723	0,69829
37	0,03297	10,36542	0,41937	9,88827	1,12090
38	0,02717	11,10256	1,03635	10,68411	1,59649
39	0,02162	11,83676	1,70345	11,48289	2,13262
40	0,01641	12,56792	2,42540	12,28870	2,73851
41	0,01230	13,17375	3,05919	12,95635	3,28918
42	0,00829	13,70496	3,62852	13,50875	3,79159
43	0,00829	13,73498	3,69826	13,62267	3,81861
44	0,00829	13,70379	3,78375	13,70379	3,78375

LE RAD 0,04076 CENTER AT ALPHA -11,81869 UPSILON 6,81056
TE RAD 0,11310 CENTER AT ALPHA 13,62212 UPSILON 3,70551

APPENDIX C

BLADE AND VANE AIRFOIL
MANUFACTURING SECTION
COORDINATES

2. Front Block Fan Rotor 2

AST FRONT BLOCK FAN ROTOR 2

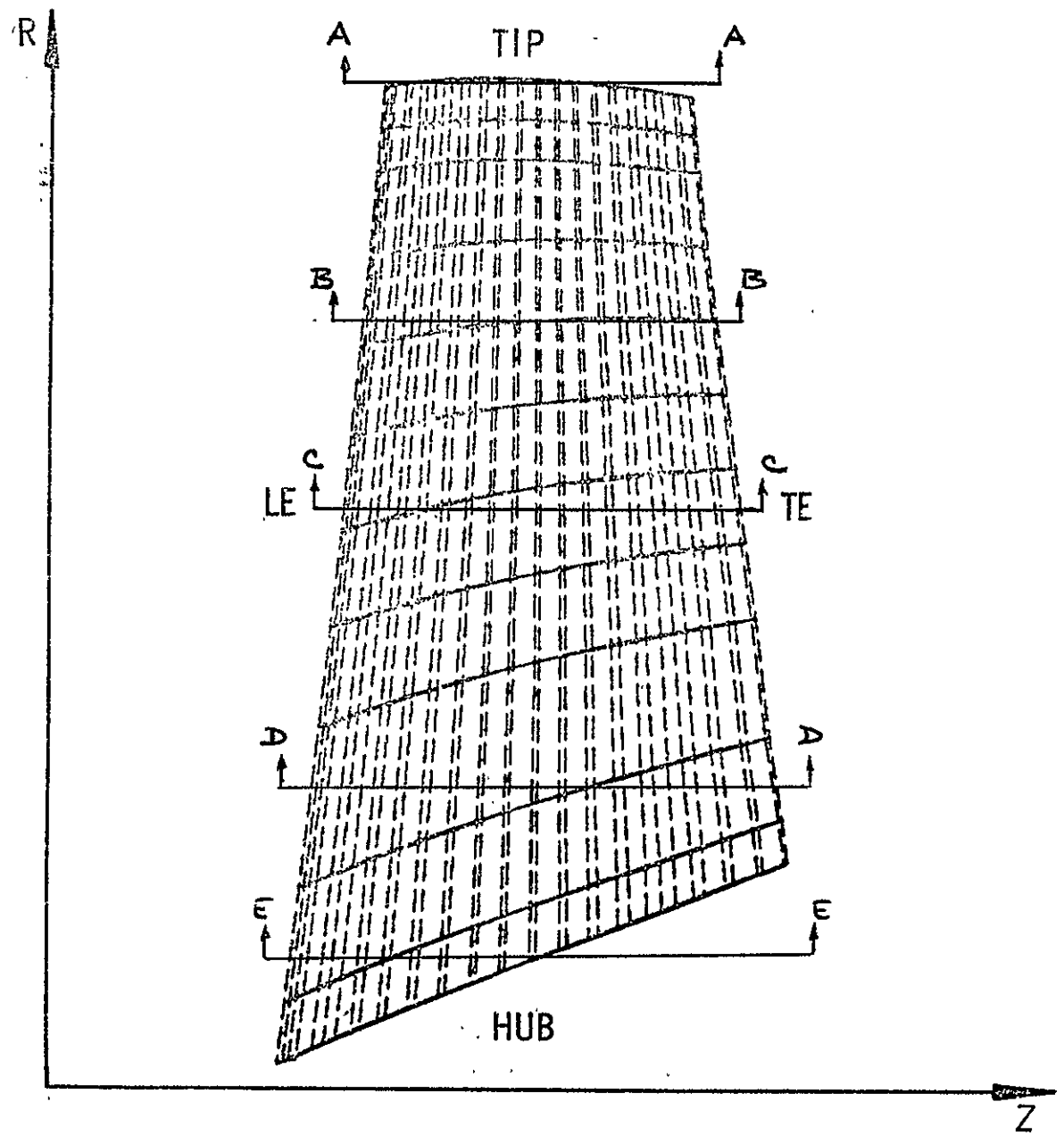

STAGE 2. ROTOR NB 42

SECTION NO 1 SECTION AA RHO 82.5500

MEANLINE DATA

PT	ALPHA	ZETA*	THICKNESS	UPSILON
1	-4.12931	63.584	0.08656	8.19362
2	-3.92536	63.383	0.10987	7.78549
3	-3.51682	63.009	0.15618	6.97644
4	-3.10704	62.755	0.20146	6.17744
5	-2.69656	62.815	0.24487	5.37991
6	-2.28369	63.522	0.28949	4.48681
7	-1.78895	64.674	0.33315	3.48739
8	-1.25357	65.462	0.37055	2.39967
9	-0.75812	65.383	0.40074	1.31103
10	-0.26251	64.230	0.42286	0.25358
11	0.23257	62.475	0.43644	-0.73397
12	0.72680	60.690	0.44152	-1.64662
13	1.21990	59.580	0.43838	-2.50367
14	1.71164	59.086	0.40846	-3.33187
15	2.20178	58.724	0.36487	-4.14439
16	2.69007	58.357	0.30602	-4.94175
17	3.17630	58.033	0.23508	-5.72623
18	3.65989	57.860	0.15588	-6.49842
19	4.06129	57.793	0.08675	-7.13747

SURFACE COORDINATES WITH ORIGIN AT SECTION AXIS

PT	T/C	UPPER ALPHA	UPPER UPSILON	LOWER ALPHA	LOWER UPSILON
1	0.00498	-4.12931	8.19362	-4.12931	8.19362
2	0.00498	-4.13656	8.18507	-4.11813	8.19426
3	0.00498	-4.13980	8.16871	-4.10321	8.18691
4	0.00498	-4.13816	8.14478	-4.08501	8.17131
5	0.00498	-4.13142	8.11360	-4.06415	8.14718
6	0.00498	-4.11888	8.07588	-4.04120	8.11421
7	0.00498	-4.10033	8.03040	-4.01635	8.07232
8	0.00498	-4.07635	7.97821	-3.98902	8.02179
9	0.00633	-3.97370	7.75924	-3.87539	7.80849
10	0.00767	-3.77926	7.34666	-3.66030	7.40672
11	0.00900	-3.58469	6.93741	-3.44534	7.00840
12	0.01031	-3.38997	6.53166	-3.23054	6.61349
13	0.01160	-3.19511	6.12827	-3.01586	6.22059
14	0.01286	-3.00010	5.72576	-2.80134	5.82812
15	0.01409	-2.80491	5.32282	-2.58700	5.43465
16	0.01528	-2.60956	4.91799	-2.37283	5.03839
17	0.01644	-2.37496	4.42590	-2.11599	4.55489
18	0.01794	-2.13998	3.92255	-1.85963	4.05869
19	0.01914	-1.90439	3.40692	-1.60369	3.54936
20	0.02026	-1.66806	2.87954	-1.34858	3.02771
21	0.02128	-1.43085	2.34261	-1.09435	2.49629
22	0.02220	-1.19259	1.79940	-0.84118	1.95894
23	0.02301	-0.95304	1.25627	-0.58930	1.42278
24	0.02371	-0.71216	0.72052	-0.33873	0.89098
25	0.02429	-0.46994	0.19767	-0.08953	0.38089
26	0.02475	-0.22640	-0.30779	0.15837	-0.11546
27	0.02509	0.01826	-0.79434	0.40515	-0.59324
28	0.02531	0.26399	-1.26191	0.65095	-1.05283
29	0.02540	0.51045	-1.71208	0.89583	-1.49665
30	0.02533	0.75801	-2.14724	1.13971	-1.92780
31	0.02504	1.00686	-2.57053	1.38229	-2.35047
32	0.02446	1.25749	-2.98547	1.62310	-2.76848
33	0.02360	1.51002	-3.39445	1.86202	-3.18371
34	0.02249	1.76432	-3.79908	2.09915	-3.59728
35	0.02114	2.02043	-4.19971	2.33446	-4.00897
36	0.01956	2.27820	-4.59601	2.56813	-4.41853
37	0.01777	2.53740	-4.98836	2.80037	-4.82637
38	0.01580	2.79789	-5.37745	3.03132	-5.23284
39	0.01367	3.05951	-5.76343	3.26113	-5.63777
40	0.01141	3.32203	-6.14639	3.49005	-6.04113
41	0.00905	3.58517	-6.52728	3.71835	-6.44366
42	0.00703	3.80478	-6.84402	3.90826	-6.77902
43	0.00499	3.99682	-7.12492	4.07666	-7.07664
44	0.00499	4.02547	-7.14291	4.08173	-7.10758
45	0.00499	4.06129	-7.13747	4.06129	-7.13747

CHORD 17.3418 STAGGER 61.887 CAMBER 5.614

AREA 5.476890 SURFACE ARC LENGTH 34.88587

	ALPHA	UPSILON
SECTION C.G.	-0.00299	0.00168
STREAMSURFACE SECTION C.G.	0.01279	-0.01781
BLADE AXIS	0.	0.
STACKING AXIS (RADIAL)	0.	0.

COORD SYSTEM ORIGIN Z 48.24019 R 0.

STAGE 2. ROTOR NR 42

SECTION NO 2 SECTION BB RHO 78.2000

MEANLINE DATA

PT	ALPHA	ZETA*	THICKNESS	UPSILON
1	-4.64612	60.343	0.11497	7.77259
2	-4.41768	60.159	0.14612	7.37348
3	-3.95915	59.873	0.20810	6.57959
4	-3.49829	59.809	0.26859	5.78683
5	-3.03505	60.006	0.32632	4.98879
6	-2.52360	60.457	0.38515	4.09547
7	-1.96303	60.899	0.44200	3.09744
8	-1.40031	60.766	0.48953	2.08623
9	-0.83574	59.697	0.52629	1.09571
10	-0.26988	57.719	0.55110	0.16314
11	0.29696	55.984	0.56313	-0.70293
12	0.86441	55.115	0.56067	-1.52836
13	1.43217	54.652	0.53925	-2.33507
14	2.00002	54.406	0.49946	-3.13128
15	2.56761	54.331	0.44301	-3.92288
16	3.13460	54.324	0.37231	-4.71288
17	3.70064	54.363	0.29041	-5.50145
18	4.26526	54.506	0.20085	-6.29108
19	4.73432	54.686	0.12313	-6.95082

SURFACE COORDINATES WITH ORIGIN AT SECTION AXIS

PT	T/C	UPPER ALPHA	UPPER UPSILON	LOWER ALPHA	LOWER UPSILON
1	0.00659	-4.64612	7.77259	-4.64612	7.77259
2	0.00659	-4.65525	7.76060	-4.63117	7.77436
3	0.00659	-4.65833	7.73864	-4.61065	7.76579
4	0.00659	-4.65476	7.70692	-4.58516	7.74655
5	0.00659	-4.64376	7.66593	-4.55545	7.71622
6	0.00659	-4.62462	7.61608	-4.52221	7.67439
7	0.00659	-4.59708	7.55751	-4.48568	7.62094
8	0.00659	-4.56189	7.48979	-4.44508	7.55630
9	0.00842	-4.47531	7.32431	-4.34792	7.39954
10	0.01024	-4.25450	6.91132	-4.09970	7.00076
11	0.01205	-4.03355	6.49827	-3.85163	6.60381
12	0.01383	-3.81240	6.08672	-3.60376	6.20806
13	0.01557	-3.59101	5.67601	-3.35613	5.81270
14	0.01726	-3.36937	5.26535	-3.10875	5.41665
15	0.01890	-3.14745	4.85348	-2.86164	5.01842
16	0.02048	-2.92518	4.43917	-2.61489	4.61680
17	0.02198	-2.69785	3.93792	-2.31939	4.12955
18	0.02396	-2.38966	3.43183	-2.02476	3.63638
19	0.02552	-2.12041	2.92186	-1.73118	3.13849
20	0.02693	-1.84984	2.40973	-1.43893	2.63825
21	0.02820	-1.57770	1.89921	-1.14824	2.13991
22	0.02931	-1.30378	1.39467	-0.85933	1.64878
23	0.03026	-1.02785	0.90120	-0.57244	1.16880
24	0.03103	-0.75004	0.42358	-0.28782	0.70546
25	0.03163	-0.47040	-0.03619	-0.00419	0.25957
26	0.03204	-0.18955	-0.47734	0.27775	-0.16987
27	0.03227	0.09215	-0.90297	0.55887	-0.58742
28	0.03230	0.37478	-1.31722	0.83907	-0.99719
29	0.03209	0.65868	-1.72298	1.11799	-1.40233
30	0.03159	0.94430	-2.12271	1.39520	-1.80508
31	0.03083	1.23171	-2.51759	1.67061	-2.20610
32	0.02981	1.52079	-2.90834	1.94437	-2.60605
33	0.02854	1.81143	-3.29583	2.21655	-3.00577
34	0.02704	2.10361	-3.68102	2.48719	-3.40593
35	0.02532	2.39728	-4.06455	2.75636	-3.80688
36	0.02339	2.69234	-4.44691	3.02412	-4.20879
37	0.02129	2.98870	-4.82827	3.29059	-4.61154
38	0.01902	3.28617	-5.20872	3.55595	-5.01509
39	0.01662	3.58457	-5.58872	3.82037	-5.41948
40	0.01411	3.88374	-5.96880	4.08403	-5.82554
41	0.01150	4.18354	-6.34945	4.34705	-6.23282
42	0.00929	4.43372	-6.66741	4.56589	-6.57303
43	0.00705	4.64612	-6.93797	4.75101	-6.46334
44	0.00705	4.68404	-6.96141	4.76099	-6.90672
45	0.00705	4.73432	-6.95082	4.73432	-6.95082

CHORD	STAGGER	CAMBER
17.4577	57.498	5.658

AREA 7.000774 SURFACE ARC LENGTH 35.07468

	ALPHA	UPSILON
SECTION C.G.	0.00619	-0.00645
STREAMSURFACE SECTION C.G.	-0.02345	0.02466
BLADE AXIS	0.	0.
STACKING AXIS (RADIAL)	0.	0.

COORD SYSTEM ORIGIN Z 48.29019 R 0.

ZPC

AST FRONT FAN R2 (STACKED ON Z-PL CG)

STAGE 2. ROTOR NR 42.

COORD SYSTEM ORIGIN Z 48.24019 R 0. MU 0. ETA 0.

SECTION NO 3 SECTION CC RHO 71.1200

MEANLINE INPUT DATA

PT	ALPHA	ZETA*	THICKNESS	UPSILON
1	-5.11568	57.096	0.13767	7.44441
2	-4.86356	57.136	0.17601	7.05540
3	-4.35726	57.266	0.25251	6.27233
4	-3.84815	57.435	0.32723	5.47953
5	-3.33631	57.608	0.39843	4.67704
6	-2.77020	57.747	0.47075	3.78323
7	-2.18902	57.352	0.54030	2.80450
8	-1.52466	55.834	0.59765	1.85534
9	-0.89693	53.976	0.64024	0.96289
10	-0.26658	52.681	0.66624	0.11730
11	0.36669	51.677	0.67474	-0.69892
12	1.00220	50.769	0.66371	-1.48975
13	1.64032	50.025	0.63274	-2.26075
14	2.28042	49.412	0.58295	-3.01626
15	2.92280	48.841	0.51627	-3.75829
16	3.56685	48.252	0.43509	-4.48733
17	4.21271	47.717	0.34230	-5.20323
18	4.85970	47.392	0.24123	-5.91056
19	5.39965	47.246	0.15343	-6.49554

SURFACE COORDINATES WITH ORIGIN AT SECTION AXIS

PT	T/C	UPPER ALPHA	UPPER UPSILON	LOWER ALPHA	LOWER UPSILON
1	0.00788	-5.11568	7.44441	-5.11568	7.44441
2	0.00788	-5.12594	7.42940	-5.09775	7.44764
3	0.00788	-5.12830	7.40278	-5.07246	7.43890
4	0.00788	-5.12209	7.36497	-5.04048	7.41777
5	0.00788	-5.10643	7.31653	-5.00266	7.38368
6	0.00788	-5.08055	7.25799	-4.95979	7.33612
7	0.00788	-5.04419	7.18949	-4.91210	7.27495
8	0.00788	-4.99823	7.11047	-4.85874	7.20072
9	0.01017	-4.92733	6.99048	-4.77826	7.08712
10	0.01246	-4.68125	6.57370	-4.49858	6.69179
11	0.01472	-4.43507	6.15581	-4.21899	6.29500
12	0.01695	-4.18866	5.73664	-3.93963	5.89647
13	0.01912	-3.94192	5.31628	-3.66060	5.49621
14	0.02124	-3.69476	4.89485	-3.38199	5.09420
15	0.02328	-3.44710	4.47234	-3.10389	4.69027
16	0.02524	-3.19880	4.04875	-2.82642	4.28447
17	0.02746	-2.89985	3.53957	-2.49445	3.79563
18	0.02953	-2.59931	3.03089	-2.16408	3.30731
19	0.03142	-2.29676	2.52712	-1.83571	2.82458
20	0.03313	-1.99195	2.03309	-1.50960	2.35205
21	0.03463	-1.68459	1.55336	-1.18603	1.89552
22	0.03591	-1.37535	1.09133	-0.86436	1.45462
23	0.03695	-1.06458	0.64544	-0.54421	1.02676
24	0.03774	-0.75238	0.21320	-0.22549	0.60904
25	0.03829	-0.43887	-0.20786	0.09192	0.19875
26	0.03859	-0.12369	-0.61989	0.40766	-0.20545
27	0.03862	0.19338	-1.02320	0.72151	-0.60381
28	0.03837	0.51227	-1.41786	1.03354	-0.99693
29	0.03784	0.83289	-1.80449	1.34384	-1.38565
30	0.03702	1.15518	-2.18385	1.65247	-1.77076
31	0.03594	1.47904	-2.55671	1.95952	-2.15300
32	0.03460	1.80452	-2.92382	2.26497	-2.53269
33	0.03301	2.13153	-3.28540	2.56888	-2.90984
34	0.03120	2.45990	-3.64160	2.87143	-3.28456
35	0.02918	2.78951	-3.99278	3.17274	-3.65709
36	0.02696	3.12032	-4.33927	3.47285	-4.02735
37	0.02456	3.45222	-4.68089	3.77187	-4.39488
38	0.02202	3.78487	-5.01753	4.07014	-4.75977
39	0.01934	4.11806	-5.35013	4.36786	-5.12284
40	0.01656	4.45179	-5.67979	4.66506	-5.48463
41	0.01368	4.78597	-6.00688	4.96180	-5.84567
42	0.01125	5.06463	-6.27770	5.20890	-6.14447
43	0.00879	5.28820	-6.49427	5.40710	-6.38434
44	0.00879	5.33886	-6.51689	5.42568	-6.43678
45	0.00879	5.39965	-6.49554	5.39965	-6.49554

LE RAD 0.02009 CENTER AT ALPHA -5.10477 UPSILON 7.42754
TE RAD 0.08109 CENTER AT ALPHA 5.38460 UPSILON -6.43600

STAGE 2. ROTOR NR 42

SECTION NO 4 SECTION DD RHO 63.5000

MEANLINE DATA

PT	ALPHA	ZETA*	THICKNESS	UPSILON
1	-5.90439	52.455	0.17213	6.85428
2	-5.61870	52.704	0.22588	6.88025
3	-5.04423	52.993	0.33360	5.72009
4	-4.46459	52.800	0.43934	4.95132
5	-3.88048	52.126	0.54049	4.18849
6	-3.23221	51.120	0.64301	3.34726
7	-2.51855	49.948	0.74009	2.49853
8	-1.79808	48.791	0.81785	1.65842
9	-1.07130	47.528	0.87338	0.84619
10	-0.33805	46.096	0.90404	0.06452
11	0.40179	44.647	0.90876	-0.68508
12	1.14836	43.198	0.88931	-1.40442
13	1.90202	41.679	0.84623	-2.09405
14	2.66331	40.067	0.78030	-2.75313
15	3.43290	38.343	0.69303	-3.38100
16	4.21125	36.479	0.58649	-3.97540
17	4.99870	34.452	0.46311	-4.53486
18	5.79555	32.331	0.32579	-5.05836
19	6.46687	30.496	0.20325	-5.46639

SURFACE COORDINATES WITH ORIGIN AT SECTION AXIS

PT	T/C	UPPER ALPHA	UPPER UPSILON	LOWER ALPHA	LOWER UPSILON
1	0.00986	-5.90439	6.85428	-5.90439	6.85428
2	0.00986	-5.91612	6.83420	-5.88199	6.86042
3	0.00986	-5.91683	6.80042	-5.84921	6.85239
4	0.00986	-5.90583	6.75349	-5.80677	6.82963
5	0.00986	-5.88218	6.69413	-5.75567	6.79137
6	0.00986	-5.84506	6.62298	-5.69677	6.73695
7	0.00986	-5.79427	6.54018	-5.63036	6.66616
8	0.00986	-5.73087	6.44492	-5.55542	6.57977
9	0.01319	-5.68682	6.37955	-5.50340	6.51887
10	0.01652	-5.40096	5.95174	-5.17070	6.12753
11	0.01983	-5.11483	5.52609	-4.83826	5.73425
12	0.02307	-4.82808	5.09819	-4.50645	5.34077
13	0.02625	-4.54040	4.67217	-4.17557	4.94951
14	0.02933	-4.25163	4.25016	-3.84577	4.56241
15	0.03229	-3.96154	3.83374	-3.51730	4.18088
16	0.03511	-3.67007	3.42412	-3.19021	3.80557
17	0.03827	-3.31832	2.94229	-2.79969	3.36388
18	0.04117	-2.96428	2.47160	-2.41145	2.93093
19	0.04376	-2.60784	2.01220	-2.02562	2.50695
20	0.04603	-2.24900	1.56408	-1.64218	2.09106
21	0.04797	-1.88769	1.12681	-1.26121	1.68260
22	0.04955	-1.52361	0.70033	-0.88302	1.28173
23	0.05076	-1.15667	0.28524	-0.50769	0.88877
24	0.05159	-0.78693	-0.11794	-0.13515	0.50375
25	0.05203	-0.41449	-0.50893	0.23469	0.12658
26	0.05210	-0.03973	-0.88779	0.60220	-0.24323
27	0.05183	0.33712	-1.25508	0.96762	-0.60606
28	0.05121	0.71602	-1.61121	1.33101	-0.96207
29	0.05027	1.09688	-1.95625	1.69241	-1.31141
30	0.04901	1.47967	-2.29023	2.05191	-1.65402
31	0.04743	1.86421	-2.61305	2.40964	-1.98983
32	0.04556	2.25028	-2.92466	2.76585	-2.31889
33	0.04340	2.63772	-3.22518	3.12069	-2.64123
34	0.04098	3.02644	-3.51463	3.47424	-2.95662
35	0.03830	3.41625	-3.79281	3.82670	-3.26479
36	0.03540	3.80686	-4.05961	4.17837	-3.56561
37	0.03229	4.19805	-4.31503	4.52945	-3.85902
38	0.02898	4.58954	-4.55917	4.88020	-4.14499
39	0.02550	4.98123	-4.79227	5.23083	-4.42352
40	0.02188	5.37290	-5.01446	5.58183	-4.69443
41	0.01812	5.76443	-5.22558	5.93218	-4.95736
42	0.01490	6.09021	-5.39300	6.22496	-5.17049
43	0.01164	6.32328	-5.50836	6.42420	-5.31249
44	0.01164	6.39611	-5.51762	6.47703	-5.37565
45	0.01164	6.46687	-5.46639	6.46687	-5.46639

CHORD 17.4599 STAGGER 44.883 CAMBER 21.959

AREA 11.378515 SURFACE ARC LENGTH 35.37815

	ALPHA	UPSILON
SECTION C.G.	0.05503	-0.01178
STREAMSURFACE SECTION C.G.	-0.20735	0.12506
BLADE AXIS	0.	0.
STACKING AXIS (RADIAL)	0.	0.

COORD SYSTEM ORIGIN Z 48.20019 R 0.

ZPC

AST FRONT FAN R2 (STACKED ON Z-PL CG)

STAGE 2. ROTOR NR 42

COORD SYSTEM ORIGIN Z 48.24819 R 0. MU 0. ETA 0.

SECTION NO 5 SECTION EE RHO 58.4200

MEANLINE INPUT DATA

PT	ALPHA	ZETA*	THICKNESS	UPSILON
1	-6.44764	50.672	0.19541	6.57499
2	-6.13931	50.810	0.26529	6.19782
3	-5.51684	50.943	0.39996	5.43201
4	-4.88736	50.544	0.53490	4.65949
5	-4.25130	49.688	0.66448	3.89676
6	-3.54388	48.403	0.79645	3.08095
7	-2.76393	46.691	0.92296	2.22762
8	-1.97621	44.613	1.02642	1.42121
9	-1.18063	42.500	1.10159	0.66545
10	-0.37747	40.403	1.14492	-0.04345
11	0.43360	38.282	1.15607	-0.70805
12	1.25315	36.167	1.13649	-1.33103
13	2.08173	33.695	1.08547	-1.91082
14	2.92036	30.803	1.00395	-2.44060
15	3.76965	27.711	0.89319	-2.91650
16	4.63155	24.403	0.75487	-3.34027
17	5.50734	20.583	0.59127	-3.70543
18	6.40121	15.929	0.40403	-4.00458
19	7.16112	11.246	0.23353	-4.19009

SURFACE COORDINATES WITH ORIGIN AT SECTION AXIS

PT	T/C	UPPER ALPHA	UPPER UPSILON	LOWER ALPHA	LOWER UPSILON
1	0.01126	-6.44764	6.57499	-6.44764	6.57499
2	0.01126	-6.46057	6.55150	-6.42205	6.58306
3	0.01126	-6.46053	6.51286	-6.38416	6.57544
4	0.01126	-6.44680	6.45967	-6.33472	6.55150
5	0.01126	-6.41836	6.39275	-6.27475	6.51041
6	0.01126	-6.37437	6.31278	-6.20514	6.45184
7	0.01126	-6.31465	6.21994	-6.12611	6.37441
8	0.01126	-6.24035	6.11325	-6.03654	6.28024
9	0.01558	-6.21218	6.07332	-6.00266	6.24411
10	0.01989	-5.90117	5.63166	-5.63322	5.84926
11	0.02418	-5.58984	5.18910	-5.26412	5.45347
12	0.02840	-5.27762	4.74725	-4.89591	5.05881
13	0.03252	-4.96401	4.30886	-4.52907	4.66839
14	0.03652	-4.64887	3.87648	-4.16378	4.28426
15	0.04037	-4.33192	3.45162	-3.80028	3.90763
16	0.04403	-4.01308	3.03543	-3.43869	3.53906
17	0.04814	-3.62771	2.54832	-3.00753	3.10797
18	0.05193	-3.23899	2.07564	-2.57973	2.68988
19	0.05535	-2.84663	1.61862	-2.15557	2.28559
20	0.05837	-2.45051	1.17840	-1.73516	1.89541
21	0.06095	-2.05060	0.75590	-1.31855	1.51919
22	0.06306	-1.64744	0.35142	-0.90517	1.15539
23	0.06468	-1.24107	-0.03591	-0.49502	0.80261
24	0.06581	-0.83134	-0.40675	-0.08823	0.46039
25	0.06646	-0.41850	-0.76124	0.31546	0.12823
26	0.06664	-0.00304	-1.09976	0.71652	-0.19458
27	0.06638	0.41486	-1.42301	1.11515	-0.50848
28	0.06569	0.83529	-1.73125	1.51124	-0.81358
29	0.06454	1.25835	-2.02441	1.90471	-1.10980
30	0.06297	1.68428	-2.30205	2.29531	-1.39625
31	0.06098	2.11267	-2.56315	2.68344	-1.67216
32	0.05859	2.54295	-2.80690	3.06969	-1.93727
33	0.05582	2.97451	-3.03282	3.45465	-2.19155
34	0.05269	3.40634	-3.24099	3.83935	-2.43580
35	0.04921	3.83837	-3.43242	4.22385	-2.67057
36	0.04540	4.27127	-3.60742	4.60747	-2.89498
37	0.04129	4.70449	-3.76493	4.99078	-3.10808
38	0.03691	5.13675	-3.90447	5.37504	-3.31004
39	0.03226	5.56784	-4.02679	5.76048	-3.50120
40	0.02738	5.99937	-4.13117	6.14547	-3.67919
41	0.02228	6.43040	-4.21302	6.53097	-3.83979
42	0.01790	6.79510	-4.26303	6.85670	-3.96084
43	0.01346	7.01915	-4.29095	7.07662	-4.03814
44	0.01346	7.10082	-4.27331	7.14507	-4.09316
45	0.01346	7.16112	-4.19009	7.16112	-4.19009

LE RAD 0.03113 CENTER AT ALPHA -6.42781 UPSILON 6.55091

TE RAD 0.13042 CENTER AT ALPHA 7.03590 UPSILON -4.16136

APPENDIX C

BLADE AND VANE AIRFOIL
MANUFACTURING SECTION
COORDINATES

3. Front Block Fan Stator 1

FRONT BLOCK FAN STATOR 1

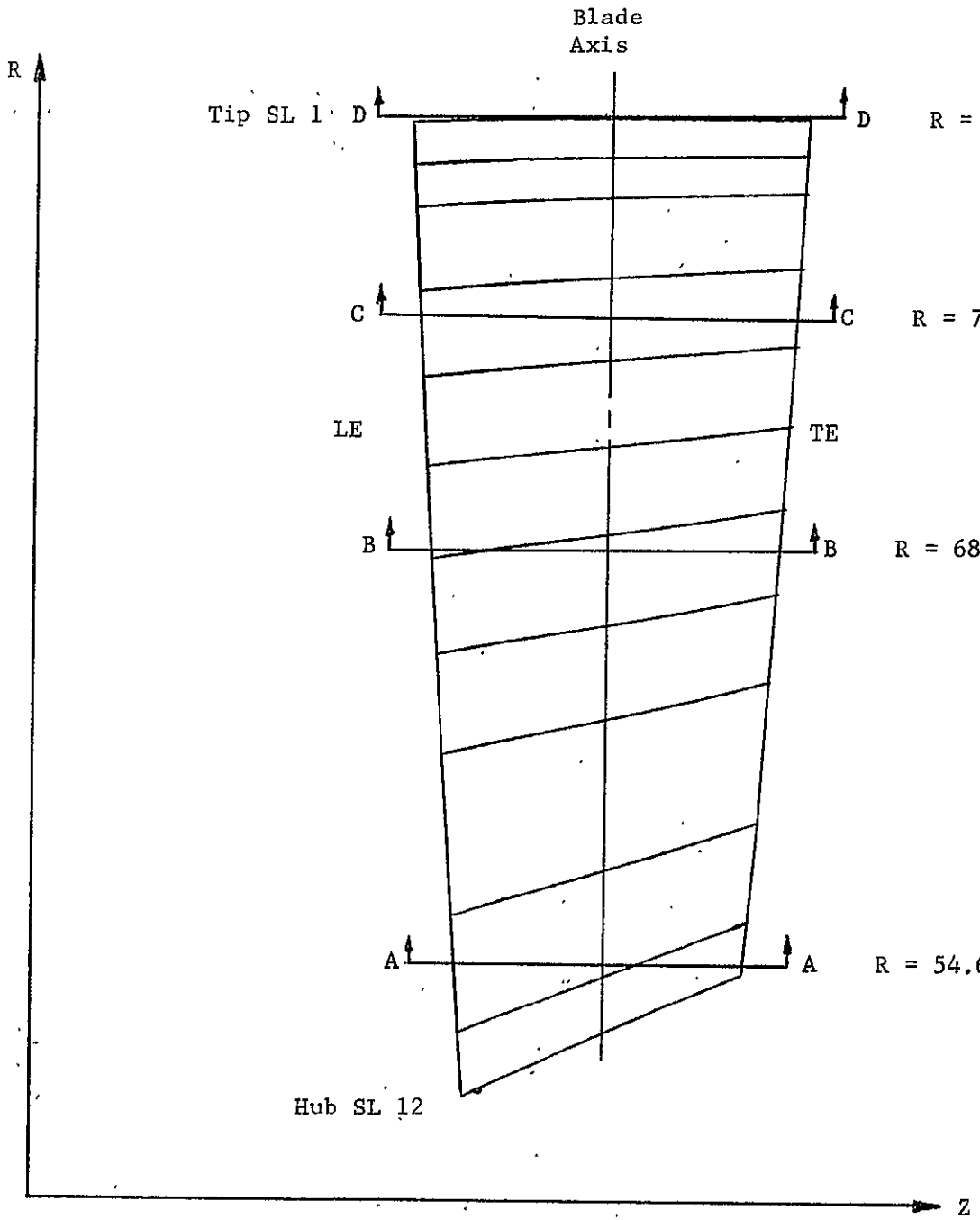

No. Vanes = 72

Aspect Ratio = 2.57

Solidity (P/L) = 2.01

STAGE 1. STATOR NR 72

SECTION NO 1 SECTION AA RHO 50.6100

MEANLINE DATA

PT	ALPHA	ZETA*	THICKNESS	UPSILON
1	-4.78127	44.645	0.10458	-3.03321
2	-4.53627	43.431	0.15030	-2.79563
3	-4.04831	40.821	0.23873	-2.35332
4	-3.56286	38.042	0.32103	-1.99365
5	-3.07993	35.211	0.39498	-1.59408
6	-2.55140	32.224	0.46427	-1.24111
7	-1.97810	29.225	0.52287	-0.90052
8	-1.40830	26.434	0.56160	-0.59995
9	-0.84218	23.723	0.57918	-0.33045
10	-0.27974	20.977	0.57564	-0.10327
11	0.27872	18.194	0.55681	0.09538
12	0.83330	15.398	0.52535	0.26279
13	1.38324	12.600	0.48259	0.40016
14	1.92860	9.800	0.43017	0.50819
15	2.46921	6.992	0.36985	0.58788
16	3.00498	4.179	0.30364	0.64023
17	3.53590	1.364	0.23364	0.66545
18	4.06207	-1.653	0.16198	0.66391
19	4.49645	-4.119	0.10249	0.64212

SURFACE COORDINATES WITH ORIGIN AT SECTION AXIS

PT	T/C	UPPER ALPHA	UPPER UPSILON	LOWER ALPHA	LOWER UPSILON
1	0.01048	-4.77208	-3.04251	-4.77208	-3.04251
2	0.01048	-4.77898	-3.02604	-4.76007	-3.04693
3	0.01048	-4.77618	-3.00640	-4.74052	-3.04347
4	0.01048	-4.76319	-2.96610	-4.71390	-3.03167
5	0.01048	-4.73933	-2.92382	-4.68075	-3.01097
6	0.01048	-4.70401	-2.87416	-4.64133	-2.98113
7	0.01048	-4.65699	-2.81737	-4.59512	-2.94265
8	0.01048	-4.59882	-2.75288	-4.49834	-2.86160
9	0.01910	-4.38152	-2.52161	-4.25324	-2.66248
10	0.02328	-4.16165	-2.29795	-4.00923	-2.47308
11	0.02733	-3.94061	-2.08340	-3.76639	-2.29302
12	0.03123	-3.71830	-1.87786	-3.52481	-2.12194
13	0.03495	-3.49465	-1.68131	-3.28457	-1.95948
14	0.03847	-3.26964	-1.49369	-3.04570	-1.80527
15	0.04176	-3.04325	-1.31494	-2.80820	-1.65886
16	0.04439	-2.76991	-1.11195	-2.52488	-1.49260
17	0.04862	-2.49484	-0.92103	-2.24328	-1.33557
18	0.05142	-2.21812	-0.74170	-1.96334	-1.18678
19	0.05376	-1.93985	-0.57355	-1.68494	-1.04530
20	0.05563	-1.66012	-0.41617	-1.40801	-0.91039
21	0.05699	-1.37903	-0.26921	-1.13244	-0.78142
22	0.05785	-1.09652	-0.13248	-0.85829	-0.65799
23	0.05816	-0.81265	-0.00604	-0.58549	-0.53981
24	0.05797	-0.52758	0.11029	-0.31390	-0.42698
25	0.05737	-0.24163	0.21682	-0.04319	-0.31993
26	0.05644	0.04480	0.31379	0.22705	-0.21878
27	0.05517	0.33152	0.40139	0.49699	-0.12339
28	0.05359	0.61842	0.47982	0.76675	-0.03367
29	0.05170	0.90540	0.54921	1.03644	0.05046
30	0.04953	1.19240	0.60969	1.30610	0.12895
31	0.04708	1.47929	0.66128	1.57588	0.20169
32	0.04439	1.76586	0.70405	1.84597	0.26860
33	0.04147	2.05197	0.73817	2.11652	0.32965
34	0.03833	2.33751	0.76381	2.38764	0.38479
35	0.03501	2.62238	0.78119	2.65943	0.43393
36	0.03154	2.90658	0.79043	2.93190	0.47687
37	0.02794	3.19000	0.79158	3.20514	0.51335
38	0.02423	3.47252	0.78475	3.47929	0.54313
39	0.02046	3.75409	0.77008	3.75438	0.56602
40	0.01664	4.03469	0.74768	4.03044	0.58172
41	0.01286	4.26777	0.72315	4.26125	0.58906
42	0.01028	4.44908	0.70028	4.44142	0.59105
43	0.01028	4.48144	0.68376	4.47752	0.60434
44	0.01028	4.49645	0.64212	4.49645	0.64212

CHORD	STAGGER	CAMBER
9.9741	21.680	48.764

AREA 4.115428 SURFACE ARC LENGTH 50.68926

	ALPHA	UPSILON
SECTION C.G.	-0.04623	-0.42192
STREAMSURFACE SECTION C.G.	-0.27009	-0.36634
BLADE AXIS	0.	0.
STACKING AXIS (RADIAL)	0.	0.

COORD SYSTEM ORIGIN Z 33.33289 R 0.

STAGE 1, STATOR NB 72

SECTION NO 2 SECTION BB RHO 68.5800

MEANLINE DATA

PT	ALPHA	ZETA*	THICKNESS	UPSILON
1	-5.74291	38.760	0.13534	-3.08896
2	-5.45283	37.711	0.20926	-2.86039
3	-4.87370	35.522	0.35441	-2.42979
4	-4.29607	33.249	0.49267	-2.03428
5	-3.71966	30.956	0.62032	-1.67242
6	-3.08708	28.502	0.74839	-1.31139
7	-2.39857	25.952	0.85558	-0.95752
8	-1.71130	23.503	0.93742	-0.60076
9	-1.02571	21.105	0.98674	-0.35984
10	-0.34152	18.708	1.00172	-0.11160
11	0.34140	16.316	0.98563	0.10401
12	1.02263	13.938	0.94290	0.28823
13	1.70224	11.580	0.87499	0.44178
14	2.38034	9.236	0.78415	0.56623
15	3.05638	6.899	0.67335	0.66254
16	3.73032	4.561	0.54621	0.72993
17	4.40234	2.211	0.40683	0.76935
18	5.07196	-0.153	0.25973	0.78159
19	5.62827	-2.140	0.13064	0.77061

SURFACE COORDINATES WITH ORIGIN AT SECTION AXIS

PT	T/C	UPPER ALPHA	UPPER UPSILON	LOWER ALPHA	LOWER UPSILON
1	0.01128	-5.73232	-3.10215	-5.73232	-3.10215
2	0.01128	-5.73968	-3.07920	-5.71696	-3.11003
3	0.01128	-5.73337	-3.04570	-5.69080	-3.10883
4	0.01128	-5.71288	-3.00229	-5.65431	-3.09799
5	0.01128	-5.67755	-2.94978	-5.60798	-3.07688
6	0.01128	-5.62680	-2.88892	-5.55200	-3.04528
7	0.01128	-5.56042	-2.81994	-5.48572	-3.00397
8	0.01128	-5.47910	-2.74201	-5.39506	-2.94765
9	0.02330	-5.25787	-2.53691	-5.09084	-2.76118
10	0.02819	-4.99204	-2.29898	-4.78811	-2.58392
11	0.03496	-4.72456	-2.06916	-4.48703	-2.41505
12	0.04056	-4.45528	-1.84766	-4.18775	-2.25432
13	0.04595	-4.18416	-1.63468	-3.89041	-2.10135
14	0.05110	-3.91129	-1.43020	-3.59462	-1.95585
15	0.05597	-3.63659	-1.23420	-3.30077	-1.81601
16	0.06141	-3.30429	-1.01006	-2.95080	-1.65680
17	0.06634	-2.96929	-0.79841	-2.60343	-1.50572
18	0.07073	-2.63209	-0.59919	-2.25845	-1.36146
19	0.07452	-2.29259	-0.41189	-1.91568	-1.22302
20	0.07768	-1.95031	-0.23646	-1.57569	-1.09023
21	0.08018	-1.60565	-0.07336	-1.23868	-0.96276
22	0.08199	-1.25933	0.07729	-0.90213	-0.83964
23	0.08307	-0.91125	0.21590	-0.56793	-0.72021
24	0.08346	-0.56106	0.34271	-0.23586	-0.60477
25	0.08319	-0.20926	0.45756	0.09462	-0.49359
26	0.08232	0.14334	0.56068	0.42429	-0.38659
27	0.08090	0.49657	0.65261	0.75333	-0.28381
28	0.07894	0.85045	0.73349	1.08172	-0.18528
29	0.07644	1.20466	0.80326	1.40978	-0.09096
30	0.07342	1.55875	0.86210	1.73796	-0.00073
31	0.06992	1.91253	0.91039	2.06646	0.08545
32	0.06595	2.26581	0.94848	2.39505	0.16763
33	0.06154	2.61859	0.97670	2.72493	0.24571
34	0.05678	2.97097	0.99513	3.05483	0.31929
35	0.05157	3.32252	1.00372	3.38555	0.38792
36	0.04609	3.67279	1.00280	3.71795	0.45142
37	0.04033	4.02171	0.99284	4.05091	0.50967
38	0.03434	4.36921	0.97429	4.38567	0.56245
39	0.02817	4.71528	0.94754	4.72187	0.60951
40	0.02187	5.05991	0.91284	5.05962	0.65038
41	0.01656	5.34891	0.87800	5.34208	0.67933
42	0.01122	5.56326	0.84788	5.54486	0.69703
43	0.01122	5.60686	0.82558	5.60019	0.71365
44	0.01122	5.62827	0.77061	5.62827	0.77061

CHORD 12.0926 STAGGER 18.824 CAMBER 40.900

AREA 8.339216 SURFACE ARC LENGTH 24.74195

	ALPHA	UPSILON
SECTION C.G.	-0.27066	-0.33088
STREAMSURFACE SECTION C.G.	-0.22346	-0.32279
BLADE AXIS	0.	0.
STACKING AXIS (RADIAL)	0.	0.

COORD SYSTEM ORIGIN Z 33.37789 R 0.

STAGE 1, STATOR NR 72

SECTION NO 3 SECTION CC RHO 76.2000

PT	ALPHA	MEANLINE ZETA*	DATA THICKNESS	UPSILON
1	-6.16830	39.389	0.15447	-3.33104
2	-5.85829	38.252	0.24452	-3.08169
3	-5.23881	35.899	0.42169	-2.61404
4	-4.62025	33.488	0.59082	-2.18529
5	-4.00248	31.084	0.74729	-1.79450
6	-3.32366	28.538	0.89958	-1.40572
7	-2.58377	25.915	1.03632	-1.02497
8	-1.80465	23.414	1.13717	-0.68604
9	-1.10639	20.976	1.19821	-0.38463
10	-0.36846	18.551	1.21710	-0.11958
11	0.36856	16.141	1.19826	0.11070
12	1.10512	13.756	1.14690	0.30724
13	1.84110	11.405	1.06460	0.47172
14	2.57624	9.081	0.95401	0.60433
15	3.31094	6.775	0.81860	0.70650
16	4.04497	4.475	0.66265	0.77941
17	4.77830	2.175	0.49109	0.82156
18	5.51076	-0.123	0.30932	0.83490
19	6.12076	-2.034	0.15418	0.82358

SURFACE COORDINATES WITH ORIGIN AT SECTION AXIS

PT	T/C	UPPER ALPHA	UPPER UPSILON	LOWER ALPHA	LOWER UPSILON
1	0.01191	-6.15605	-3.34637	-6.15605	-3.34637
2	0.01191	-6.16505	-3.31987	-6.13822	-3.35539
3	0.01191	-6.15860	-3.28116	-6.10818	-3.35394
4	0.01191	-6.13614	-3.23089	-6.06640	-3.34144
5	0.01191	-6.09698	-3.16996	-6.01339	-3.31725
6	0.01191	-6.04036	-3.09915	-5.94932	-3.28118
7	0.01191	-5.96619	-3.01870	-5.87339	-3.23419
8	0.01191	-5.87519	-2.92772	-5.78558	-3.17954
9	0.02563	-5.65394	-2.71418	-5.45375	-2.97936
10	0.03235	-5.36961	-2.44979	-5.12363	-2.78960
11	0.03894	-5.08334	-2.19449	-4.79545	-2.60918
12	0.04532	-4.79469	-1.94846	-4.46964	-2.43798
13	0.05148	-4.50358	-1.71199	-4.14630	-2.27576
14	0.05735	-4.21005	-1.48550	-3.82538	-2.12189
15	0.06291	-3.91417	-1.26903	-3.50681	-1.97563
16	0.06809	-3.55628	-1.02238	-3.12735	-1.80883
17	0.07470	-3.19521	-0.78963	-2.75108	-1.65030
18	0.07967	-2.83071	-0.57075	-2.37824	-1.49934
19	0.08395	-2.46310	-0.36604	-2.00845	-1.35502
20	0.08751	-2.09313	-0.17541	-1.64112	-1.21616
21	0.09031	-1.72050	0.00159	-1.27642	-1.08192
22	0.09232	-1.34485	0.16487	-0.91472	-0.95211
23	0.09349	-0.96669	0.31394	-0.55554	-0.82634
24	0.09387	-0.58679	0.44904	-0.19810	-0.70433
25	0.09352	-0.20538	0.57082	0.15784	-0.58611
26	0.09251	0.17743	0.67968	0.51237	-0.47200
27	0.09087	0.56104	0.77581	0.86611	-0.36213
28	0.08862	0.94488	0.85944	1.21961	-0.25620
29	0.08576	1.32896	0.93091	1.57287	-0.15398
30	0.08233	1.71335	0.99039	1.92583	-0.05567
31	0.07834	2.09757	1.03794	2.27895	0.03855
32	0.07383	2.48114	1.07384	2.63272	0.12866
33	0.06883	2.86377	1.09851	2.98703	0.21464
34	0.06339	3.24521	1.11252	3.34333	0.29648
35	0.05754	3.62568	1.11640	3.70021	0.37403
36	0.05134	4.00535	1.11014	4.05788	0.44657
37	0.04482	4.38350	1.09367	4.41708	0.51347
38	0.03805	4.75958	1.06770	4.77834	0.57471
39	0.03107	5.13387	1.03308	5.14140	0.63030
40	0.02394	5.50652	0.99013	5.50609	0.67968
41	0.01793	5.81567	0.94810	5.81139	0.71563
42	0.01189	6.04699	0.91294	6.04167	0.73934
43	0.01189	6.09605	0.88708	6.09413	0.76356
44	0.01189	6.12076	0.82358	6.12076	0.82358

CHORD 12.9657 STAGGER 18.761 CAMBER 41.478

AREA 10.901278 SURFACE ARC LENGTH 26.77760

	ALPHA	UPSILON
SECTION C.G.	-0.27068	-0.35031
STREAMSURFACE SECTION C.G.	-0.24446	-0.30390
BLADE AXIS	0.	0.
STACKING AXIS (RADIAL)	0.	0.

COORD SYSTEM ORIGIN Z 33.37789 R 0.

STAGE 1. STATOR NR 72

SECTION NO 4 SECTION DD RHO 82.9056

MEANLINE DATA

PT	ALPHA	ZETA*	THICKNESS	UPSILON
1	-6.41560	46.199	0.17279	-4.10801
2	-6.09442	44.783	0.27795	-3.78133
3	-5.45234	41.818	0.48469	-3.17612
4	-4.81030	38.740	0.68160	-2.63127
5	-4.16850	35.663	0.86283	-2.10434
6	-3.46284	32.447	1.03771	-1.66733
7	-2.69329	29.229	1.19205	-1.20827
8	-1.92358	26.242	1.30193	-0.80428
9	-1.15418	23.366	1.36252	-0.44854
10	-0.38456	20.496	1.37219	-0.13845
11	0.38481	17.633	1.34291	0.12768
12	1.15443	14.802	1.27937	0.35153
13	1.92382	12.019	1.18340	0.53476
14	2.69346	9.280	1.05777	0.67986
15	3.46286	6.568	0.90619	0.78683
16	4.23251	3.864	0.73307	0.85730
17	5.00191	1.162	0.54353	0.89045
18	5.77155	-1.535	0.34309	0.88794
19	6.41266	-3.772	0.17197	0.85807

SURFACE COORDINATES WITH ORIGIN AT SECTION AXIS

PT	T/C	UPPER ALPHA	UPPER UPSILON	LOWER ALPHA	LOWER UPSILON
1	0.01257	-6.40013	-4.12308	-6.40013	-4.12308
2	0.01257	-6.41356	-4.09462	-6.37928	-4.13082
3	0.01257	-6.41134	-4.05065	-6.34615	-4.12539
4	0.01257	-6.39282	-3.99178	-6.30137	-4.10619
5	0.01257	-6.35712	-3.91888	-6.24560	-4.07257
6	0.01257	-6.30347	-3.83269	-6.17905	-4.02432
7	0.01257	-6.23163	-3.73346	-6.10070	-3.96244
8	0.01257	-6.14204	-3.62036	-5.99682	-3.88016
9	0.02778	-5.90508	-3.33212	-5.64330	-3.61020
10	0.03523	-5.61484	-2.99656	-5.29212	-3.35771
11	0.04250	-5.32186	-2.67496	-4.94369	-3.12036
12	0.04954	-5.02530	-2.36718	-4.59884	-2.89821
13	0.05630	-4.72518	-2.07408	-4.25754	-2.69078
14	0.06272	-4.42198	-1.79559	-3.91933	-2.49618
15	0.06876	-4.11561	-1.53099	-3.58429	-2.31285
16	0.07545	-3.74356	-1.23127	-3.18664	-2.10626
17	0.08145	-3.36695	-0.95083	-2.79356	-1.91249
18	0.08669	-2.98615	-0.68936	-2.40466	-1.72955
19	0.09112	-2.60151	-0.44643	-2.01961	-1.55562
20	0.09469	-2.21342	-0.22153	-1.63801	-1.38913
21	0.09737	-1.82180	-0.01405	-1.25993	-1.22899
22	0.09911	-1.42640	0.17593	-0.88563	-1.07459
23	0.09988	-1.02773	0.34817	-0.51460	-0.92539
24	0.09982	-0.62674	0.50349	-0.14590	-0.78172
25	0.09908	-0.22412	0.64301	0.22117	-0.64414
26	0.09769	0.17977	0.76710	0.58698	-0.51267
27	0.09569	0.58052	0.87594	0.95192	-0.38714
28	0.09308	0.98974	0.96972	1.31640	-0.26739
29	0.08987	1.39487	1.04867	1.68096	-0.15318
30	0.08610	1.79937	1.11330	2.04616	-0.04423
31	0.08178	2.20339	1.16427	2.41184	0.05952
32	0.07696	2.60705	1.20173	2.77787	0.15767
33	0.07166	3.00956	1.22575	3.14506	0.24999
34	0.06593	3.41023	1.23693	3.51408	0.33656
35	0.05981	3.80942	1.23601	3.88459	0.41728
36	0.05334	4.20733	1.22305	4.25638	0.49146
37	0.04657	4.60303	1.19809	4.63037	0.55853
38	0.03954	4.99593	1.16219	5.00716	0.61869
39	0.03233	5.38695	1.11628	5.38584	0.67188
40	0.02496	5.77640	1.05946	5.76609	0.71645
41	0.01875	6.09821	1.00375	6.08568	0.74625
42	0.01251	6.33287	0.96003	6.32224	0.76555
43	0.01251	6.38737	0.92946	6.38126	0.79136
44	0.01251	6.41266	0.85807	6.41266	0.85807

CHORD 13.7470 STAGGER 21.249 CAMBER 48.906

AREA 13.116504 SURFACE ARC LENGTH 28.70537

	ALPHA	UPSILON
SECTION C.G.	-0.37594	-0.47632
STREAMSURFACE SECTION C.G.	-0.37398	-0.48118
BLADE AXIS	0.	0.
STACKING AXIS (RADIAL)	0.	0.

COORD SYSTEM ORIGIN Z 33.37789 R 0.

APPENDIX C

BLADE AND VANE AIRFOIL
MANUFACTURING SECTION
COORDINATES

4. Front Block Fan Stator 2

FRONT BLOCK FAN STATOR 2

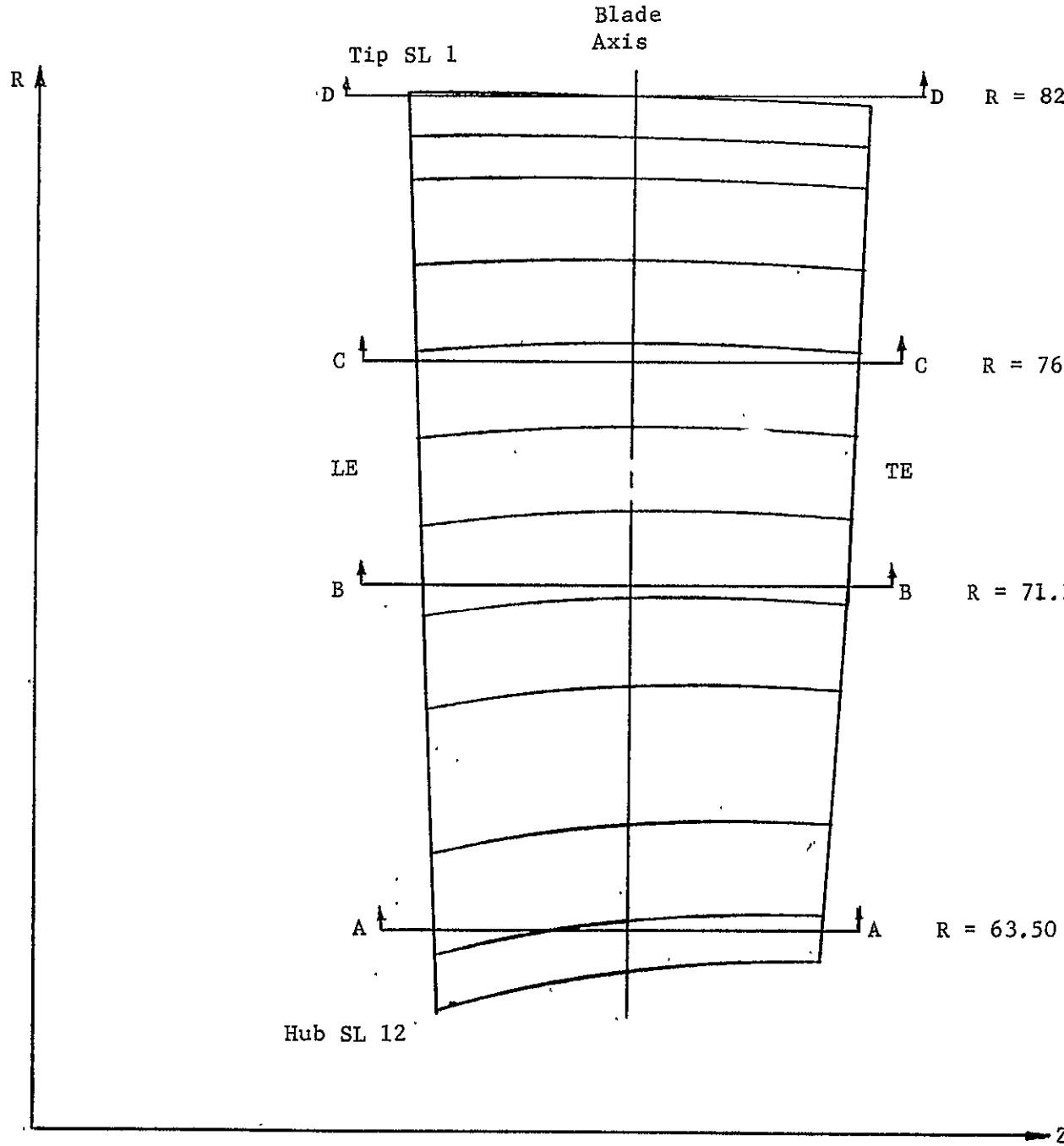

STAGE 2. STATOR NB 94

SECTION NO 1 SECTION AA RHO 63.5000

MEANLINE DATA

PT	ALPHA	ZETA*	THICKNESS	UPSILON
1	-4.38194	42.607	0.02908	18.54144
2	-4.34678	42.384	0.08278	18.57335
3	-4.29446	42.046	0.12539	18.62126
4	-4.03160	40.312	0.22688	18.85047
5	-3.68144	37.898	0.31365	19.13505
6	-3.24314	34.788	0.38945	19.45840
7	-2.71734	31.083	0.45158	19.80040
8	-2.19134	27.624	0.49249	20.09622
9	-1.66546	24.434	0.51780	20.35323
10	-1.13964	21.419	0.52767	20.57497
11	-0.43838	17.457	0.51548	20.82215
12	0.43847	12.500	0.46577	21.05698
13	1.31573	7.628	0.38896	21.21257
14	1.84234	4.758	0.33518	21.27019
15	2.36897	1.909	0.27861	21.30040
16	2.89583	-0.933	0.22153	21.30371
17	3.42310	-3.768	0.16760	21.28141
18	3.95024	-6.584	0.12138	21.23306
19	4.12595	-7.517	0.11002	21.21181
20	4.38938	-8.908	0.09884	21.17482

SURFACE COORDINATES WITH ORIGIN AT SECTION AXIS

PT	T/C	UPPER ALPHA	UPPER UPSILON	LOWER ALPHA	LOWER UPSILON
1	0.00317	-4.38194	18.54144	-4.38194	18.54144
2	0.00317	-4.38597	18.54749	-4.37606	18.53673
3	0.00317	-4.38829	18.55506	-4.36855	18.53359
4	0.00317	-4.38885	18.56406	-4.35947	18.53210
5	0.00317	-4.38756	18.57439	-4.34893	18.53240
6	0.00317	-4.38432	18.58597	-4.33706	18.53459
7	0.00317	-4.37907	18.59872	-4.32392	18.53875
8	0.00317	-4.37183	18.61265	-4.30948	18.54486
9	0.00317	-4.36273	18.62793	-4.29356	18.55272
10	0.01371	-4.33658	18.66778	-4.25188	18.57515
11	0.01841	-4.26228	18.76341	-4.15075	18.63698
12	0.02479	-4.10417	18.93776	-3.95801	18.76704
13	0.02987	-3.94197	19.10222	-3.76936	18.89003
14	0.03428	-3.77679	19.25973	-3.58368	19.01225
15	0.03799	-3.60879	19.40927	-3.40084	19.13031
16	0.04255	-3.35303	19.61929	-3.13031	19.29955
17	0.04627	-3.09401	19.81423	-2.86305	19.45892
18	0.04933	-2.83220	19.99491	-2.59858	19.60824
19	0.05180	-2.56835	20.16166	-2.33616	19.74794
20	0.05379	-2.30333	20.31562	-2.07490	19.87915
21	0.05537	-2.03723	20.45832	-1.81472	20.00264
22	0.05655	-1.76985	20.59022	-1.55582	20.11863
23	0.05731	-1.50150	20.71131	-1.29789	20.22761
24	0.05762	-1.23254	20.82194	-1.04057	20.33042
25	0.05747	-0.96290	20.92262	-0.78392	20.42764
26	0.05627	-0.51206	21.06909	-0.35764	20.57742
27	0.05400	-0.06015	21.18962	0.06758	20.71182
28	0.05083	0.39201	21.28507	0.49255	20.83057
29	0.04691	0.84349	21.35650	0.91821	20.93343
30	0.04243	1.29355	21.40563	1.34528	21.02049
31	0.03955	1.56289	21.42515	1.60222	21.06510
32	0.03656	1.83180	21.43731	1.85958	21.10363
33	0.03350	2.10010	21.44206	2.11757	21.13578
34	0.03039	2.36766	21.43957	2.37629	21.16143
35	0.02725	2.63439	21.43012	2.63584	21.18052
36	0.02416	2.90027	21.41428	2.89624	21.19305
37	0.02116	3.16548	21.39255	3.15730	21.19893
38	0.01829	3.43018	21.36485	3.41888	21.19777
39	0.01559	3.69423	21.33131	3.68111	21.18913
40	0.01325	3.95770	21.29327	3.94393	21.17271
41	0.01259	4.04545	21.27989	4.03160	21.16546
42	0.01201	4.13319	21.26633	4.11928	21.15721
43	0.01154	4.22102	21.25265	4.20688	21.14791
44	0.01079	4.34800	21.23204	4.33311	21.13254
45	0.01079	4.37840	21.21451	4.36791	21.14089
46	0.01079	4.38938	21.17482	4.38938	21.17482

CHORD	STAGGER	CAMBER
9.1581	16.711	51.514

AREA 3.463111 SURFACE ARC LENGTH 19.08075

	ALPHA	UPSILON
SECTION C.G.	-0.61196	20.51515
STREAMSURFACE SECTION C.G.	-0.59767	20.52033
BLADE AXIS	0.	20.94983
STACKING AXIS (RADIAL)	0.	19.30240

COORD SYSTEM ORIGIN Z 60.55512 R 0. MU 0. ETA -16.0784

STAGE 2. STATOR NB 94

SECTION NO 2 SECTION BB RHO 71.1200

MEANLINE DATA

PT	ALPHA	ZETA*	THICKNESS	UPSILON
1	-4.71867	40.488	0.03437	18.55366
2	-4.68113	40.279	0.10024	18.58558
3	-4.62474	39.966	0.15340	18.63309
4	-4.34279	38.358	0.27991	18.86299
5	-3.96645	36.133	0.38966	19.14929
6	-3.49555	33.275	0.48668	19.47611
7	-2.93005	29.867	0.56878	19.82382
8	-2.36384	26.646	0.62371	20.12811
9	-1.79714	23.632	0.65870	20.39424
10	-1.23010	20.756	0.67493	20.62548
11	-0.47314	16.980	0.66242	20.88412
12	0.47366	12.273	0.60081	21.13109
13	1.42181	7.644	0.50144	21.29737
14	1.99119	4.908	0.43071	21.36037
15	2.56071	2.186	0.35575	21.39571
16	3.13070	-0.539	0.27973	21.40335
17	3.70097	-3.265	0.20735	21.38403
18	4.27113	-5.979	0.14536	21.33765
19	4.46137	-6.877	0.12998	21.31614
20	4.74647	-8.219	0.11491	21.27874

SURFACE COORDINATES WITH ORIGIN AT SECTION AXIS

PT	T/C	UPPER ALPHA	UPPER UPSILON	LOWER ALPHA	LOWER UPSILON
1	0.00349	-4.71867	18.55366	-4.71867	18.55366
2	0.00349	-4.72357	18.56148	-4.71171	18.54758
3	0.00349	-4.72641	18.57100	-4.70274	18.54328
4	0.00349	-4.72710	18.58215	-4.69183	18.54083
5	0.00349	-4.72555	18.59480	-4.67906	18.54034
6	0.00349	-4.72165	18.60884	-4.66452	18.54193
7	0.00349	-4.71533	18.62419	-4.64828	18.54565
8	0.00349	-4.70661	18.64086	-4.63031	18.55147
9	0.00349	-4.69565	18.65903	-4.61044	18.55921
10	0.01562	-4.67342	18.69267	-4.57461	18.57471
11	0.02109	-4.59536	18.79248	-4.46337	18.63210
12	0.02851	-4.42721	18.97524	-4.25292	18.75507
13	0.03448	-4.25348	19.14716	-4.04804	18.87678
14	0.03969	-4.07667	19.31082	-3.84624	18.99505
15	0.04409	-3.89674	19.46617	-3.64757	19.11046
16	0.04954	-3.62204	19.68492	-3.35436	19.27696
17	0.05408	-3.34347	19.88815	-3.06502	19.43401
18	0.05786	-3.06197	20.07667	-2.77862	19.58216
19	0.06094	-2.77803	20.25129	-2.49464	19.72221
20	0.06341	-2.49225	20.41307	-2.21252	19.85462
21	0.06540	-2.20497	20.56311	-1.93189	19.97967
22	0.06693	-1.91632	20.70190	-1.65263	20.09765
23	0.06800	-1.62653	20.82964	-1.37451	20.20908
24	0.06854	-1.33573	20.94635	-1.09740	20.31477
25	0.06848	-1.04389	21.05213	-0.82134	20.41536
26	0.06720	-0.55558	21.20495	-0.36313	20.57169
27	0.06460	-0.06598	21.32954	0.09379	20.71360
28	0.06088	0.42386	21.42707	0.55045	20.84096
29	0.05619	0.91298	21.49887	1.00785	20.95360
30	0.05077	1.40055	21.54677	1.46679	21.05115
31	0.04725	1.69224	21.56484	1.74301	21.10221
32	0.04359	1.98327	21.57517	2.01989	21.14736
33	0.03983	2.27354	21.57790	2.29752	21.18632
34	0.03600	2.56296	21.57320	2.57601	21.21887
35	0.03214	2.85144	21.56131	2.85544	21.24478
36	0.02831	3.13892	21.54270	3.13587	21.26386
37	0.02458	3.42550	21.51783	3.41720	21.27588
38	0.02100	3.71127	21.48702	3.69934	21.28054
39	0.01765	3.99632	21.45065	3.98219	21.27737
40	0.01474	4.28084	21.40961	4.26558	21.26525
41	0.01391	4.37558	21.39511	4.36015	21.25899
42	0.01319	4.47025	21.38049	4.45478	21.25151
43	0.01260	4.56497	21.36590	4.54936	21.24277
44	0.01167	4.69767	21.34896	4.68157	21.22860
45	0.01167	4.73326	21.32477	4.72186	21.23875
46	0.01167	4.74647	21.27874	4.74647	21.27874

CHORD	STAGGER	CAMBER
9.8496	16.062	48.707

AREA 4.713849 SURFACE ARC LENGTH 20.47458

	ALPHA	UPSILON
SECTION C.G.	-0.63089	20.58531
STREAMSURFACE SECTION C.G.	-0.64204	20.58025
BLADE AXIS	0.	21.01802
STACKING AXIS (RADIAL)	0.	20.49869

COORD SYSTEM ORIGIN Z 60.55512 R 0. TH 0. ETA =16.0744

STAGE 2. STATOR NB 94

SECTION NO 3 SECTION CC RHO 76.2000

PT	ALPHA	MEANLINE ZETA*	DATA THICKNESS	UPSILON
1	-4.89625	42.274	0.03844	19.19444
2	-4.85723	42.070	0.11505	19.22952
3	-4.79878	41.762	0.17618	19.28205
4	-4.50622	40.183	0.32316	19.53577
5	-4.11589	37.965	0.45144	19.85336
6	-3.62735	35.064	0.56628	20.21481
7	-3.04062	31.549	0.66352	20.60006
8	-2.45306	28.201	0.73007	20.93786
9	-1.86504	25.065	0.77335	21.23290
10	-1.27648	22.066	0.79293	21.48955
11	-0.49116	18.098	0.77959	21.77648
12	0.49150	13.083	0.70633	22.05113
13	1.47482	8.104	0.58760	22.23479
14	2.06518	5.147	0.50314	22.30380
15	2.65574	2.195	0.41373	22.34157
16	3.24646	-0.774	0.32315	22.34920
17	3.83694	-3.753	0.23761	22.32550
18	4.42777	-6.722	0.16434	22.27129
19	4.62481	-7.704	0.14630	22.24620
20	4.92015	-9.168	0.12858	22.20217

SURFACE COORDINATES WITH ORIGIN AT SECTION AXIS

PT	T/C	UPPER ALPHA	UPPER UPSILON	LOWER ALPHA	LOWER UPSILON
1	0.00374	-4.89625	19.19444	-4.89625	19.19444
2	0.00374	-4.90225	19.20327	-4.88791	19.18750
3	0.00374	-4.90599	19.21409	-4.87738	19.18261
4	0.00374	-4.90741	19.22680	-4.86475	19.17988
5	0.00374	-4.90638	19.24130	-4.85012	19.17941
6	0.00374	-4.90279	19.25744	-4.83361	19.18134
7	0.00374	-4.89657	19.27516	-4.81529	19.18575
8	0.00374	-4.88774	19.29446	-4.79513	19.19259
9	0.00374	-4.87646	19.31553	-4.77293	19.20165
10	0.01721	-4.85704	19.34847	-4.73913	19.21688
11	0.02325	-4.77852	19.45940	-4.62131	19.27976
12	0.03157	-4.60802	19.66193	-4.39916	19.41405
13	0.03826	-4.43124	19.85301	-4.18328	19.54830
14	0.04411	-4.25026	20.03571	-3.97161	19.67876
15	0.04909	-4.06535	20.20905	-3.76386	19.80518
16	0.05529	-3.78276	20.45251	-3.45747	19.98724
17	0.06045	-3.49567	20.67882	-3.15558	20.15962
18	0.06475	-3.20486	20.88928	-2.85740	20.32249
19	0.06830	-2.91099	21.08468	-2.56229	20.47632
20	0.07121	-2.61473	21.26594	-2.26957	20.62148
21	0.07357	-2.31658	21.43395	-1.97873	20.75837
22	0.07539	-2.01679	21.58915	-1.68953	20.88775
23	0.07662	-1.71544	21.73186	-1.40190	21.01038
24	0.07725	-1.41262	21.86223	-1.11574	21.12682
25	0.07724	-1.10850	21.98039	-0.83088	21.23756
26	0.07588	-0.59944	22.15088	-0.35830	21.41010
27	0.07295	-0.08848	22.28948	0.11238	21.56790
28	0.06869	0.42334	22.39728	0.58220	21.71022
29	0.06332	0.93434	22.47548	1.05284	21.83630
30	0.05711	1.44318	22.52638	1.52564	21.94592
31	0.05038	1.74743	22.54886	1.81037	22.00357
32	0.04889	2.05101	22.55451	2.09578	22.05458
33	0.04458	2.35348	22.55540	2.38229	22.09858
34	0.04020	2.65456	22.54803	2.67019	22.13562
35	0.03578	2.95455	22.53294	2.95919	22.16566
36	0.03140	3.25362	22.51032	3.24910	22.18794
37	0.02716	3.55152	22.48036	3.54018	22.20173
38	0.02310	3.84818	22.44358	3.83251	22.20696
39	0.01929	4.14389	22.40066	4.12578	22.20341
40	0.01599	4.43899	22.35262	4.41967	22.18959
41	0.01505	4.53726	22.33569	4.51772	22.18237
42	0.01424	4.63553	22.31853	4.61578	22.17363
43	0.01358	4.73382	22.30126	4.71381	22.16328
44	0.01292	4.83688	22.27737	4.84655	22.14712
45	0.01252	4.90627	22.25400	4.89185	22.13781
46	0.01252	4.92015	22.20217	4.92015	22.20217

CHORD 10.2668 STAGGER 17.035 CAMBER 51.441

AREA 5.765058 SURFACE ARC LENGTH 21.44711

	ALPHA	UPSILON
SECTION C.G.	-0.67695	21.43984
STREAMSURFACE SECTION C.G.	-0.70927	21.42010
BLADE AXIS	0.	21.92550
STACKING AXIS (RADIAL)	0.	21.96288

COORD SYSTEM ORIGIN Z 69.55512 R 0. MU 0. ETA -16.0784

STAGE 2. STATOR NB 94

SECTION NO 4 SECTION DD RHO 82.1182

PT	ALPHA	MEANLINE ZETA*	DATA THICKNESS	UPSILON
1	-5.02222	50.917	0.04403	19.95739
2	-4.98191	50.702	0.14078	20.00670
3	-4.92300	50.366	0.21208	20.07872
4	-4.62361	48.639	0.39019	20.43013
5	-4.22366	46.130	0.54335	20.86888
6	-3.72333	42.561	0.67657	21.35649
7	-3.12297	38.130	0.79170	21.86976
8	-2.51894	33.903	0.86993	22.30879
9	-1.91632	30.111	0.92124	22.68631
10	-1.31159	26.560	0.93310	23.00949
11	-0.50466	21.804	0.91392	23.36832
12	0.50529	15.553	0.81677	23.70953
13	1.51596	9.228	0.67026	23.92735
14	2.12330	5.481	0.56920	24.00312
15	2.73073	1.747	0.46437	24.04021
16	3.33817	-2.026	0.36125	24.04315
17	3.94355	-5.851	0.26481	23.99717
18	4.55210	-9.634	0.18321	23.91749
19	4.75262	-10.881	0.16361	23.87982
20	5.05590	-12.722	0.14419	23.81200

SURFACE COORDINATES WITH ORIGIN AT SECTION AXIS

PT	T/C	UPPER ALPHA	UPPER UPSILON	LOWER ALPHA	LOWER UPSILON
1	0.00408	-5.02222	19.95739	-5.02222	19.95739
2	0.00408	-5.03122	19.96695	-5.01106	19.95050
3	0.00408	-5.03798	19.97914	-4.99779	19.94632
4	0.00408	-5.04236	19.99382	-4.98252	19.94496
5	0.00408	-5.04418	20.01085	-4.96546	19.94657
6	0.00408	-5.04323	20.03006	-4.94679	19.95131
7	0.00408	-5.03937	20.05133	-4.92664	19.95928
8	0.00408	-5.03262	20.07469	-4.90496	19.97044
9	0.00408	-5.02329	20.10038	-4.88144	19.98455
10	0.01977	-5.00360	20.14816	-4.83928	20.01206
11	0.02654	-4.93008	20.29298	-4.71124	20.10834
12	0.03635	-4.76672	20.56440	-4.47147	20.30618
13	0.04408	-4.59332	20.82150	-4.24175	20.50110
14	0.05058	-4.41268	21.06603	-4.01926	20.68772
15	0.05697	-4.22643	21.29633	-3.80239	20.86477
16	0.06294	-3.94122	21.61737	-3.48291	21.11624
17	0.06875	-3.65044	21.91635	-3.16900	21.35202
18	0.07360	-3.35264	22.19431	-2.86212	21.56977
19	0.07753	-3.04981	22.44872	-2.56026	21.77040
20	0.08079	-2.74540	22.68172	-2.25998	21.95769
21	0.08354	-2.43893	22.89777	-1.96176	22.13306
22	0.08546	-2.12821	23.09639	-1.66780	22.29739
23	0.08633	-1.81406	23.27548	-1.37726	22.45276
24	0.08647	-1.49896	23.43725	-1.08768	22.59971
25	0.08624	-1.18339	23.58496	-0.79856	22.73775
26	0.08461	-0.85491	23.79978	-0.31922	22.95081
27	0.08088	-0.12229	23.97340	0.15597	23.14620
28	0.07551	0.41300	24.10668	0.62849	23.32089
29	0.06911	0.94694	24.20102	1.10236	23.47172
30	0.06193	1.47685	24.25943	1.58027	23.59924
31	0.05734	1.79294	24.27873	1.86886	23.66474
32	0.05259	2.10787	24.28663	2.15862	23.72141
33	0.04777	2.42038	24.28361	2.45080	23.76910
34	0.04292	2.72976	24.27189	2.74611	23.80904
35	0.03812	3.03889	24.25286	3.04166	23.84155
36	0.03341	3.34933	24.22311	3.33591	23.86285
37	0.02884	3.65728	24.18002	3.63265	23.86976
38	0.02449	3.96092	24.12819	3.93370	23.86536
39	0.02045	4.26367	24.07165	4.23563	23.85276
40	0.01698	4.56739	24.00782	4.53660	23.82720
41	0.01600	4.66872	23.98430	4.63684	23.81461
42	0.01516	4.77003	23.95972	4.73709	23.79954
43	0.01446	4.87116	23.93429	4.83752	23.78199
44	0.01356	5.00243	23.90043	4.96908	23.75619
45	0.01336	5.04451	23.87113	5.02071	23.76459
46	0.01336	5.05590	23.81200	5.05590	23.81200

CHORD	STAGGER	CAMBER
10.7901	20.930	63.866

AREA 7.218416 SURFACE ARC LENGTH 23.02185

	ALPHA	UPSILON
SECTION C.G.	-0.83811	22.85920
STREAMSURFACE SECTION C.G.	-0.91376	22.80684
BLADE AXIS	0.	23.55667
STACKING AXIS (RADIAL)	0.	23.66867

COORD SYSTEM ORIGIN Z 60.55512 R 0. MU 0. ETA -14.0784

APPENDIX C

BLADE AND VANE AIRFOIL
MANUFACTURING SECTION
COORDINATES

5. Front Block Fan IGV Strut

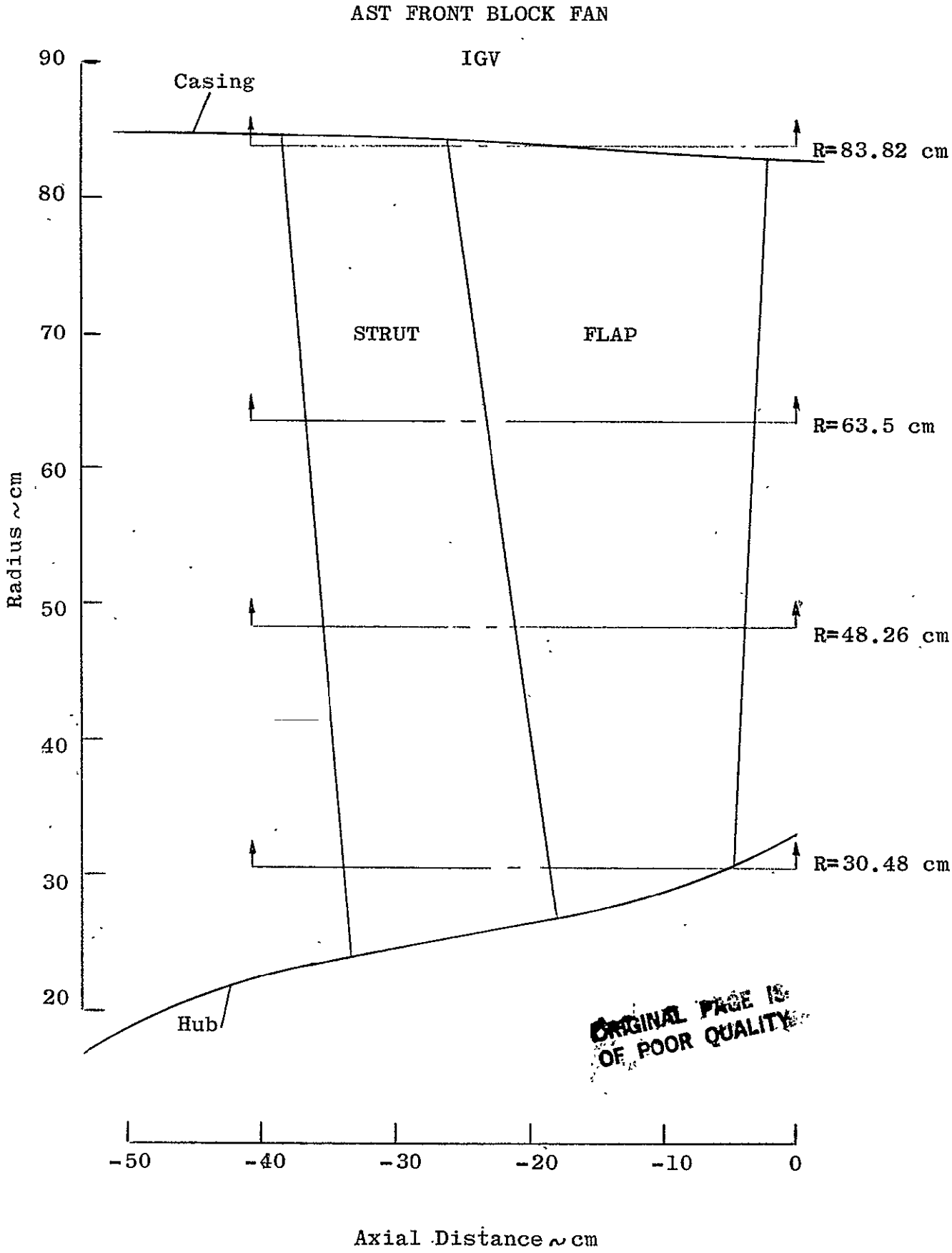

AST FRONT BLOCK FAN IGV STRUT SECTIONS (CM) *SAG* STATOR 0

SECTION AA RADIUS 30.480000 R/R 30.480000

SURFACE COORDINATES WITH ORIGIN AT S.P.

PT.	T/C	LOWER Z	LOWER R-THETA	UPPER Z	UPPER R-THETA
1	0.022233	-15.283177	-0.000000	-15.283177	-0.000000
2	0.022233	-15.227117	-0.154013	-15.227117	0.154013
3	0.022233	-15.114998	-0.228701	-15.114998	0.228701
4	0.037511	-14.901097	-0.286643	-14.901097	0.286643
5	0.046637	-14.519018	-0.356384	-14.519018	0.356384
6	0.059716	-13.754859	-0.456322	-13.754859	0.456322
7	0.069609	-12.990700	-0.531921	-12.990700	0.531921
8	0.077512	-12.226541	-0.592313	-12.226541	0.592313
9	0.083891	-11.462383	-0.641063	-11.462383	0.641063
10	0.089604	-10.698224	-0.684719	-10.698224	0.684719
11	0.094332	-9.934065	-0.720845	-9.934065	0.720845
12	0.098393	-9.169906	-0.751878	-9.169906	0.751878
13	0.101687	-8.405747	-0.777053	-8.405747	0.777053
14	0.104334	-7.641588	-0.797281	-7.641588	0.797281
15	0.106424	-6.877430	-0.813252	-6.877430	0.813252
16	0.108067	-6.113271	-0.825803	-6.113271	0.825803
17	0.109062	-5.349112	-0.833407	-5.349112	0.833407
18	0.109500	-4.584953	-0.836754	-4.584953	0.836754
19	0.109500	-3.820794	-0.836754	-3.820794	0.836754
20	0.109500	-3.056635	-0.836754	-3.056635	0.836754
21	0.109500	-2.292477	-0.836754	-2.292477	0.836754
22	0.109500	-1.986813	-0.836754	-1.986813	0.836754
23	0.109500	-1.833981	-0.836754	-1.833981	0.836754
24	0.109500	-1.681149	-0.836754	-1.681149	0.836754
25	0.109500	-1.528318	-0.836754	-1.528318	0.836754
26	0.109500	-1.375486	-0.836754	-1.375486	0.836754
27	0.109500	-1.222654	-0.836754	-1.222654	0.836754
28	0.109500	-0.916991	-0.836754	-0.916991	0.836754
29	0.109500	-0.836703	-0.836754	-0.836754	0.836754
30	0.109500	-0.278901	-0.623664	-0.278918	0.623680
31	0.109500	0.	-0.000000	0.	-0.000000

LE RADIUS 0.239591 CENTER AT Z -15.043585 R-THETA -0.000000
TE RADIUS 0.836754 CENTER AT Z -0.836754 R-THETA -0.000000

CHORD	SOLIDITY	STAGGER	CAMBER
15.283177	1.276848	0.	0.

AREA	C.G. Z	C.G. R-THETA	S.P. Z	S.P. R-THETA
21.574004	-6.866399	0.	15.283177	0.000000

SURFACE ARC LENGTH 31.778

AST FRONT BLOCK FAN IGV STRUT SECTIONS (CM) *SAG* STATOR 0

SECTION BB RADIUS 48.260000 R/R 48.260000

SURFACE COORDINATES WITH ORIGIN AT S.P.

PT.	T/C	LOWER Z	LOWER R-THETA	UPPER Z	UPPER R-THETA
1	0.023991	-14.255213	-0.000000	-14.255213	-0.000000
2	0.023991	-14.199055	-0.158854	-14.199055	0.158854
3	0.023991	-14.086741	-0.238290	-14.086741	0.238290
4	0.041588	-13.898832	-0.296426	-13.898832	0.296426
5	0.052117	-13.542452	-0.371468	-13.542452	0.371468
6	0.067176	-12.829691	-0.478803	-12.829691	0.478803
7	0.078576	-12.116931	-0.560057	-12.116931	0.560057
8	0.087637	-11.404170	-0.624643	-11.404170	0.624643
9	0.095004	-10.691409	-0.677153	-10.691409	0.677153
10	0.101576	-9.978649	-0.723992	-9.978649	0.723992
11	0.107027	-9.265888	-0.762844	-9.265888	0.762844
12	0.111682	-8.553128	-0.796025	-8.553128	0.796025
13	0.115466	-7.840367	-0.822994	-7.840367	0.822994
14	0.118551	-7.127606	-0.844985	-7.127606	0.844985
15	0.120965	-6.414846	-0.862193	-6.414846	0.862193
16	0.122833	-5.702085	-0.875504	-5.702085	0.875504
17	0.124002	-4.989324	-0.883837	-4.989324	0.883837
18	0.124500	-4.276564	-0.887387	-4.276564	0.887387
19	0.124500	-3.563803	-0.887387	-3.563803	0.887387
20	0.124500	-2.851043	-0.887387	-2.851043	0.887387
21	0.124500	-2.138282	-0.887387	-2.138282	0.887387
22	0.124500	-1.853178	-0.887387	-1.853178	0.887387
23	0.124500	-1.710626	-0.887387	-1.710626	0.887387
24	0.124500	-1.568073	-0.887387	-1.568073	0.887387
25	0.124500	-1.425521	-0.887387	-1.425521	0.887387
26	0.124500	-1.282969	-0.887387	-1.282969	0.887387
27	0.124500	-1.140417	-0.887387	-1.140417	0.887387
28	0.124500	-1.013875	-0.887387	-1.013902	0.887387
29	0.124500	-0.887333	-0.887387	-0.887387	0.887387
30	0.124500	-0.295778	-0.661403	-0.295796	0.661419
31	0.124500	0.	-0.000000	0.	-0.000000

LE RADIUS 0.252757 CENTER AT Z -14.002456 R-THETA -0.000000
TE RADIUS 0.887387 CENTER AT Z -0.887387 R-THETA -0.000000

CHORD	SOLIDITY	STAGGER	CAMBER
14.255213	0.752189	0.	0.

AREA	C.G. Z	C.G. R-THETA	S.P. Z	S.P. R-THETA
21.252029	-6.403911	0.	14.255213	0.000000

SURFACE ARC LENGTH 29.804

AST FRONT BLOCK FAN IGV STRUT SECTIONS (CM) *SAG* STATOR 0

SECTION CC RADIUS 63.500000 R/R 63.500000

SURFACE COORDINATES WITH ORIGIN AT S.P.

PT.	T/C	LOWER Z	LOWER R-THETA	UPPER Z	UPPER R-THETA
1	0.025239	-13.374101	-0.000000	-13.374101	-0.000000
2	0.025239	-13.318969	-0.160016	-13.318969	0.160016
3	0.025239	-13.208705	-0.242030	-13.208705	0.242030
4	0.044861	-13.039748	-0.299990	-13.039748	0.299990
5	0.056615	-12.705396	-0.378590	-12.705396	0.378590
6	0.073402	-12.036690	-0.490841	-12.036690	0.490841
7	0.086117	-11.367985	-0.575868	-11.367985	0.575868
8	0.096182	-10.699280	-0.643171	-10.699280	0.643171
9	0.104414	-10.030575	-0.698219	-10.030575	0.698219
10	0.111732	-9.361870	-0.747160	-9.361870	0.747160
11	0.117815	-8.693165	-0.787837	-8.693165	0.787837
12	0.122985	-8.024460	-0.822407	-8.024460	0.822407
13	0.127194	-7.355755	-0.850549	-7.355755	0.850549
14	0.130668	-6.687050	-0.873782	-6.687050	0.873782
15	0.133366	-6.018345	-0.891826	-6.018345	0.891826
16	0.135426	-5.349640	-0.905598	-5.349640	0.905598
17	0.136751	-4.680935	-0.914459	-4.680935	0.914459
18	0.137300	-4.012230	-0.918132	-4.012230	0.918132
19	0.137300	-3.343525	-0.918132	-3.343525	0.918132
20	0.137300	-2.674820	-0.918132	-2.674820	0.918132
21	0.137300	-2.006115	-0.918132	-2.006115	0.918132
22	0.137300	-1.738633	-0.918132	-1.738633	0.918132
23	0.137300	-1.604892	-0.918132	-1.604892	0.918132
24	0.137300	-1.471151	-0.918132	-1.471151	0.918132
25	0.137300	-1.337410	-0.918132	-1.337410	0.918132
26	0.137300	-1.203669	-0.918132	-1.203669	0.918132
27	0.137300	-1.069928	-0.918132	-1.069928	0.918132
28	0.137300	-0.994002	-0.918132	-0.994030	0.918132
29	0.137300	-0.918076	-0.918132	-0.918132	0.918132
30	0.137300	-0.306025	-0.684318	-0.306044	0.684335
31	0.137300	0.	-0.000000	0.	-0.000000

LE RADIUS 0.259784 CENTER AT Z -13.114316 R-THETA -0.000000
TE RADIUS 0.918132 CENTER AT Z -0.918132 R-THETA -0.000000

CHORD	SOLIDITY	STAGGER	CAMBER
13.374101	0.536329	0.	0.

AREA	C.G. Z	C.G. R-THETA	S.P. Z	S.P. R-THETA
20.555887	-6.007511	0.	13.374101	0.000000

SURFACE ARC LENGTH 28.093

AST FRONT BLOCK FAN IGV STRUT SECTIONS (CM) *SAG* STATOR 0

SECTION DD RADIUS 83.820000 R/R 83.820000

SURFACE COORDINATES WITH ORIGIN AT S.P.

PT.	T/C	LOWER Z	LOWER R-THETA	UPPER Z	UPPER R-THETA
1	0.026557	-12.199284	-0.000000	-12.199284	-0.000000
2	0.026557	-12.146875	-0.157658	-12.146875	0.157658
3	0.026557	-12.042055	-0.241013	-12.042055	0.241013
4	0.048945	-11.894302	-0.298546	-11.894302	0.298546
5	0.062378	-11.589320	-0.380481	-11.589320	0.380481
6	0.081523	-10.979356	-0.497262	-10.979356	0.497262
7	0.096037	-10.369392	-0.585790	-10.369392	0.585790
8	0.107462	-9.759428	-0.655482	-9.759428	0.655482
9	0.116881	-9.149463	-0.712931	-9.149463	0.712931
10	0.125218	-8.539499	-0.763787	-8.539499	0.763787
11	0.132166	-7.929535	-0.806168	-7.929535	0.806168
12	0.138034	-7.319571	-0.841956	-7.319571	0.841956
13	0.142820	-6.709606	-0.871151	-6.709606	0.871151
14	0.146834	-6.099642	-0.895637	-6.099642	0.895637
15	0.149922	-5.489678	-0.914473	-5.489678	0.914473
16	0.152238	-4.879714	-0.928600	-4.879714	0.928600
17	0.153782	-4.269750	-0.938018	-4.269750	0.938018
18	0.154400	-3.659785	-0.941785	-3.659785	0.941785
19	0.154400	-3.049821	-0.941785	-3.049821	0.941785
20	0.154400	-2.439857	-0.941785	-2.439857	0.941785
21	0.154400	-1.829893	-0.941785	-1.829893	0.941785
22	0.154400	-1.585907	-0.941785	-1.585907	0.941785
23	0.154400	-1.463914	-0.941785	-1.463914	0.941785
24	0.154400	-1.341921	-0.941785	-1.341921	0.941785
25	0.154400	-1.219929	-0.941785	-1.219929	0.941785
26	0.154400	-1.097936	-0.941785	-1.097936	0.941785
27	0.154400	-0.975943	-0.941785	-0.975943	0.941785
28	0.154400	-0.958835	-0.941785	-0.958864	0.941785
29	0.154400	-0.941727	-0.941785	-0.941785	0.941785
30	0.154400	-0.313909	-0.701948	-0.313928	0.701965
31	0.154400	0.	-0.000000	0.	-0.000000

LE RADIUS 0.263337 CENTER AT Z -11.935948 R-THETA -0.000000
TE RADIUS 0.941785 CENTER AT Z -0.941785 R-THETA -0.000000

CHORD	SOLIDITY	STAGGER	CAMBER
12.199285	0.370619	0.	0.

AREA	C.G. Z	C.G. R-THETA	S.P. Z	S.P. R-THETA
19.141828	-5.479087	0.	12.199284	0.000000

SURFACE ARC LENGTH 25.787

APPENDIX C

BLADE AND VANE AIRFOIL
MANUFACTURING SECTION
COORDINATES

6. Front Block Fan IGV Flap

AST FRONT BLOCK FAN IGV FLAP *SAG* STATOR 0

NB 16 SECTION AA RADIUS 30.48000 R/R 30.480000

SURFACE COORDINATES WITH ORIGIN AT S.P.

PT.	T/C	LOWER Z	LOWER R-THETA	UPPER Z	UPPER R-THETA
1	0.	-0.660400	-0.057777	-0.660400	-0.057777
2	0.041091	-0.471559	-0.314699	-0.519041	0.228033
3	0.056715	-0.297431	-0.403435	-0.362969	0.345658
4	0.077130	0.044564	-0.509370	-0.044564	0.509370
5	0.091140	0.382858	-0.573000	0.277542	0.630777
6	0.101608	0.719107	-0.613242	0.631693	0.728797
7	0.116008	1.387827	-0.650563	1.253773	0.881673
8	0.124523	2.053146	-0.649019	1.919254	0.995684
9	0.128950	2.716104	-0.620476	2.587096	1.082696
10	0.130200	3.377226	-0.570953	3.246774	1.148728
11	0.126196	4.695713	-0.428956	4.549887	1.237841
12	0.115714	6.010457	-0.244177	5.876743	1.284172
13	0.100837	7.322661	-0.030376	7.206139	1.301480
14	0.082315	8.632759	0.207501	8.537641	1.294714
15	0.061132	9.941320	0.462948	9.870680	1.270376
16	0.036977	11.248164	0.738023	11.205436	1.226412
17	0.026538	11.770453	0.853181	11.739787	1.203697
18	0.023804	11.900953	0.882793	11.873447	1.197196
19	0.021177	12.031516	0.911695	12.007044	1.191405
20	0.018443	12.162016	0.941307	12.140704	1.184904
21	0.015686	12.292503	0.971069	12.274377	1.178253
22	0.010076	12.488314	1.016121	12.475036	1.167889
23	0.010076	12.530324	1.042135	12.520926	1.149564
24	0.010076	12.547600	1.097772	12.547600	1.097772

LE RADIUS 0. CENTER AT Z -0.660400 R-THETA -0.057777
TE RADIUS 0.076929 CENTER AT Z 12.470964 R-THETA 1.091367

CHORD	SOLIDITY	STAGGER	CAMBER
13.258452	1.107690	5.000000	0.

AREA	C.G. Z	C.G. R-THETA	S.P. Z	S.P. R-THETA
15.937597	5.006214	0.437987	0.660400	0.057777

SURFACE ARC LENGTH 27.158

THROAT	NL	NU	SPACING	AT/S
10.213028	9	10	11.969458	0.853257

AST FRONT BLOCK FAN IGV FLAP *SAG* STATOR 0

NB 16 SECTION BB RADIUS 48.26000 R/R 48.260000

SURFACE COORDINATES WITH ORIGIN AT S.P.

PT.	T/C	LOWER Z	LOWER R-THETA	UPPER Z	UPPER R-THETA
1	0.	-0.838617	-0.073369	-0.838617	-0.073369
2	0.036357	-0.602288	-0.359924	-0.655638	0.249870
3	0.050181	-0.382491	-0.457512	-0.456126	0.384143
4	0.068244	0.050071	-0.572310	-0.050071	0.572310
5	0.080640	0.478473	-0.639576	0.360143	0.712945
6	0.089902	0.904577	-0.680564	0.772656	0.827303
7	0.102643	1.752542	-0.714044	1.601925	1.007522
8	0.110177	2.596686	-0.703857	2.435014	1.144073
9	0.114094	3.438177	-0.663334	3.270757	1.250290
10	0.115200	4.277605	-0.599239	4.108562	1.332934
11	0.111636	5.952224	-0.422615	5.788410	1.449787
12	0.102278	7.622591	-0.197392	7.472510	1.518041
13	0.089010	9.290089	0.060615	9.159478	1.553512
14	0.072516	10.955221	0.345672	10.848812	1.561933
15	0.053493	12.618497	0.651941	12.540003	1.549141
16	0.031910	14.279896	0.979674	14.233071	1.514886
17	0.022604	14.943961	1.116413	14.910792	1.495539
18	0.020185	15.109910	1.151374	15.080291	1.489925
19	0.017791	15.275877	1.186126	15.249770	1.484521
20	0.015372	15.441825	1.221088	15.419269	1.478907
21	0.012862	15.607707	1.256806	15.588833	1.472537
22	0.007864	15.874803	1.314366	15.851867	1.462231
23	0.007864	15.916529	1.339463	15.907317	1.444762
24	0.007864	15.933717	1.394019	15.933717	1.394019

LE RADIUS 0. CENTER AT Z -0.838617 R-THETA -0.073369
TE RADIUS 0.074776 CENTER AT Z 15.859225 R-THETA 1.387502

CHORD	SOLIDITY	STAGGER	CAMBER
16.836401	0.888387	5.000000	0.

AREA	C.G. Z	C.G. R-THETA	S.P. Z	S.P. R-THETA
22.667250	6.336416	0.554364	0.838617	0.073369

SURFACE ARC LENGTH 34.329

THROAT	NL	NU	SPACING	AT/S
16.968622	9	10	18.951642	0.895364

AST FRONT BLOCK FAN IGV FLAP *SAG* STATOR 0

NB 16 SECTION CC RADIUS 63.50000 R/R 63.500000

SURFACE COORDINATES WITH ORIGIN AT S.P.

PT.	T/C	LOWER Z	LOWER R-THETA	UPPER Z	UPPER R-THETA
1	0.	-0.991374	-0.086734	-0.991374	-0.086734
2	0.032254	-0.715555	-0.384811	-0.771506	0.254710
3	0.044518	-0.457074	-0.484710	-0.534299	0.397976
4	0.060543	0.052512	-0.600210	-0.052512	0.600210
5	0.071540	0.557736	-0.665862	0.433637	0.752596
6	0.079757	1.060550	-0.703955	0.922198	0.877423
7	0.091060	2.061728	-0.729279	1.903768	1.076215
8	0.097744	3.058899	-0.708807	2.889344	1.229211
9	0.101219	4.053286	-0.656522	3.877704	1.350393
10	0.102200	5.045511	-0.579514	4.868227	1.446854
11	0.099022	7.025503	-0.374545	6.853731	1.588820
12	0.090656	9.000994	-0.118133	8.843735	1.679344
13	0.078805	10.973463	0.172820	10.836761	1.735326
14	0.064093	12.943450	0.492143	12.832270	1.762940
15	0.047003	14.911375	0.835032	14.829839	1.765986
16	0.027696	16.877377	1.199904	16.829333	1.749050
17	0.019387	17.663269	1.351667	17.629639	1.736061
18	0.017241	17.859682	1.390291	17.829775	1.732131
19	0.015063	18.056069	1.429223	18.029938	1.727892
20	0.012917	18.252482	1.467847	18.230075	1.723962
21	0.010638	18.448779	1.507792	18.430326	1.718710
22	0.006176	18.781236	1.574987	18.769401	1.710266
23	0.006176	18.820079	1.597736	18.811604	1.694609
24	0.006176	18.836102	1.647945	18.836102	1.647945

LE RADIUS 0. CENTER AT Z -0.991374 R-THETA -0.086734
TE RADIUS 0.068286 CENTER AT Z 18.768076 R-THETA 1.641993

CHORD	SOLIDITY	STAGGER	CAMBER
19.903214	0.798160	5.000000	0.

AREA	C.G. Z	C.G. R-THETA	S.P. Z	S.P. R-THETA
28.025800	7.469378	0.653486	0.991374	0.086734

SURFACE ARC LENGTH 40.434

THROAT	NL	NU	SPACING	AT/S
22.839727	10	11	24.936371	0.915920

AST FRONT BLOCK FAN IGV FLAP *SAG* STATOR 0

VB 16 SECTION DD RADIUS 83.82000 R/R 83.820000

SURFACE COORDINATES WITH ORIGIN AT S.P.

PT.	T/C	LOWER Z	LOWER R-THETA	UPPER Z	UPPER R-THETA
1	0.	-1.195050	-0.104553	-1.195050	-0.104553
2	0.026826	-0.868240	-0.398999	-0.924335	0.242169
3	0.037026	-0.558813	-0.494756	-0.636237	0.390203
4	0.050354	0.052647	-0.601755	-0.052647	0.601755
5	0.059500	0.659734	-0.658778	0.535316	0.763331
6	0.066334	1.264404	-0.688171	1.125696	0.897278
7	0.075735	2.469283	-0.695965	2.310917	1.114178
8	0.081294	3.670146	-0.657844	3.500154	1.285164
9	0.084184	4.868217	-0.587828	4.692183	1.424254
10	0.085000	6.064120	-0.493026	5.886380	1.538559
11	0.082340	8.451439	-0.252125	8.279261	1.715871
12	0.075310	10.834189	0.040987	10.676711	1.840972
13	0.065365	13.213891	0.368942	13.077209	1.931231
14	0.053040	15.591105	0.725338	15.480195	1.993047
15	0.038590	17.966097	1.107129	17.885403	2.029469
16	0.022355	20.339223	1.510252	20.292477	2.044559
17	0.015385	21.287976	1.677190	21.255804	2.044907
18	0.013600	21.525119	1.719432	21.496681	2.044486
19	0.011730	21.762174	1.762690	21.737646	2.043049
20	0.009945	21.999318	1.804933	21.978522	2.042628
21	0.007990	22.236284	1.849207	22.219576	2.040176
22	0.004250	22.660248	1.927074	22.650620	2.037121
23	0.004250	22.692585	1.945341	22.685637	2.024746
24	0.004250	22.705950	1.986512	22.705950	1.986512

LE RADIUS 0. CENTER AT Z -1.195050 R-THETA -0.104553
TE RADIUS 0.055435 CENTER AT Z 22.650725 R-THETA 1.981685

CHORD	SOLIDITY	STAGGER	CAMBER
23.992298	0.728894	5.000000	0.

AREA	C.G. Z	C.G. R-THETA	S.P. Z	S.P. R-THETA
33.746803	8.969505	0.784730	1.195050	0.104553

SURFACE ARC LENGTH 48.526

THROAT	NL	NU	SPACING	AT/S
30.786906	10	11	32.916009	0.935317

APPENDIX C

BLADE AND VANE AIRFOIL
MANUFACTURING SECTION
COORDINATES

7. Rear Block Fan Rotor

REAR BLOCK FAN ROTOR

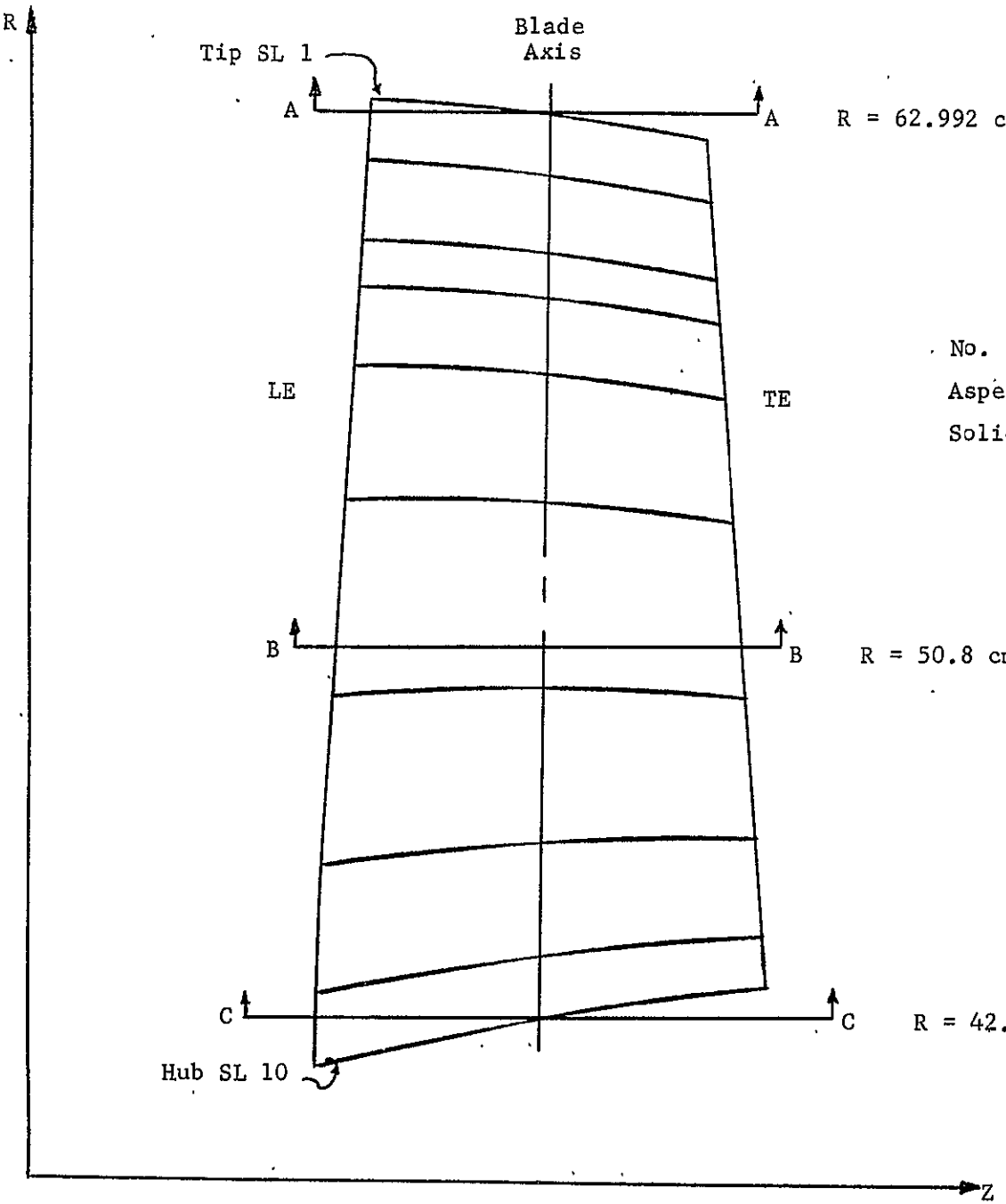

STAGE 4, ROTOR NB 40

SECTION NO 1 SECTION AA RHO 62.9920

MEANLINE DATA

PT	ALPHA	ZETA*	THICKNESS	UPSILON
1	-3.70686	57.859	0.06501	5.78020
2	-3.55907	57.198	0.09282	5.48513
3	-3.18339	56.004	0.14774	4.91618
4	-2.80768	55.352	0.20048	4.36705
5	-2.43225	55.441	0.24975	3.82411
6	-2.01951	56.248	0.29846	3.21780
7	-1.56991	57.540	0.34327	2.52797
8	-1.12078	58.682	0.37796	1.80552
9	-0.67257	59.206	0.40127	1.05939
10	-0.22517	58.897	0.41239	0.31114
11	0.22119	58.097	0.41106	-0.41757
12	0.66672	57.263	0.39756	-1.12128
13	1.11079	56.859	0.37247	-1.80550
14	1.55357	56.898	0.33684	-2.48335
15	1.99507	57.166	0.29193	-3.16392
16	2.43559	57.460	0.23926	-3.84978
17	2.87429	57.697	0.18069	-4.53968
18	3.31158	57.901	0.11822	-5.23283
19	3.67455	58.078	0.06472	-5.81311

SURFACE COORDINATES WITH ORIGIN AT SECTION AXIS

PT	T/C	UPPER ALPHA	UPPER UPSILON	LOWER ALPHA	LOWER UPSILON
1	0.00472	-3.74686	5.78020	-3.74686	5.78020
2	0.00472	-3.75220	5.77147	-3.73666	5.78128
3	0.00472	-3.75262	5.75526	-3.72189	5.77456
4	0.00472	-3.74736	5.73190	-3.70311	5.75971
5	0.00472	-3.73581	5.70184	-3.68094	5.73632
6	0.00472	-3.71757	5.66532	-3.65574	5.70416
7	0.00472	-3.69301	5.62210	-3.62707	5.66353
8	0.00672	-3.60019	5.46358	-3.52245	5.51369
9	0.00870	-3.42577	5.17134	-3.32581	5.23736
10	0.01066	-3.25109	4.88535	-3.12941	4.96738
11	0.01258	-3.07616	4.60448	-2.93327	4.70230
12	0.01445	-2.90102	4.32719	-2.73735	4.44022
13	0.01626	-2.72566	4.05179	-2.54163	4.17918
14	0.01830	-2.55008	3.77678	-2.34614	3.91745
15	0.01965	-2.37428	3.50067	-2.15088	3.65330
16	0.02152	-2.16298	3.16569	-1.91689	3.33055
17	0.02323	-1.95113	2.82418	-1.68306	2.99913
18	0.02478	-1.73843	2.47512	-1.45047	2.65851
19	0.02614	-1.52473	2.11838	-1.21929	2.30869
20	0.02732	-1.30987	1.75445	-0.98886	1.95038
21	0.02830	-1.09366	1.38419	-0.75978	1.58479
22	0.02906	-0.87587	1.00982	-0.53229	1.21469
23	0.02961	-0.65643	0.63432	-0.30645	0.84312
24	0.02993	-0.43529	0.26071	-0.08231	0.47317
25	0.03003	-0.21252	-0.10803	0.14021	0.10746
26	0.02990	0.01166	-0.47036	0.36131	-0.25318
27	0.02955	0.23716	-0.82577	0.58110	-0.60847
28	0.02899	0.46382	-1.17454	0.79973	-0.95913
29	0.02821	0.69153	-1.51754	1.01730	-1.30620
30	0.02723	0.92014	-1.85627	1.23397	-1.65141
31	0.02604	1.14966	-2.19264	1.44974	-1.99648
32	0.02468	1.38008	-2.52822	1.66460	-2.34267
33	0.02313	1.61143	-2.86430	1.87853	-2.69092
34	0.02143	1.84374	-3.20145	2.09151	-3.04139
35	0.01958	2.07692	-3.53978	2.30361	-3.39409
36	0.01759	2.31090	-3.87949	2.51492	-3.74907
37	0.01549	2.54560	-4.22070	2.72550	-4.10628
38	0.01329	2.78093	-4.56322	2.93545	-4.46531
39	0.01101	3.01675	-4.90674	3.14492	-4.82543
40	0.00867	3.25291	-5.25167	3.35404	-5.18819
41	0.00670	3.44994	-5.54056	3.52808	-5.49170
42	0.00670	3.62890	-5.80349	3.68595	-5.76787
43	0.00670	3.64794	-5.81705	3.69978	-5.79086
44	0.00670	3.67455	-5.81311	3.67455	-5.81311

CHORD 13.7953 STAGGER 57.375 CAMBER -0.158

AREA 3.962378 SURFACE ARC LENGTH 27.60307

	ALPHA	UPSILON
SECTION C.G.	-0.02821	0.02192
STREAMSURFACE SECTION C.G.	0.	0.
BLADE AXIS	0.	0.
STACKING AXIS (RADIAL)	0.	0.

COORD SYSTEM ORIGIN Z 122.58126 R 0.

STAGE 4. ROTOR NB 40

SECTION NO 2 SECTION BB RHO 50.8000

MEANLINE DATA

PT	ALPHA-	ZETA*	THICKNESS	UPSILON
1	-4.38259	56.153	0.11964	5.43124
2	-4.15823	55.210	0.16727	5.10283
3	-3.70934	53.451	0.26145	4.47758
4	-3.25958	52.310	0.35229	3.88476
5	-2.80934	51.913	0.43740	3.30746
6	-2.31357	51.835	0.52183	2.67604
7	-1.77235	51.721	0.60011	1.98869
8	-1.23077	51.357	0.66134	1.30650
9	-0.68897	50.516	0.70332	0.63765
10	-0.14720	49.083	0.72455	-0.00441
11	0.39426	47.372	0.72432	-0.61106
12	0.93554	45.864	0.70264	-1.18277
13	1.47653	45.054	0.66035	-1.73142
14	2.01686	44.895	0.59899	-2.27059
15	2.55632	45.099	0.52077	-2.80963
16	3.09494	45.371	0.42848	-3.35270
17	3.63204	45.603	0.32538	-3.89908
18	4.16810	45.818	0.21511	-4.44867
19	4.61355	46.005	0.12056	-4.90858

SURFACE COORDINATES WITH ORIGIN AT SECTION AXIS

PT	T/C	UPPER ALPHA	UPPER UPSILON	LOWER ALPHA	LOWER UPSILON
1	0.00873	-4.38259	5.43124	-4.38259	5.43124
2	0.00873	-4.39247	5.41461	-4.36342	5.43009
3	0.00873	-4.39268	5.38446	-4.33539	5.42288
4	0.00873	-4.38225	5.34143	-4.29936	5.39702
5	0.00873	-4.36004	5.28630	-4.25632	5.35586
6	0.00873	-4.32534	5.21954	-4.20678	5.29905
7	0.00873	-4.27883	5.14068	-4.14979	5.22722
8	0.01221	-4.22639	5.05426	-4.08897	5.14983
9	0.01568	-4.02003	4.72120	-3.84553	4.84655
10	0.01918	-3.81304	4.39770	-3.60271	4.55351
11	0.02246	-3.60549	4.08293	-3.36045	4.26914
12	0.02573	-3.39755	3.77498	-3.11859	3.99061
13	0.02889	-3.18922	3.47158	-2.87711	3.71524
14	0.03193	-2.98044	3.17107	-2.63608	3.44108
15	0.03482	-2.77104	2.87209	-2.39568	3.16681
16	0.03808	-2.51861	2.51468	-2.10834	2.83717
17	0.04107	-2.26473	2.15871	-1.82246	2.50686
18	0.04377	-2.00914	1.80452	-1.53827	2.17629
19	0.04617	-1.75166	1.45270	-1.25599	1.84602
20	0.04823	-1.49209	1.10405	-0.97579	1.51686
21	0.04994	-1.23013	0.75946	-0.69797	1.19001
22	0.05129	-0.96548	0.42048	-0.42286	0.86745
23	0.05227	-0.69815	0.08912	-0.15042	0.55079
24	0.05285	-0.42824	-0.23317	0.11944	0.24097
25	0.05305	-0.15587	-0.54528	0.38684	-0.06135
26	0.05286	0.11873	-0.84661	0.65200	-0.35618
27	0.05228	0.39511	-1.13681	0.91539	-0.64417
28	0.05131	0.67267	-1.41680	1.17760	-0.92729
29	0.04997	0.95126	-1.68835	1.43878	-1.20737
30	0.04826	1.23074	-1.95334	1.69906	-1.48620
31	0.04621	1.51126	-2.21373	1.95838	-1.76531
32	0.04382	1.79273	-2.47116	2.21662	-2.04572
33	0.04112	2.07542	-2.72700	2.47369	-2.32825
34	0.03813	2.35938	-2.98222	2.72951	-2.61321
35	0.03489	2.64459	-3.23748	2.98406	-2.90074
36	0.03141	2.93106	-3.49304	3.23736	-3.19062
37	0.02772	3.21864	-3.74894	3.48955	-3.48261
38	0.02386	3.50716	-4.00524	3.74079	-3.77646
39	0.01986	3.79643	-4.26203	3.99129	-4.07194
40	0.01576	4.08628	-4.51946	4.24121	-4.36891
41	0.01229	4.32815	-4.73462	4.44915	-4.61741
42	0.00880	4.52523	-4.91032	4.61835	-4.82036
43	0.00880	4.56598	-4.92676	4.63337	-4.86150
44.	0.00880	4.61355	-4.90858	4.61355	-4.90858

CHORD	STAGGER	CAMBER
13.7056	48.975	10.149

AREA 4.905326 SURFACE ARC LENGTH 27.60185

	ALPHA	UPSILON
SECTION C.G.	-0.00076	-0.00296
STREAMSURFACE SECTION C.G.	0.	0.
BLADE AXIS	0.	0.
STACKING AXIS (RADIAL)	0.	0.

COORD SYSTEM ORIGIN Z 122.54128 R 0.

STAGE 4, ROTOR NR 40

SECTION NO 3 SECTION CC RHO 42.3672

MEANLINE DATA

PT	ALPHA	ZETA*	THICKNESS	UPSILON
1	-4.66998	57.303	0.15579	5.34252
2	-4.42418	56.424	0.21722	4.98619
3	-3.93160	54.612	0.33927	4.20899
4	-3.43770	53.131	0.45754	3.57341
5	-2.98279	52.104	0.56885	2.92599
6	-2.39722	50.889	0.67962	2.21876
7	-1.80067	48.975	0.78271	1.52802
8	-1.20267	46.541	0.86422	0.86768
9	-0.60291	43.935	0.92192	-0.26264
10	-0.00158	41.611	0.95401	-0.29382
11	0.60141	39.571	0.95918	-0.81022
12	1.20600	37.632	0.93660	-1.29344
13	1.81189	35.492	0.88677	-1.74399
14	2.41968	33.070	0.81108	-2.15902
15	3.02866	30.486	0.71124	-2.53814
16	3.63850	27.929	0.58993	-2.88089
17	4.24906	25.556	0.45042	-3.19219
18	4.86029	23.352	0.29733	-3.47289
19	5.37082	21.602	0.16311	-3.68528

SURFACE COORDINATES WITH ORIGIN AT SECTION AXIS

PT	T/C	UPPER ALPHA	UPPER UPSILON	LOWER ALPHA	LOWER UPSIL
1	0.01154	-4.66998	5.34252	-4.66998	5.3425
2	0.01154	-4.68353	5.32097	-4.64471	5.3456
3	0.01154	-4.68485	5.28155	-4.60825	5.3307
4	0.01154	-4.67273	5.22505	-4.56169	5.2961
5	0.01154	-4.64569	5.15241	-4.50626	5.2419
6	0.01154	-4.60288	5.06420	-4.44257	5.1671
7	0.01154	-4.54517	4.95982	-4.36933	5.0727
8	0.01618	-4.50994	4.89784	-4.32797	5.0188
9	0.02081	-4.48370	4.50752	-4.05217	4.6667
10	0.02539	-4.05660	4.12895	-3.77723	4.3277
11	0.02989	-3.82863	3.76165	-3.50317	4.0003
12	0.03428	-3.59990	3.40599	-3.22985	3.6826
13	0.03853	-3.37032	3.05404	-2.95740	3.3704
14	0.04261	-3.13971	2.71069	-2.68597	3.0643
15	0.04649	-2.90762	2.37317	-2.41601	2.7634
16	0.05084	-2.62657	1.97679	-2.09462	2.4107
17	0.05084	-2.34251	1.59177	-1.77623	2.0685
18	0.05845	-2.05526	1.21952	-1.46103	1.7389
19	0.06165	-1.76459	0.86126	-1.14926	1.4218
20	0.06440	-1.47032	0.51812	-0.84107	1.1183
21	0.06671	-1.17305	0.19140	-0.53590	0.8281
22	0.06855	-0.87334	-0.11932	-0.23317	0.5491
23	0.06990	-0.57127	-0.41914	0.06721	0.2795
24	0.07076	-0.26699	-0.69694	0.36538	0.0193
25	0.07113	0.03928	-0.96554	0.66156	-0.2340
26	0.07098	0.34736	-1.22180	0.95593	-0.4816
27	0.07031	0.65751	-1.46676	1.24823	-0.7234
28	0.06914	0.96981	-1.70073	1.53837	-0.9602
29	0.06748	1.28446	-1.92381	1.82617	-1.1912
30	0.06533	1.60144	-2.13552	2.11163	-1.4159
31	0.06271	1.92006	-2.33505	2.39547	-1.6343
32	0.05968	2.23979	-2.52238	2.67819	-1.8468
33	0.05614	2.56069	-2.69788	2.95973	-2.0533
34	0.05223	2.88266	-2.86142	3.24020	-2.2535
35	0.04794	3.20480	-3.01265	3.52052	-2.4476
36	0.04329	3.52649	-3.15236	3.80127	-2.6365
37	0.03831	3.84795	-3.28176	4.08226	-2.8206
38	0.03305	4.16916	-3.40142	4.36350	-2.9996
39	0.02755	4.49003	-3.51160	4.64507	-3.1734
40	0.02186	4.81035	-3.61206	4.92721	-3.3410
41	0.01700	5.07592	-3.68839	5.16367	-3.4763
42	0.01208	5.26125	-3.73942	5.33084	-3.5700
43	0.01208	5.32046	-3.73576	5.37074	-3.6155
44	0.01208	5.37082	-3.68528	5.37082	-3.6857

CHORD 13.5025 STAGGER 41.95° CAMBER 35.104

AREA 9.110736 SURFACE ARC LENGTH 27.66462

	ALPHA	UPSILON
SECTION C.G.	0.06787	-0.02784
STREAMSURFACE SECTION C.G.	0.	0.
BLADE AXIS	0.	0.
STACKING AXIS (RADIAL)	0.	0.

COORD SYSTEM ORIGIN Z 122.94128 R 0.

APPENDIX C

BLADE AND VANE AIRFOIL
MANUFACTURING SECTION
COORDINATES

8. Rear Block Fan IGV Strut

REAR BLOCK FAN IGV STRUT SECTIONS (CM) *SAG* STATOR 0

SECTION AA RADIUS 48.260000 R/R 48.260000

SURFACE COORDINATES WITH ORIGIN AT S.P.

PT.	T/C	LOWER Z	LOWER R-THETA	UPPER Z	UPPER R-THETA
1	0.017530	-6.350000	-0.000000	-6.350000	-0.000000
2	0.017530	-6.331632	-0.048808	-6.331632	0.048808
3	0.017530	-6.294895	-0.071570	-6.294895	0.071570
4	0.029867	-6.191250	-0.094828	-6.191250	0.094828
5	0.037242	-6.032500	-0.118242	-6.032500	0.118242
6	0.047802	-5.715000	-0.151770	-5.715000	0.151770
7	0.055792	-5.397500	-0.177140	-5.397500	0.177140
8	0.062163	-5.080000	-0.197368	-5.080000	0.197368
9	0.067320	-4.762500	-0.213741	-4.762500	0.213741
10	0.071931	-4.445000	-0.228382	-4.445000	0.228382
11	0.075750	-4.127500	-0.240508	-4.127500	0.240508
12	0.079024	-3.810000	-0.250901	-3.810000	0.250901
13	0.081682	-3.492500	-0.259339	-3.492500	0.259339
14	0.083829	-3.175000	-0.266156	-3.175000	0.266156
15	0.085518	-2.857500	-0.271521	-2.857500	0.271521
16	0.086838	-2.540000	-0.275712	-2.540000	0.275712
17	0.087648	-2.222500	-0.278282	-2.222500	0.278282
18	0.088000	-1.905000	-0.279400	-1.905000	0.279400
19	0.088000	-1.587500	-0.279400	-1.587500	0.279400
20	0.088000	-1.270000	-0.279400	-1.270000	0.279400
21	0.088000	-0.952500	-0.279400	-0.952500	0.279400
22	0.088000	-0.825500	-0.279400	-0.825500	0.279400
23	0.088000	-0.762000	-0.279400	-0.762000	0.279400
24	0.088000	-0.698500	-0.279400	-0.698500	0.279400
25	0.088000	-0.635000	-0.279400	-0.635000	0.279400
26	0.088000	-0.571500	-0.279400	-0.571500	0.279400
27	0.088000	-0.508000	-0.279400	-0.508000	0.279400
28	0.088000	-0.381000	-0.279400	-0.381000	0.279400
29	0.088000	-0.279332	-0.279400	-0.279400	0.279400
30	0.088000	-0.093111	-0.208232	-0.093133	0.208252
31	0.088000	0.	-0.000000	0.	-0.000000

LE RADIUS 0.074029 CENTER AT Z -6.275971 R-THETA -0.000000
TE RADIUS 0.279400 CENTER AT Z -0.279400 R-THETA -0.000000

CHORD	SOLIDITY	STAGGER	CAMBER
6.350000	0.753893	0.	0.

AREA	C.G. Z	C.G. R-THETA	S.P. Z	S.P. R-THETA
2.999059	-2.843799	0.	6.350000	0.000000

SURFACE ARC LENGTH 13.095

REAR BLOCK FAN IGV STRUT SECTIONS (CM) *SAG* STATOR 0

SECTION BB RADIUS 55.880000 R/R 55.880000

SURFACE COORDINATES WITH ORIGIN AT S.P.

PT.	T/C	LOWER Z	LOWER R-THETA	UPPER Z	UPPER R-THETA
1	0.018900	-6.350000	-0.000000	-6.350000	-0.000000
2	0.018900	-6.330280	-0.053728	-6.330280	0.053728
3	0.018900	-6.290840	-0.079541	-6.290840	0.079541
4	0.033100	-6.191250	-0.105093	-6.191250	0.105093
5	0.041600	-6.032500	-0.132080	-6.032500	0.132080
6	0.053750	-5.715000	-0.170656	-5.715000	0.170656
7	0.062950	-5.397500	-0.199866	-5.397500	0.199866
8	0.070250	-5.080000	-0.223044	-5.080000	0.223044
9	0.076200	-4.762500	-0.241935	-4.762500	0.241935
10	0.081500	-4.445000	-0.258763	-4.445000	0.258763
11	0.085900	-4.127500	-0.272733	-4.127500	0.272733
12	0.089650	-3.810000	-0.284639	-3.810000	0.284639
13	0.092700	-3.492500	-0.294323	-3.492500	0.294323
14	0.095200	-3.175000	-0.302260	-3.175000	0.302260
15	0.097150	-2.857500	-0.308451	-2.857500	0.308451
16	0.098650	-2.540000	-0.313214	-2.540000	0.313214
17	0.099600	-2.222500	-0.316230	-2.222500	0.316230
18	0.100000	-1.905000	-0.317500	-1.905000	0.317500
19	0.100000	-1.587500	-0.317500	-1.587500	0.317500
20	0.100000	-1.270000	-0.317500	-1.270000	0.317500
21	0.100000	-0.952500	-0.317500	-0.952500	0.317500
22	0.100000	-0.825500	-0.317500	-0.825500	0.317500
23	0.100000	-0.762000	-0.317500	-0.762000	0.317500
24	0.100000	-0.698500	-0.317500	-0.698500	0.317500
25	0.100000	-0.635000	-0.317500	-0.635000	0.317500
26	0.100000	-0.571500	-0.317500	-0.571500	0.317500
27	0.100000	-0.508000	-0.317500	-0.508000	0.317500
28	0.100000	-0.381000	-0.317500	-0.381000	0.317500
29	0.100000	-0.317423	-0.317500	-0.317500	0.317500
30	0.100000	-0.105807	-0.236627	-0.105833	0.236651
31	0.100000	0.	-0.000000	0.	-0.000000

LE RADIUS 0.083052 CENTER AT Z -6.266949 R-THETA -0.000000
TE RADIUS 0.317500 CENTER AT Z -0.317500 R-THETA -0.000000

CHORD	SOLIDITY	STAGGER	CAMBER
6.350000	0.651089	0.	0.

AREA	C.G. Z	C.G. R-THETA	S.P. Z	S.P. R-THETA
3.395317	-2.842575	0.	6.350000	0.000000

SURFACE ARC LENGTH 13.151

REAR BLOCK FAN IGV STRUT SECTIONS (CM) *SAG* STATOR - 0

SECTION CC RADIUS 63.500000 R/R 63.500000

SURFACE COORDINATES WITH ORIGIN AT S.P.

PT.	T/C	LOWER Z	LOWER R-THETA	UPPER Z	UPPER R-THETA
1	0.020026	-6.350000	-0.000000	-6.350000	-0.000000
2	0.020026	-6.329222	-0.058096	-6.329222	0.058096
3	0.020026	-6.287664	-0.086804	-6.287664	0.086804
4	0.036131	-6.191250	-0.114717	-6.191250	0.114717
5	0.045786	-6.032500	-0.145369	-6.032500	0.145369
6	0.059562	-5.715000	-0.189108	-5.715000	0.189108
7	0.070000	-5.397500	-0.222250	-5.397500	0.222250
8	0.078243	-5.080000	-0.248422	-5.080000	0.248422
9	0.085008	-4.762500	-0.269900	-4.762500	0.269900
10	0.091011	-4.445000	-0.288961	-4.445000	0.288961
11	0.096006	-4.127500	-0.304820	-4.127500	0.304820
12	0.100240	-3.810000	-0.318262	-3.810000	0.318262
13	0.103690	-3.492500	-0.329214	-3.492500	0.329214
14	0.106557	-3.175000	-0.338318	-3.175000	0.338318
15	0.108774	-2.857500	-0.345359	-2.857500	0.345359
16	0.110454	-2.540000	-0.350693	-2.540000	0.350693
17	0.111552	-2.222500	-0.354178	-2.222500	0.354178
18	0.112000	-1.905000	-0.355600	-1.905000	0.355600
19	0.112000	-1.587500	-0.355600	-1.587500	0.355600
20	0.112000	-1.270000	-0.355600	-1.270000	0.355600
21	0.112000	-0.952500	-0.355600	-0.952500	0.355600
22	0.112000	-0.825500	-0.355600	-0.825500	0.355600
23	0.112000	-0.762000	-0.355600	-0.762000	0.355600
24	0.112000	-0.698500	-0.355600	-0.698500	0.355600
25	0.112000	-0.635000	-0.355600	-0.635000	0.355600
26	0.112000	-0.571500	-0.355600	-0.571500	0.355600
27	0.112000	-0.508000	-0.355600	-0.508000	0.355600
28	0.112000	-0.381000	-0.355600	-0.381000	0.355600
29	0.112000	-0.355513	-0.355600	-0.355600	0.355600
30	0.112000	-0.118504	-0.265023	-0.118533	0.265049
31	0.112000	0.	-0.000000	0.	-0.000000

LE RADIUS 0.091606 CENTER AT Z -6.258395 R-THETA -0.000000
TE RADIUS 0.355600 CENTER AT Z -0.355600 R-THETA -0.000000

CHORD	SOLIDITY	STAGGER	CAMBER
6.350000	0.572958	0.	0.

AREA	C.G. Z	C.G. R-THETA	S.P. Z	S.P. R-THETA
3.788554	-2.841342	0.	6.350000	0.000000

SURFACE ARC LENGTH 13.207

APPENDIX C

BLADE AND VANE AIRFOIL
MANUFACTURING SECTION
COORDINATES

9. Rear Block Fan IGV Flap

AST REAR BLOCK FAN IGV FLAP SECTIONS (CM) *SAG* STATOR 3

NB 36 SECTION AA RADIUS 48.26000 R/R 48.260000

SURFACE COORDINATES WITH ORIGIN AT S.P.

PT.	T/C	LOWER Z	LOWER R-THETA	UPPER Z	UPPER R-THETA
1	0.	-0.370515	-0.032416	-0.370515	-0.032416
2	0.035663	-0.266326	-0.156448	-0.289447	0.107824
3	0.049223	-0.169302	-0.198586	-0.201214	0.166170
4	0.066941	0.021700	-0.248027	-0.021700	0.248027
5	0.079100	0.210898	-0.276869	0.159617	0.309285
6	0.088185	0.399101	-0.294324	0.341929	0.359155
7	0.100683	0.773667	-0.308214	0.708393	0.437877
8	0.108073	1.146578	-0.303180	1.076512	0.497675
9	0.111915	1.518339	-0.284999	1.445782	0.544326
10	0.113000	1.889205	-0.256603	1.815946	0.580761
11	0.109517	2.629107	-0.178867	2.558105	0.632689
12	0.100389	3.367178	-0.080214	3.302094	0.663700
13	0.087439	4.104010	0.032598	4.047322	0.680551
14	0.071326	4.839817	0.157134	4.793575	0.685678
15	0.052839	5.574854	0.290462	5.540598	0.682014
16	0.031798	6.309064	0.433252	6.288449	0.668887
17	0.022713	6.602531	0.492847	6.587806	0.661157
18	0.020340	6.675865	0.508123	6.662678	0.658848
19	0.018035	6.749221	0.523147	6.737528	0.656790
20	0.015662	6.822554	0.538422	6.812401	0.654481
21	0.013244	6.895874	0.553865	6.887288	0.652004
22	0.008362	7.012079	0.578491	7.006003	0.647941
23	0.008362	7.031702	0.590271	7.027374	0.639747
24	0.008362	7.039787	0.615901	7.039787	0.615901

LE RADIUS 0. CENTER AT Z -0.370515 R-THETA -0.032416
TE RADIUS 0.035116 CENTER AT Z 7.004804 R-THETA 0.612845

CHORD	SOLIDITY	STAGGER	CAMBER
7.438608	0.883135	5.000000	0.

AREA	C.G. Z	C.G. R-THETA	S.P. Z	S.P. R-THETA
4.348912	2.805355	0.245437	0.370515	0.032416

SURFACE ARC LENGTH 15.161

THROAT	NL	NU	SPACING	AT/S
7.563049	9	10	8.422952	0.897910

AST REAR BLOCK FAN IGV FLAP SECTIONS (CM) *SAG* STATOR 0

NB 36 SECTION BB RADIUS 55.88000 R/R 55.880000

SURFACE COORDINATES WITH ORIGIN AT S.P.

PT.	T/C	LOWER Z	LOWER R-THETA	UPPER Z	UPPER R-THETA
1	0.	-0.399237	-0.034929	-0.399237	-0.034929
2	0.035663	-0.286971	-0.168576	-0.311884	0.116183
3	0.049223	-0.182426	-0.213980	-0.216811	0.179051
4	0.066941	0.023382	-0.267254	-0.023382	0.267254
5	0.079100	0.227247	-0.298332	0.171990	0.333261
6	0.088185	0.430039	-0.317139	0.368435	0.386997
7	0.100683	0.833642	-0.332106	0.763307	0.471821
8	0.108073	1.235460	-0.326682	1.159963	0.536254
9	0.111915	1.636039	-0.307092	1.557858	0.586522
10	0.113000	2.035655	-0.276494	1.956716	0.625781
11	0.109497	2.832906	-0.192652	2.756414	0.681654
12	0.100288	3.628163	-0.086027	3.558105	0.714743
13	0.087236	4.422079	0.035937	4.361138	0.732494
14	0.071021	5.214889	0.170533	5.165276	0.737613
15	0.052263	6.006811	0.315279	5.970302	0.732582
16	0.031019	6.797865	0.469951	6.776197	0.717625
17	0.021866	7.114058	0.534436	7.098783	0.709026
18	0.019493	7.193077	0.550895	7.179460	0.706538
19	0.017119	7.272095	0.567355	7.260136	0.704050
20	0.014747	7.351114	0.583815	7.340812	0.701562
21	0.012260	7.430093	0.600725	7.421528	0.698622
22	0.007345	7.559303	0.628342	7.553570	0.693873
23	0.007345	7.577859	0.639444	7.573772	0.686161
24	0.007345	7.585505	0.663645	7.585505	0.663645

LE RADIUS 0. CENTER AT Z -0.399237 R-THETA -0.034929
TE RADIUS 0.033127 CENTER AT Z 7.552504 R-THETA 0.660763

CHORD	SOLIDITY	STAGGER	CAMBER
8.015243	0.821832	5.000000	0.

AREA	C.G. Z	C.G. R-THETA	S.P. Z	S.P. R-THETA
5.033438	3.012988	0.263602	0.399237	0.034929

SURFACE ARC LENGTH 16.332

THROAT	NL	NU	SPACING	AT/S
8.824229	10	11	9.752892	0.904781

AST REAR BLOCK FAN IGV FLAP SECTIONS (CM) *SAG* STATOR 0

NB 36 SECTION CC RADIUS 63.50000 R/R 63.500000

SURFACE COORDINATES WITH ORIGIN AT S.P.

PT.	T/C	LOWER Z	LOWER R-THETA	UPPER Z	UPPER R-THETA
1	0.	-0.427959	-0.037442	-0.427959	-0.037442
2	0.035663	-0.307617	-0.180703	-0.334322	0.124541
3	0.049223	-0.195550	-0.229374	-0.232409	0.191933
4	0.066941	-0.025064	-0.286481	-0.025064	0.286481
5	0.079100	0.243596	-0.319795	0.184363	0.357236
6	0.088185	0.460977	-0.339955	0.394941	0.414838
7	0.100683	0.893616	-0.355999	0.818221	0.505765
8	0.108073	1.324342	-0.350184	1.243413	0.574834
9	0.111915	1.753739	-0.329185	1.669934	0.628718
10	0.113000	2.182105	-0.296386	2.097487	0.670802
11	0.109477	3.036704	-0.206424	2.954724	0.730606
12	0.100186	3.889143	-0.091780	3.814121	0.765728
13	0.087033	4.740137	0.039393	4.674964	0.784321
14	0.070715	5.589946	0.184107	5.536992	0.789373
15	0.051686	6.438739	0.340428	6.400035	0.782819
16	0.030239	7.286627	0.507097	7.263984	0.765916
17	0.021018	7.625542	0.576511	7.609803	0.756408
18	0.018645	7.710246	0.594155	7.696284	0.753741
19	0.016204	7.794924	0.612089	7.782789	0.750784
20	0.013831	7.879627	0.629733	7.869270	0.748117
21	0.011277	7.964262	0.648150	7.955818	0.744676
22	0.006328	8.107034	0.678889	8.101757	0.739206
23	0.006328	8.124164	0.689092	8.120398	0.732132
24	0.006328	8.131224	0.711390	8.131224	0.711390

LE RADIUS 0. CENTER AT Z -0.427959 R-THETA -0.037442
TE RADIUS 0.030482 CENTER AT Z 8.100858 R-THETA 0.708738

CHORD	SOLIDITY	STAGGER	CAMBER
8.591878	0.775242	5.000000	0.

AREA	C.G. Z	C.G. R-THETA	S.P. Z	S.P. R-THETA
5.765492	3.219131	0.281637	0.427959	0.037442

SURFACE ARC LENGTH 17.502

THROAT	NL	NU	SPACING	AT/S
10.085477	10	11	11.082831	0.910009

APPENDIX D

LIST OF SYMBOLS AND NOMENCLATURE

APPENDIX D

LIST OF SYMBOLS AND NOMENCLATURE

Symbol	Description	Units
A	Area	m^2 or cm^2
C_P	Specific Heat at Constant Pressure	calorie per gram degree C
C	Blade Chord	cm
CH'	Static Pressure-Rise Coefficient: $CH' = \left\{2g\ \bar{C}_p\ \bar{T}_{S_1}\ \left[\left(\bar{P}_{S_2}/\bar{P}_{S_1}\right)^{\frac{\gamma-1}{\gamma}} - 1\right] - \left(U_2^2 - U_1^2\right)\right\} \div \left(V_1'\right)^2$	
CP	Constant Pitch	
D or D-Factor	Diffusion Factor: $D_{rotor} = 1 - (V'_2/V'_1) + (r_2 V_{\theta_2} - r_1 V_{\theta_1})/(2\ \bar{r}\ \sigma\ V'_1)$ $D_{stator} = 1 - (V_2/V_1) + (r_1 V_{\theta_1} - r_2 V_{\theta_2})/(2\ \bar{r}\ \sigma\ V_1)$	
d	Diameter	m
i	Incidence Angle	degrees
HP	High Pressure	---
IGV	Inlet Guide Vane	---
I.D.	Inner Diameter	---
K_t	Stress Concentration Factor	
LP	Low Pressure	
M	Mach Number	
N	Engine Speed	rpm
N_B	Number of Blades	
N_V	Number of Vanes	
NCT	Near Constant Tip	

LIST OF SYMBOLS AND NOMENCLATURE (Continued)

Symbol	Description	Units
O.D.	Outer Diameter	
P, p	Static Pressure	Newton/m^2
P_T	Total Pressure	Newton/m^2
q	Dynamic Pressure (Total Pressure - Static Pressure, Incompressible)	Newton/m^2
R or r	Radius	cm
rpm	Revolutions per Minute	
R1, R2	Rotor 1, Rotor 2, Respectively	
$\bar{r}$	Mean Radius	cm
S1, S2	Stator 1, Stator 2, Respectively	
SL	Streamline	
Stall Margin(%)	$\frac{\left(\frac{P/P}{W}\right)_{\text{stall}} - \left(\frac{P/P}{W}\right)_{\text{operating line}}}{\left(\frac{P/P}{W}\right)_{\text{operating line}}} \times 100$	
Ti	Titanium	
T	Temperature	K
t	Thickness (Blade)	cm
U	Rotor Speed	m/sec
V	Velocity	m/sec
W	Airflow	kg/sec
Z	Axial Distance	cm
β	Flow Angle	degrees

LIST OF SYMBOLS AND NOMENCLATURE (Continued)

Symbol	Description	Units
γ	Specific Heat Ratio	
δ	Pressure Correction ($P_T/1.0133 \times 10^5$ N/m^2)	
δ^o	Deviation Angle	degrees
θ	Temperature Correction ($T_{T_1}/288.15$ K)	
λ	Effective Area Coefficient: $A_{effective}/A_{physical}$	
ρ	Air Density	kg/m^3
σ	Solidity	
ψ	Percent Flow Streamfunction	
ϕ	Slope of Meridional Streamline	degrees
η	Efficiency	
$\bar{\omega}$	Total Pressure Loss Coefficient:	

$$\text{Rotor } \bar{\omega} = \frac{P'_{T_{2_{id}}} - P'_{T_2}}{P'_{T_1} - P_{S_1}}$$

$$\text{Stator } \bar{\bar{\omega}} = \frac{P_{T_1} - P_{T_2}}{P_{T_1} - P_{S_1}}$$

Subscripts

ad Adiabatic

id Ideal

poly Polytropic

m Meridional Direction

T Total

S Static

1 Inlet

2 Exit

Superscripts

' Relative to Rotor

o Degrees

LIST OF SYMBOLS AND NOMENCLATURE (Concluded)

Subscripts

1	Leading Edge
2	Trailing Edge
Sta	Blade Row Exit Station
I	Cascade Inlet Capture
m or max	Maximum
r	Radial
S or s	Static Condition
T	Total
TH	Throat
Z	Axial Direction
θ	Tangential Direction
∞	Free Stream
0	Total or Stagnation Conditions

References

1. Koch, C.C. and Smith, L.H., Jr.; "Loss Sources and Magnitudes in Axial-Flow Compressors," Transactions of ASME Journal of Engineering for Power, Vol. 98, Series A, No. 3, July 1976, Page 411.

2. Seyler, D.R. and Smith, L.H.; "Single Stage Experimental Evaluation of High Mach Number Compressor Rotor Blading Part 1 - Design of Rotor Blading, NASA CR-54581, April 1, 1967.

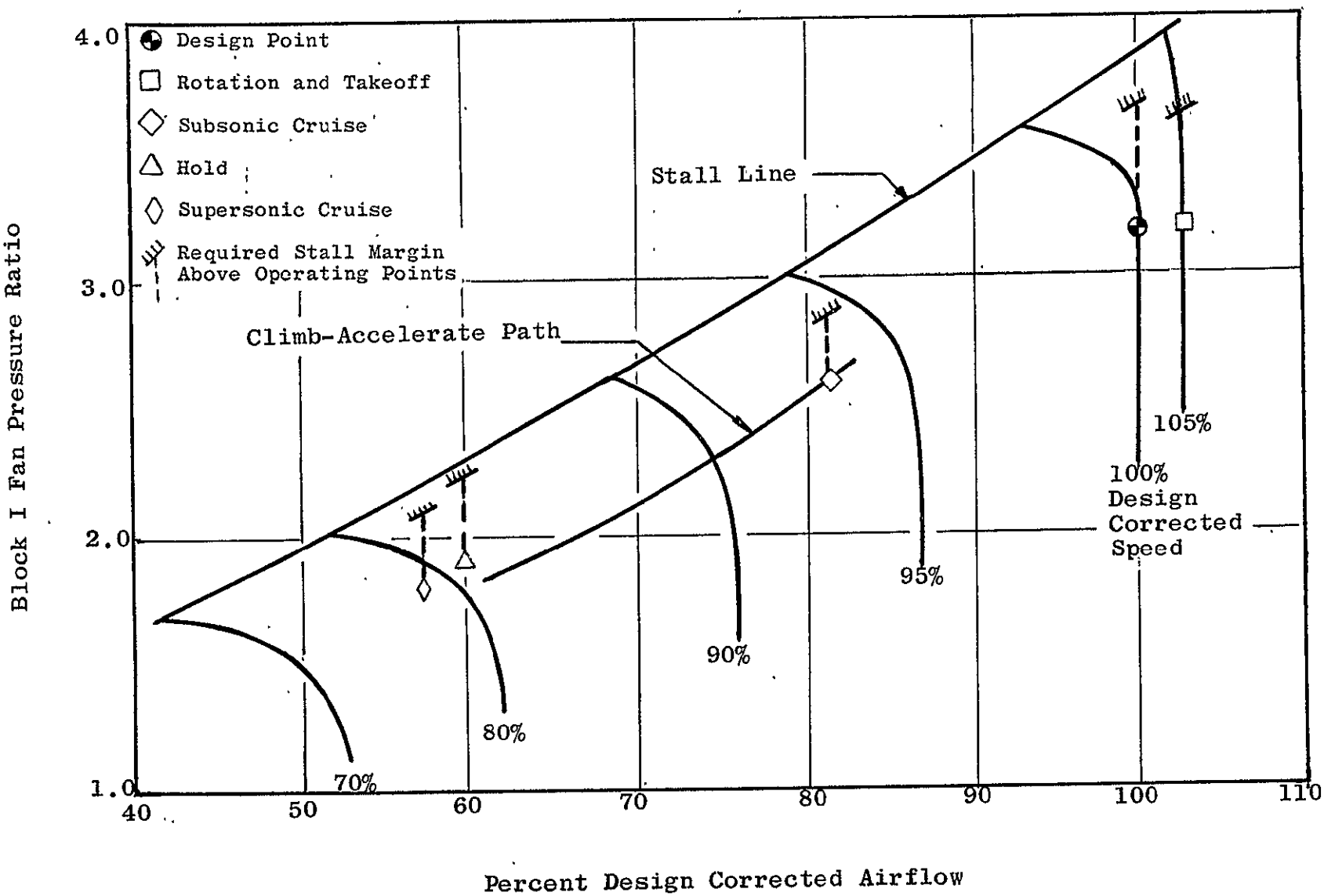

Figure 1. Stall Margin Requirements for a Typical AST Front Block Performance Map.

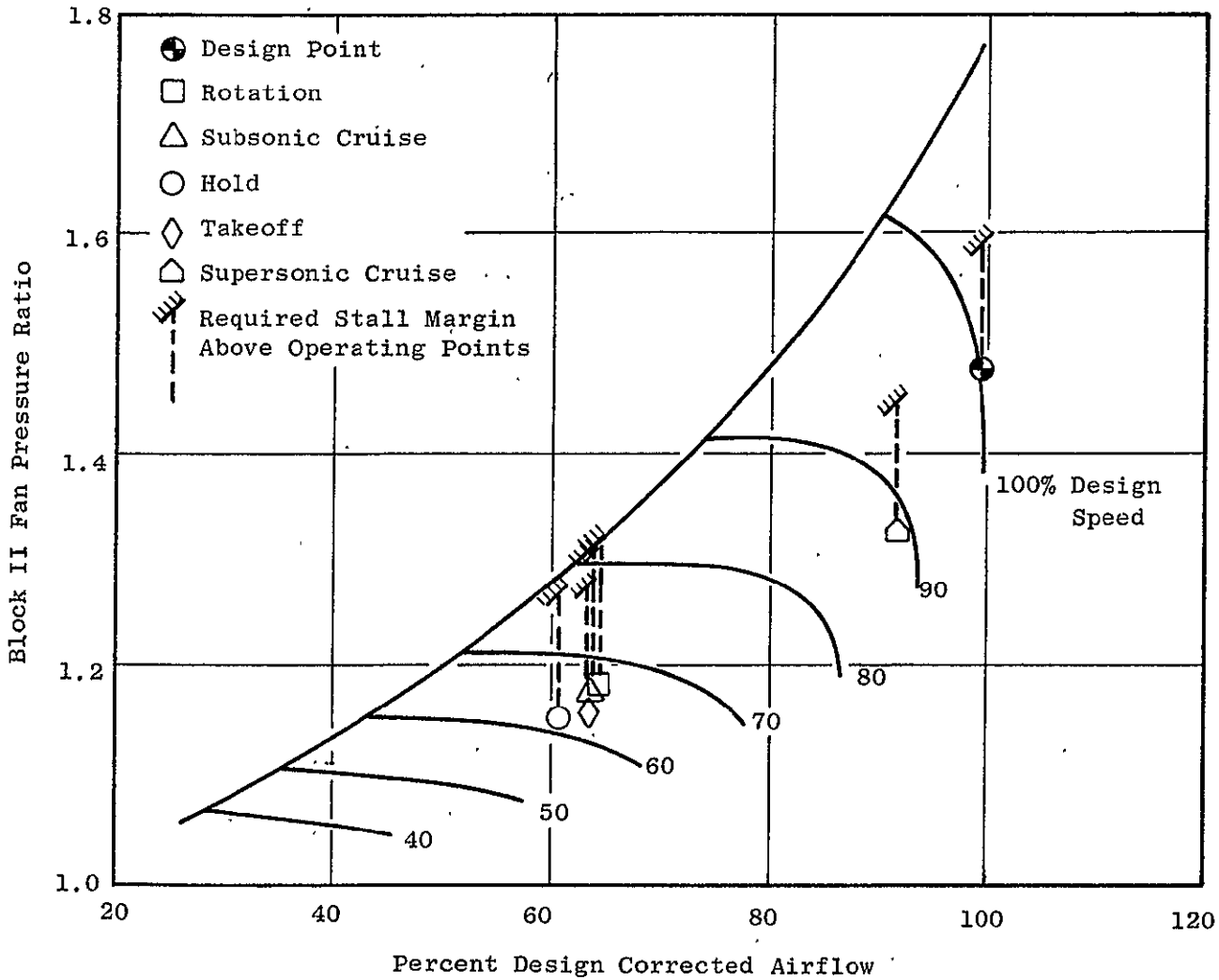

Figure 2. Stall Margin Requirements for a Typical AST Rear Block Performance Map.

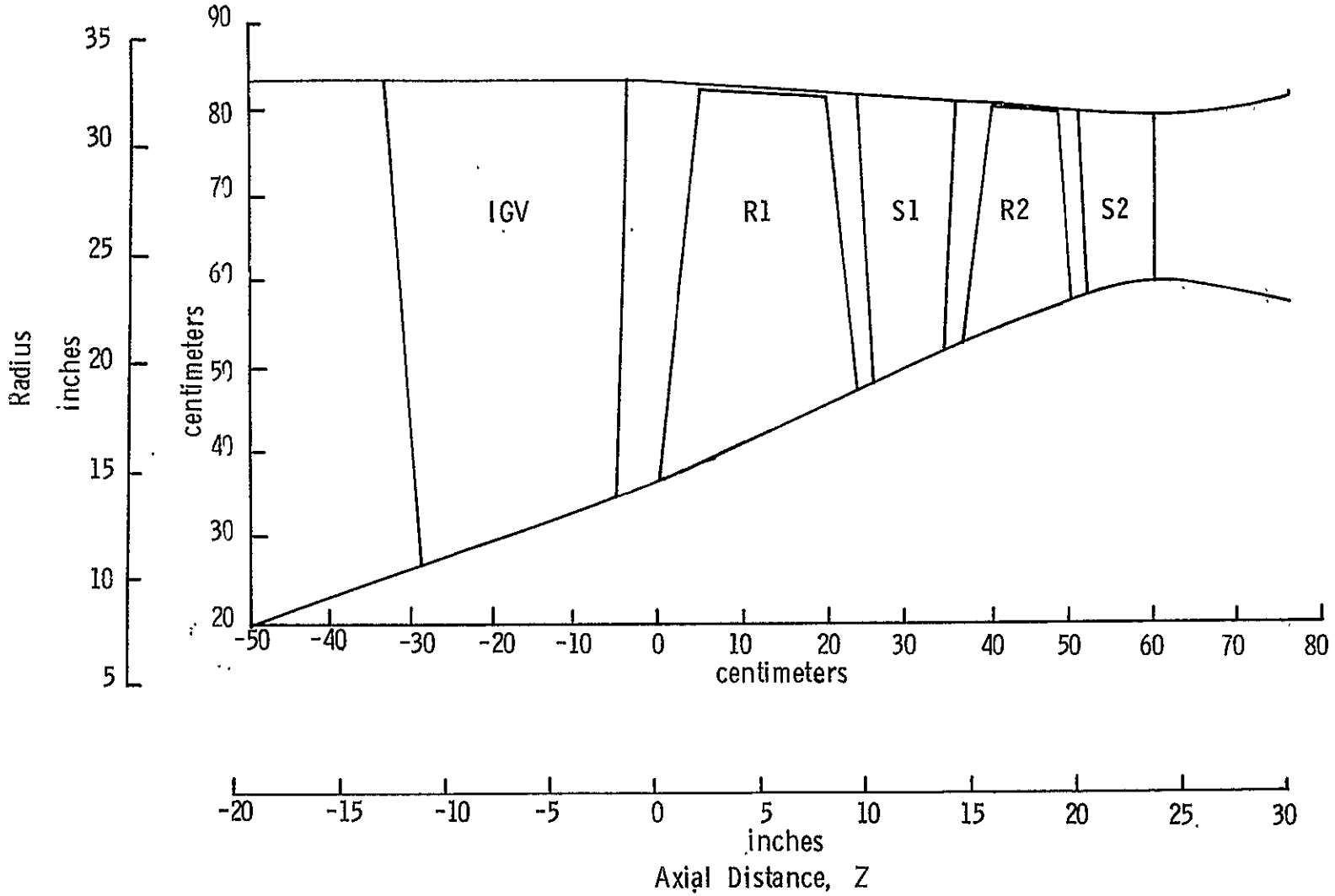

Figure 3. Front Block Fan Screening Study - Two-Stage Tapered Casing Nominal Fan Design Flowpath.

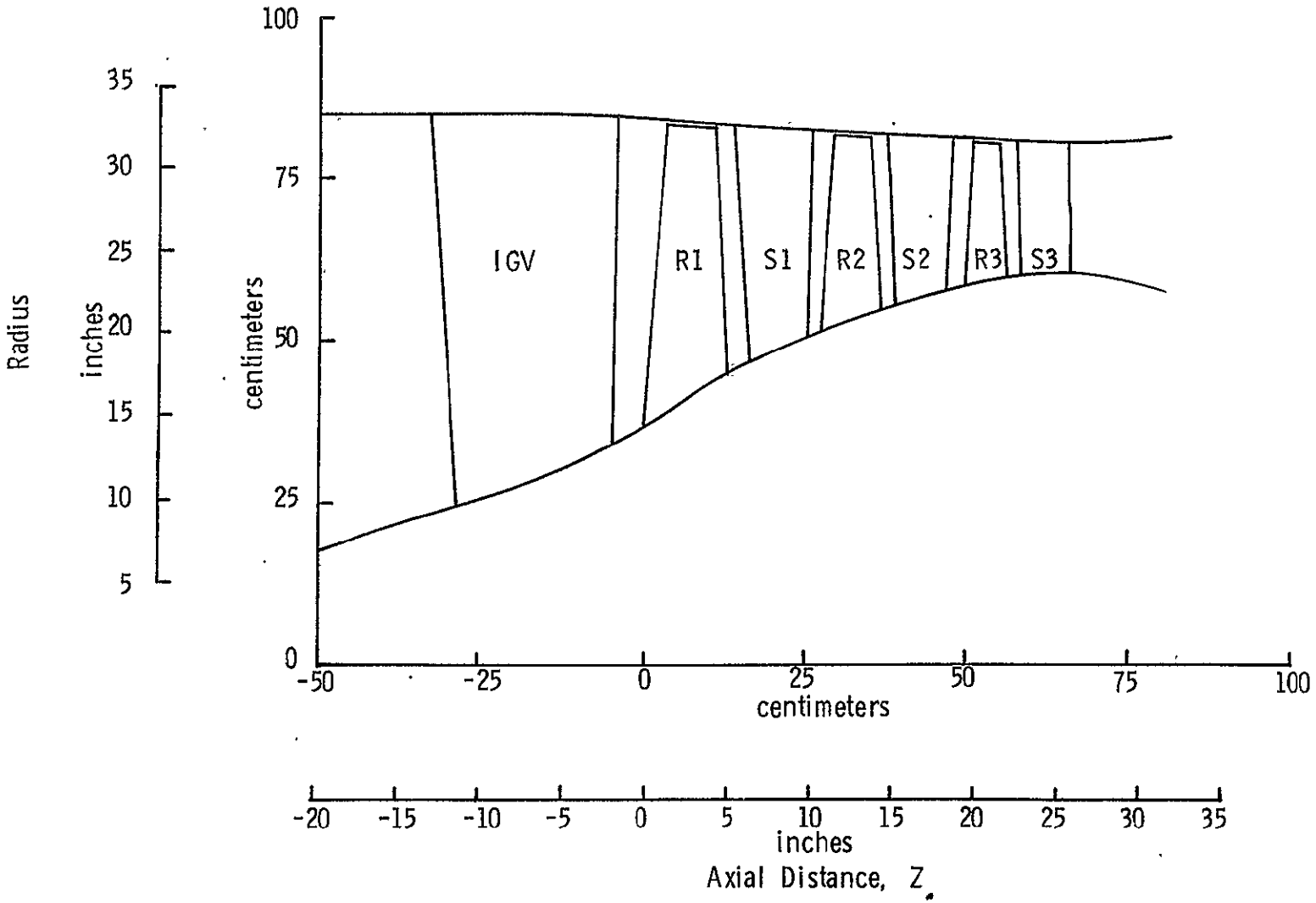

Figure 4. Front Block Fan Screening Study -Three-Stage Near Constant Tip Fan Design Flowpath.

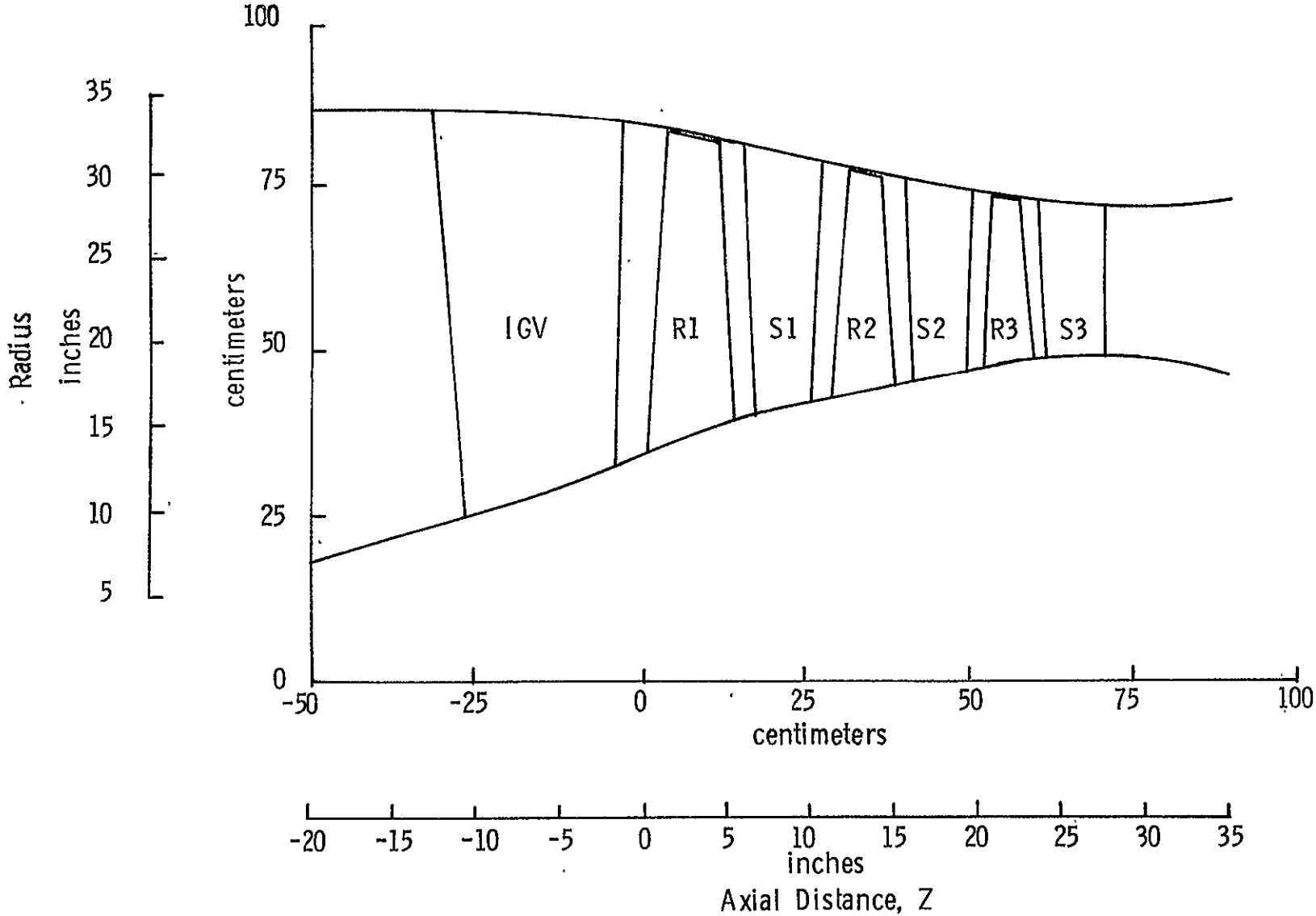

Figure 5. Front Block Fan Screening Study - Three-Stage Constant Pitch Nominal Fan Design Flowpath.

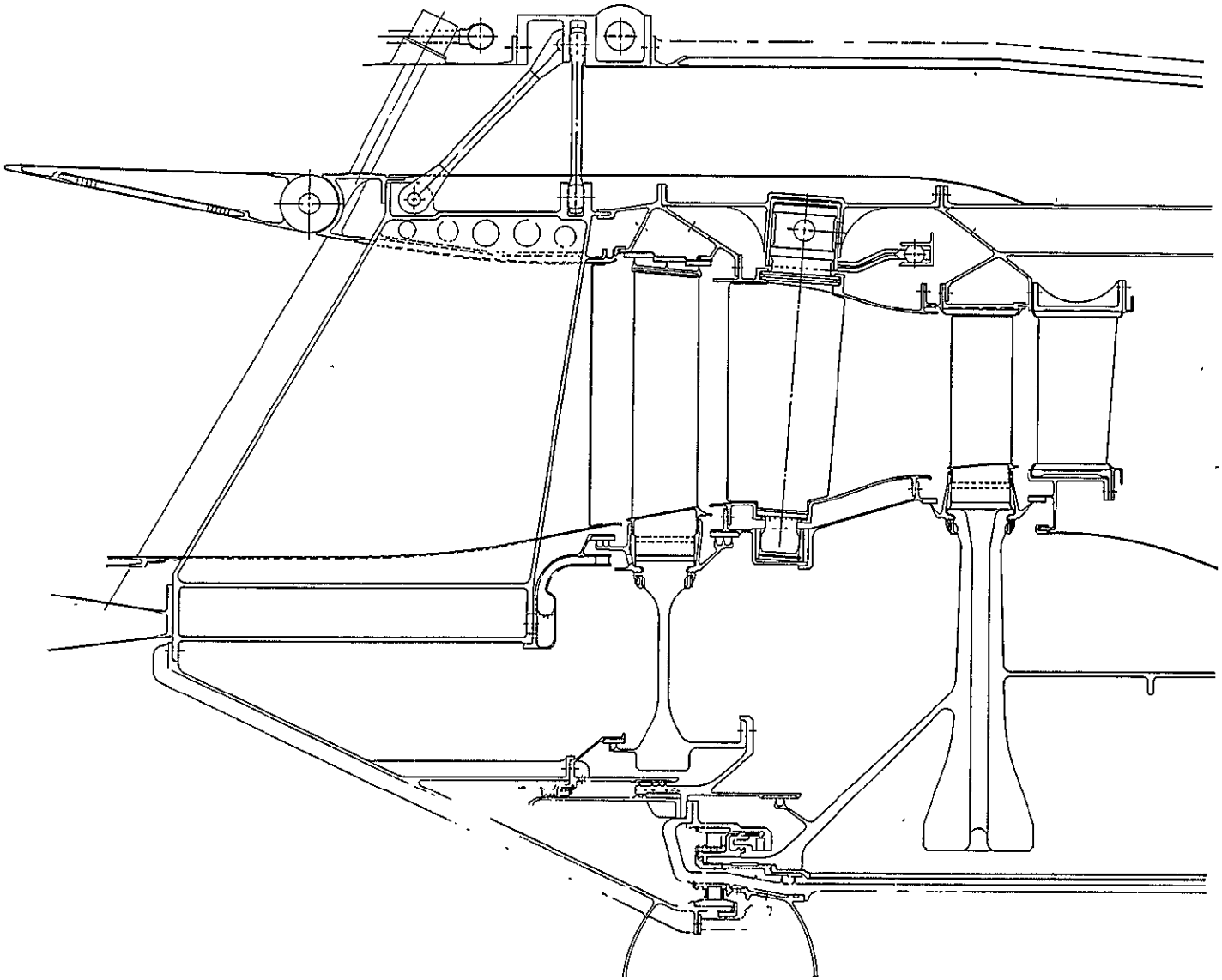

Figure 6. AST Turbine Components - Preliminary Mechanical Layout.

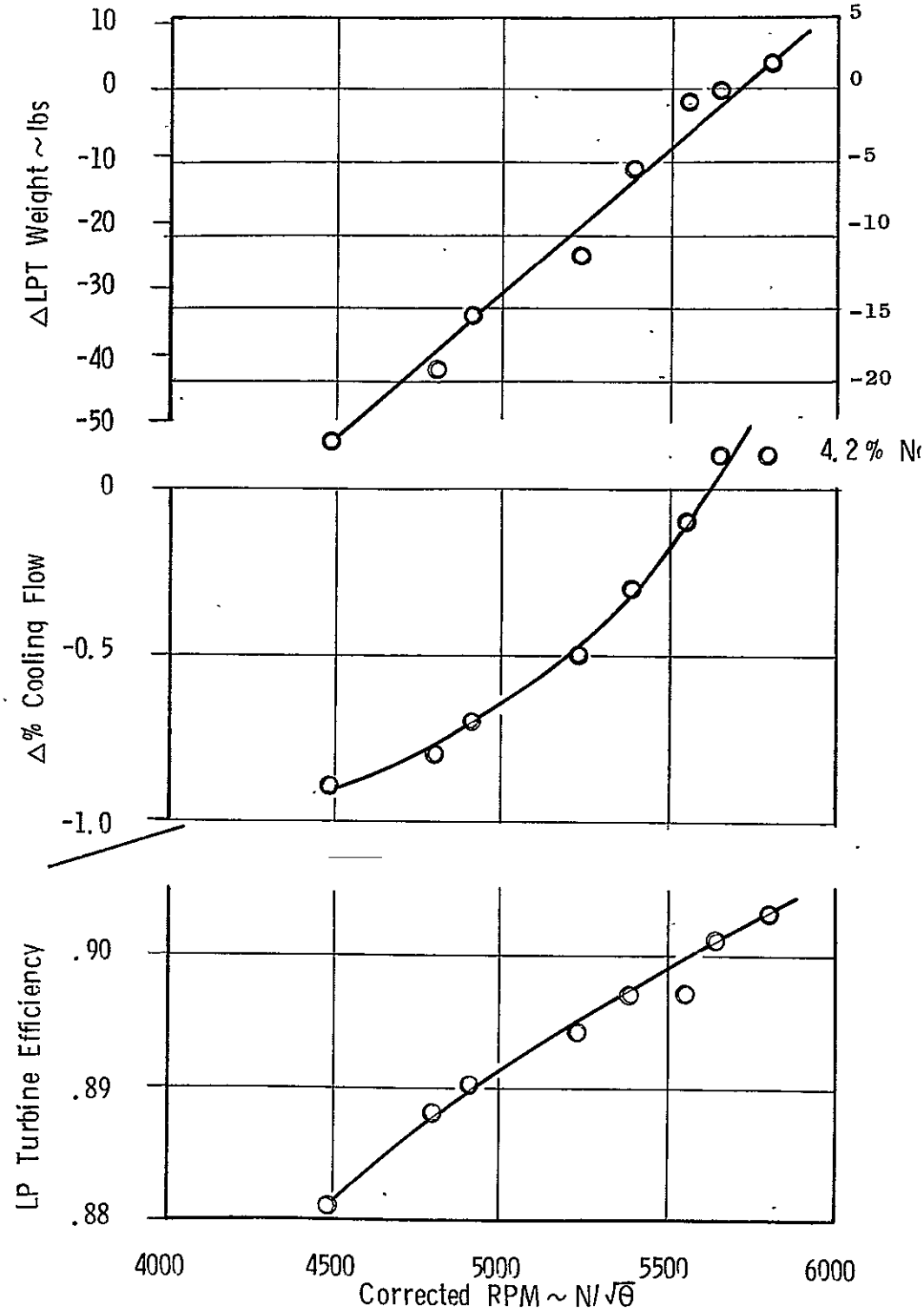

Figure 7. AST LP Turbine Derivatives on Weight, Cooling Flow and Efficiency.

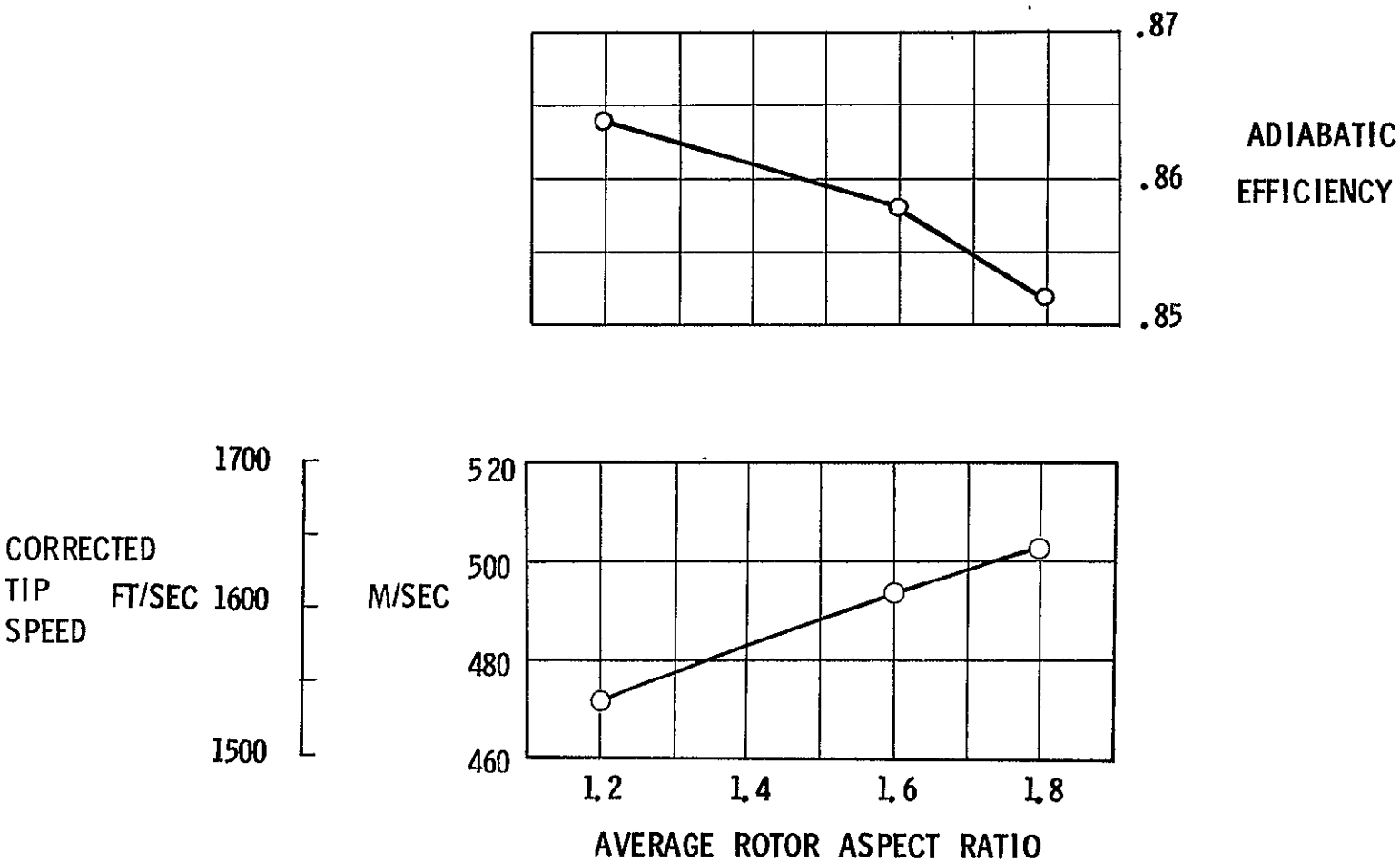

Figure 8. Front Block Fan Parametric Screening Results - Two Stage - Effect of Aspect Ratio Variation.

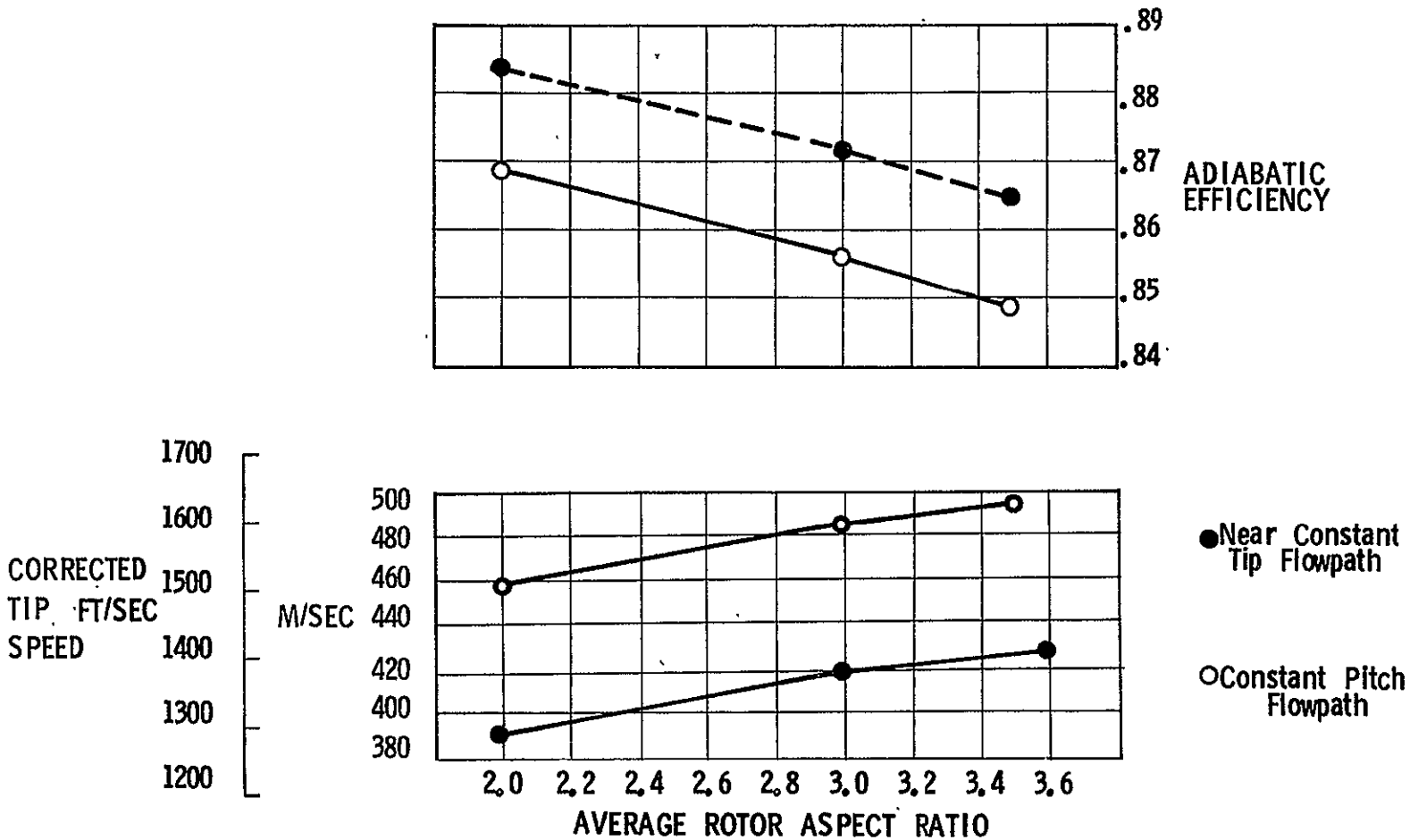

Figure 9. Front Block Fan Parametric Screening Results - Three Stage - Effect of Aspect Ratio Variation.

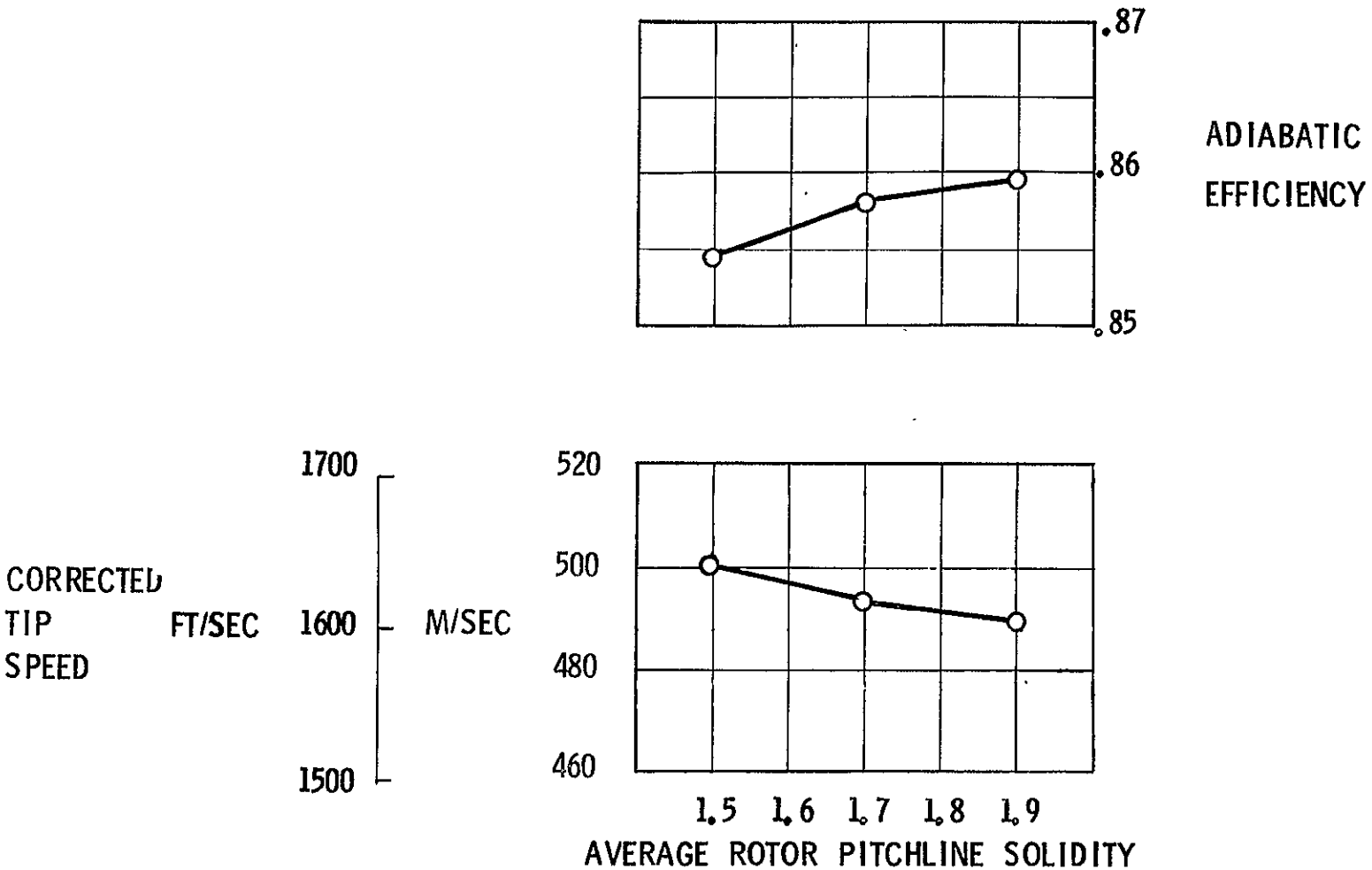

Figure 10. Front Block Fan Parametric Screening Results - Two Stage - Effect of Solidity Variation.

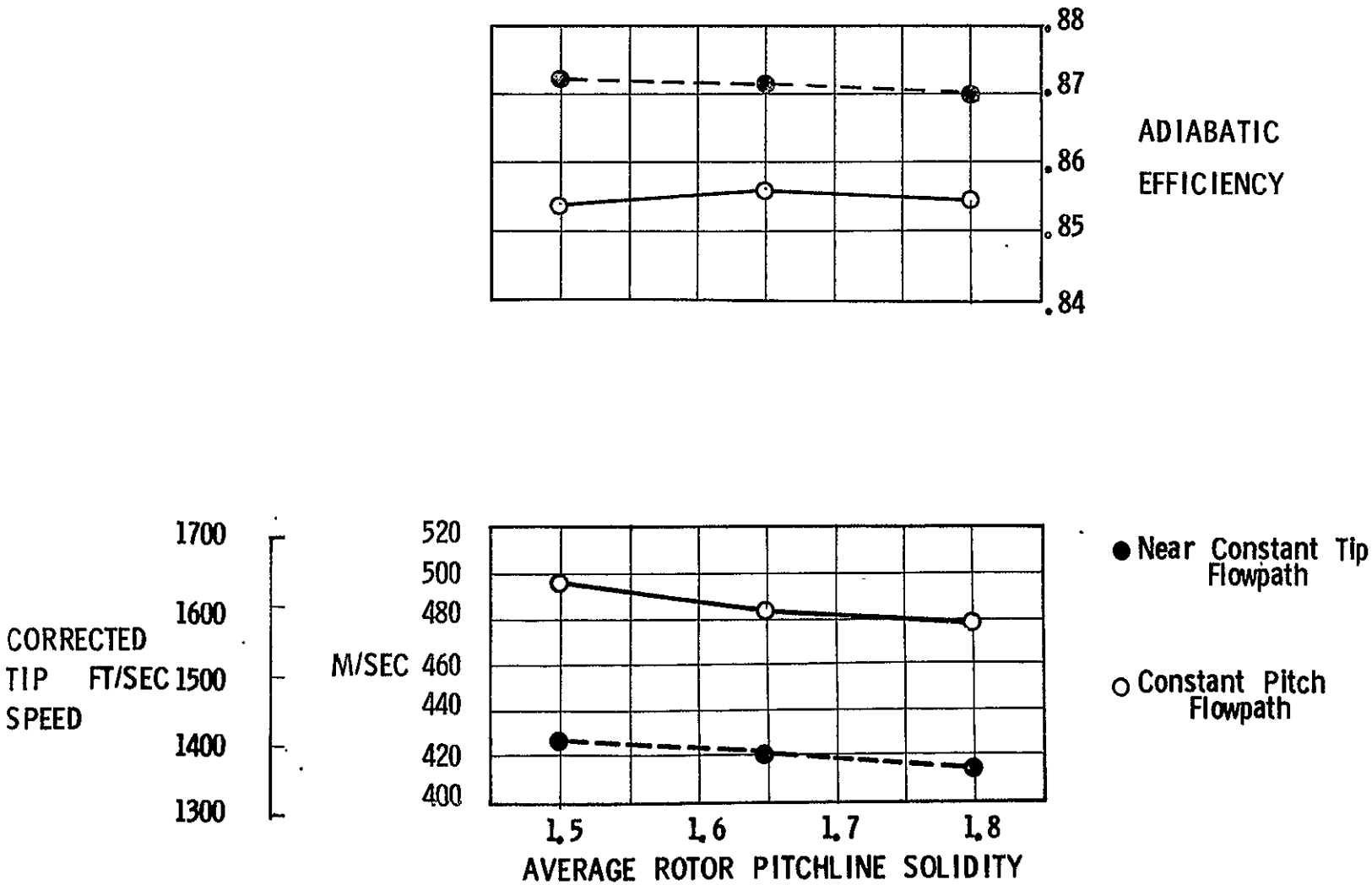

Figure 11. Front Block Fan Parametric Screening Results - Three Stage - Effect of Solidity Variation.

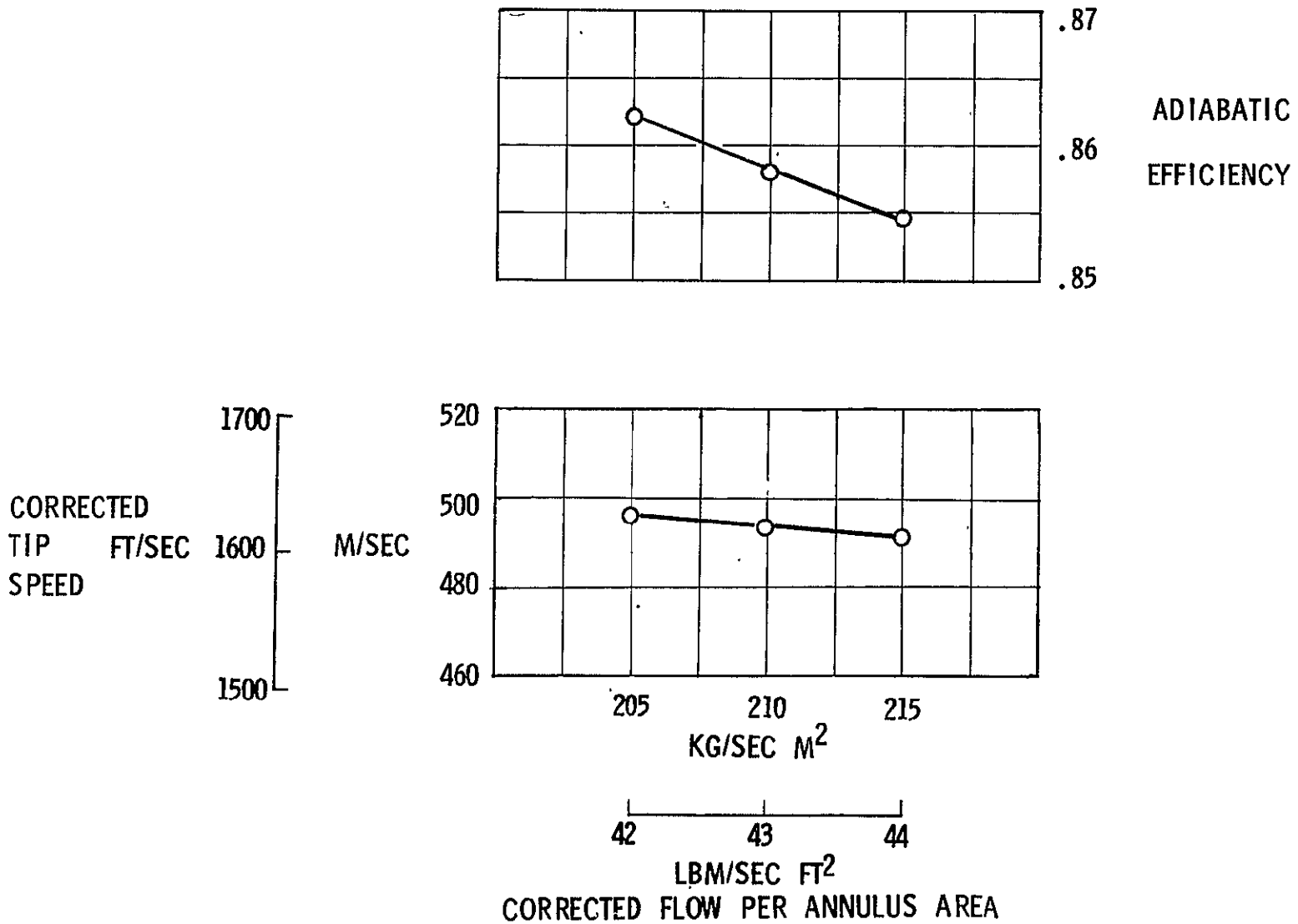

Figure 12. Front Block Fan Parametric Screening Results - Two Stage - Effect of Flow/Annulus Variation.

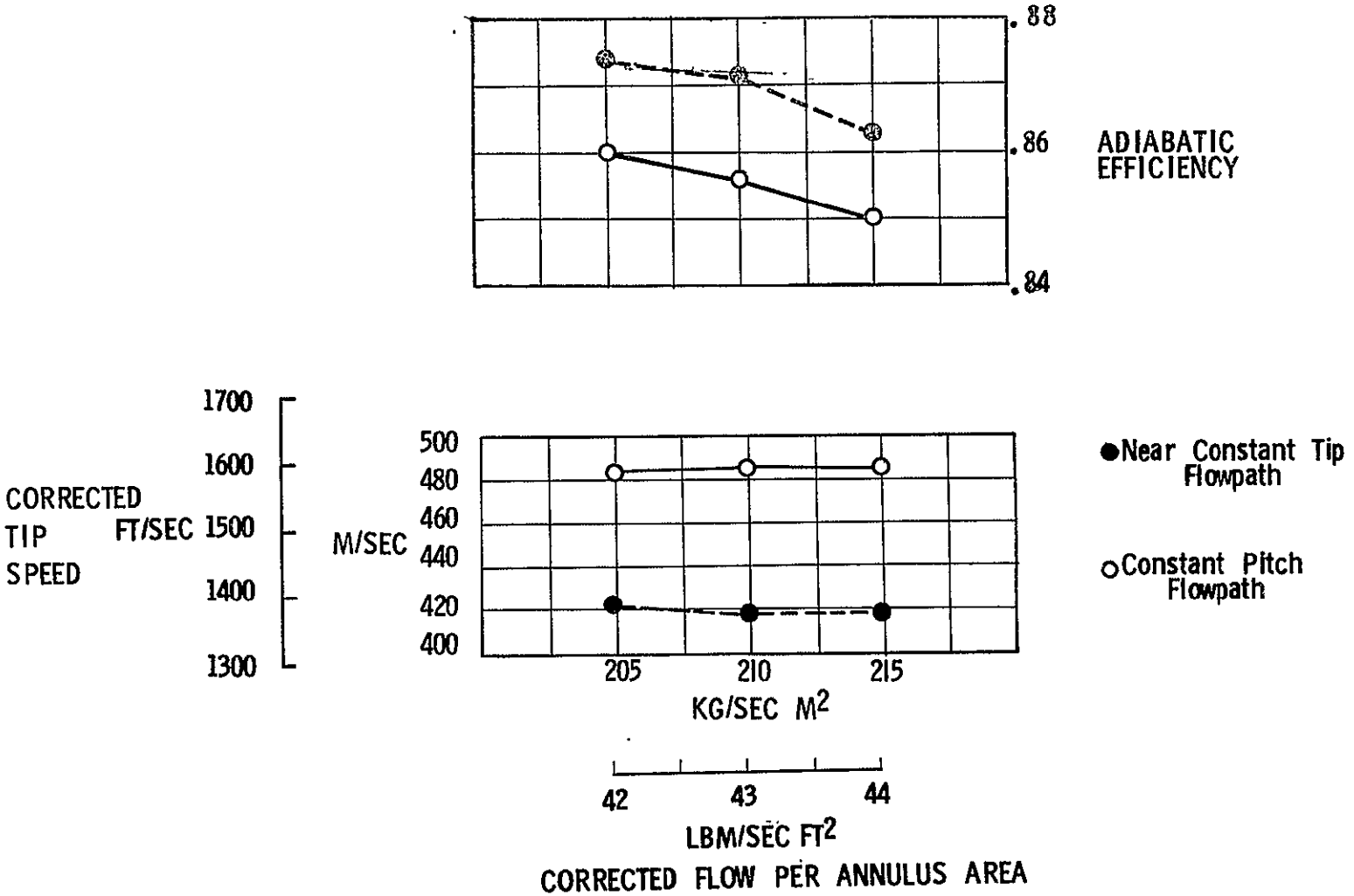

Figure 13. Front Block Fan Parametric Screening Results - Three Stage - Effect of Flow/Annulus Variation.

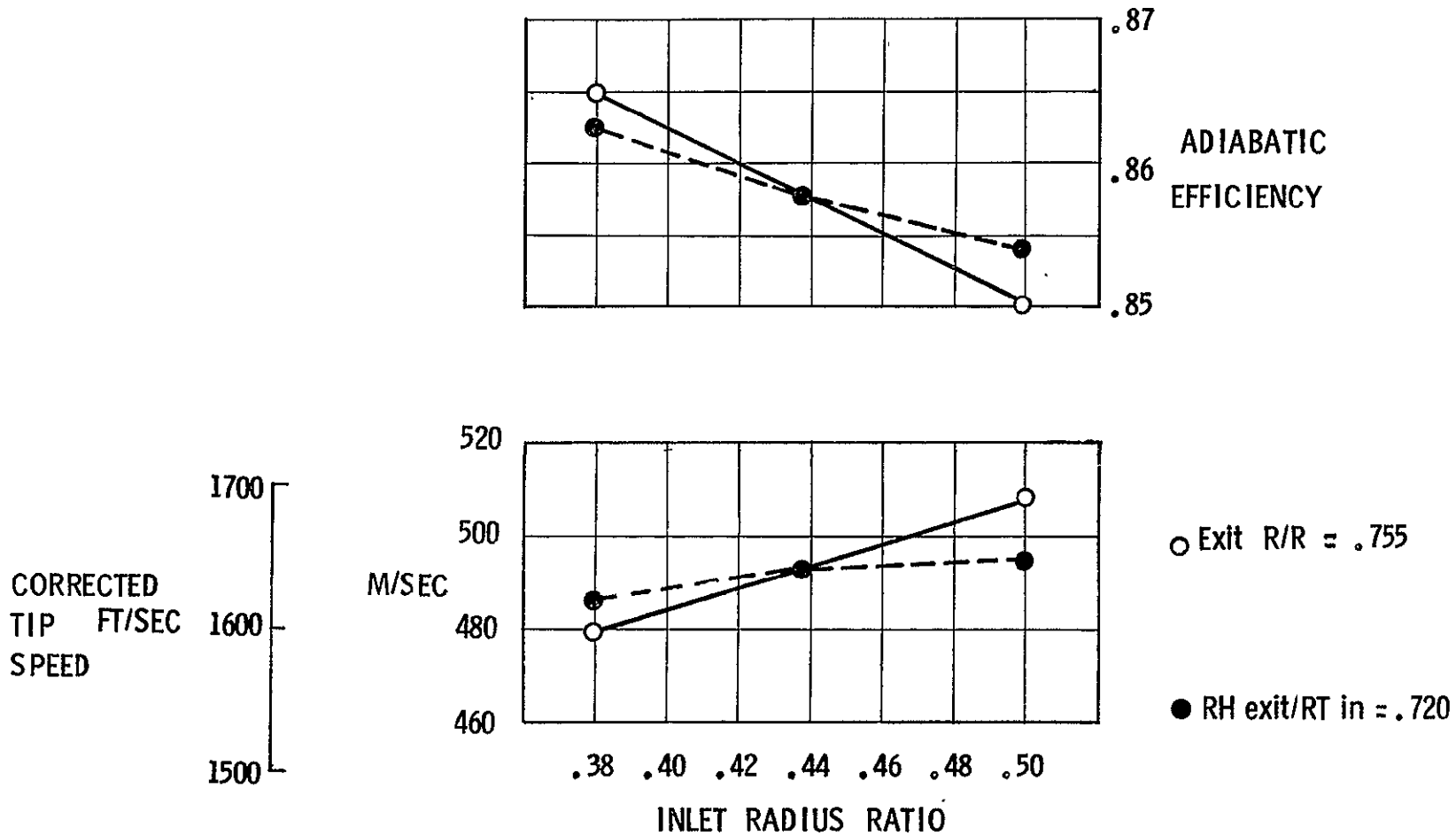

Figure 14. Front Block Fan Parametric Screening Results - Two Stage - Effect of Inlet Radius Ratio Variation.

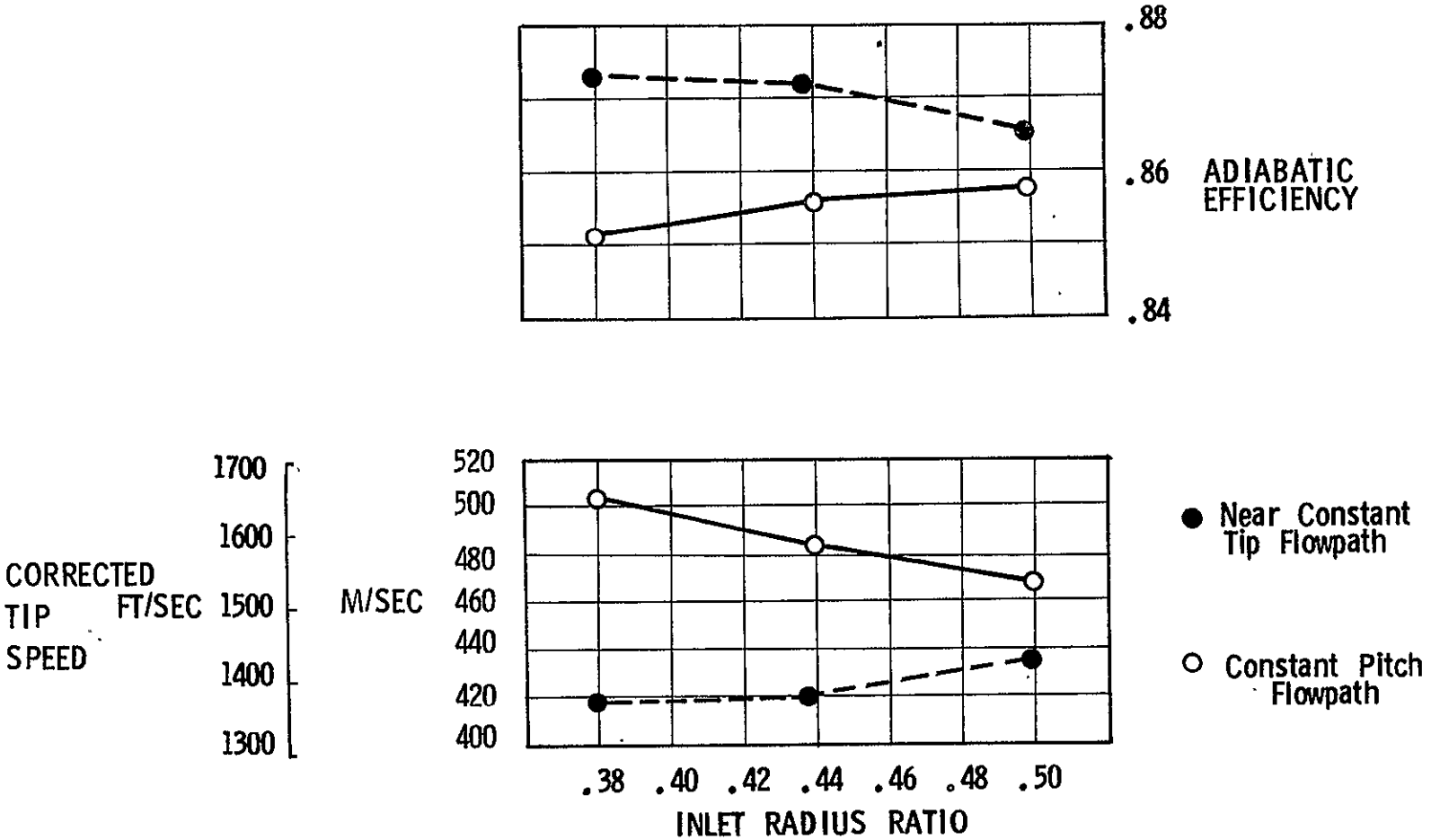

Figure 15. Front Block Fan Parametric Screening Results - Three Stage - Effect of Inlet Radius Ratio Variation.

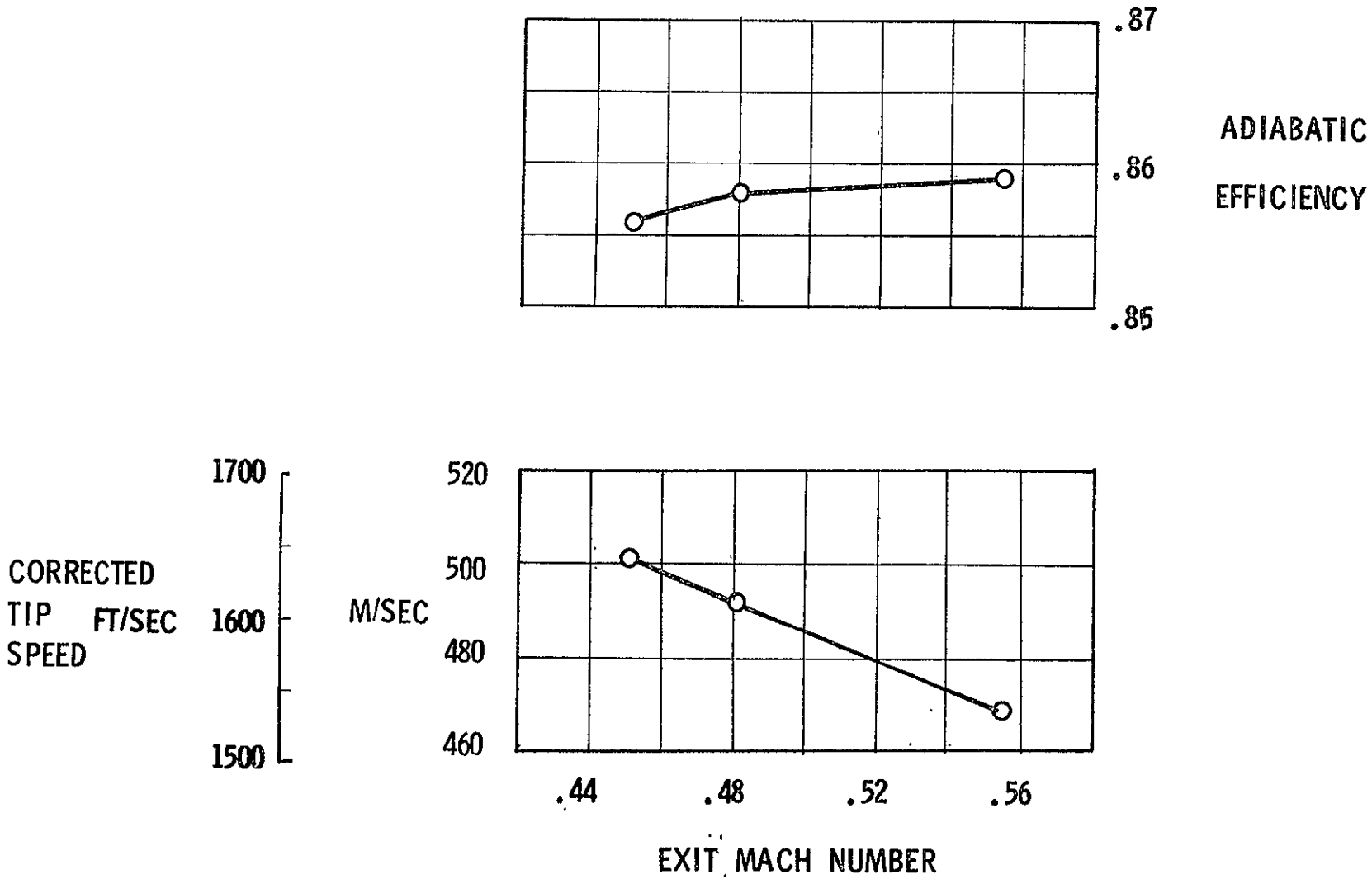

Figure 16. Front Block Fan Parametric Screening Results - Two Stage - Effect of Exit Mach No. Variation.

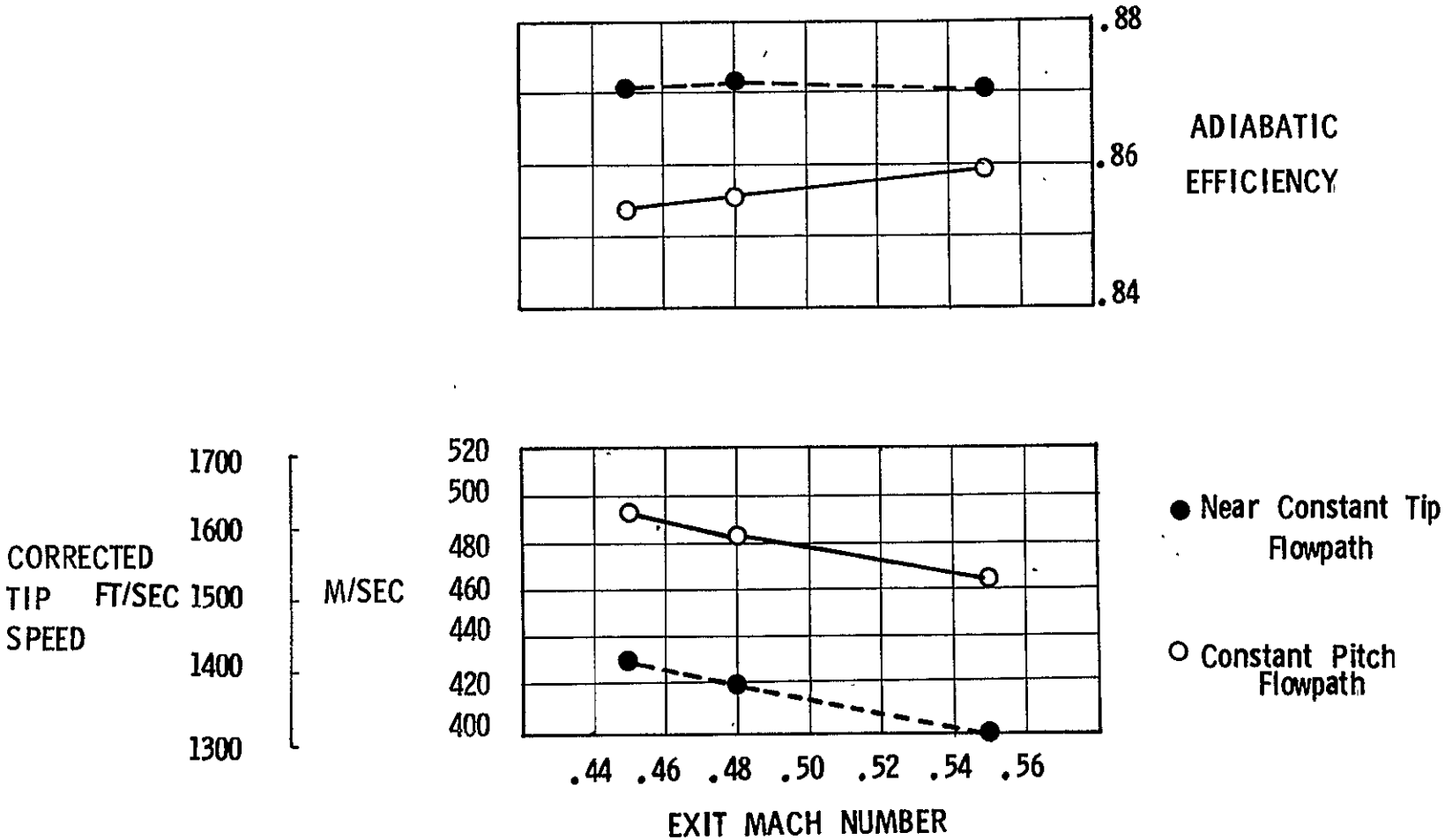

Figure 17. Front Block Fan Parametric Screening Results - Three Stage - Effect of Exit Mach No. Variation.

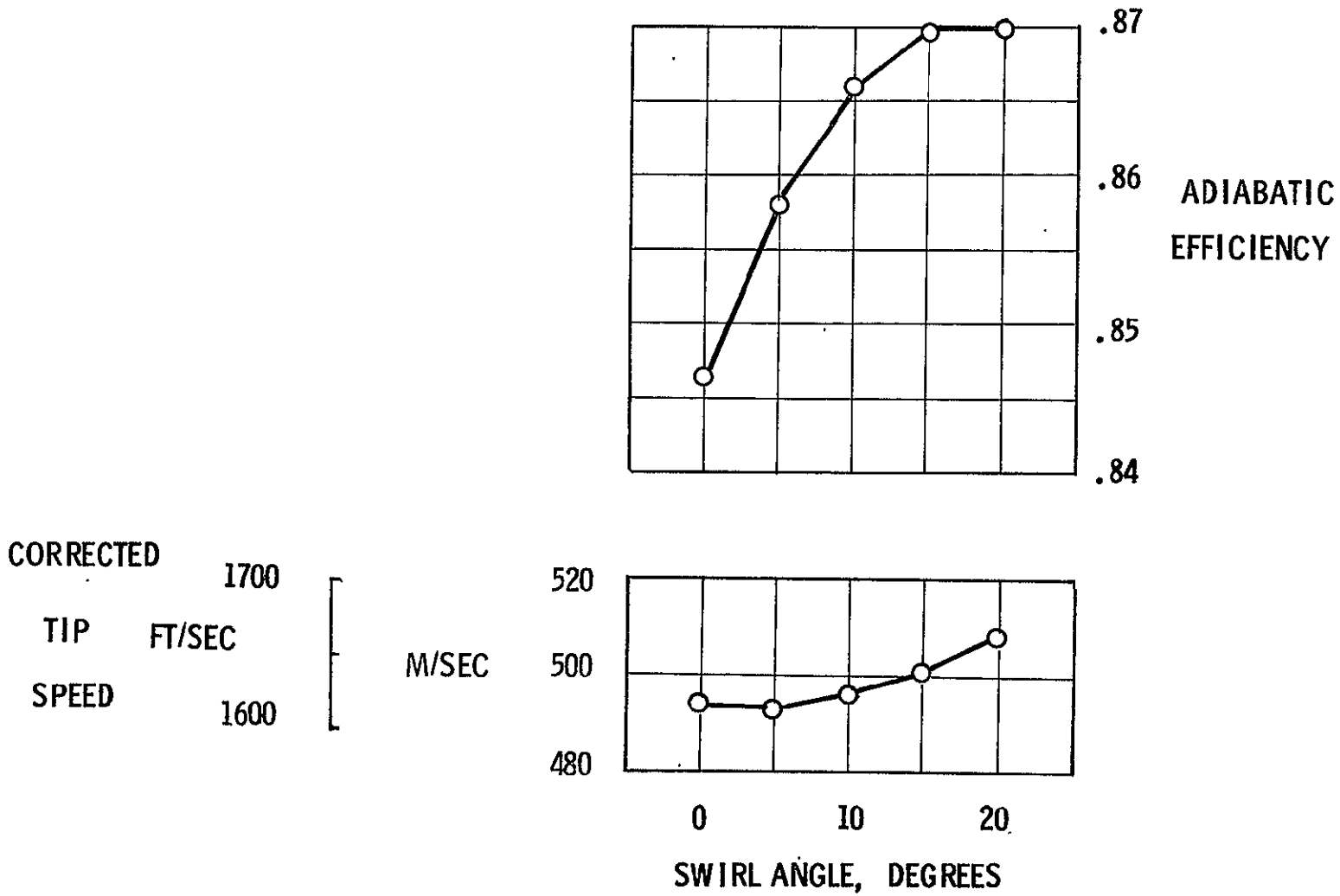

Figure 18. Front Block Fan Parametric Screening Results - Two Stage - Effect of Swirl Angle Variation.

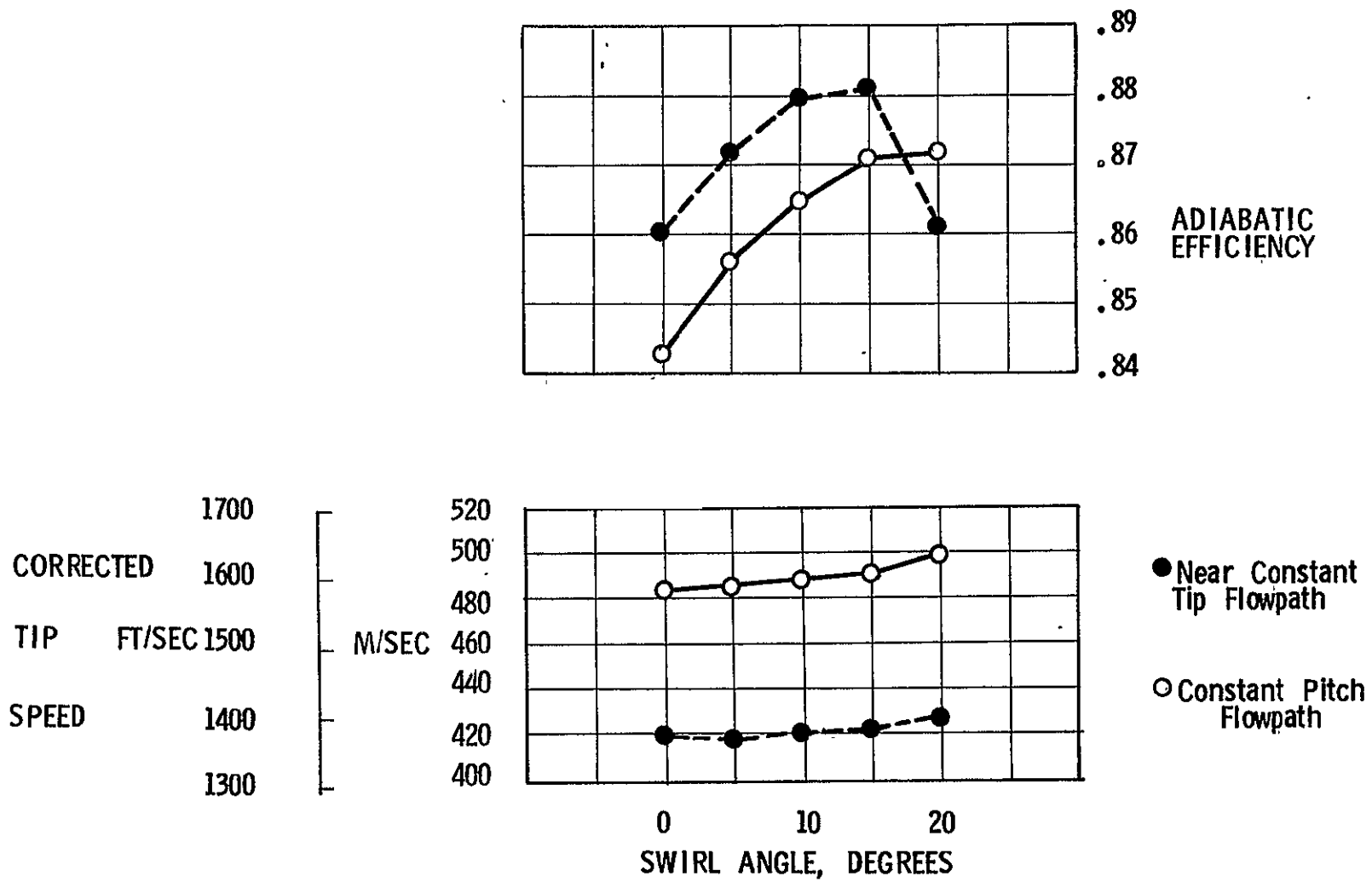

Figure 19. Front Block Fan Parametric Screening Results - Three Stage - Effect of Swirl Angle Variation.

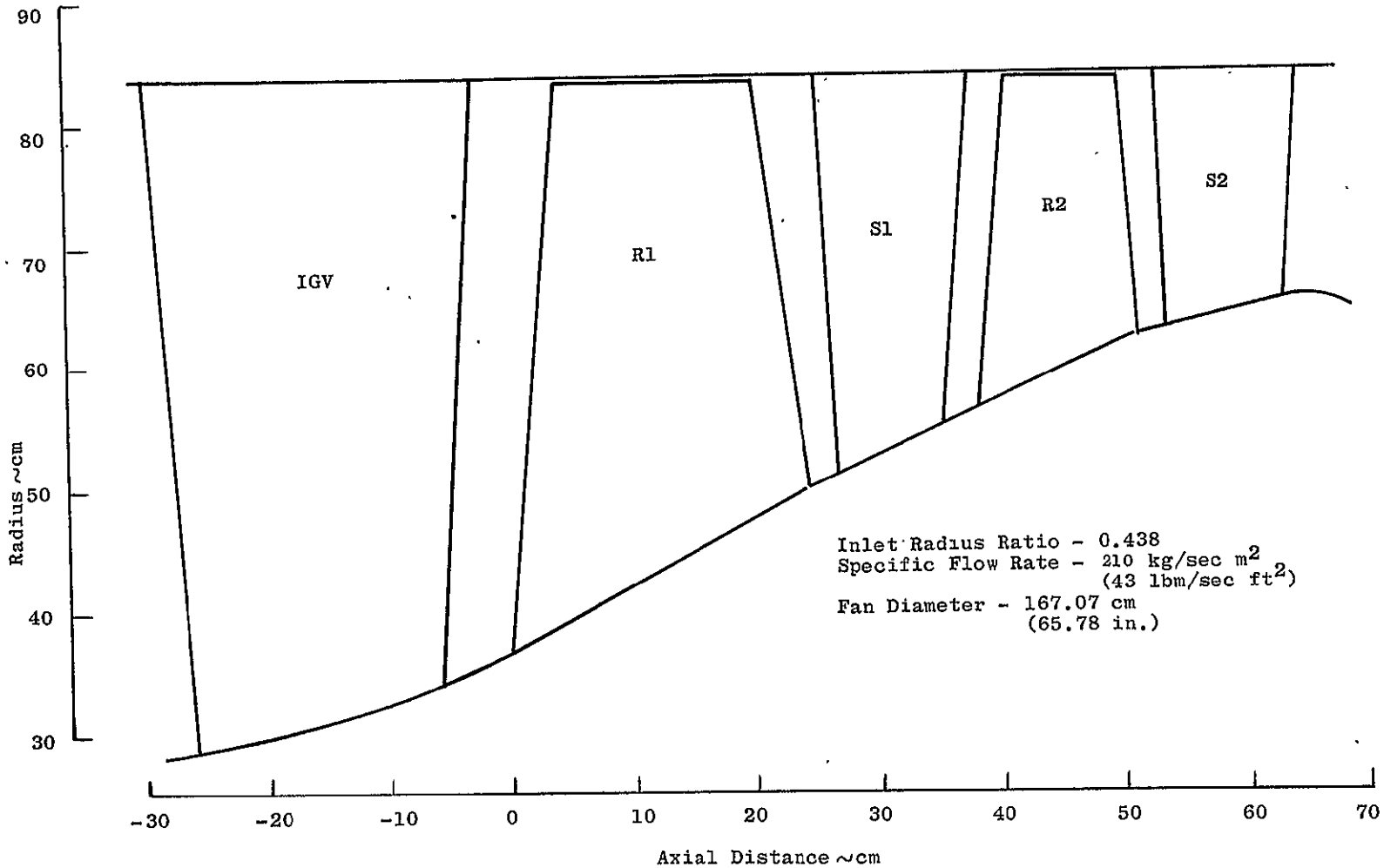

Figure 20. AST Front Block Fan Flowpath - Constant Tip - Inlet Radius Ratio = 0.438.

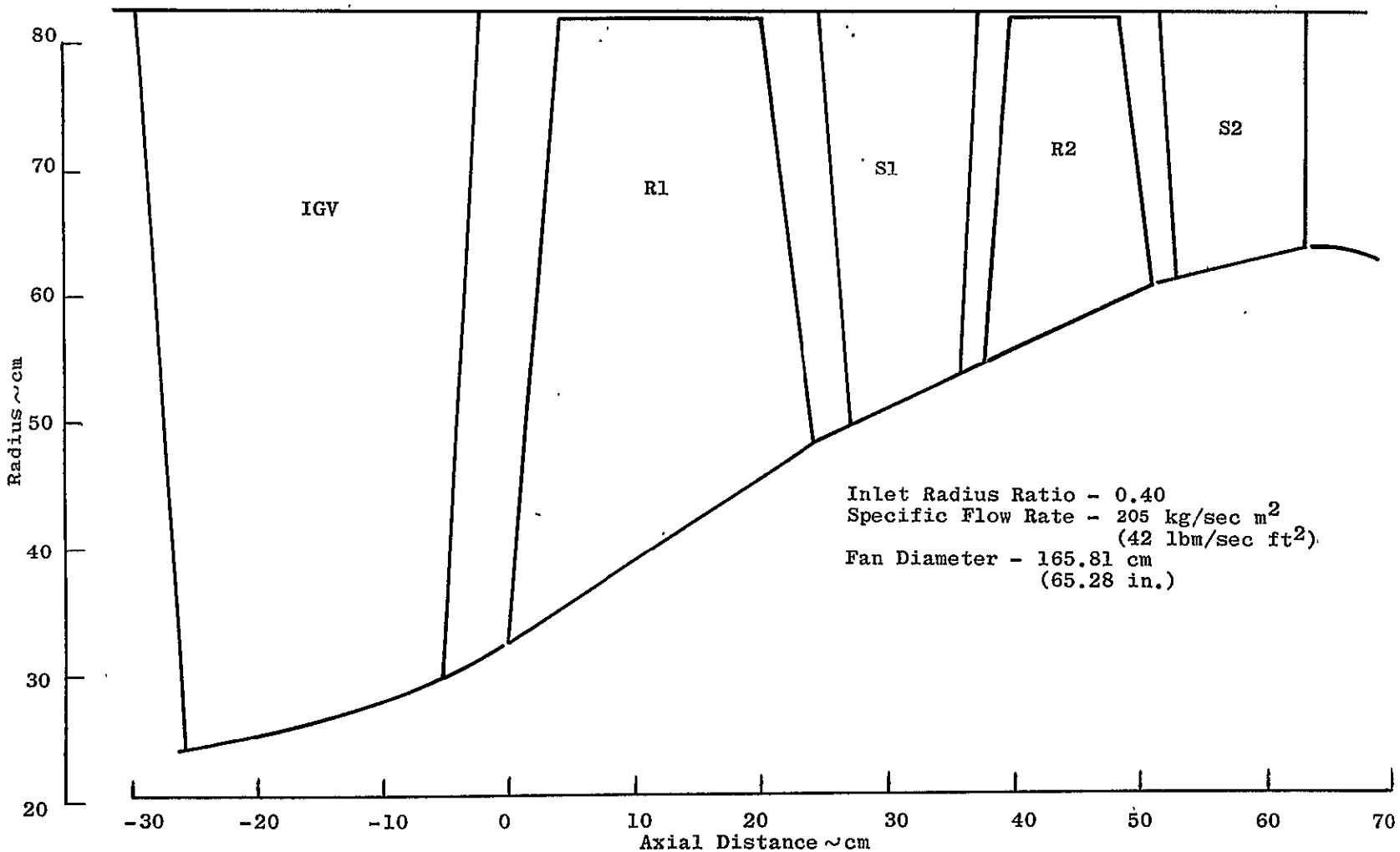

Figure 21. AST Front Block Fan Flowpath - Constant Tip - Inlet Radius Ratio = 0.400.

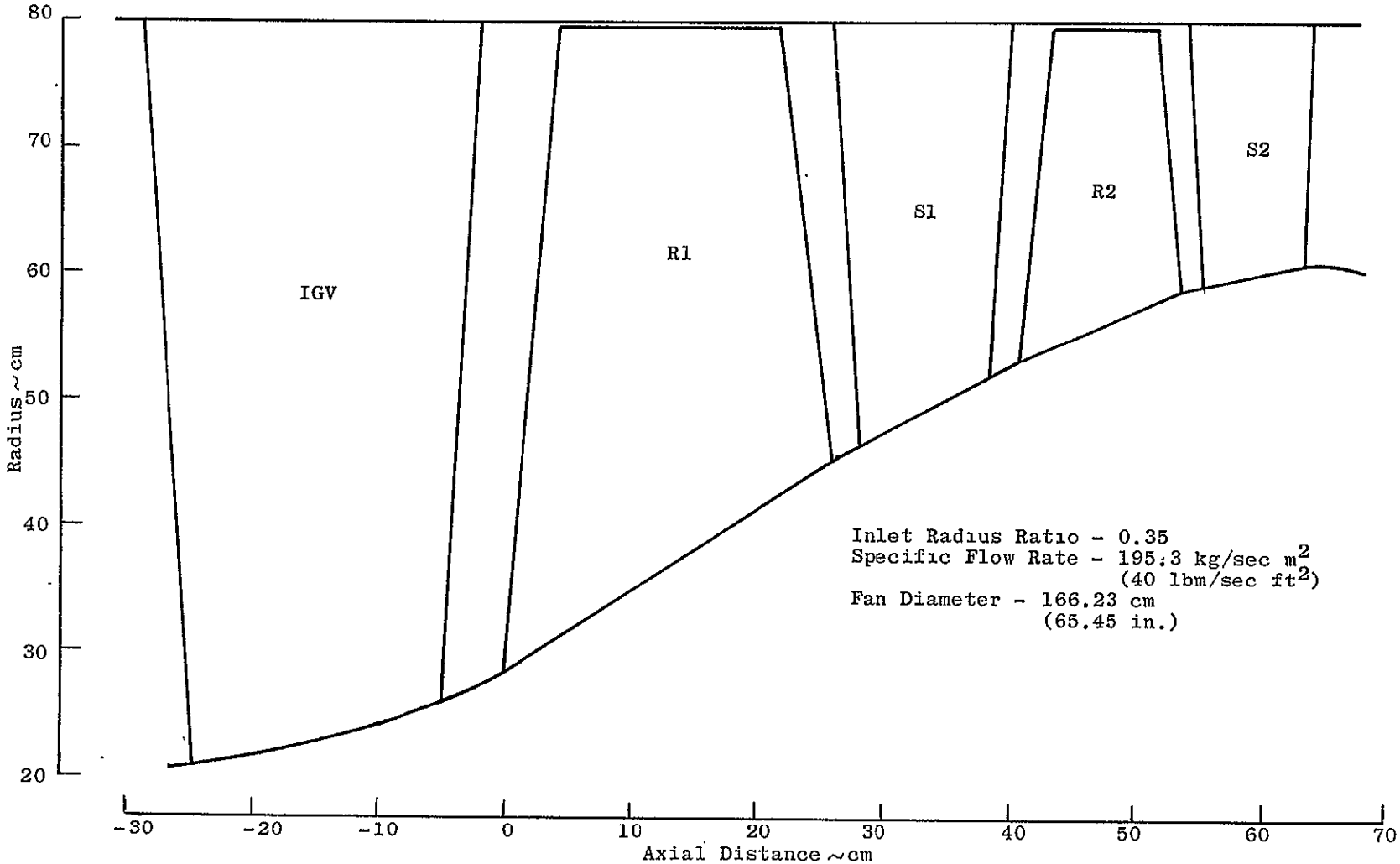

Figure 22. AST Front Block Fan Flowpath - Constant Tip - Inlet Radius Ratio = 0.350.

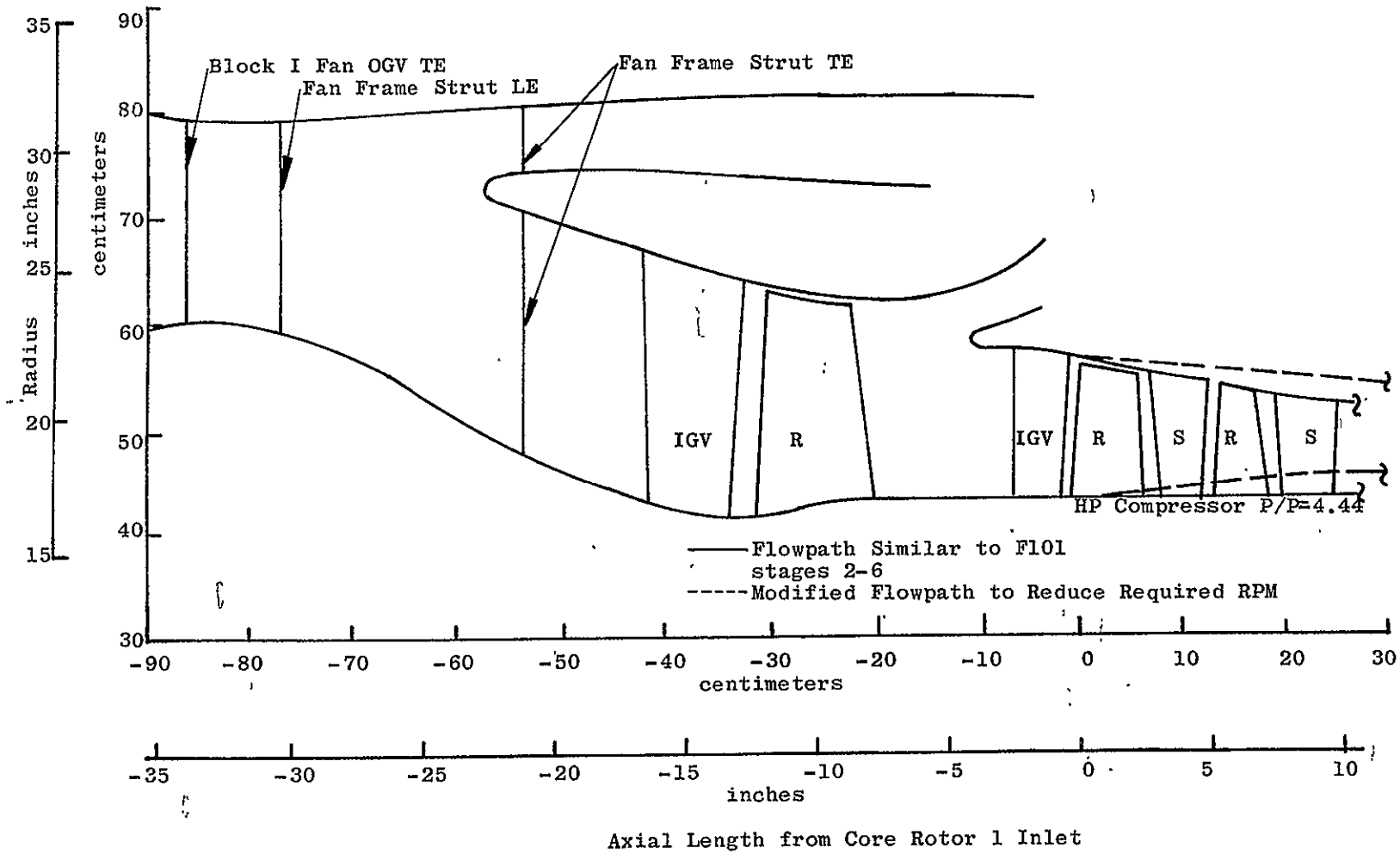

Figure 23. AST Rear Block Fan and Compressor Inlet Nominal Design Flowpath.

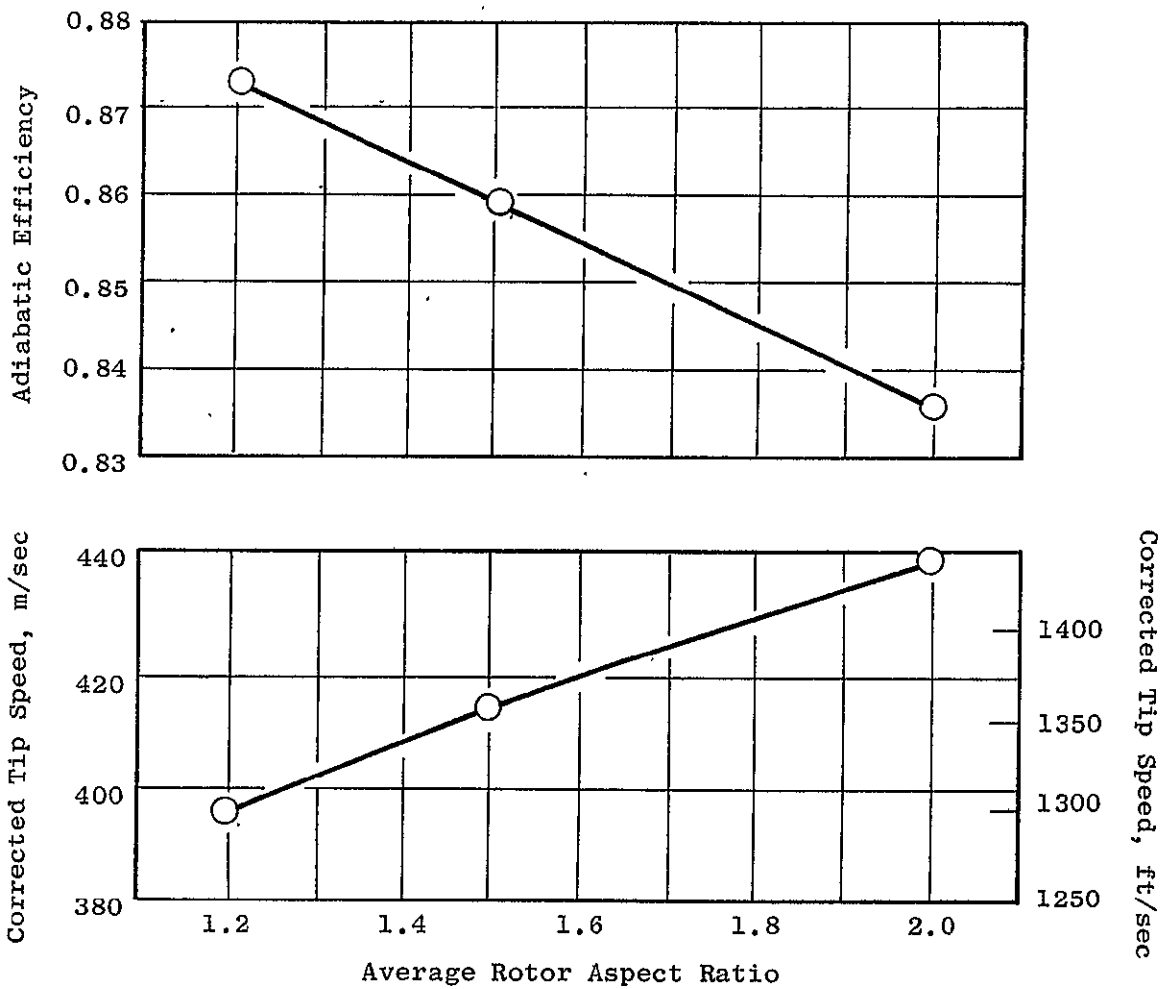

Figure 24. Rear Block Fan Parametric Screening Results - Effect of Aspect Ratio Variation.

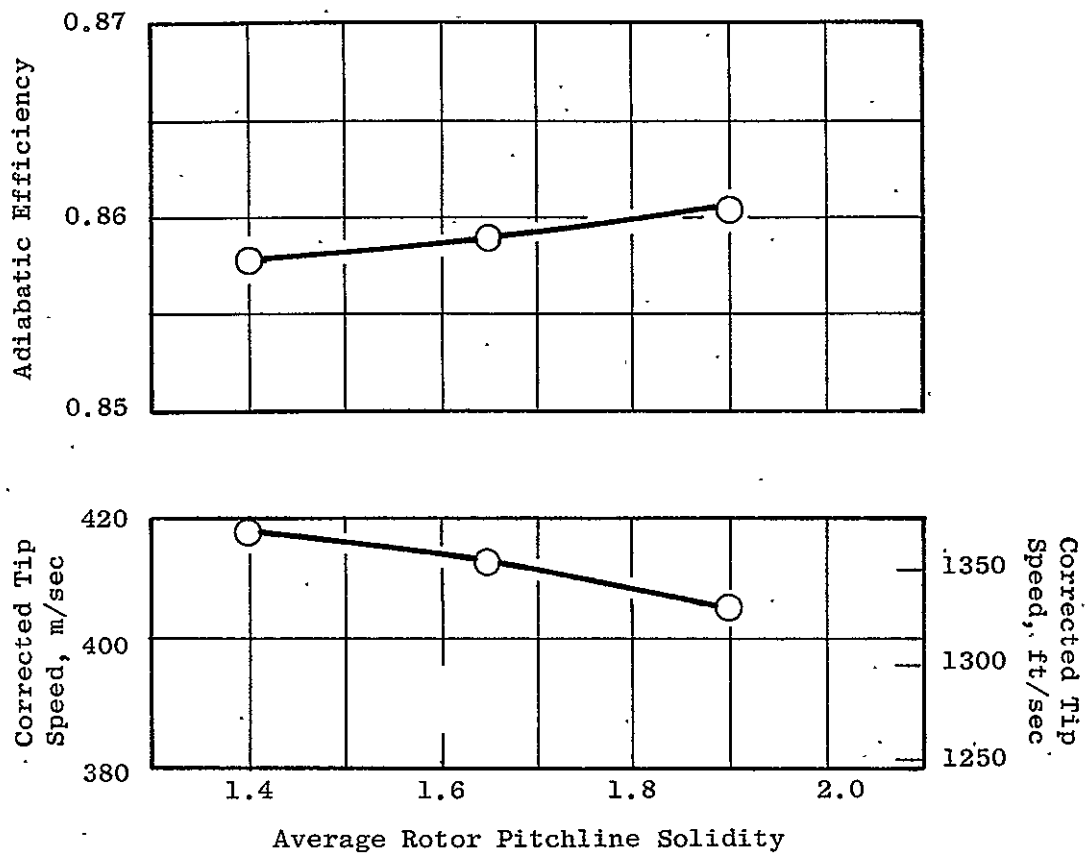

Figure 25. Rear Block Fan Parametric Screening Results - Effect of Solidity Variation.

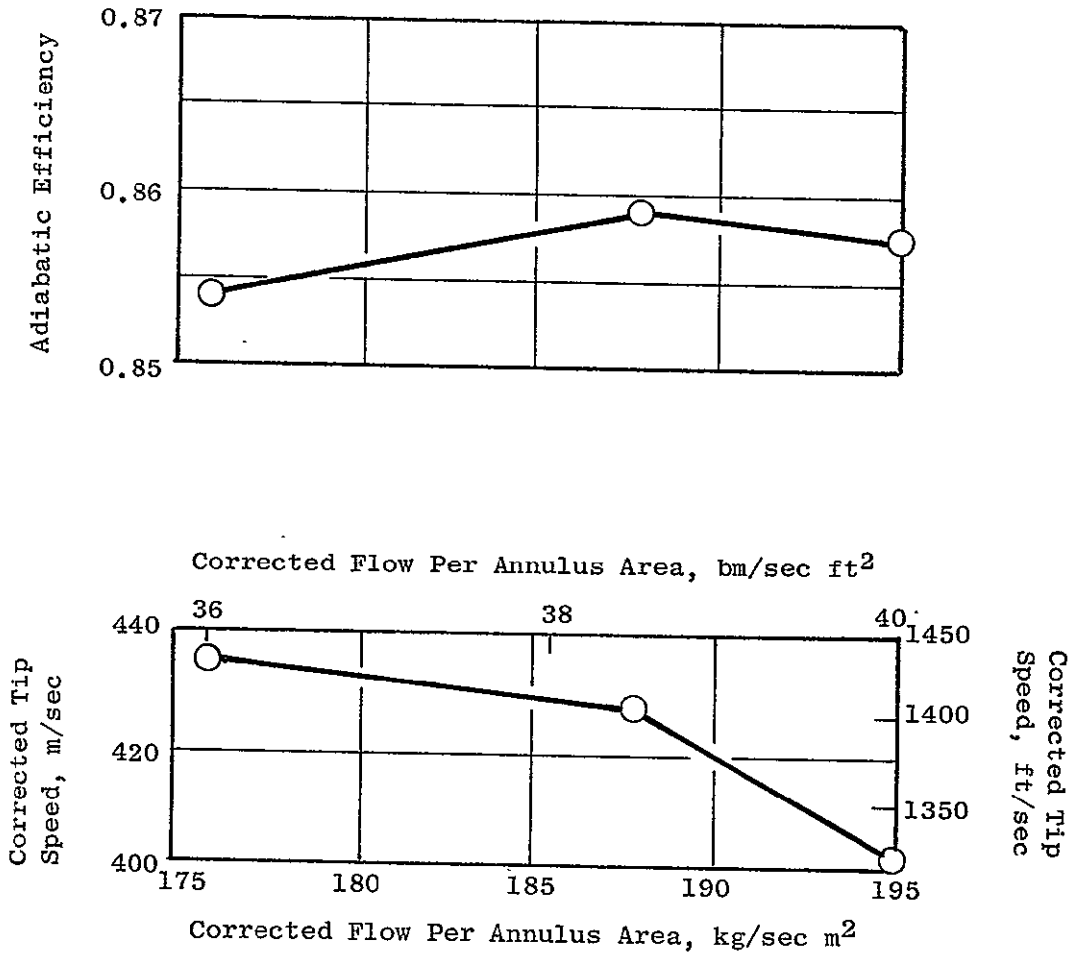

Figure 26. Rear Block Fan Parametric Screening Results - Effect of Flow/Annulus Variation.

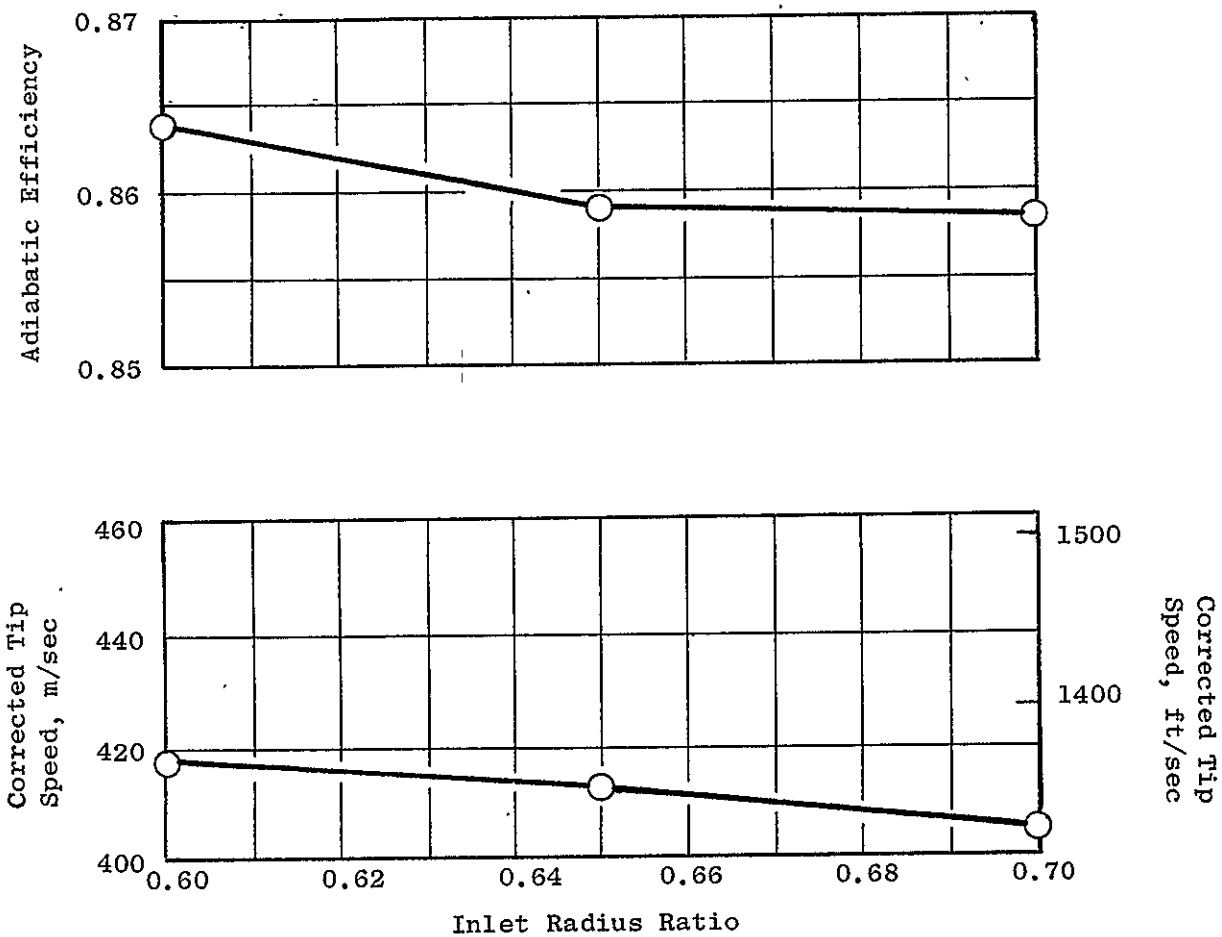

Figure 27. Rear Block Fan Parametric Screening Results - Effect of Inlet Radius Ratio Variations.

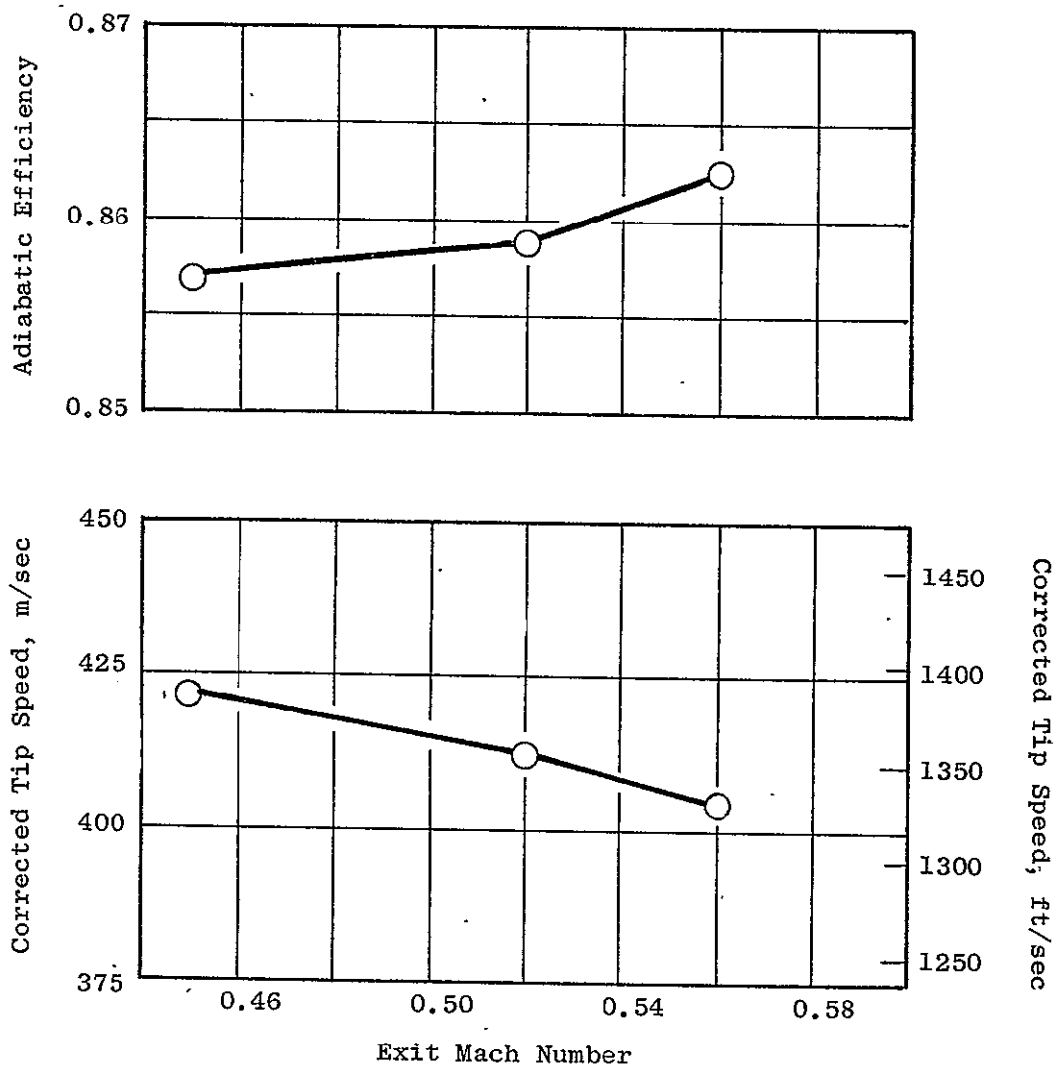

Figure 28. Rear Block Fan Parametric Screening Results - Effect of Exit Mach No. Variation.

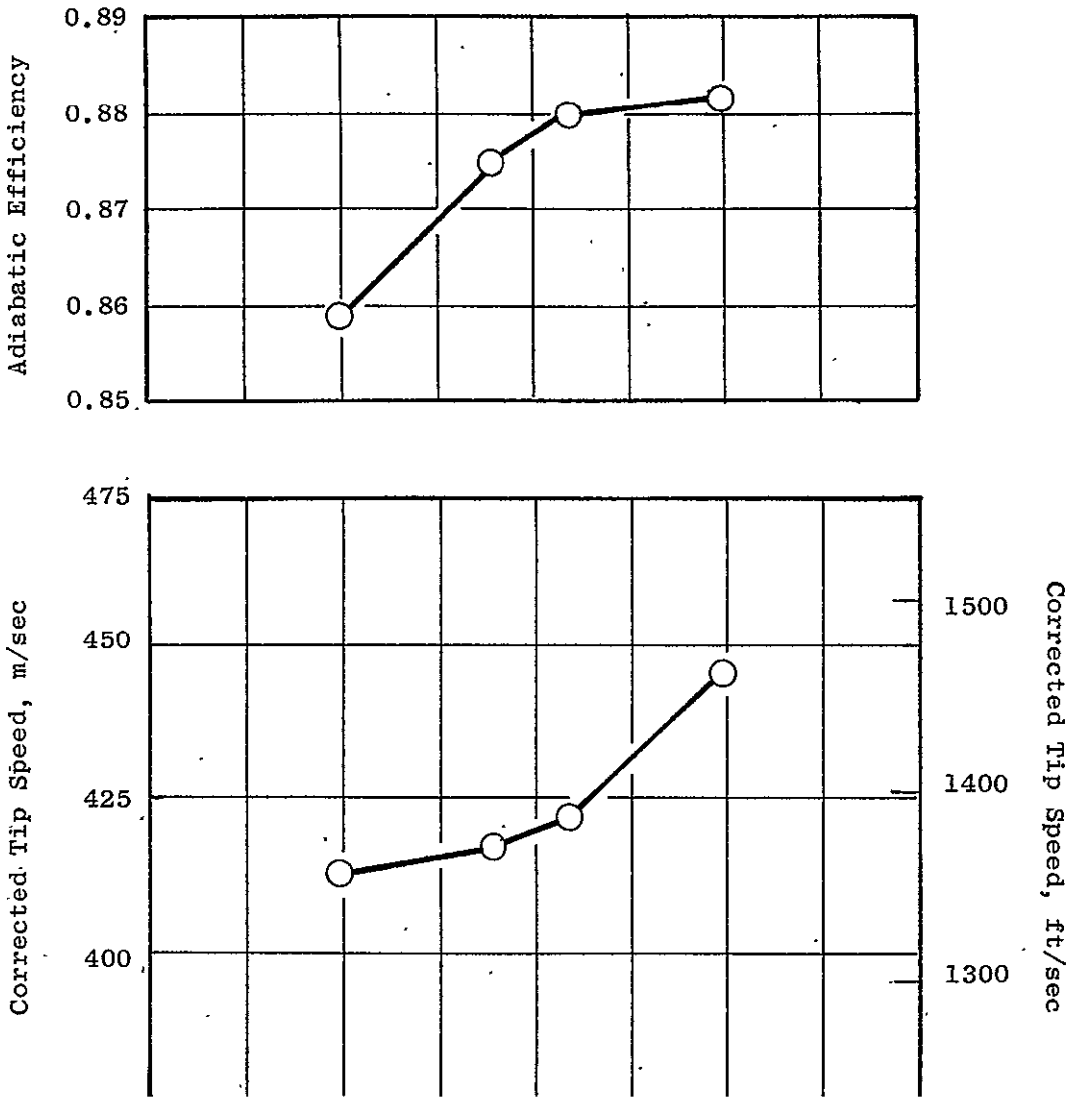
Adiabatic Efficiency
0.89
0.88
0.87
0.86
0.85
Corrected Tip Speed, m/sec
475
450
425
400
1500
1400
1300
Corrected Tip Speed, ft/sec

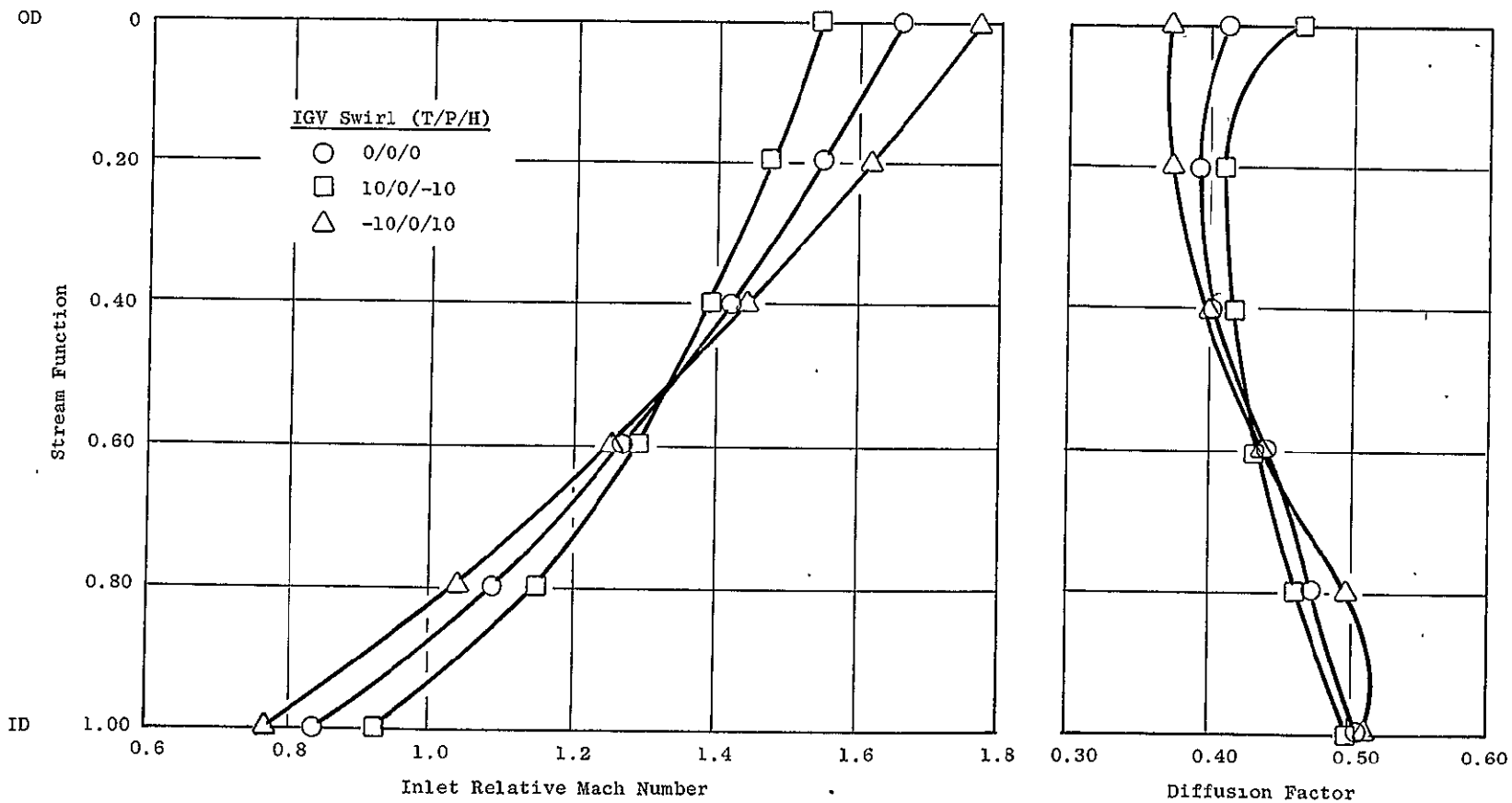

Figure 30. Front Block Fan Rotor 1 Design Parameters - Various IGV Swirls.

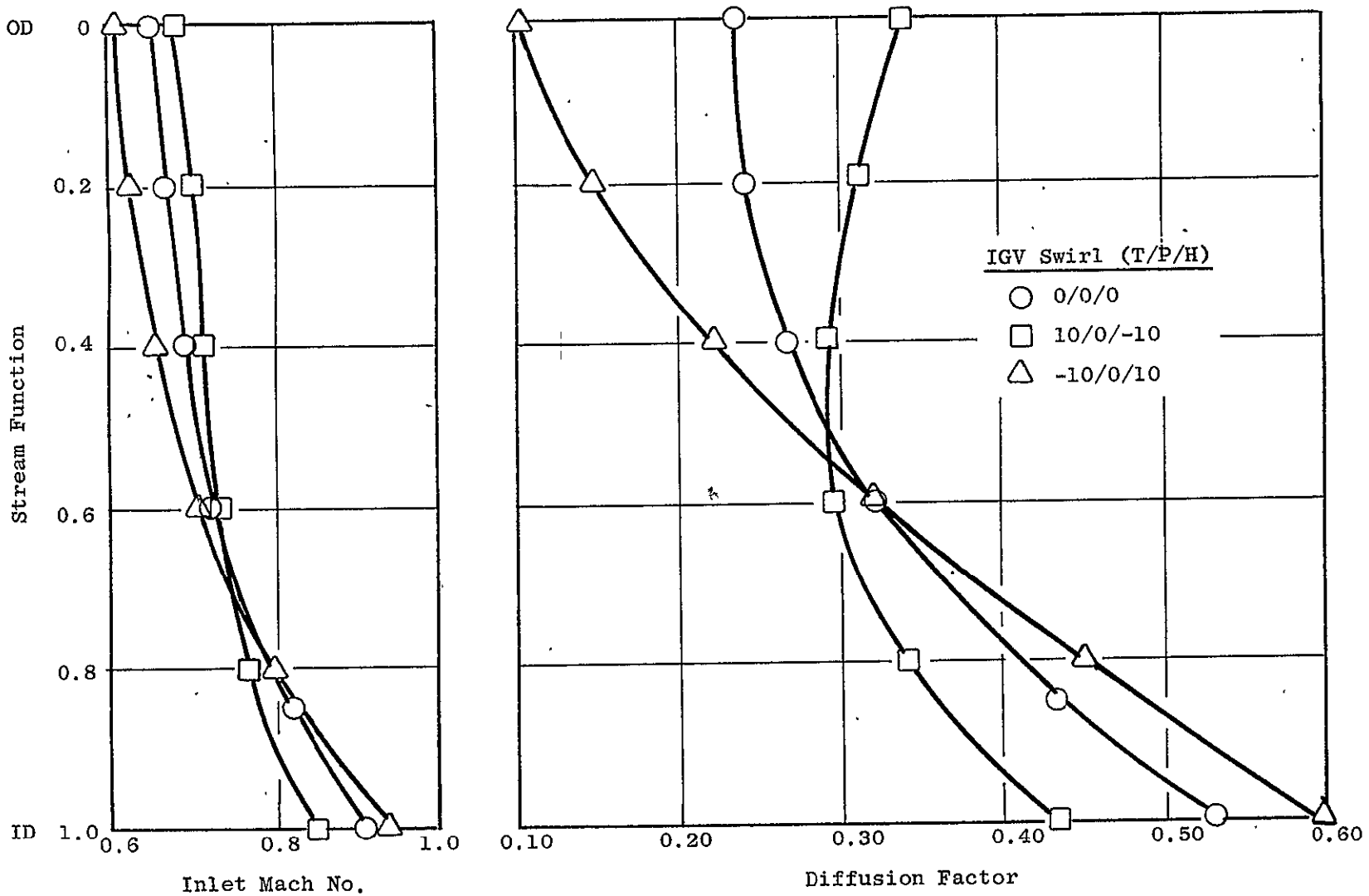

Figure 31. Front Block Fan Stator 1 Design Parameters - Various IGV Swirls.

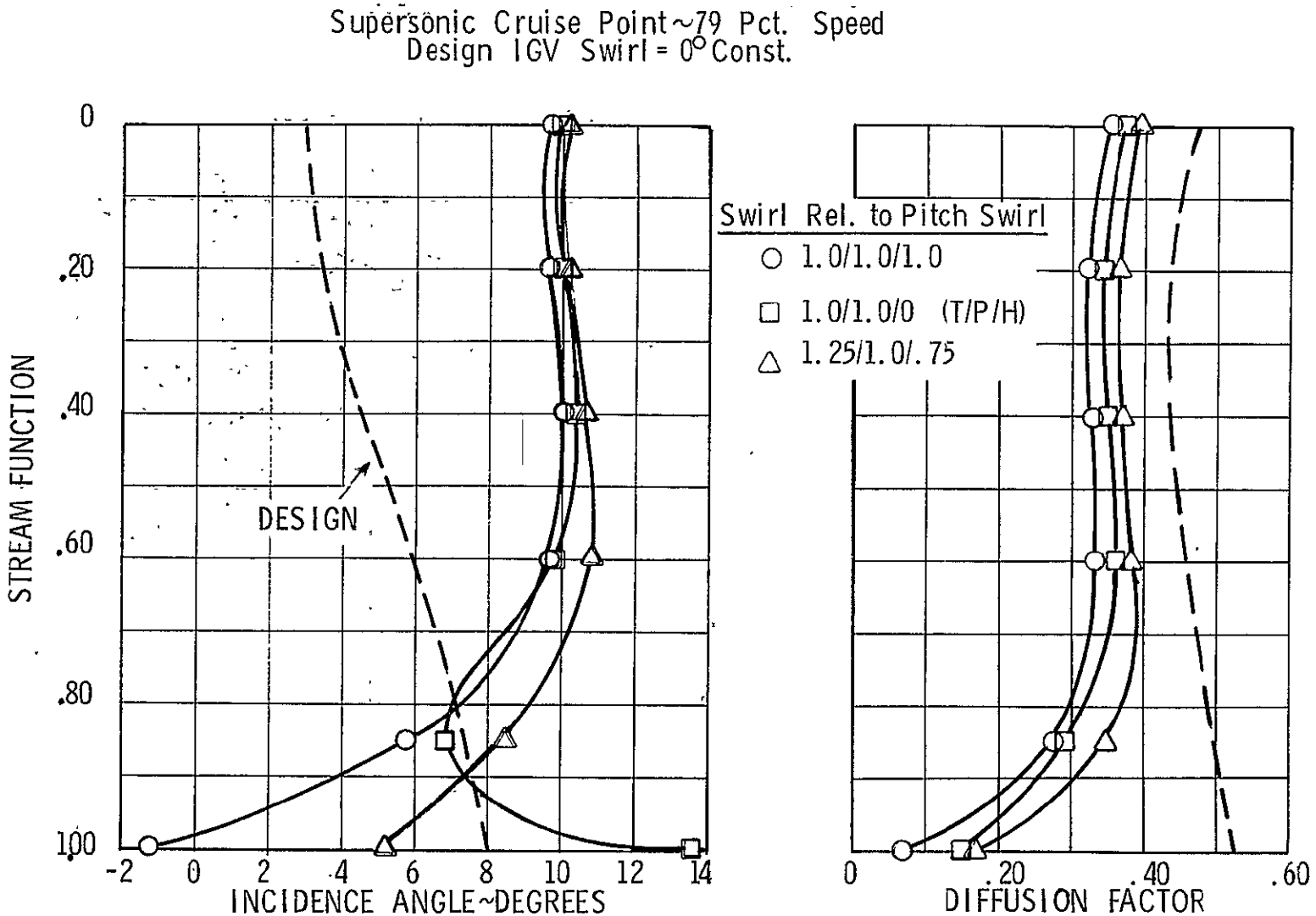

Figure 32. Front Block Fan Rotor 1 Off-Design Parameters - Design IGV Swirl = 0° Constant.

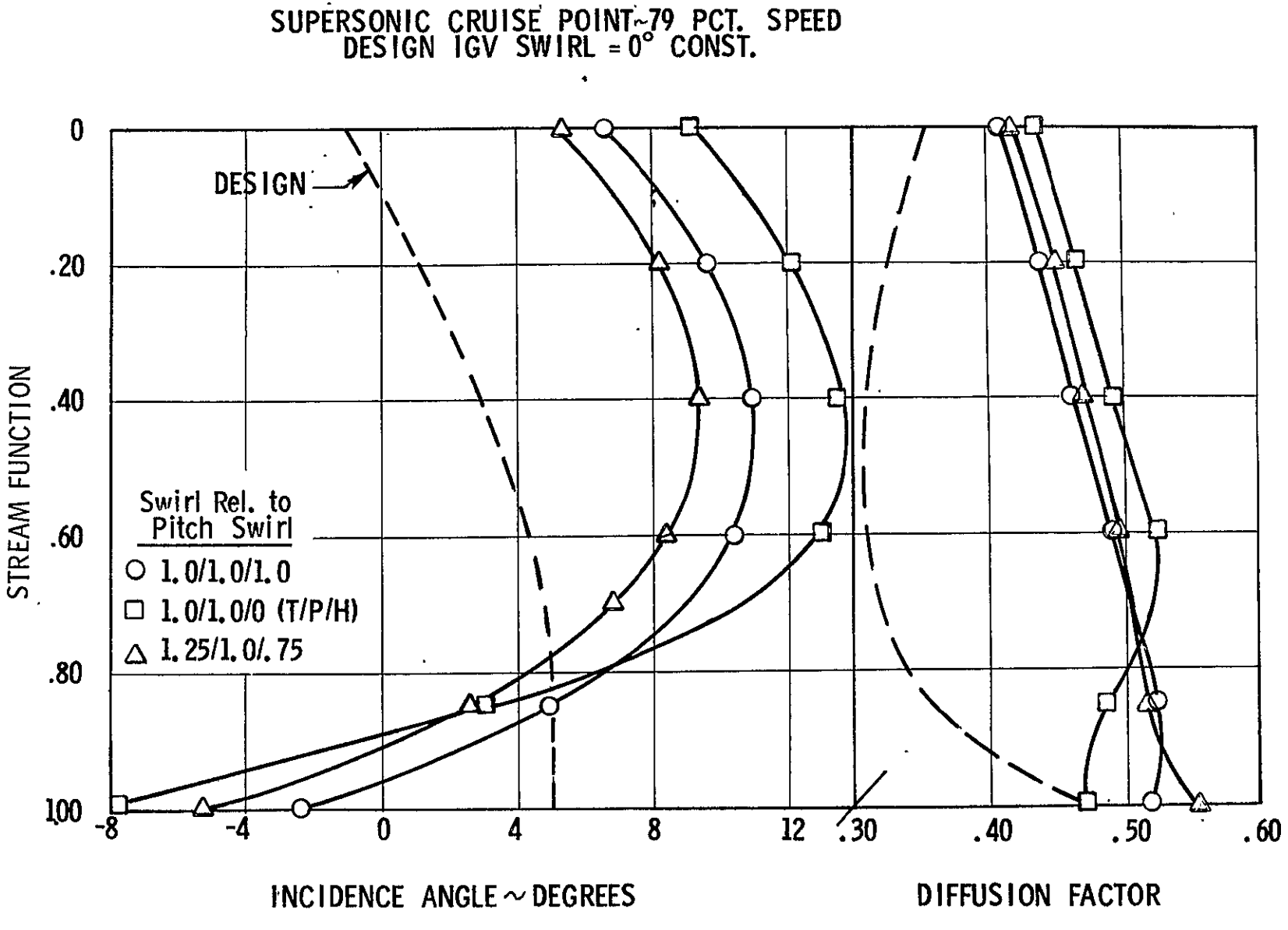

Figure 33. Front Block Fan Stator 1 Off-Design Parameters - Design IGV Swirl = 0° Constant.

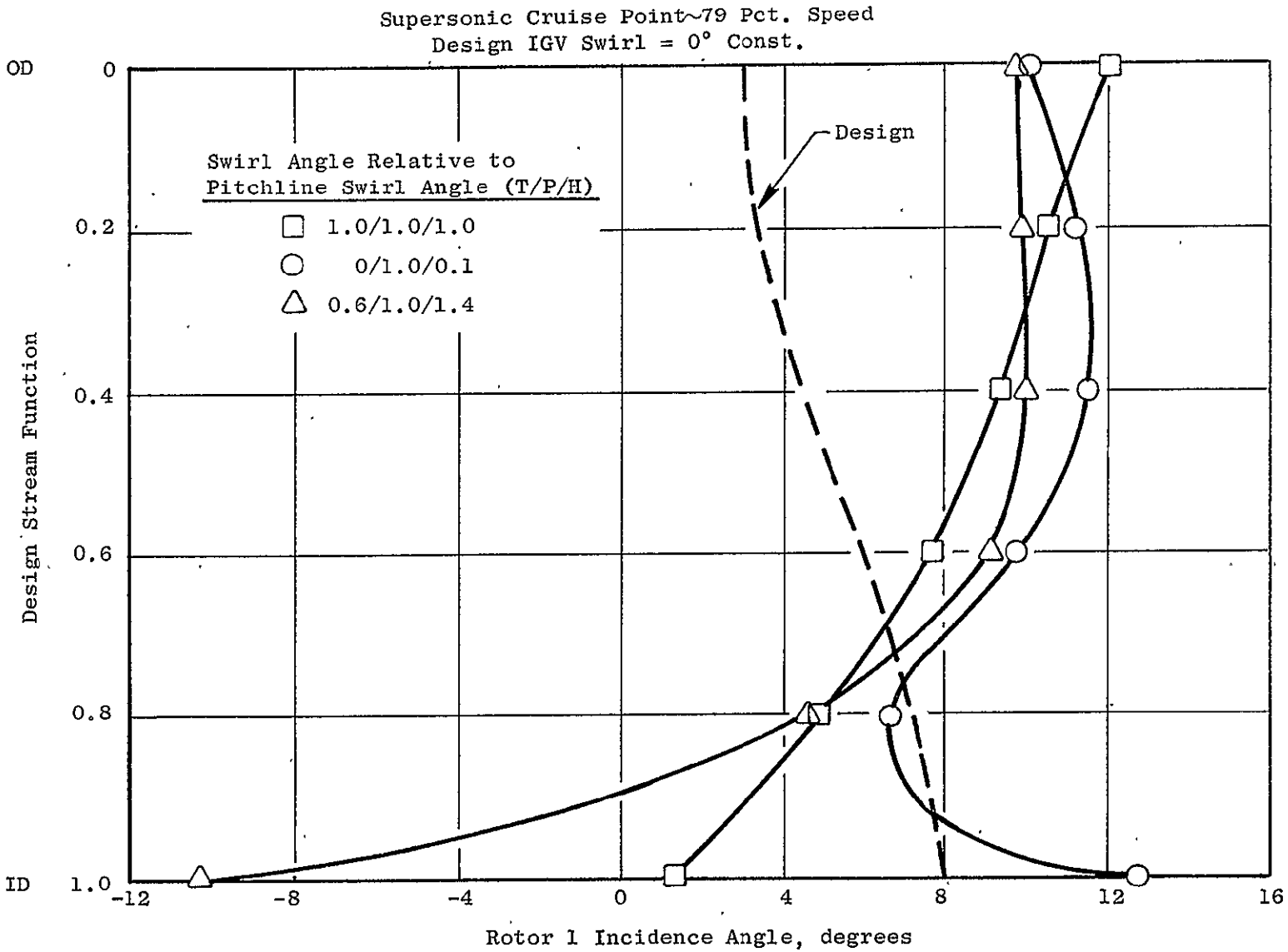

Figure 34. Front Block Fan Rotor 1 Off-Design Parameters - Design IGV Swirl = 10°/0°/-10°.

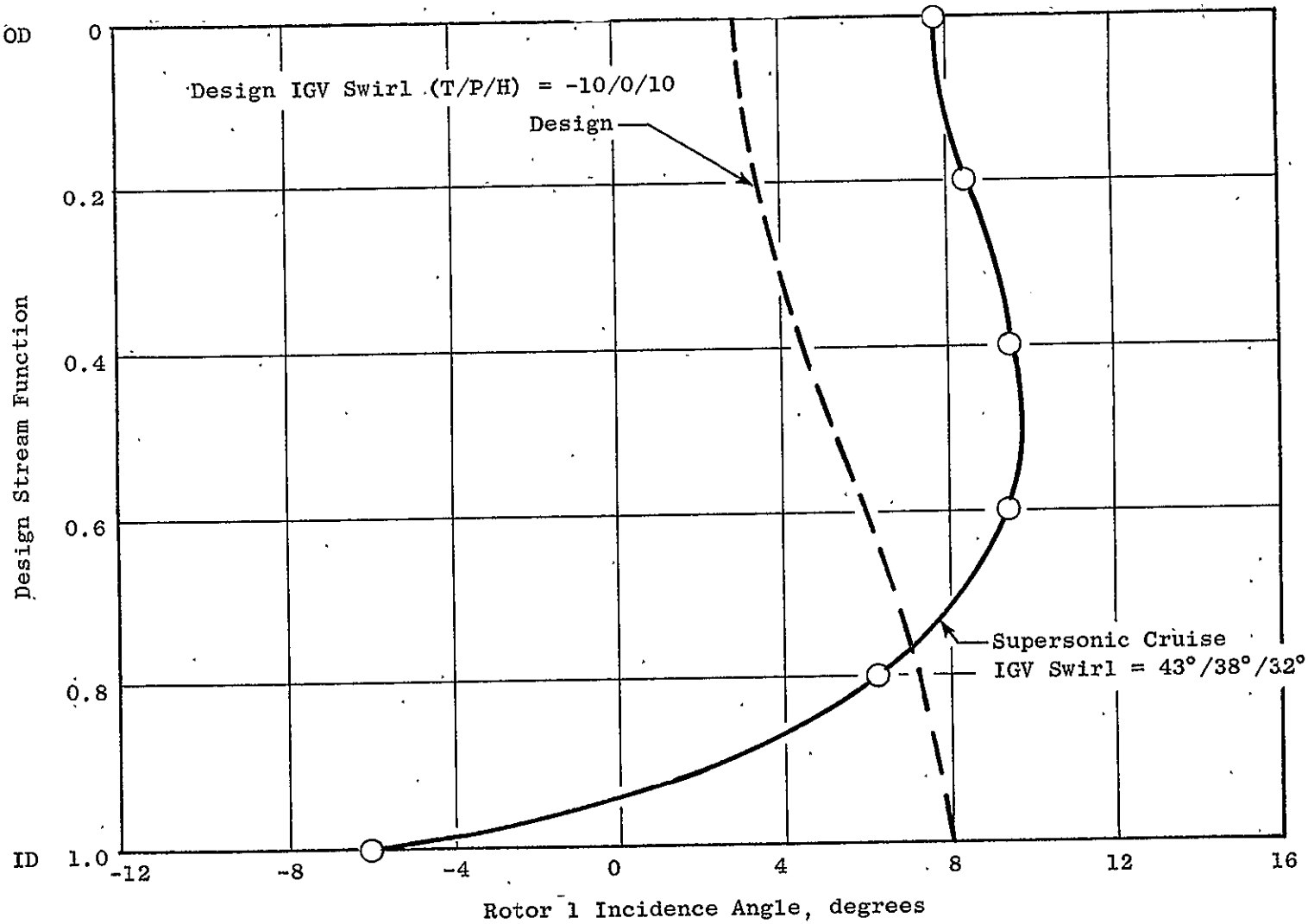

Figure 35. Front Block Fan Rotor 1 Incidence Angle at Design and Supersonic Cruise.

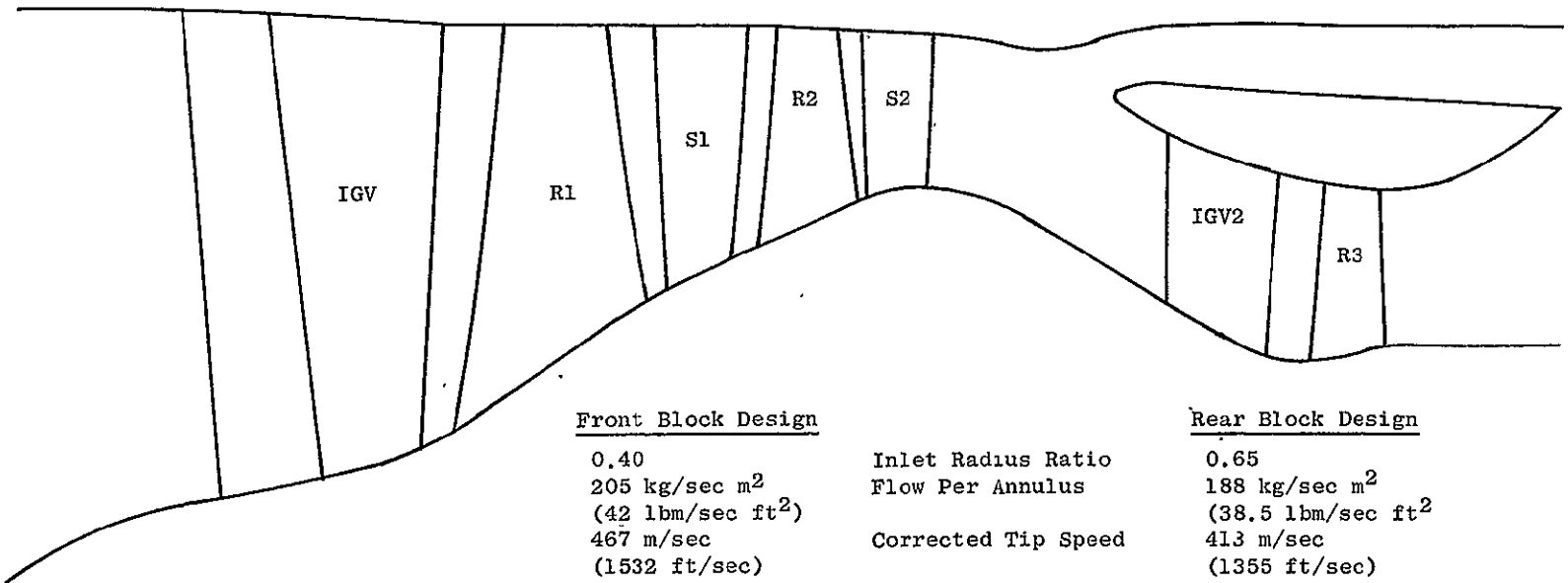

Front Block Design		Rear Block Design
0.40	Inlet Radius Ratio	0.65
205 kg/sec m^2 (42 lbm/sec ft^2)	Flow Per Annulus	188 kg/sec m^2 (38.5 lbm/sec ft^2
467 m/sec (1532 ft/sec)	Corrected Tip Speed	413 m/sec (1355 ft/sec)
3.17	Pressure Ratio	1.48

Figure 36. Front and Rear Block Fan Flowpath - Recommended Configuration.

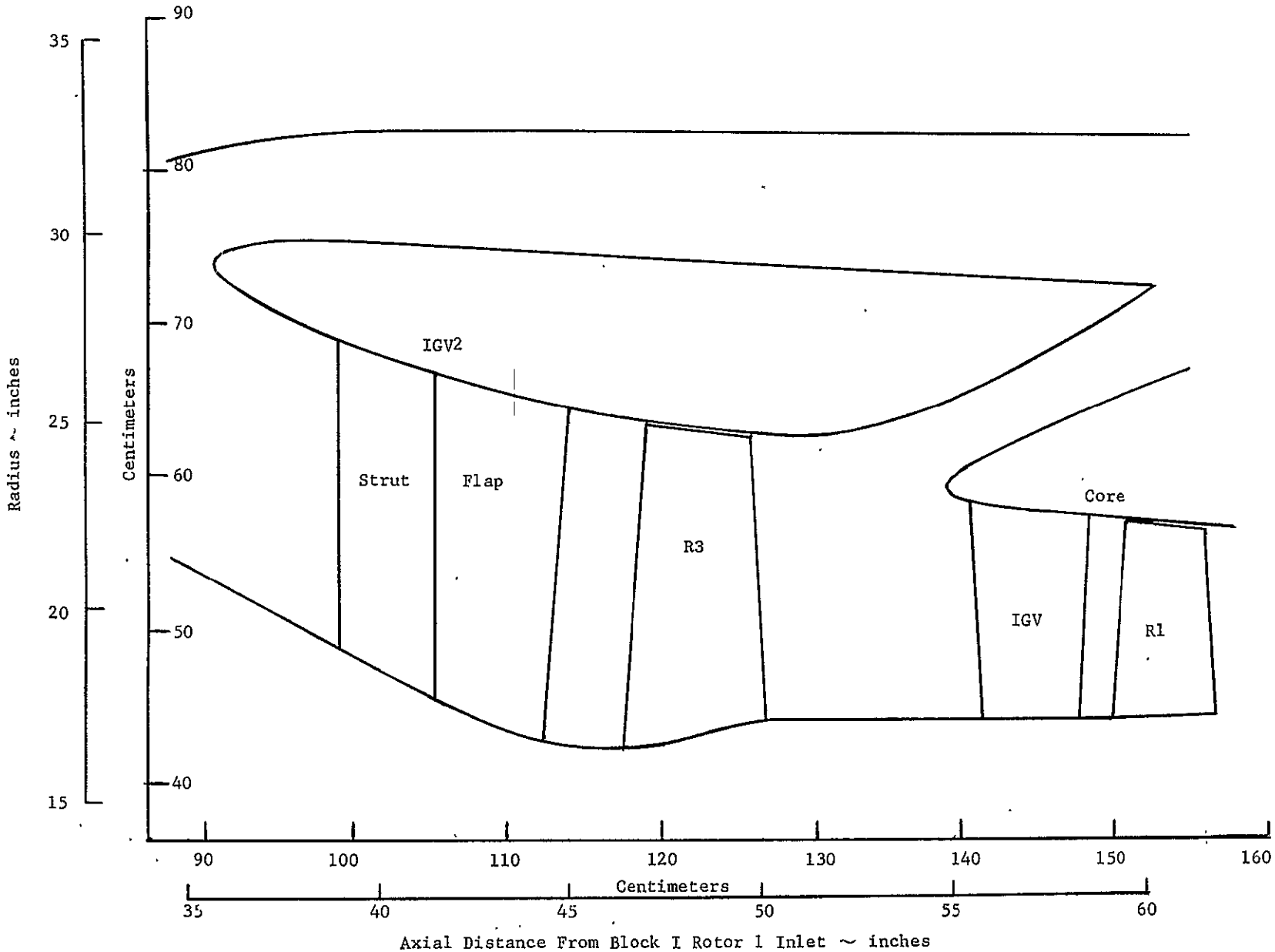

Figure 37. Rear Block Fan Flowpath.

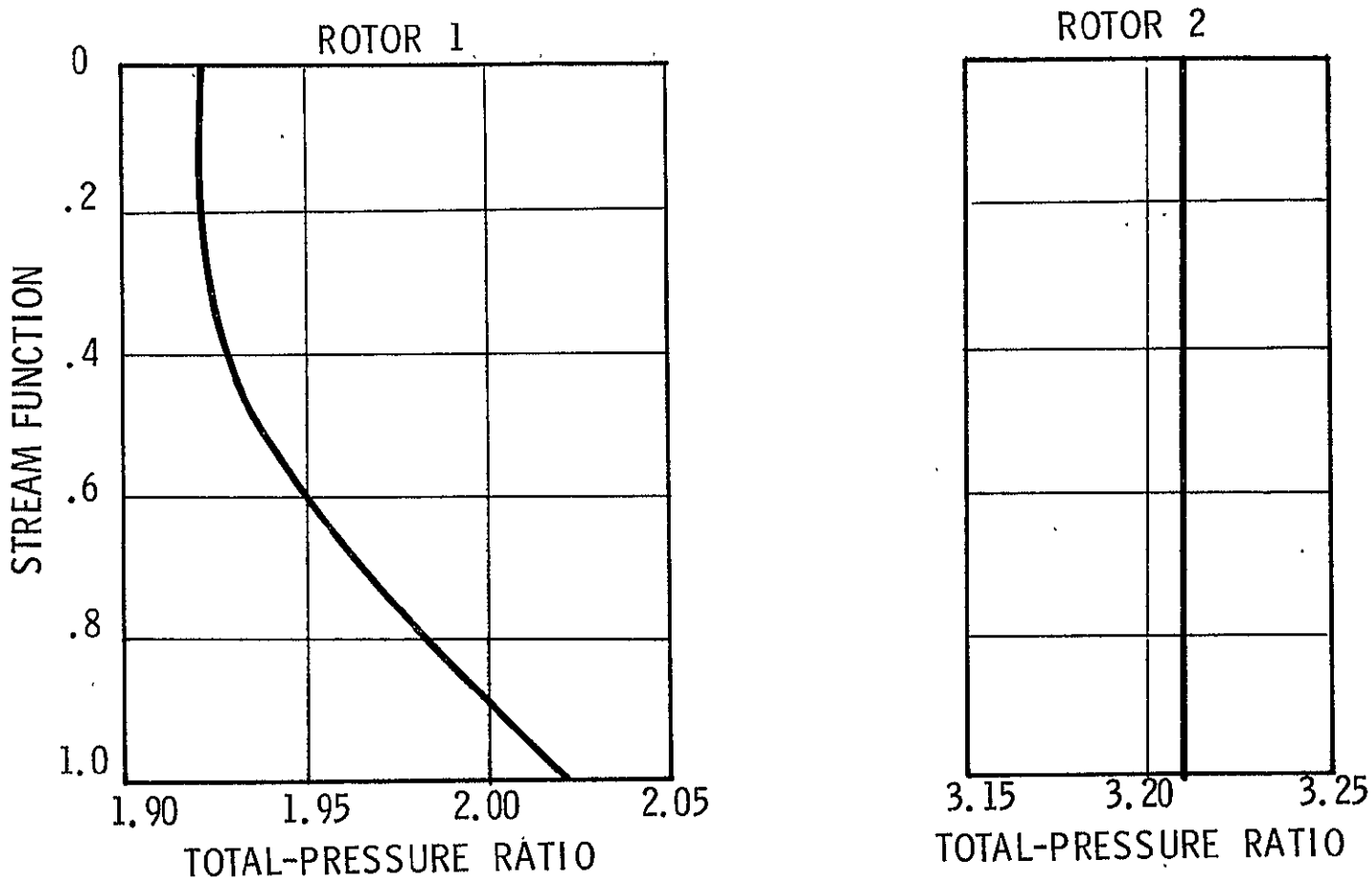

Figure 38. Front Block Fan Design Rotor Exit Total-Pressure Ratio.

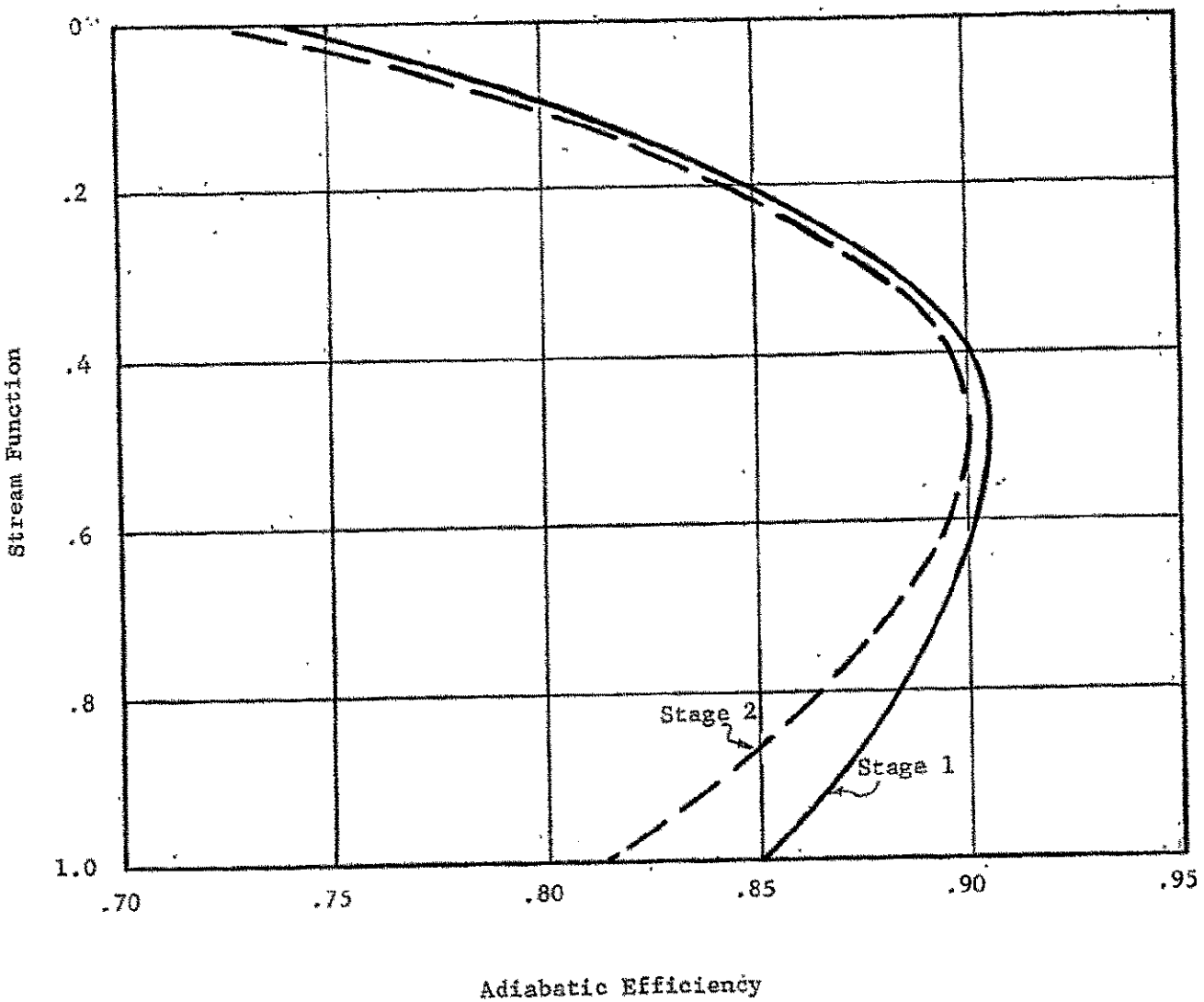

Figure 39. Front Block Fan Design Stage Exit Adiabatic Efficiency.

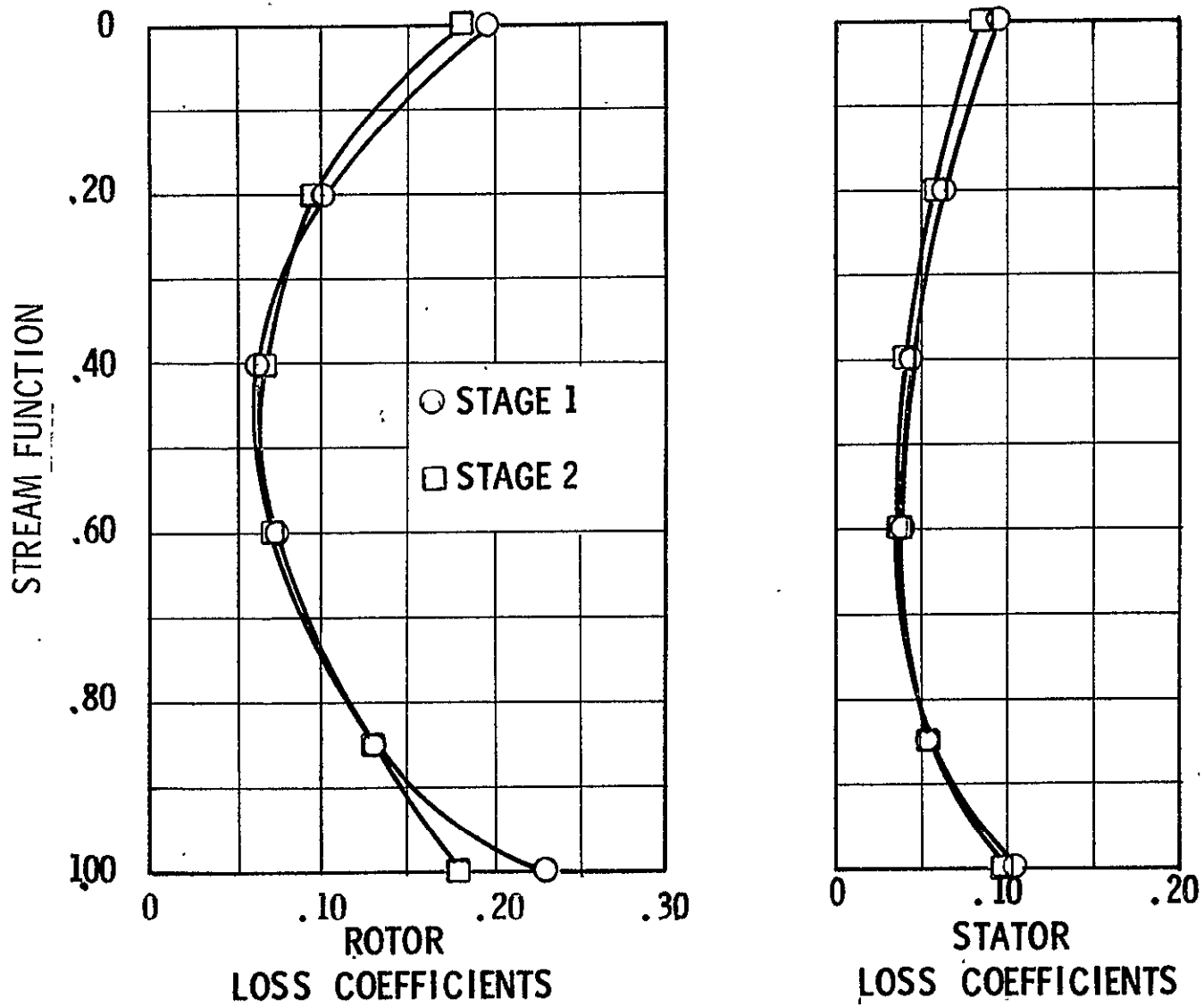

Figure 40. Front Block Fan Design Parameters - Loss Coefficients.

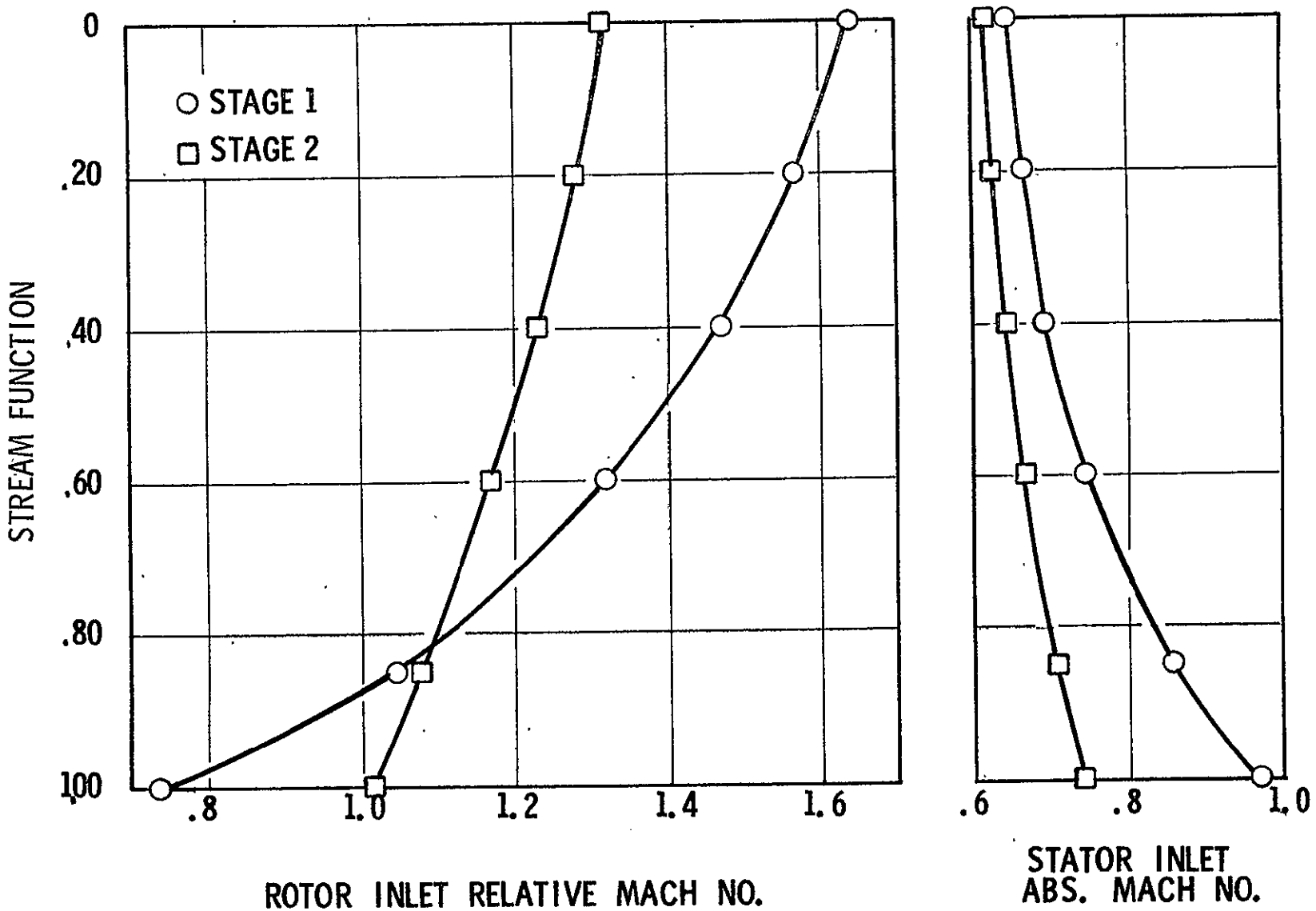

Figure 41. Front Block Fan Design Parameters - Mach Numbers.

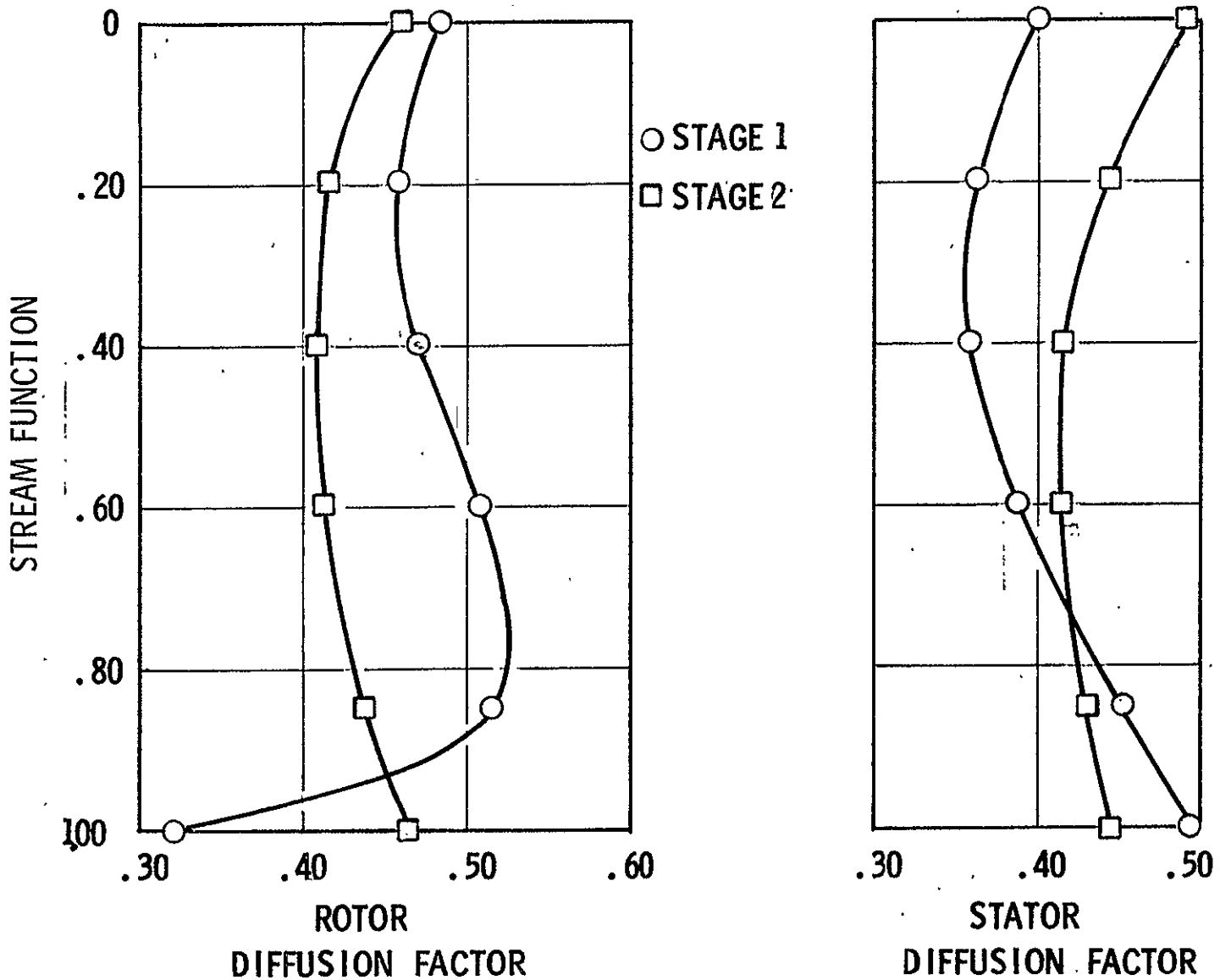

Figure 42. Front Block Fan Design Parameters - Diffusion Factors.

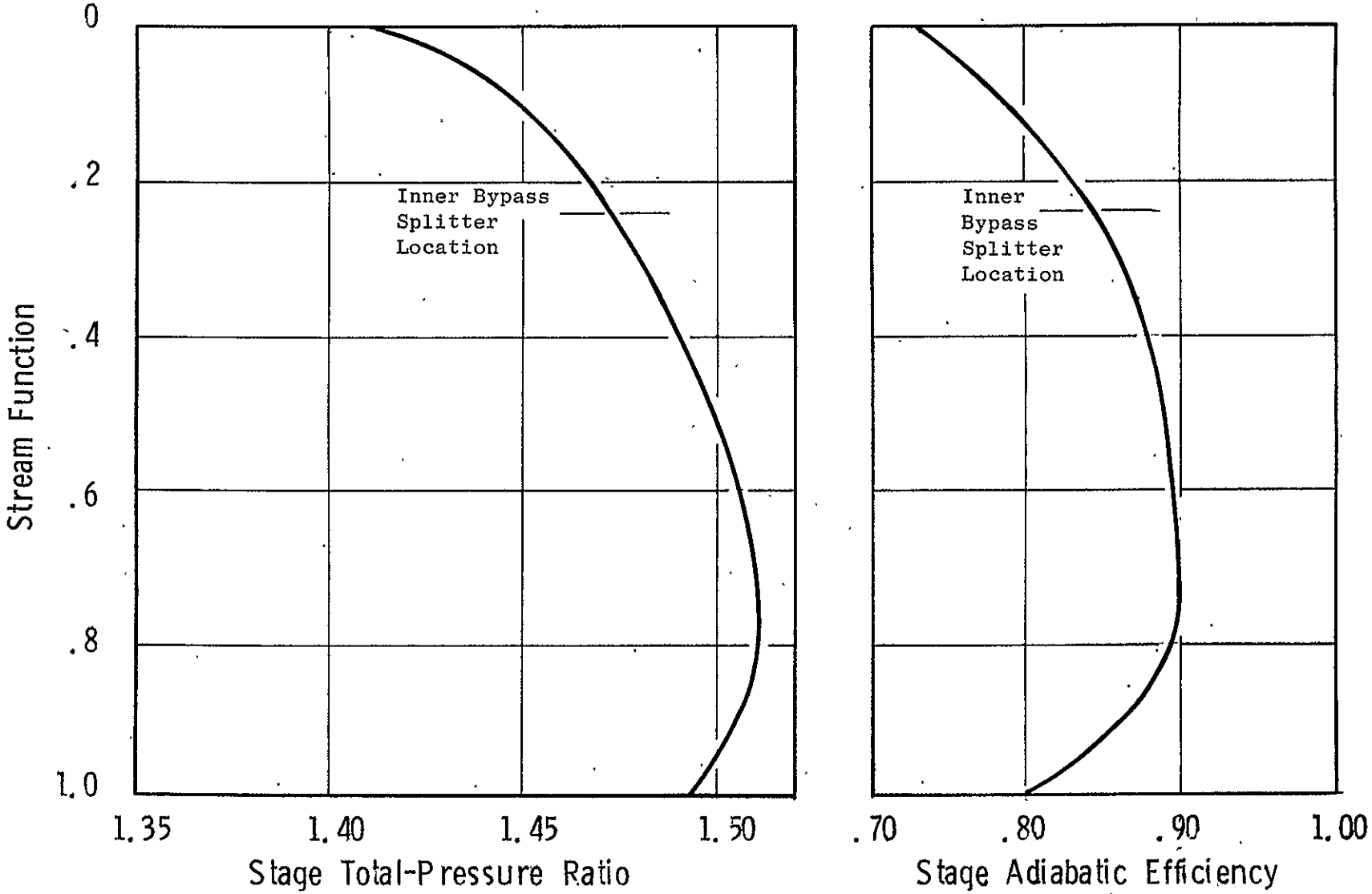

Figure 43. Rear Block Fan Design Parameters - Stage Total-Pressure Ratio and Adiabatic Efficiency.

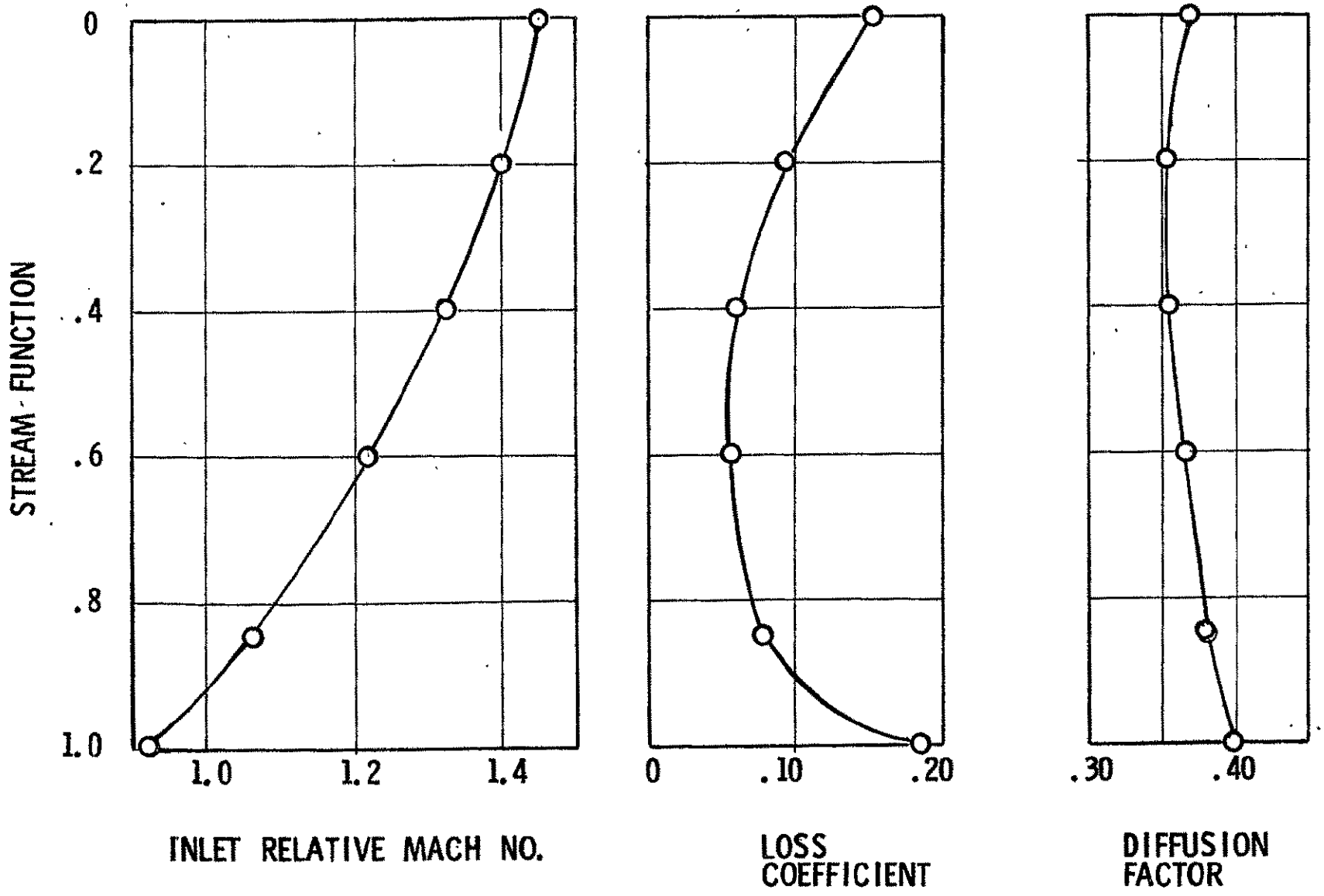

Figure 44. Rear Block Fan Design Parameters - Mach No., Loss Coefficient, and Diffusion Factor.

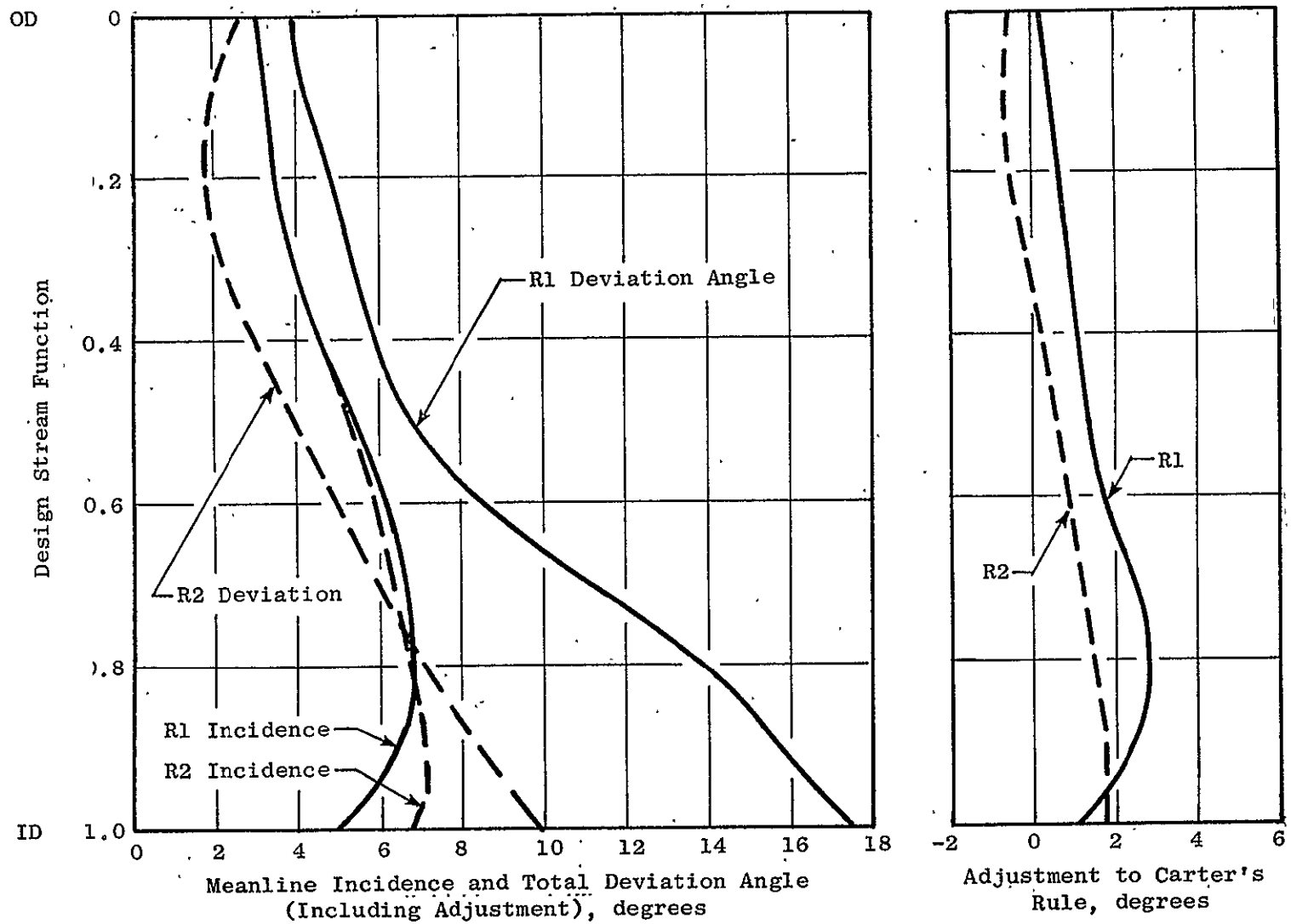

Figure 45. Front Block Fan Rotor Incidence, Deviation and Adjustment Angles at Aerodynamic Design Point.

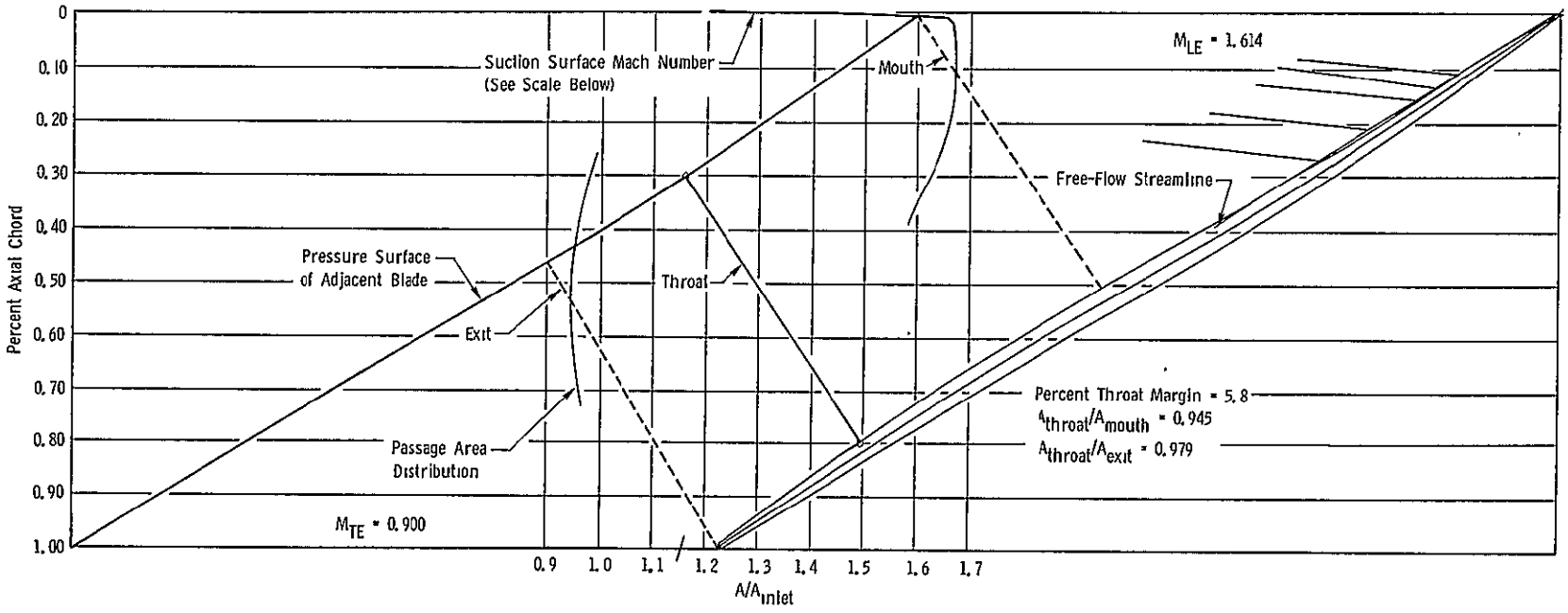

Figure 46. Front Block Fan Rotor 1 Streamline 3 (Near Tip) Airfoil Section.

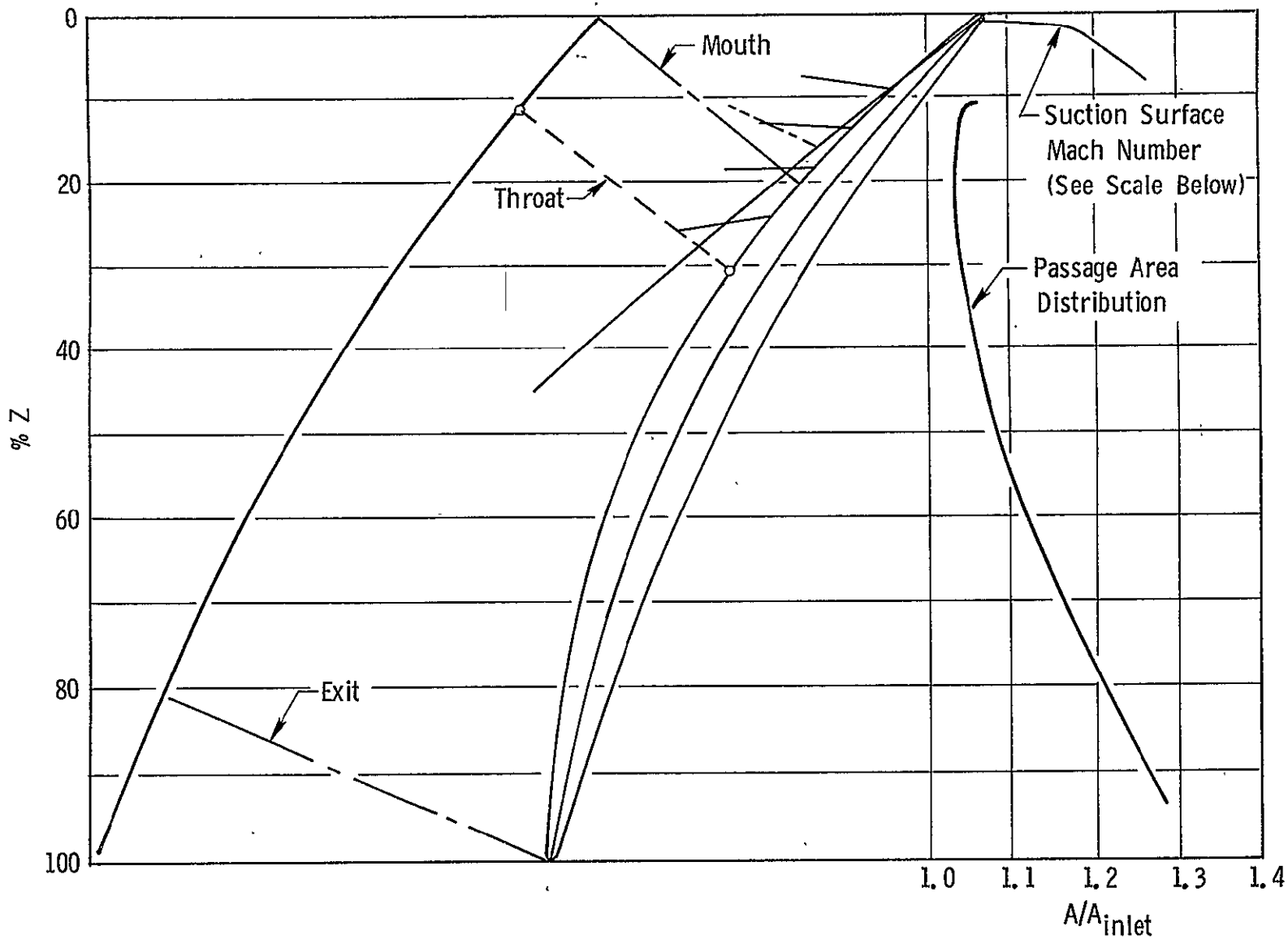

Figure 47. Front Block Fan Rotor 1 Streamline 10 (Near Hub) Airfoil Section.

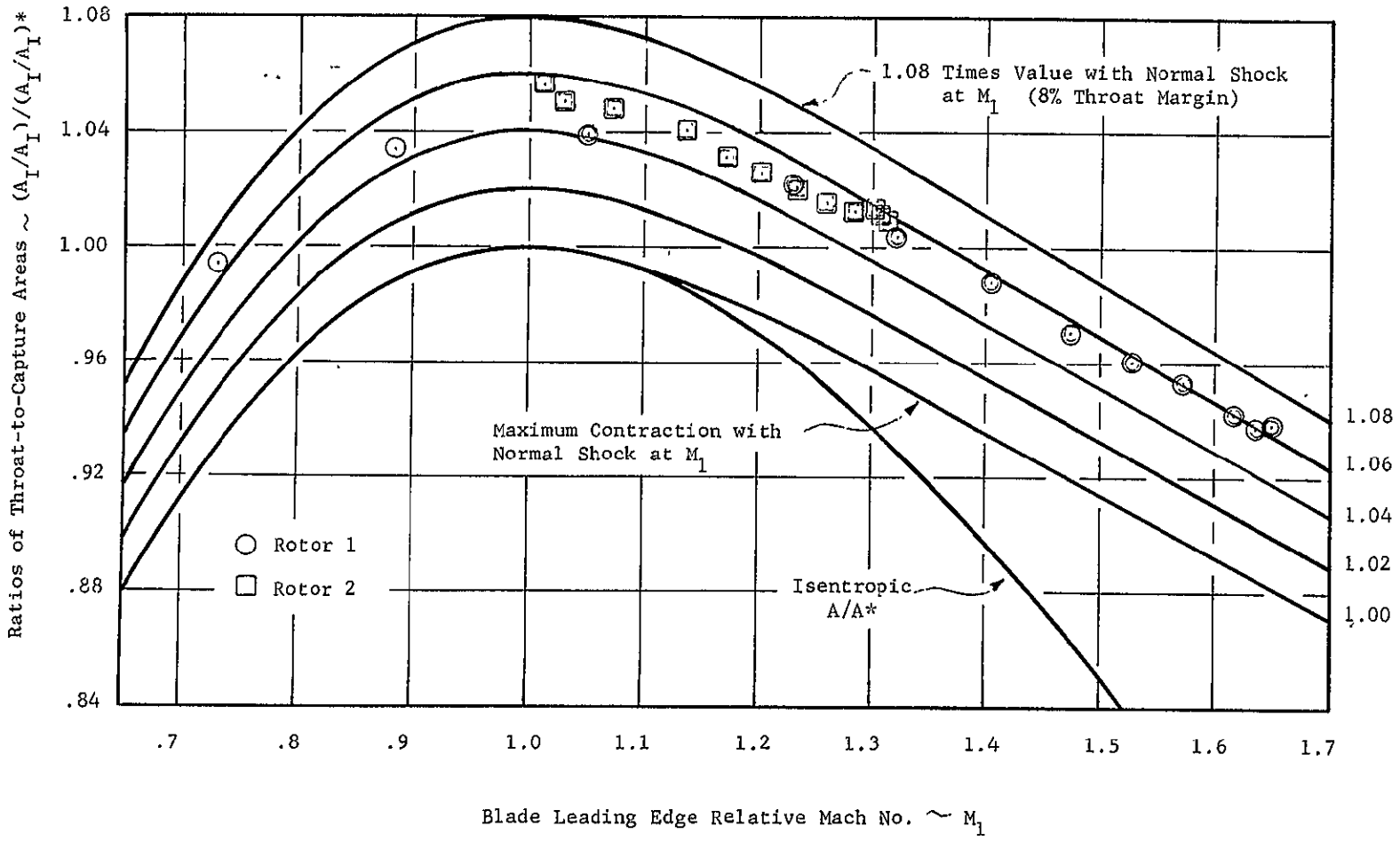

Figure 48. Front Block Fan Rotor Airfoil Design Throat Margins.

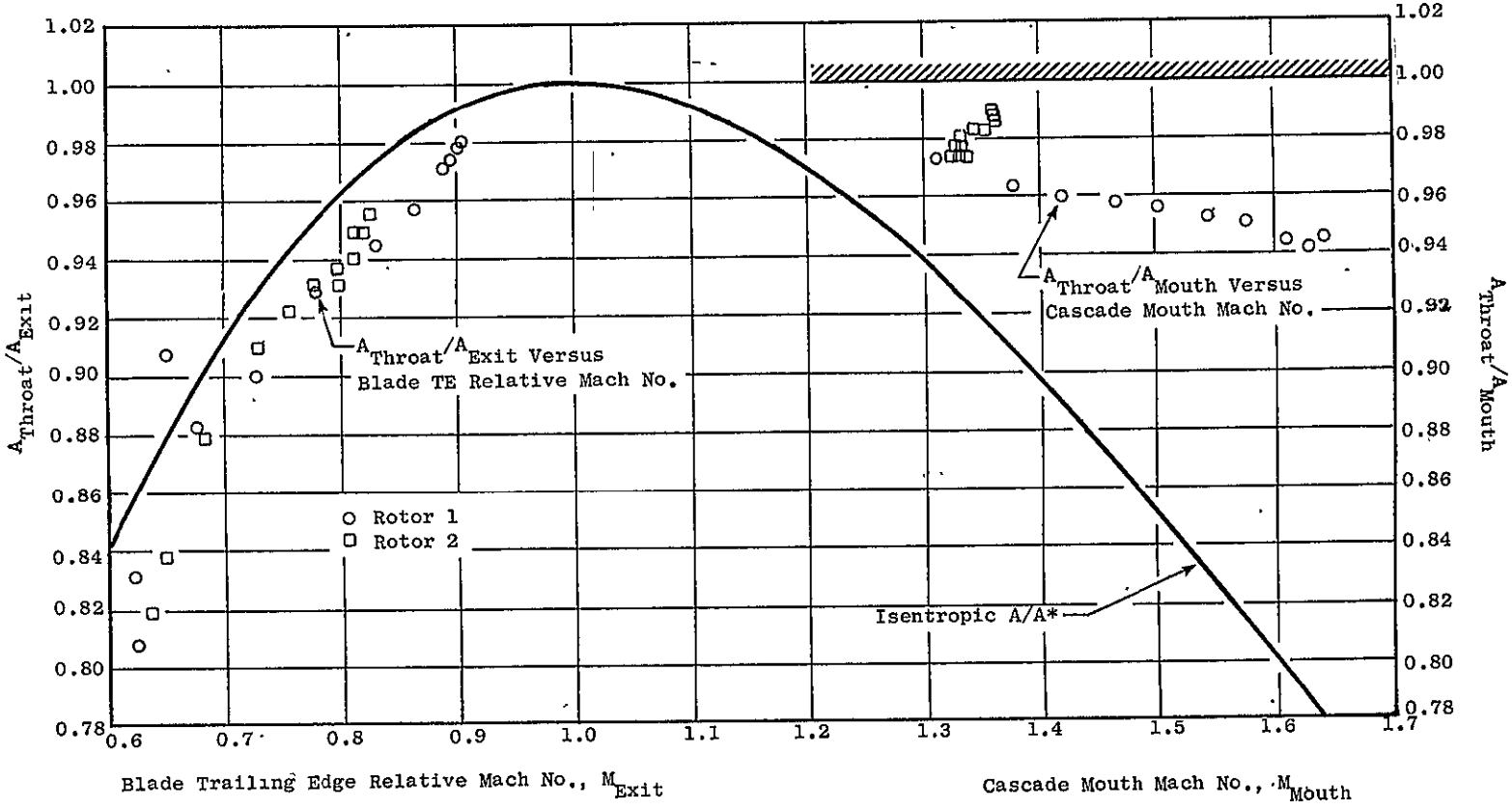

Figure 49. Front Block Fan Rotor Airfoil Design Passage Area Ratios.

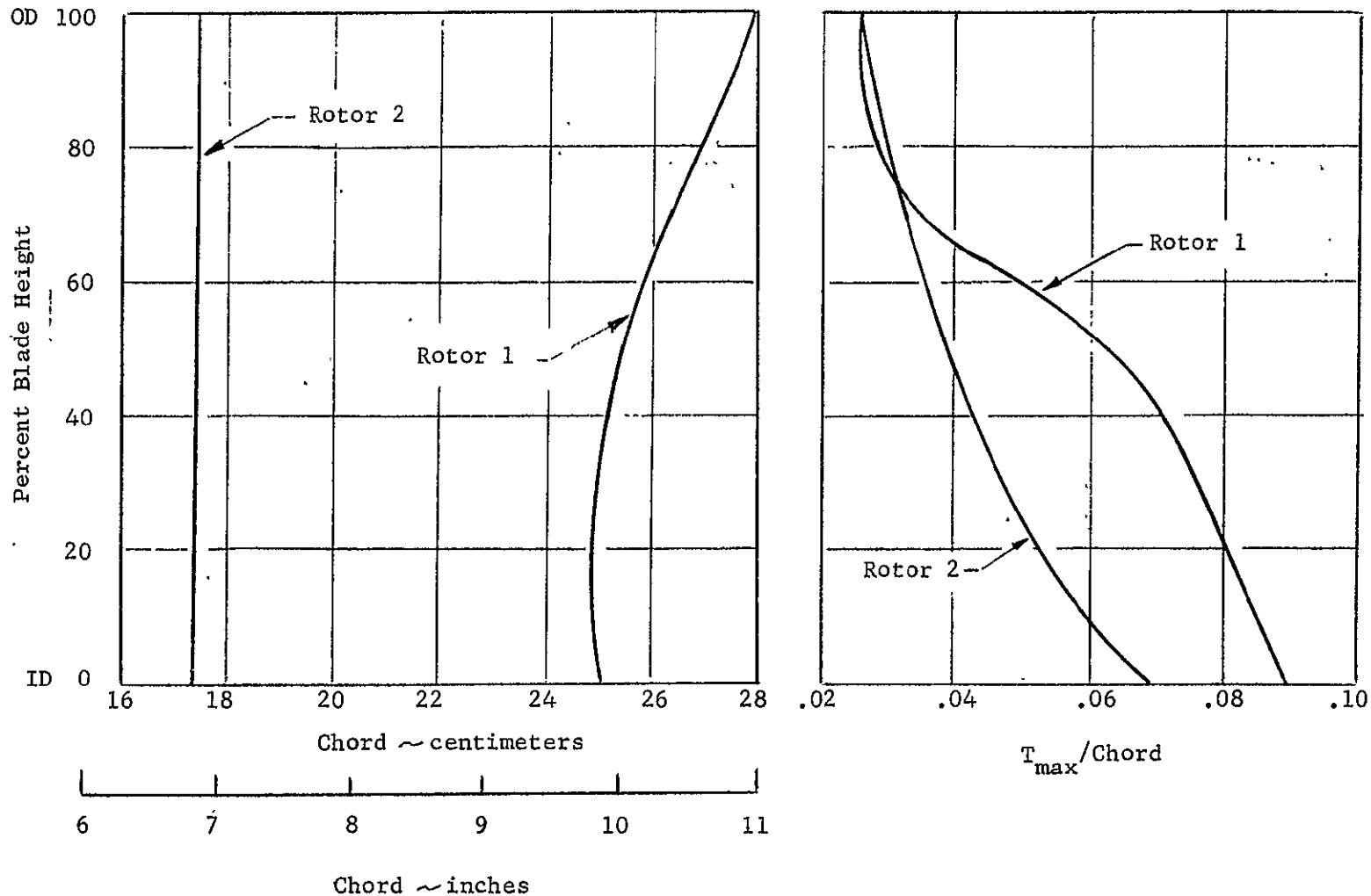

Figure 50. Front Block Fan Rotor Chord and Tm/c Distributions.

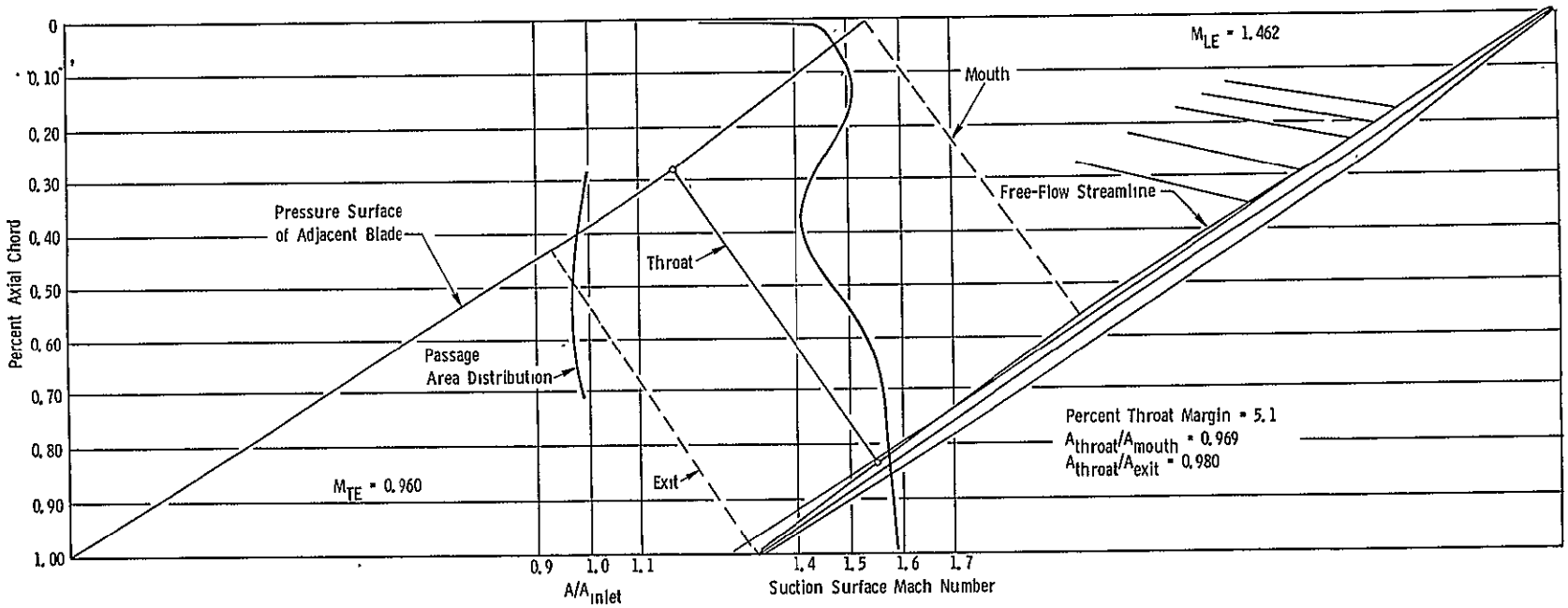

Figure 51. Rear Block Fan Rotor Streamline 1 (Tip) Airfoil Section.

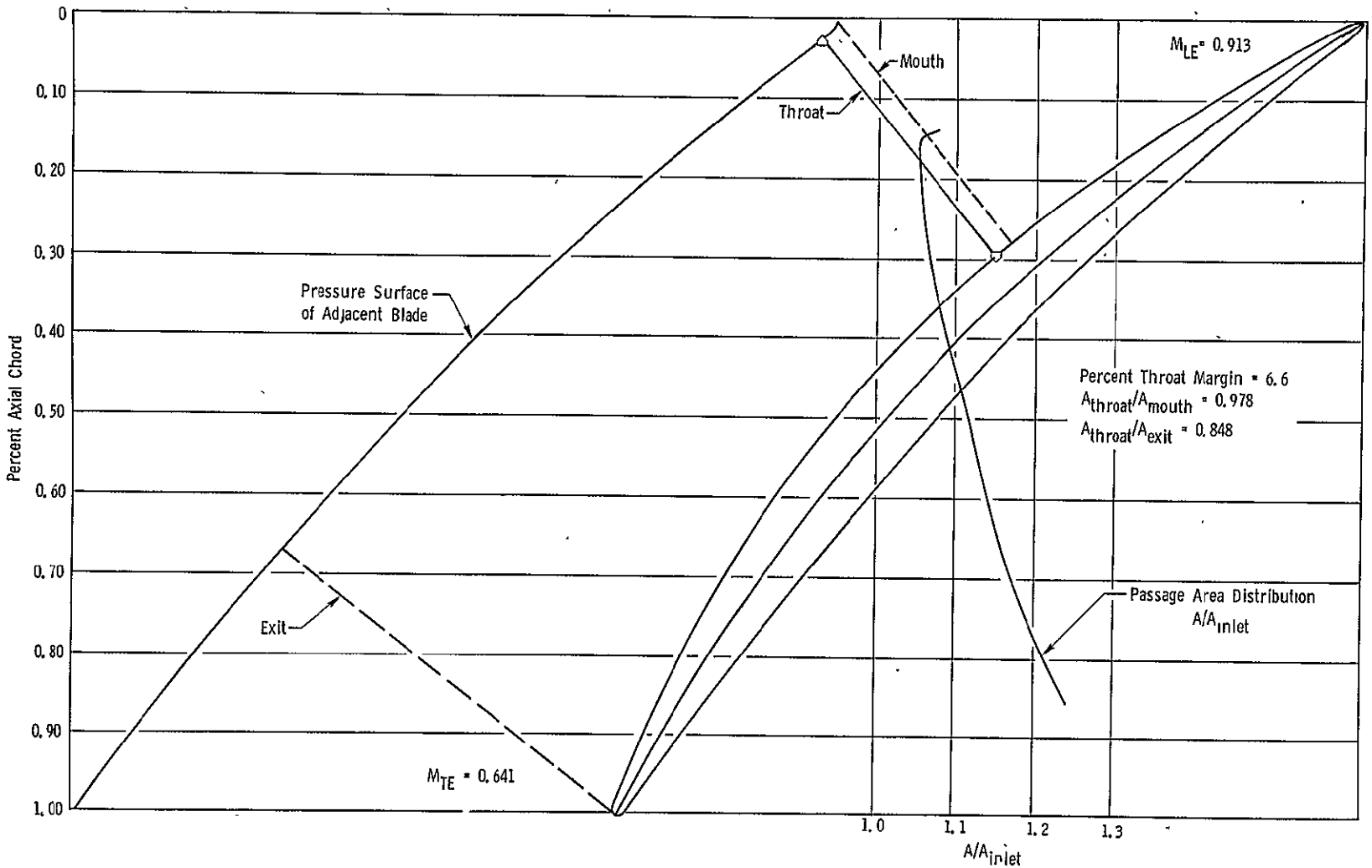

Figure 52. Rear Block Fan Rotor Streamline 10 (Hub) Airfoil Section.

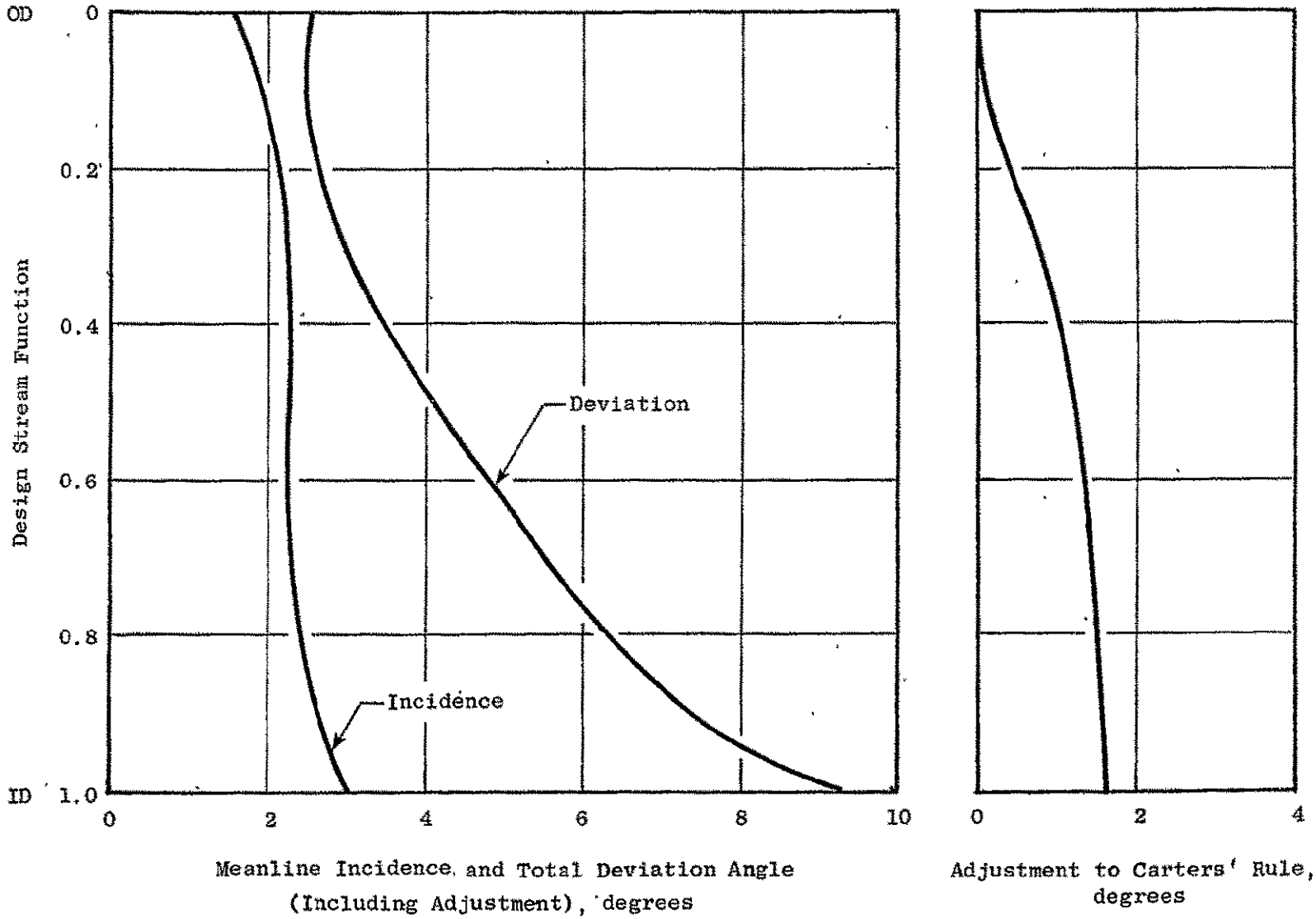

Figure 53. Rear Block Fan Rotor Incidence, Deviation and Adjustment Angles at Aerodynamic Design Point

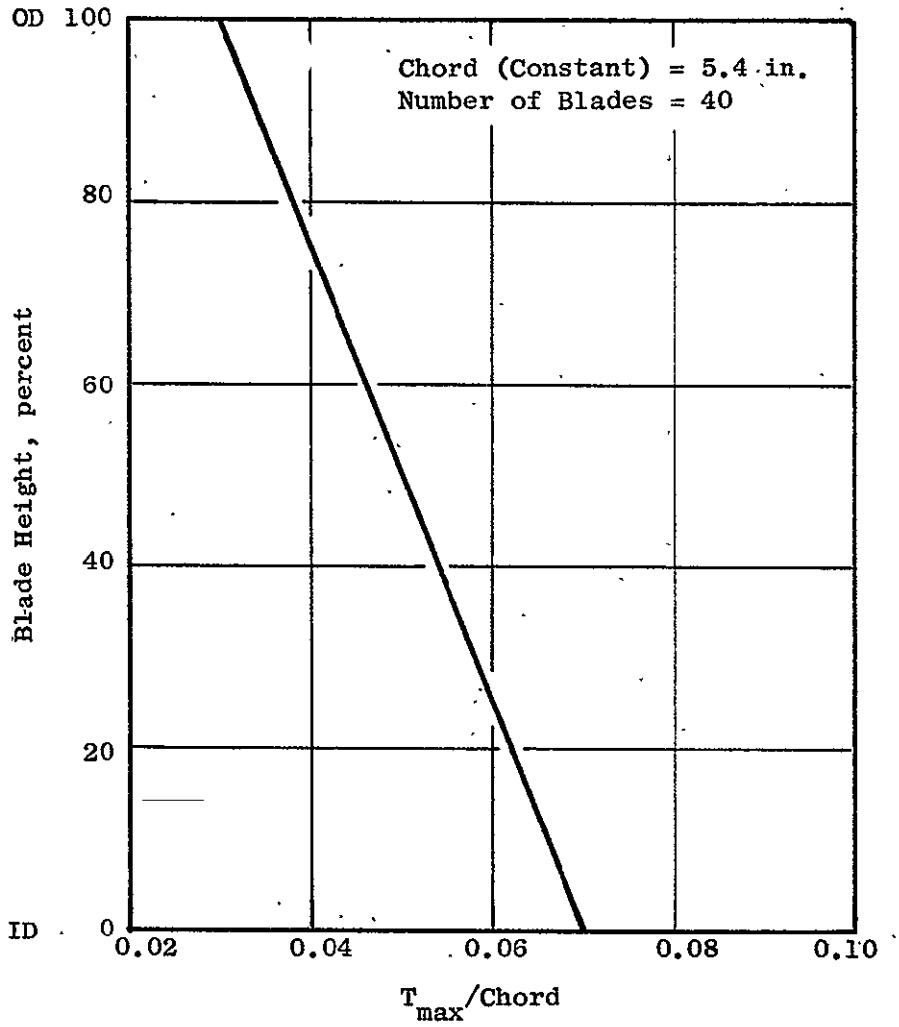

Figure 54. Rear Block Fan Rotor Tm/c Distribution.

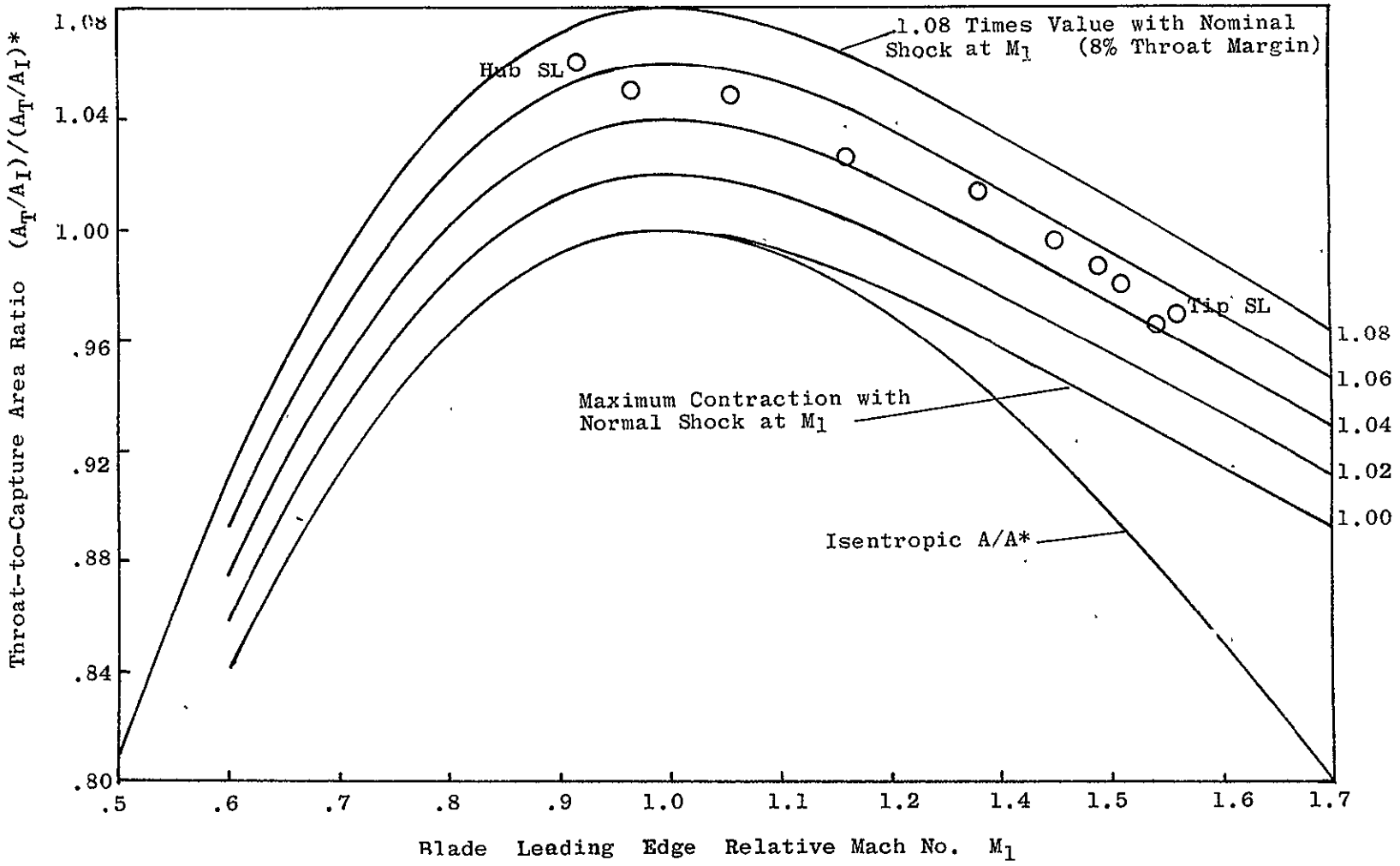

Figure 55. Rear Block Fan Rotor Airfoil Design Throat Margins.

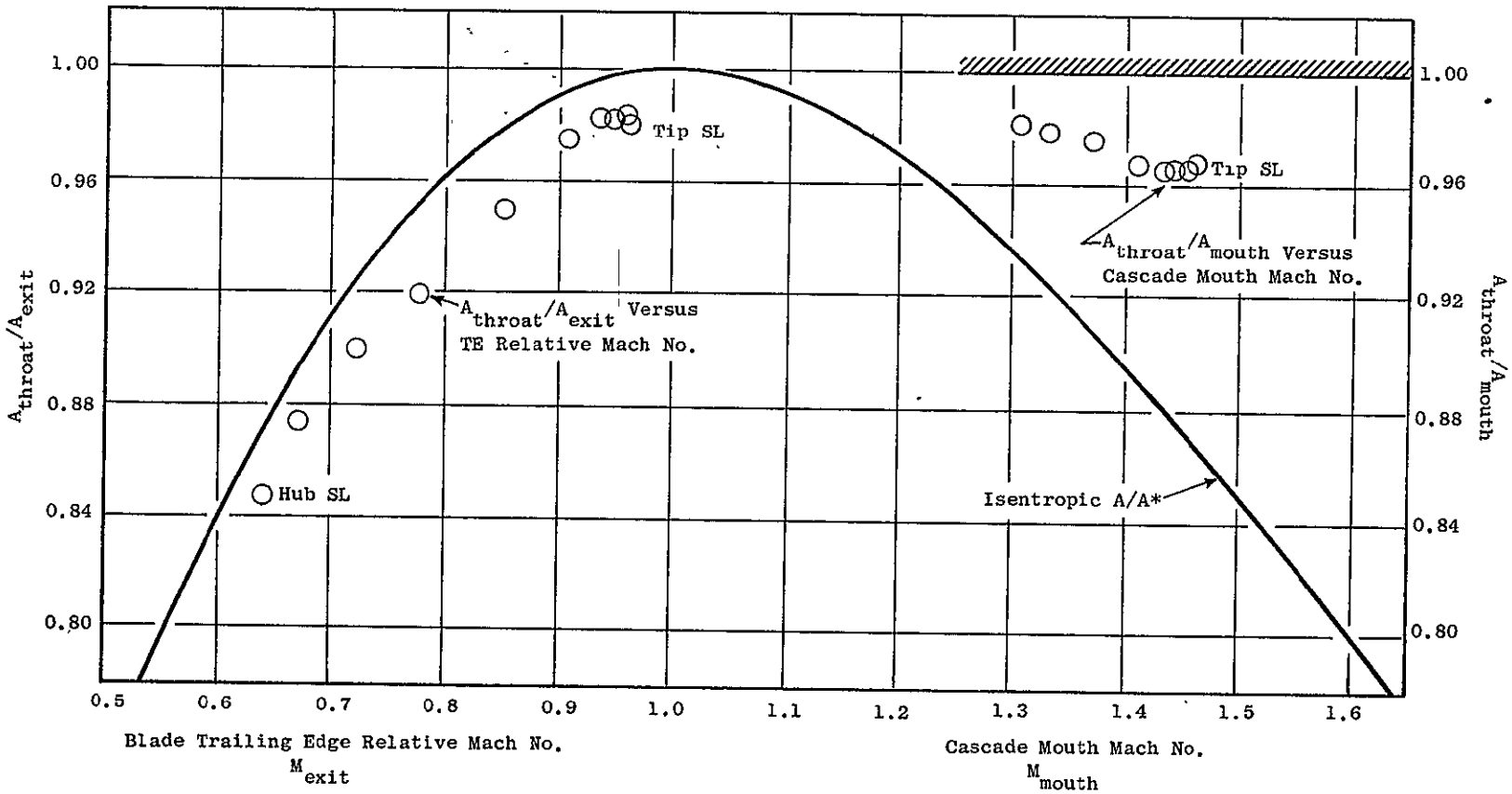

Figure 56. Rear Block Fan Rotor Airfoil Design Passage Area Ratios.

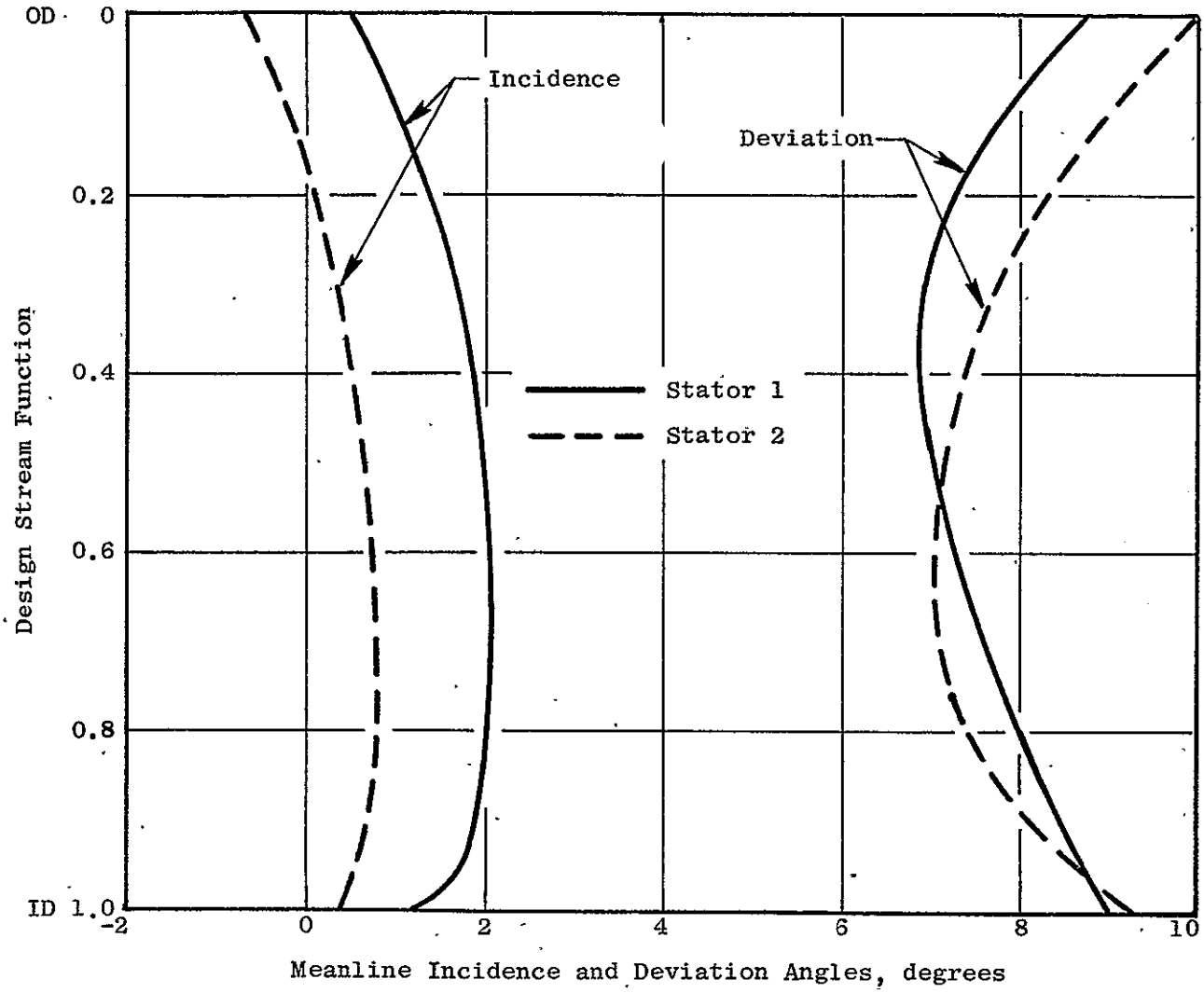

Figure 57. Front Block Fan Stator Incidence and Deviation Angles at Aerodynamic Design Point.

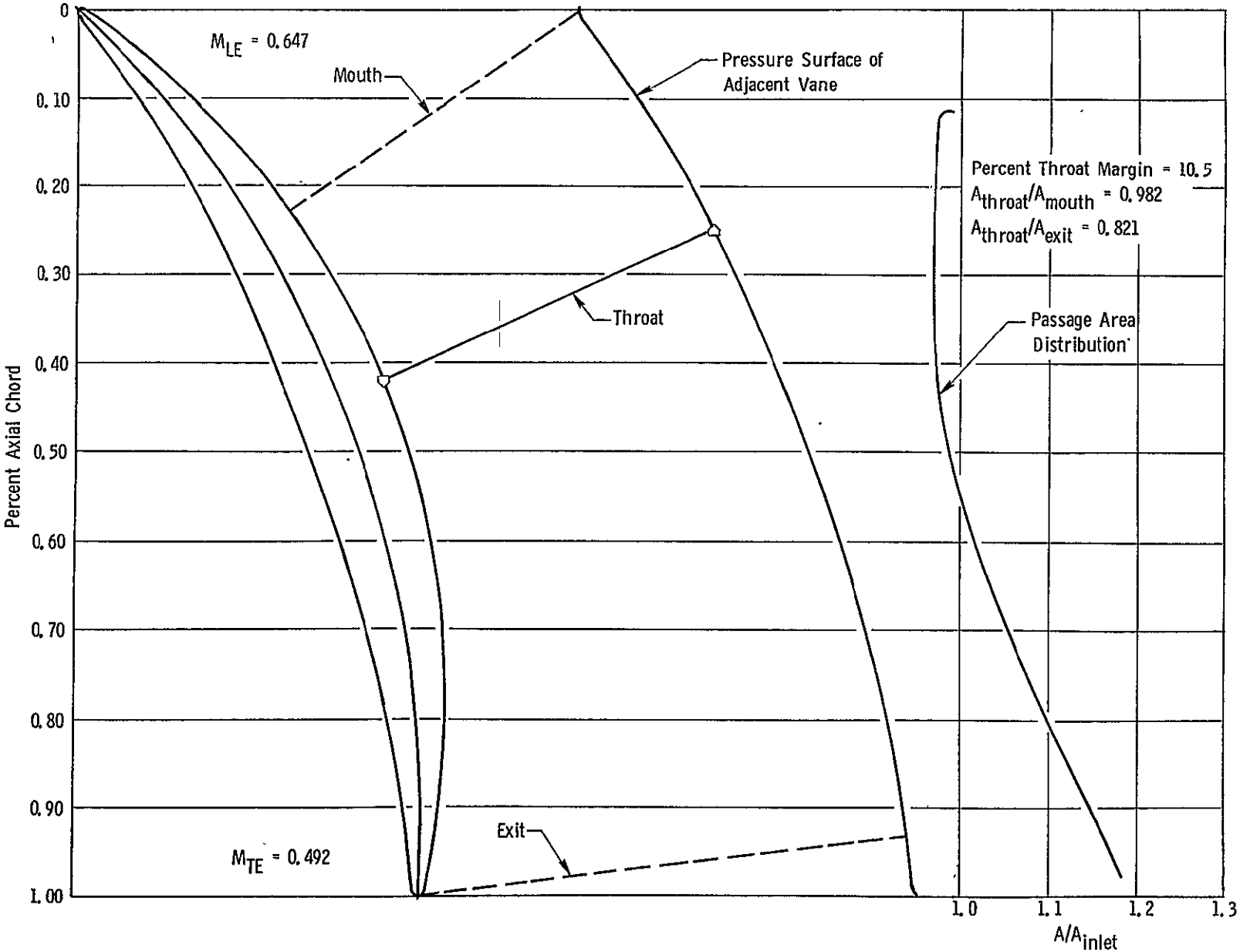

Figure 58. Front Block Fan Stator 1 Tip Streamline Airfoil Section.

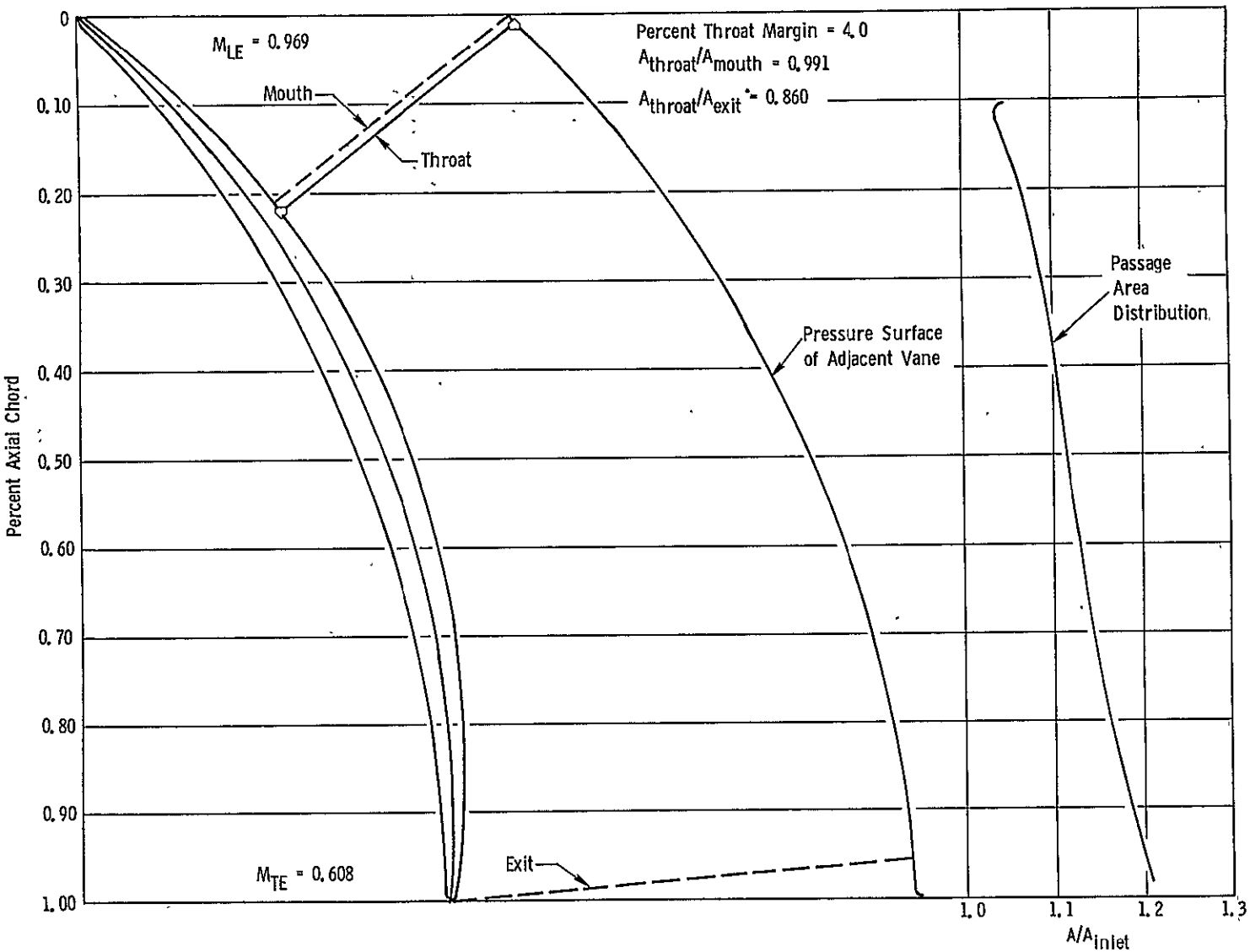

Figure 59. Front Block Fan Stator 1 Hub Streamline Airfoil Section. .

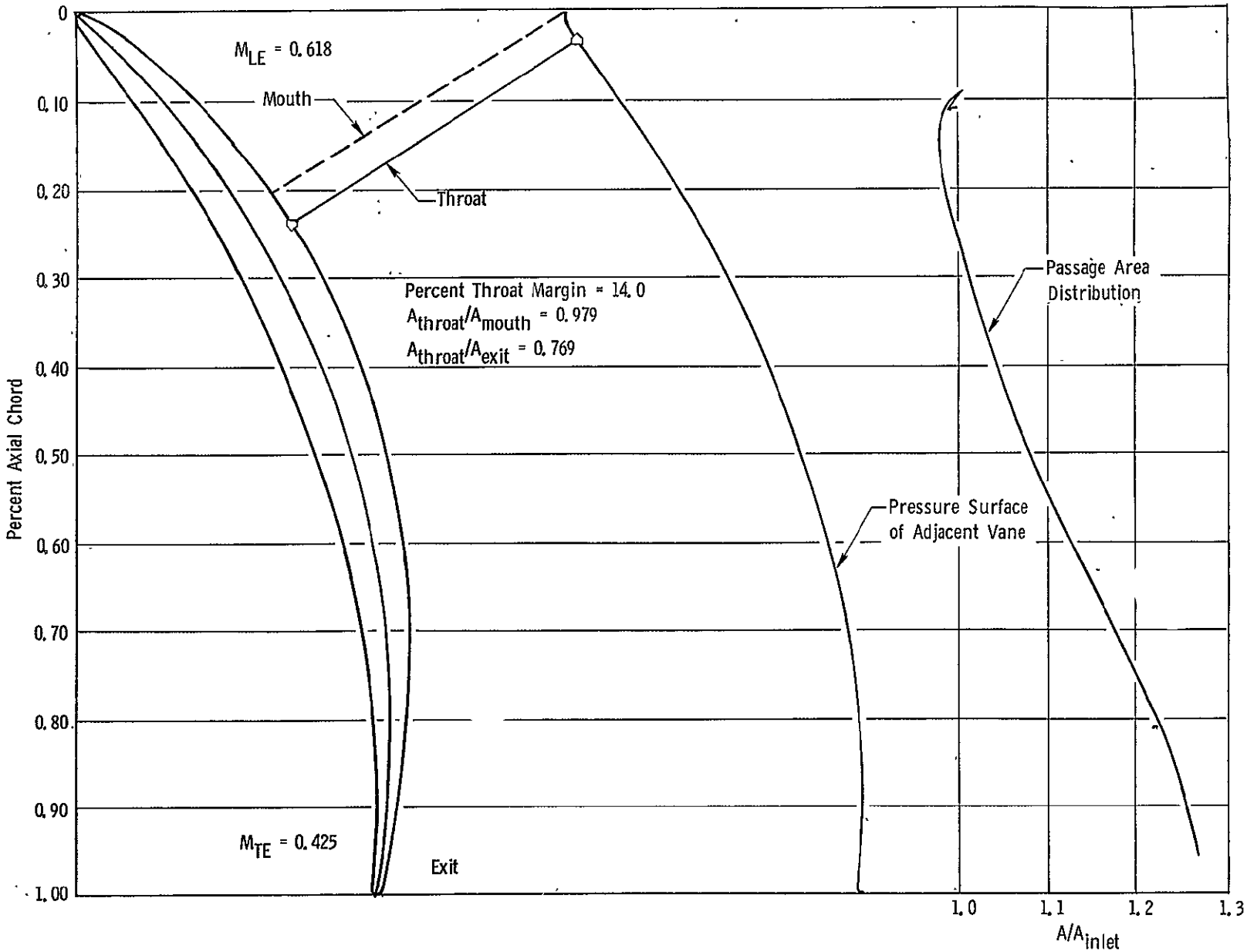

Figure 60. Front Block Fan Stator 2 Tip Streamline Airfoil Section.

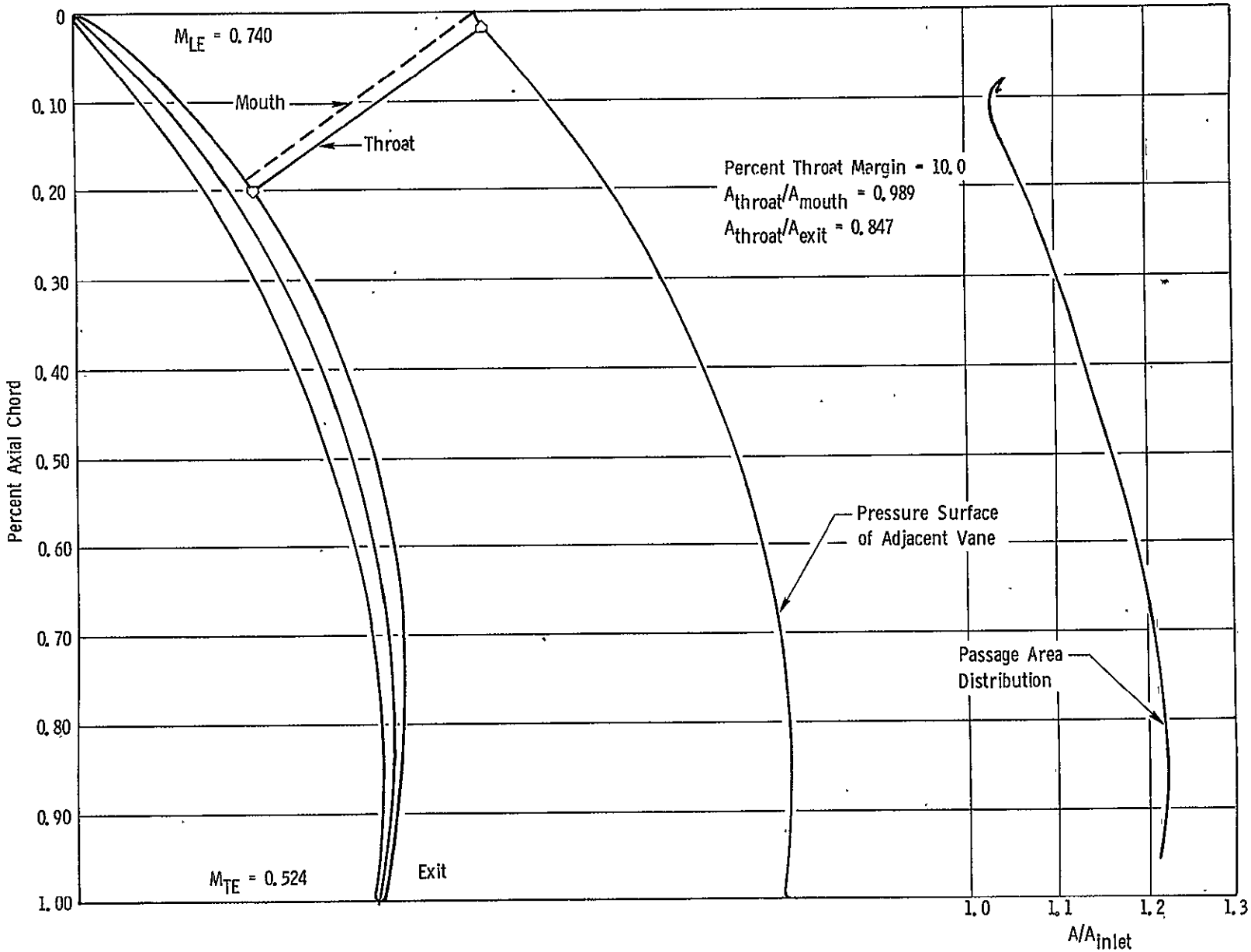

Figure 61. Front Block Fan Stator 2 Hub Streamline Airfoil Section.

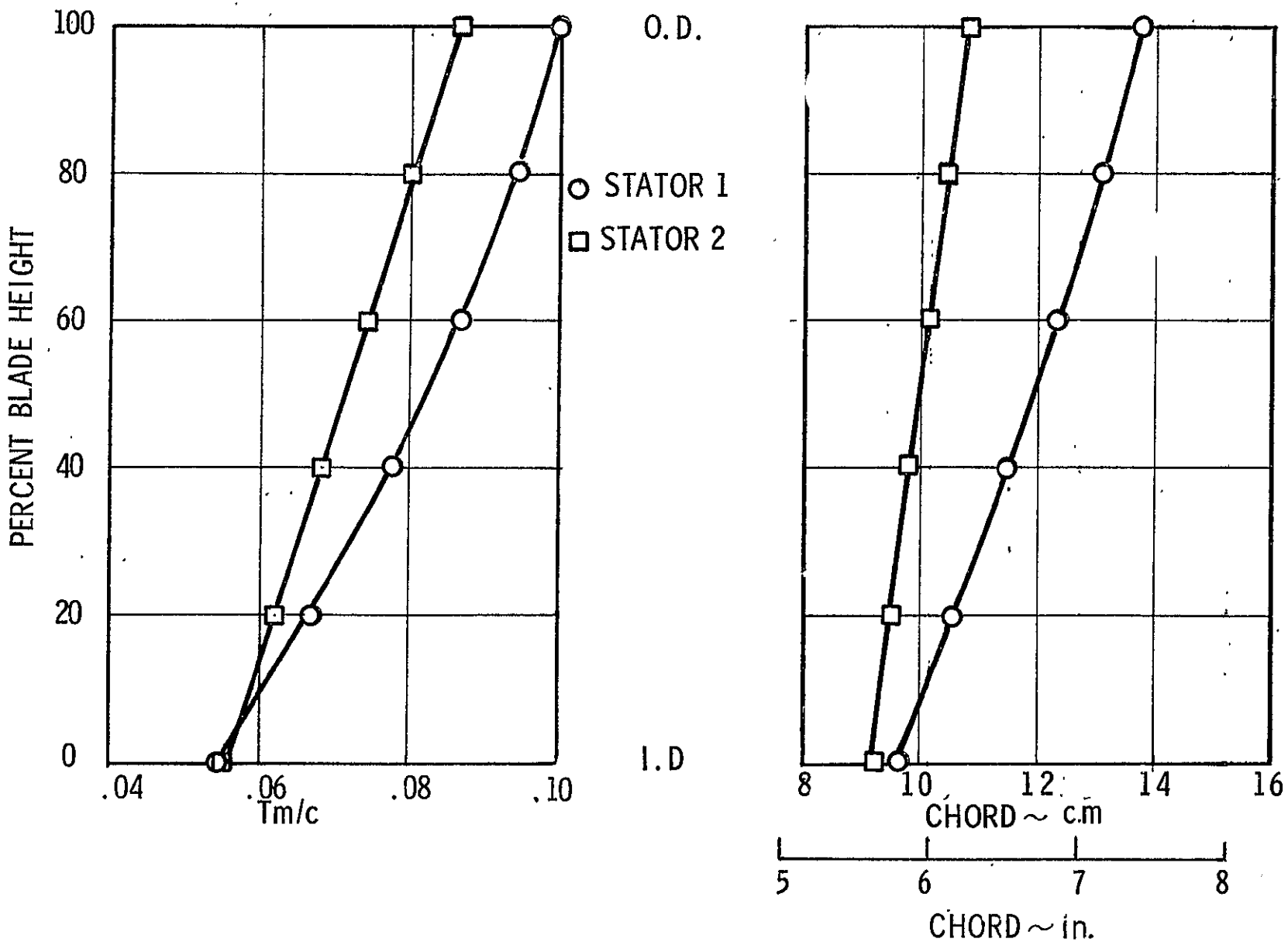

Figure 62. Front Block Fan Stator Tm/c and Chord Distributions.

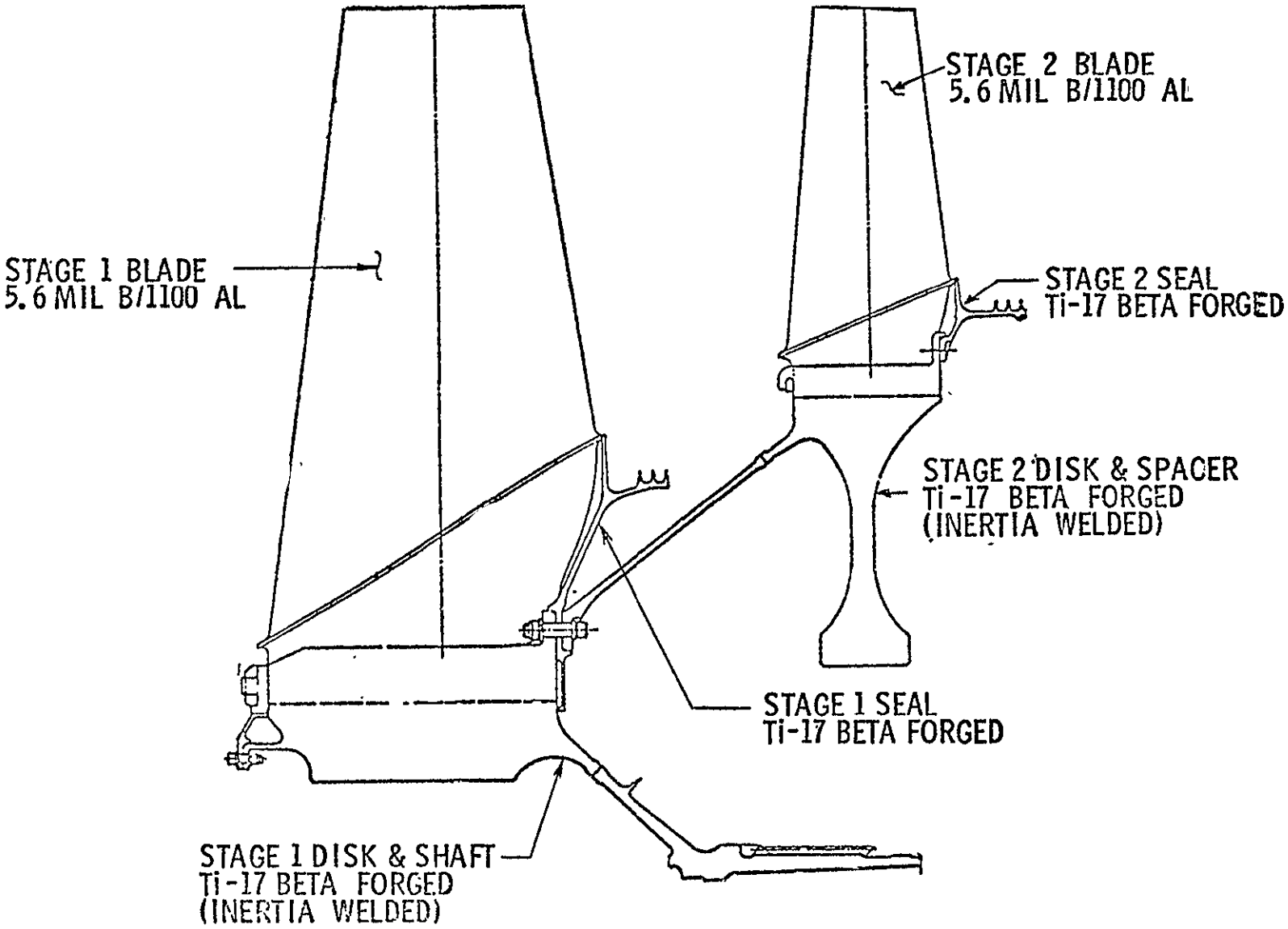

Figure 63. Front Block Fan Rotor Materials and Mechanical Configuration.

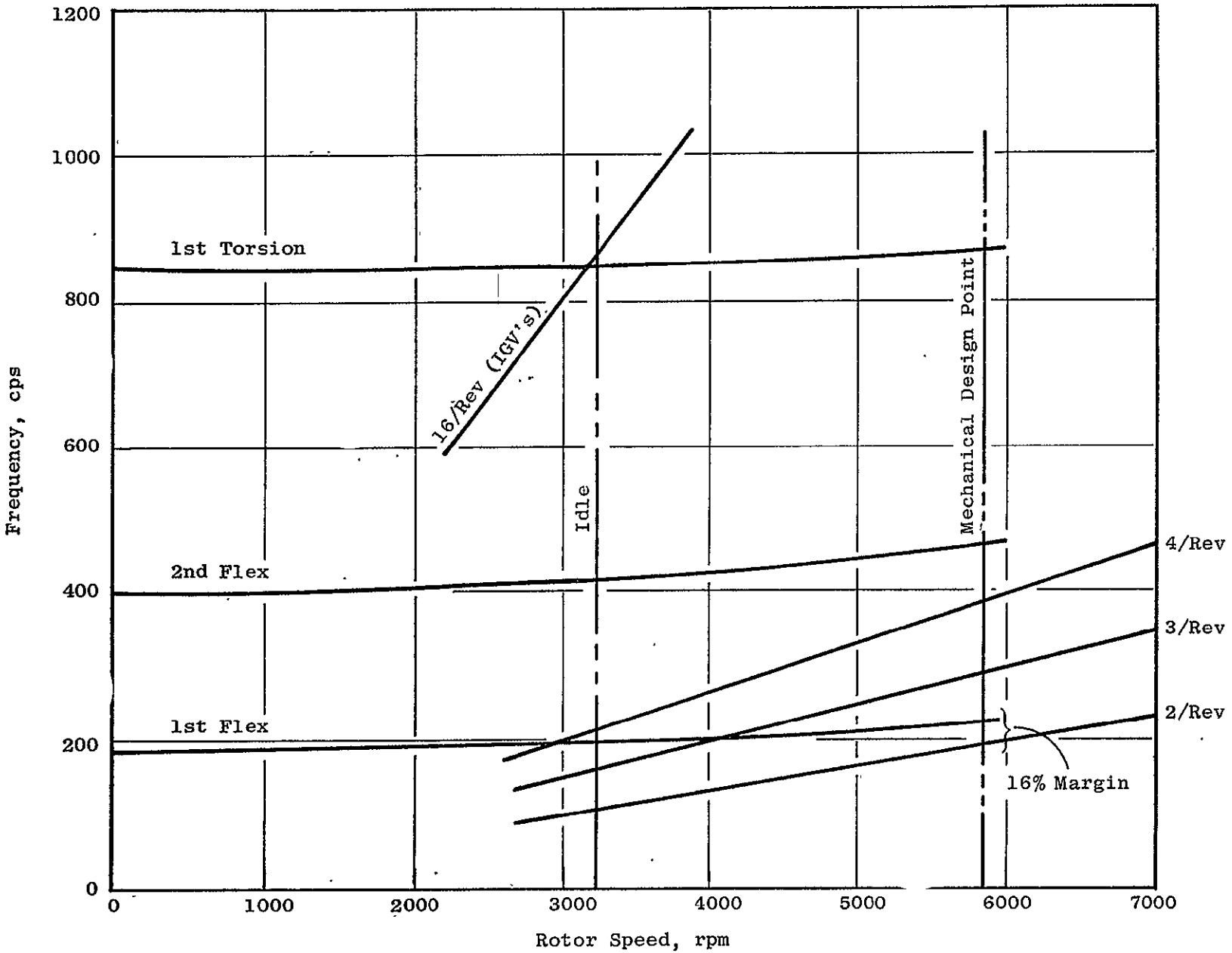

Figure 64. Front Block Fan Rotor Stage 1 Blade Campbell Diagram.

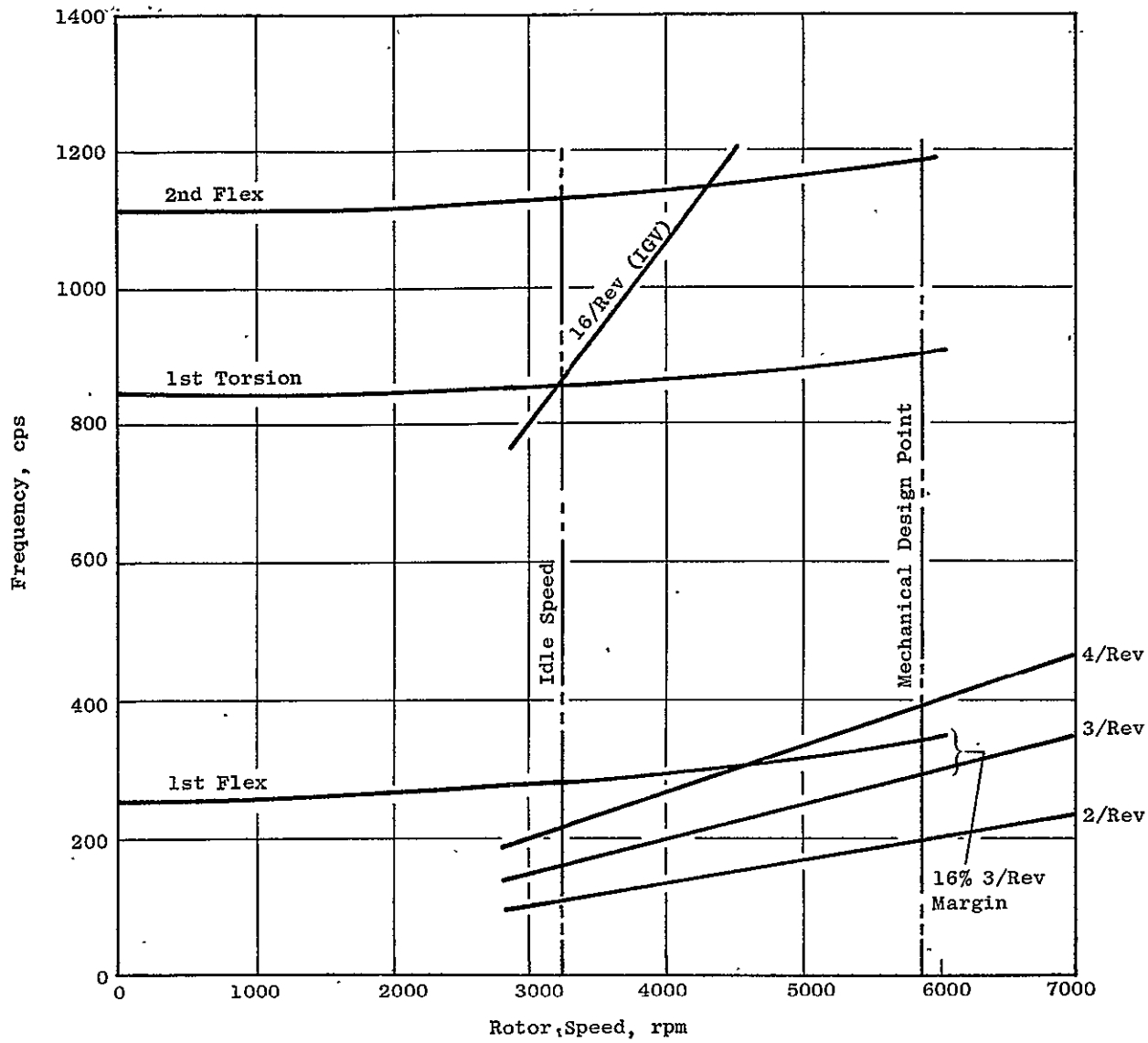

Figure 65. Front Block Fan Rotor Stage 2 Blade Campbell Diagram.

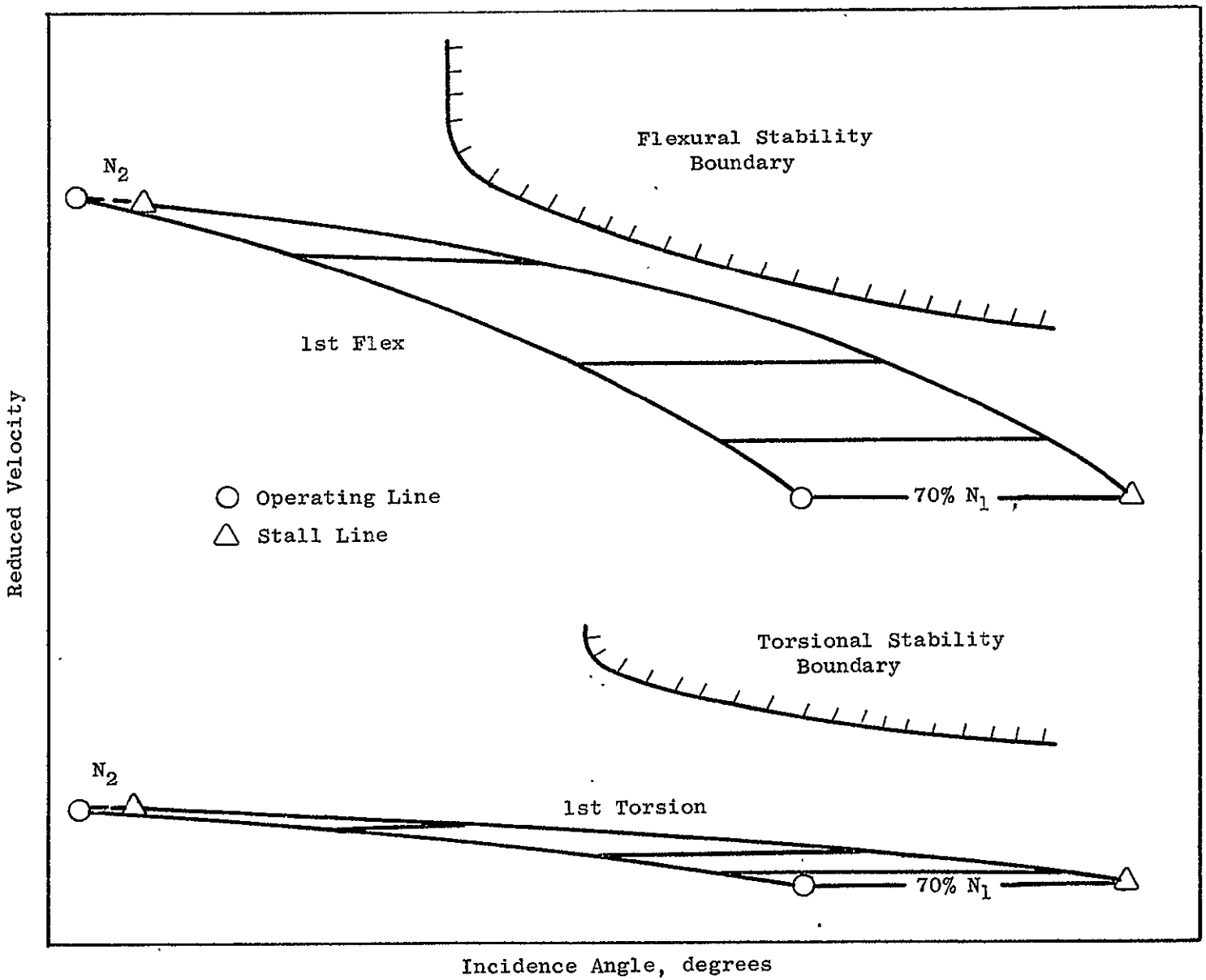

Figure 66. Front Block Fan Rotor Stage 1 Blade Stability Plot.

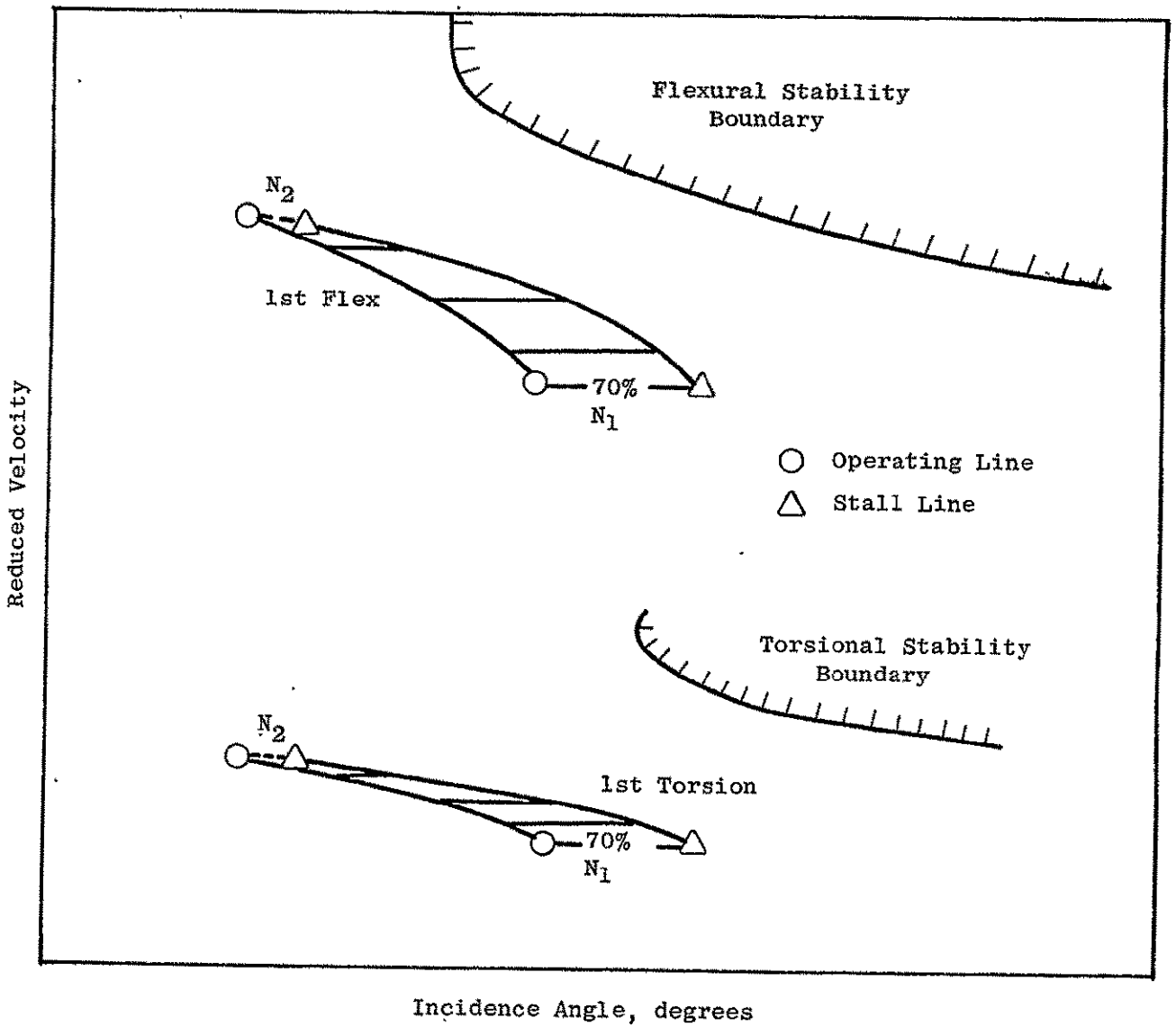

Figure 67. Front Block Fan Rotor Stage 2 Blade Stability Plot.

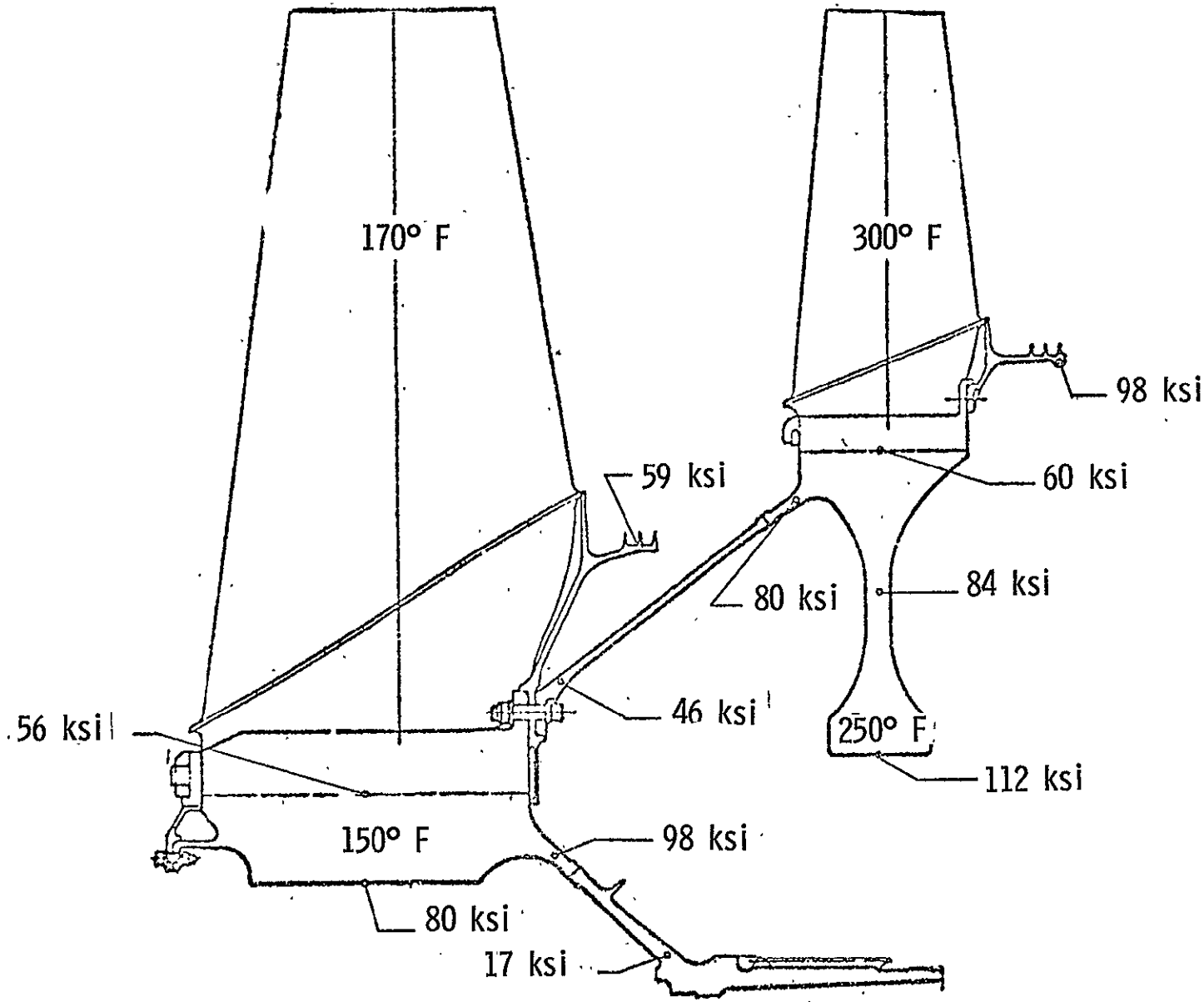

Figure 68. Front Block Fan Rotor Design Point Temperatures and Stresses.

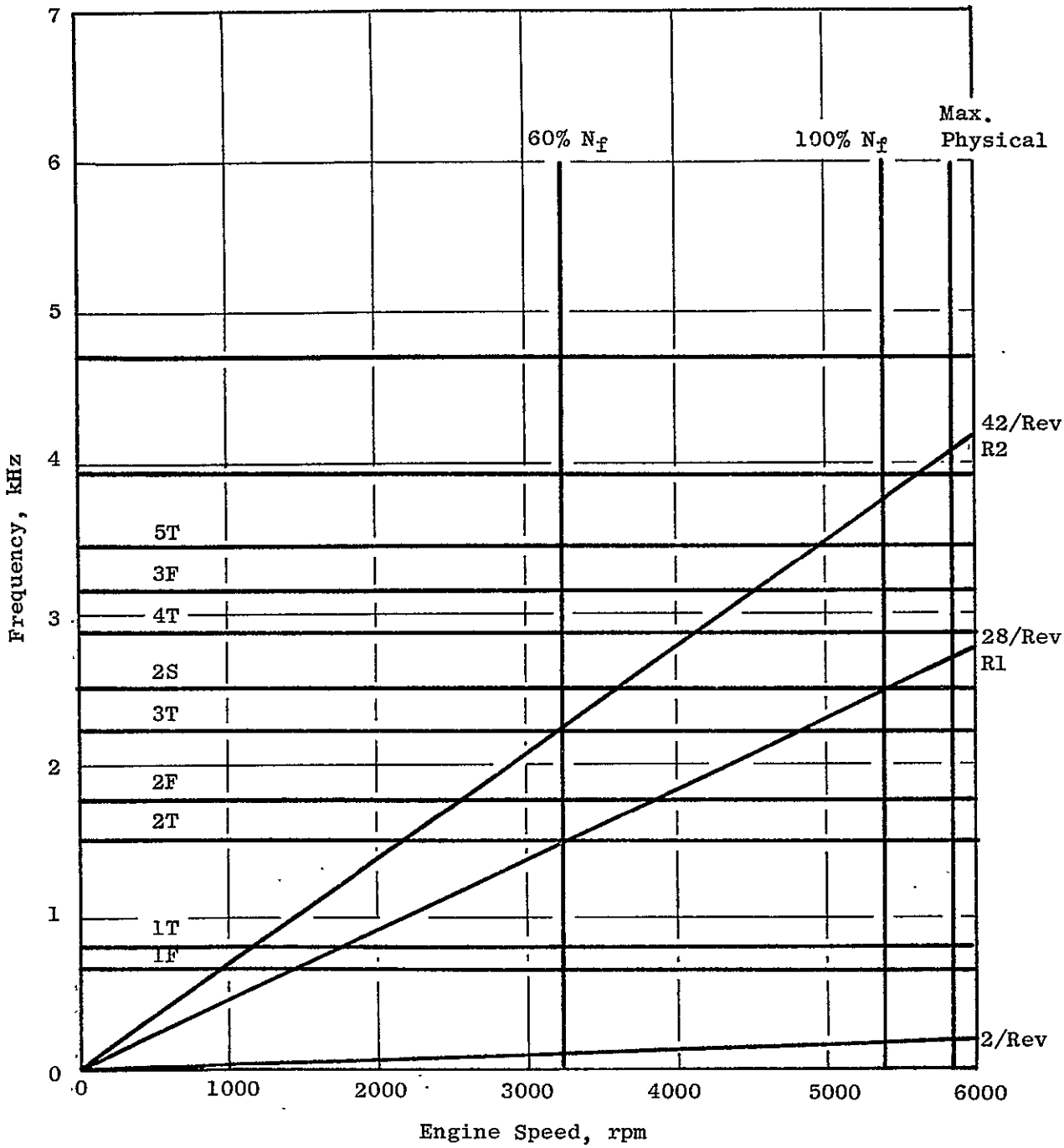

Figure 69. Front Block Fan Stator 1 Campbell Diagram - Full Size Fan, Solid Vane.

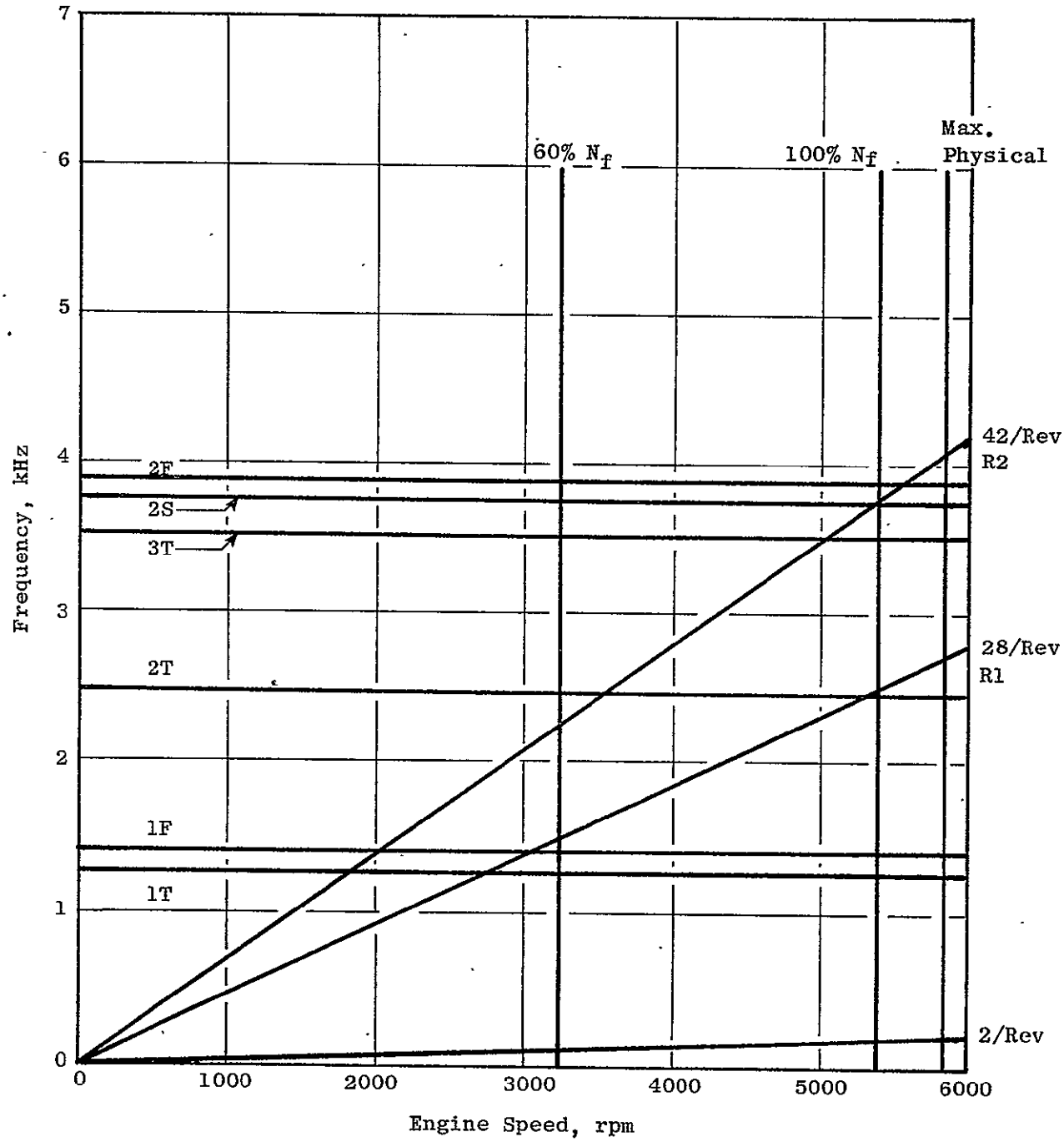

Figure 70. Front Block Fan Stator 2 Campbell Diagram - Full Size Fan, Solid Vane.

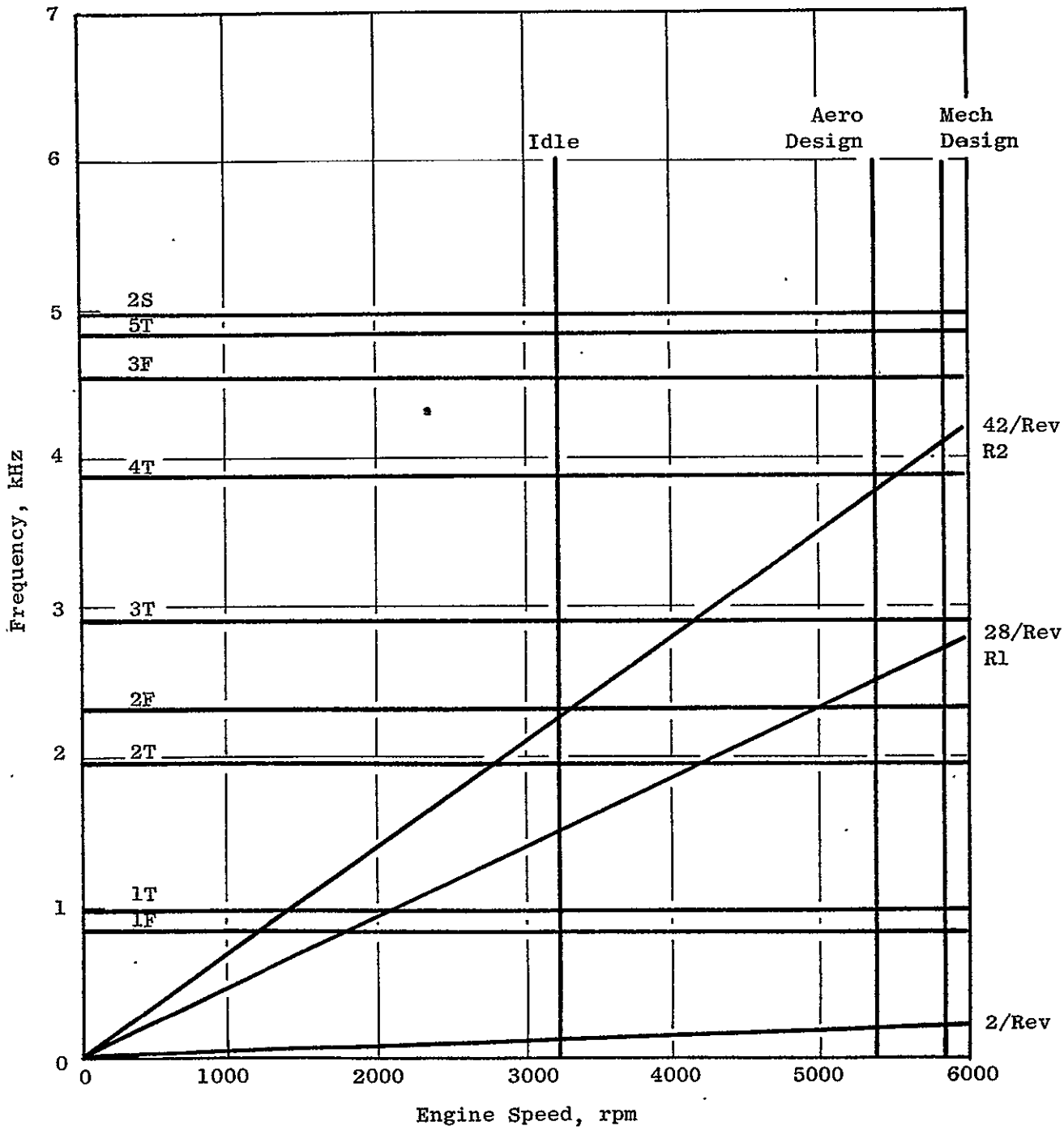

Figure 71. Front Block Fan Stator 1 Campbell Diagram - Full Size Fan, Hollow Vane.

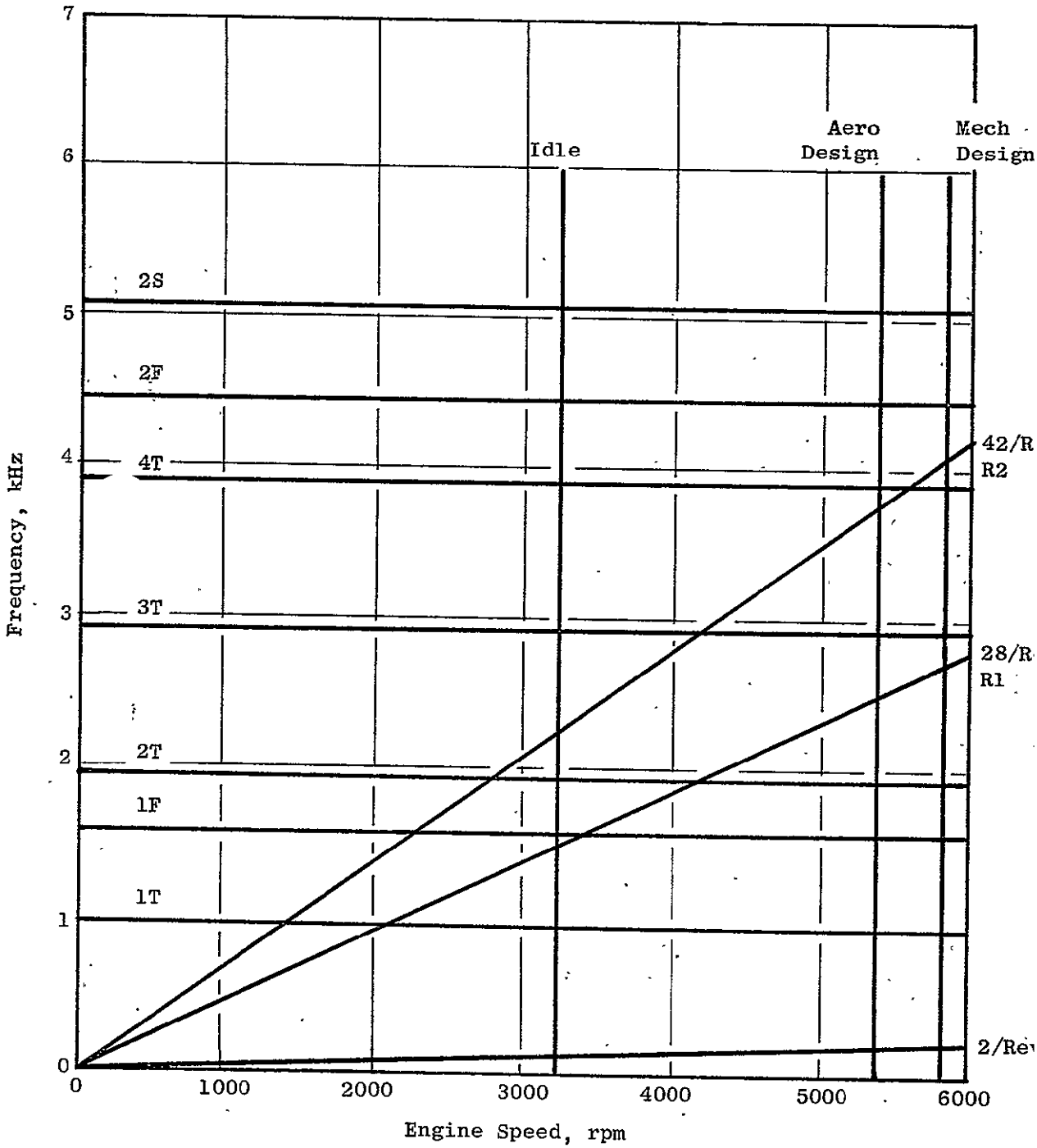

Figure 72. Front Block Fan Stator 2 Campbell Diagram - Full Size Fan, Hollow Vane.

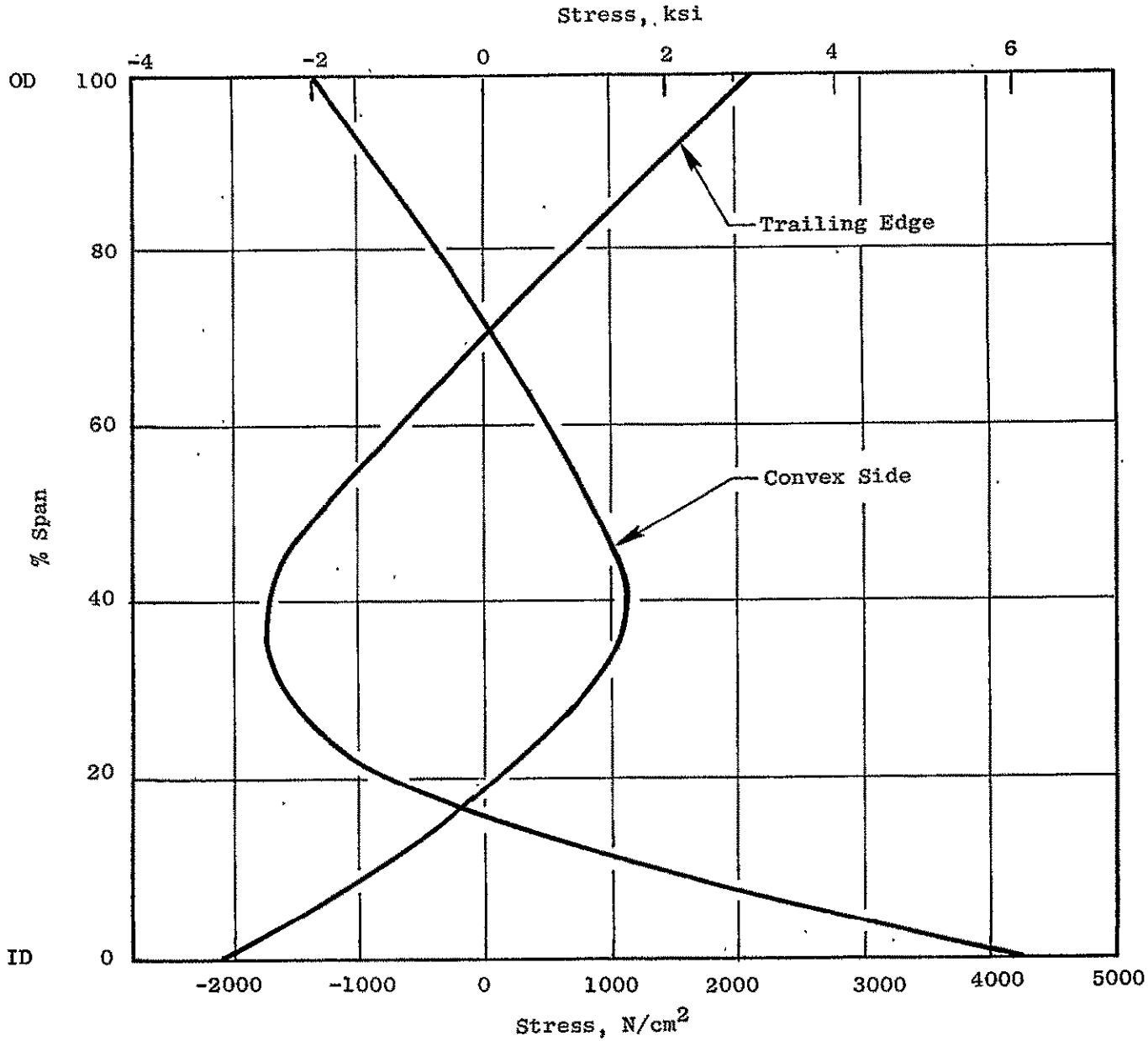

Figure 73. Front Block Fan Stator 1 Steady-State Stress.

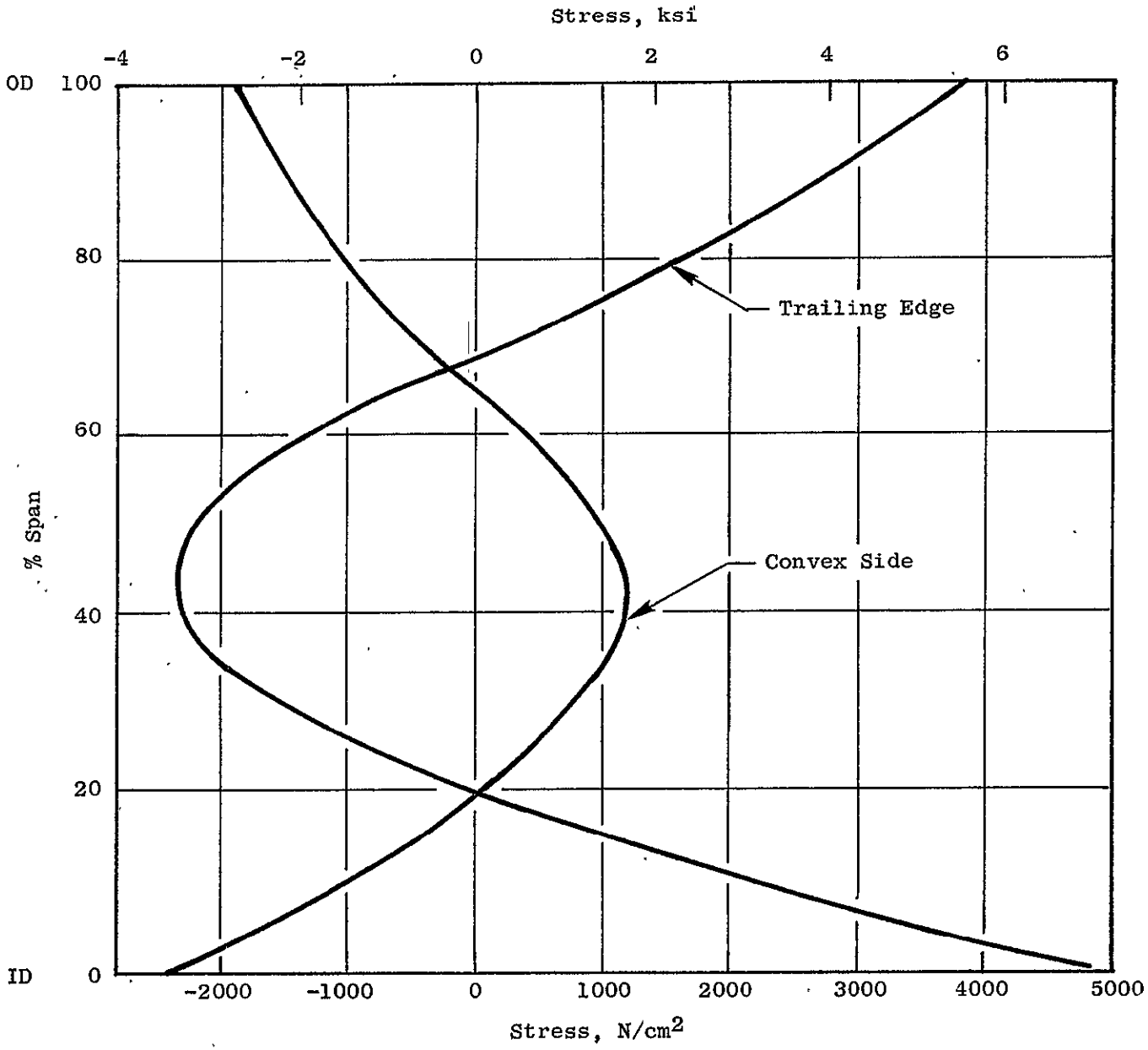

Figure 74. Front Block Fan Stator 2 Steady-State Stress.

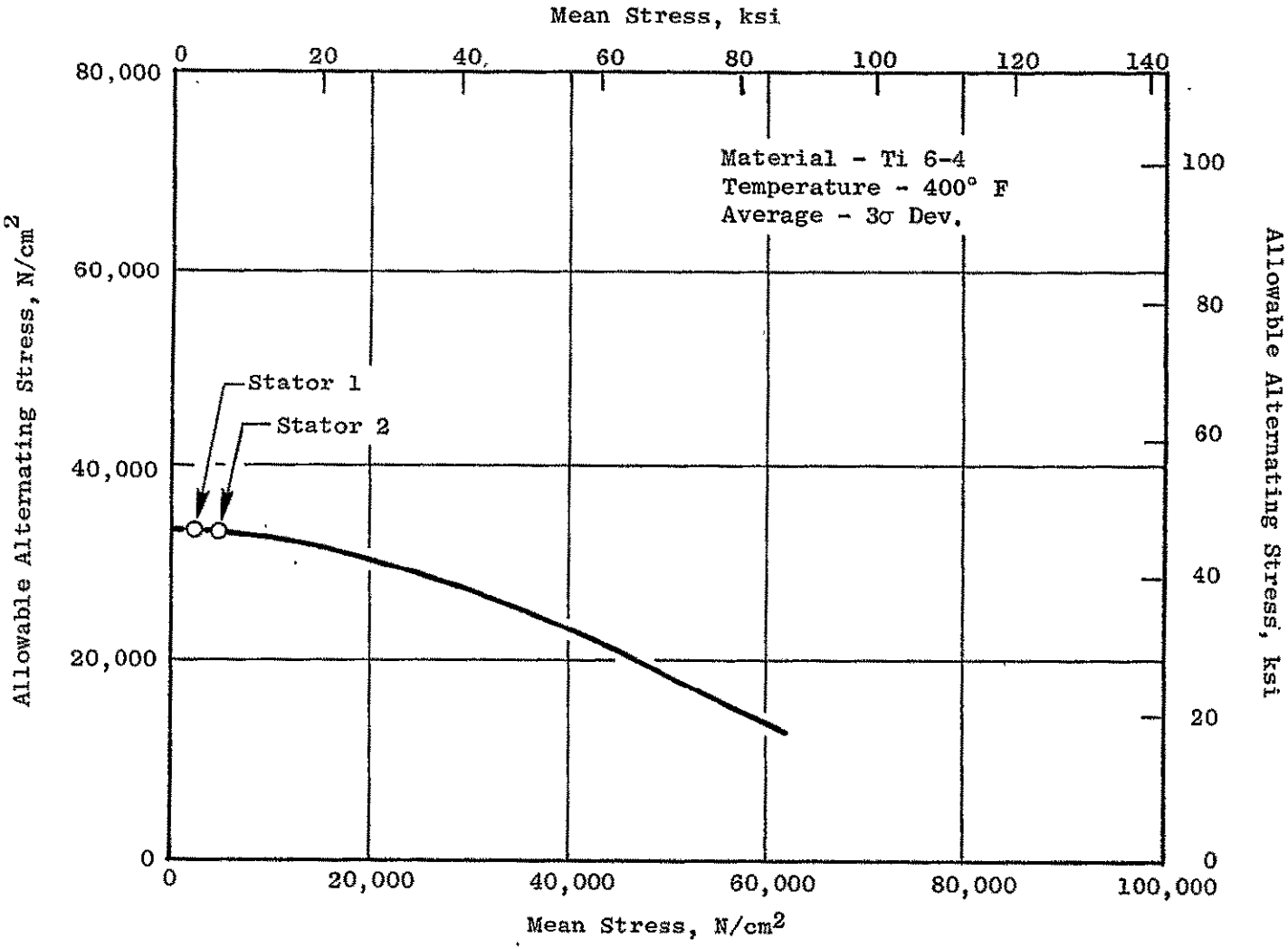

Figure 75. Front Block Fan Stator Fatigue Limit Diagram - Stators.

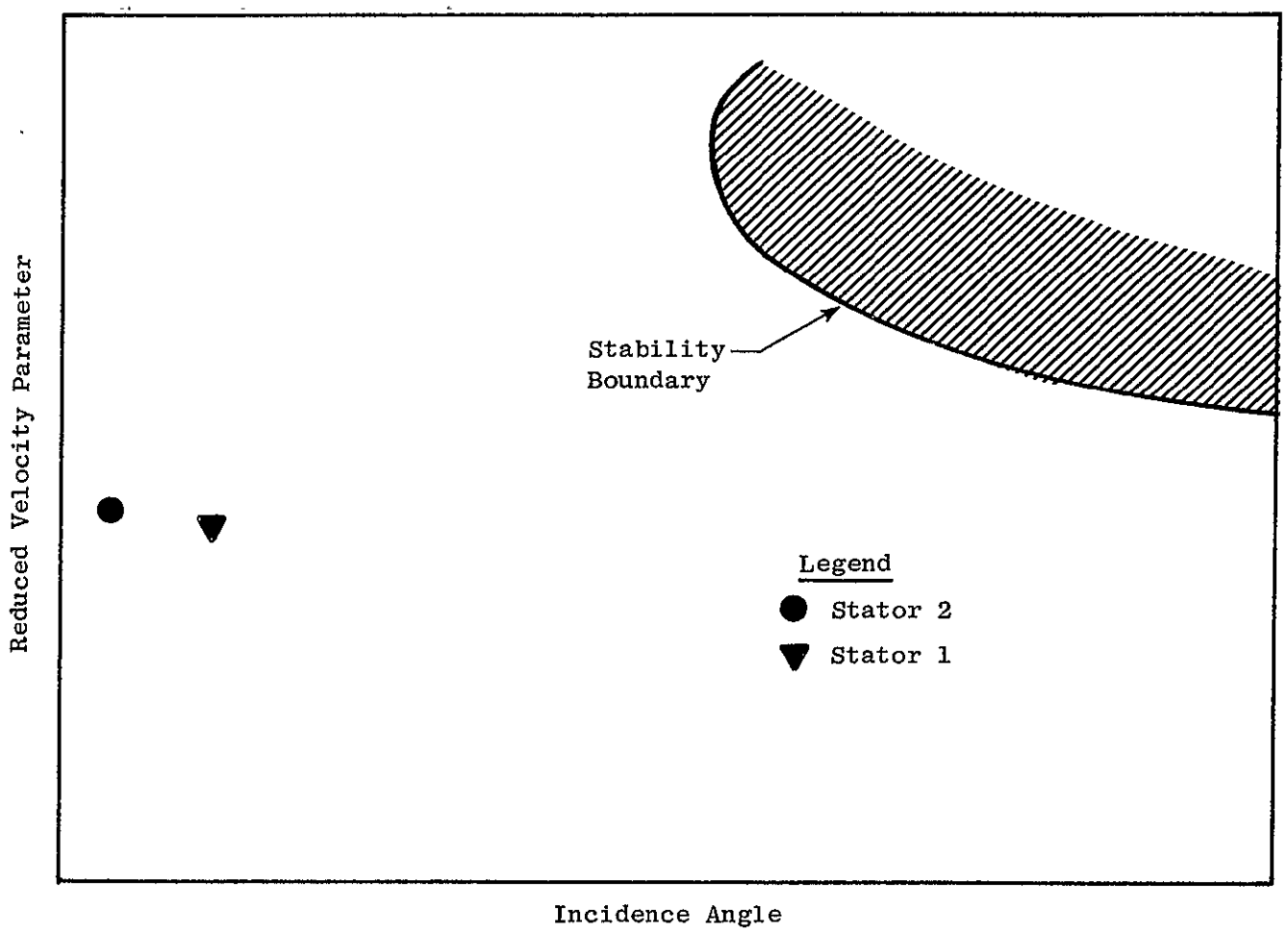

Figure 76. Front Block Fan Stator Torsional Stability Plot.

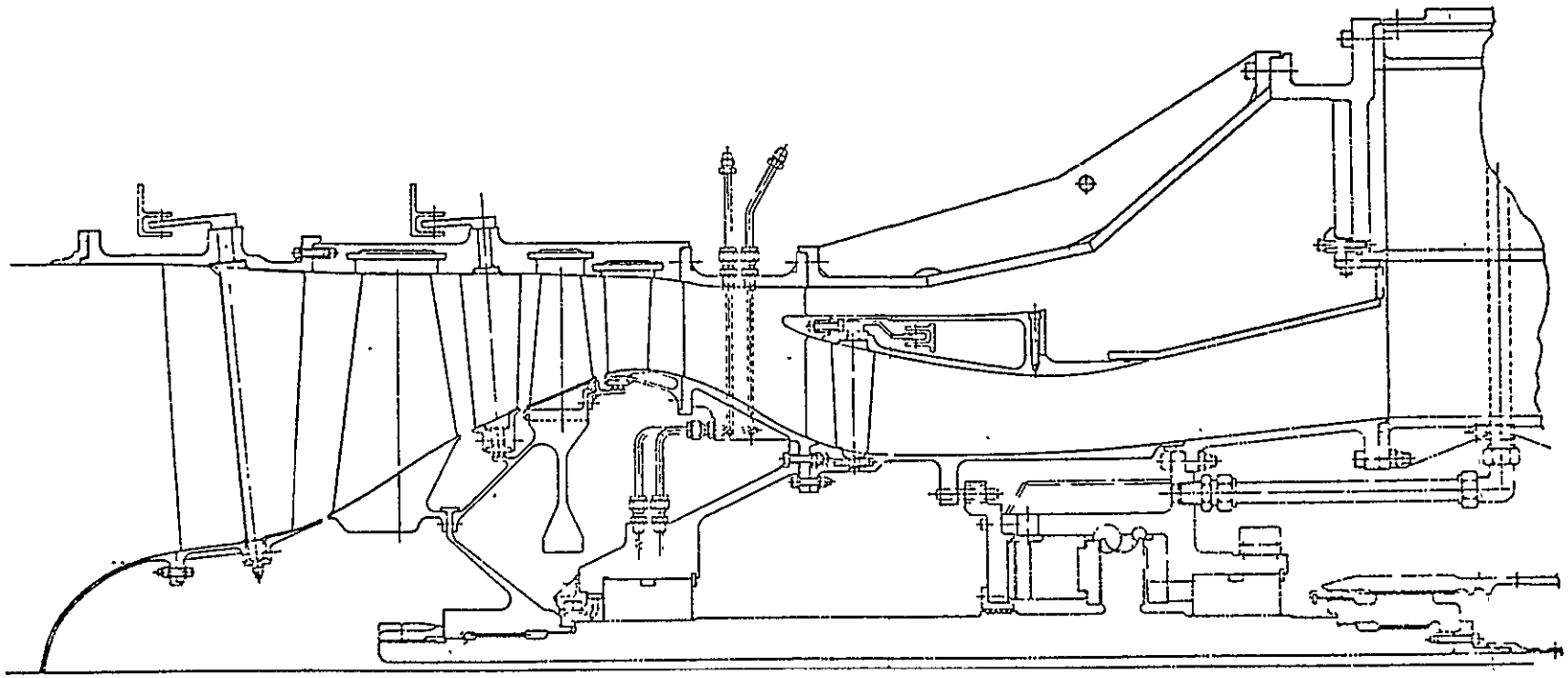

Figure 77. Front Block Fan Component Test Vehicle.

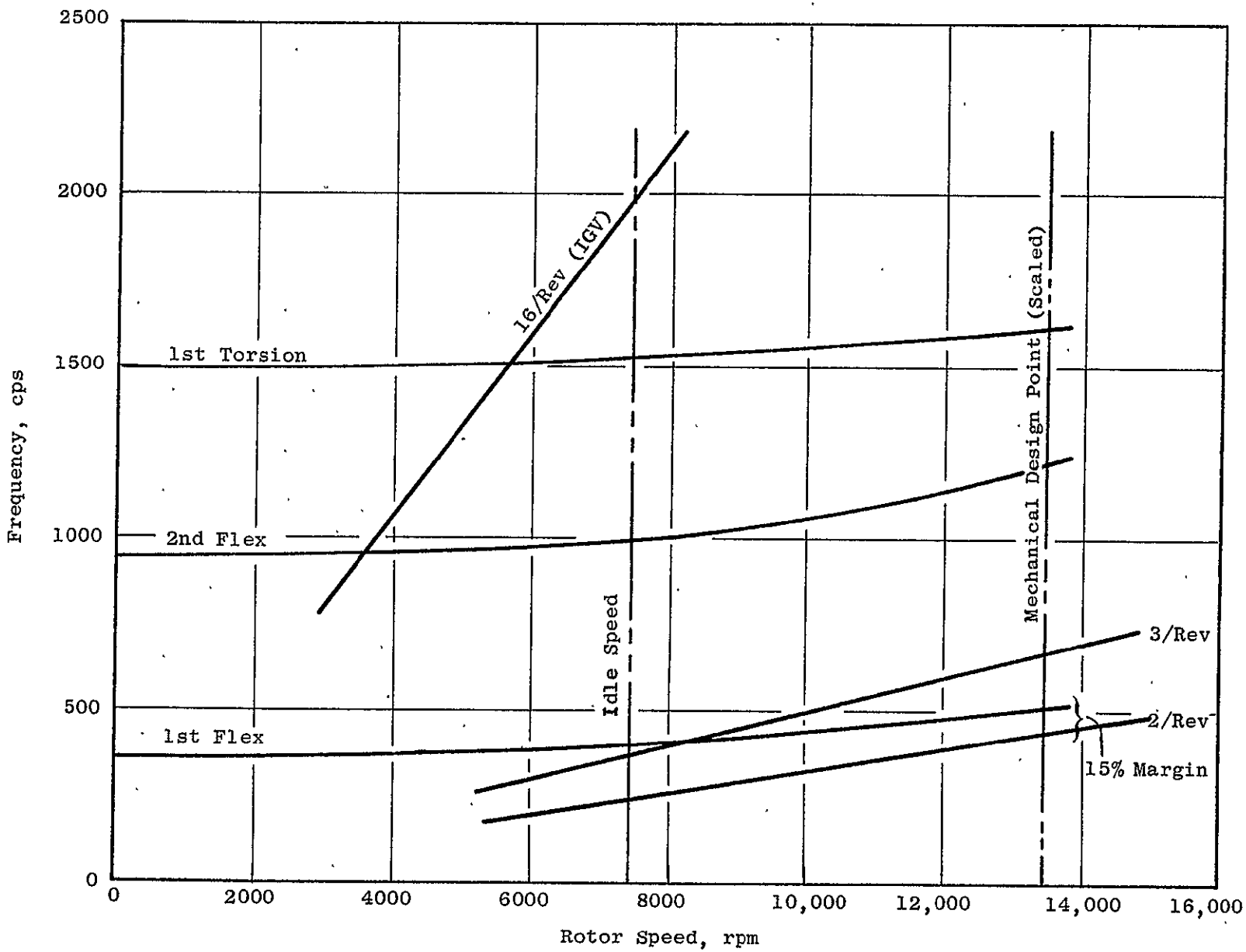

Figure 78. Front Block Fan Component Rotor 1 Campbell Diagram.

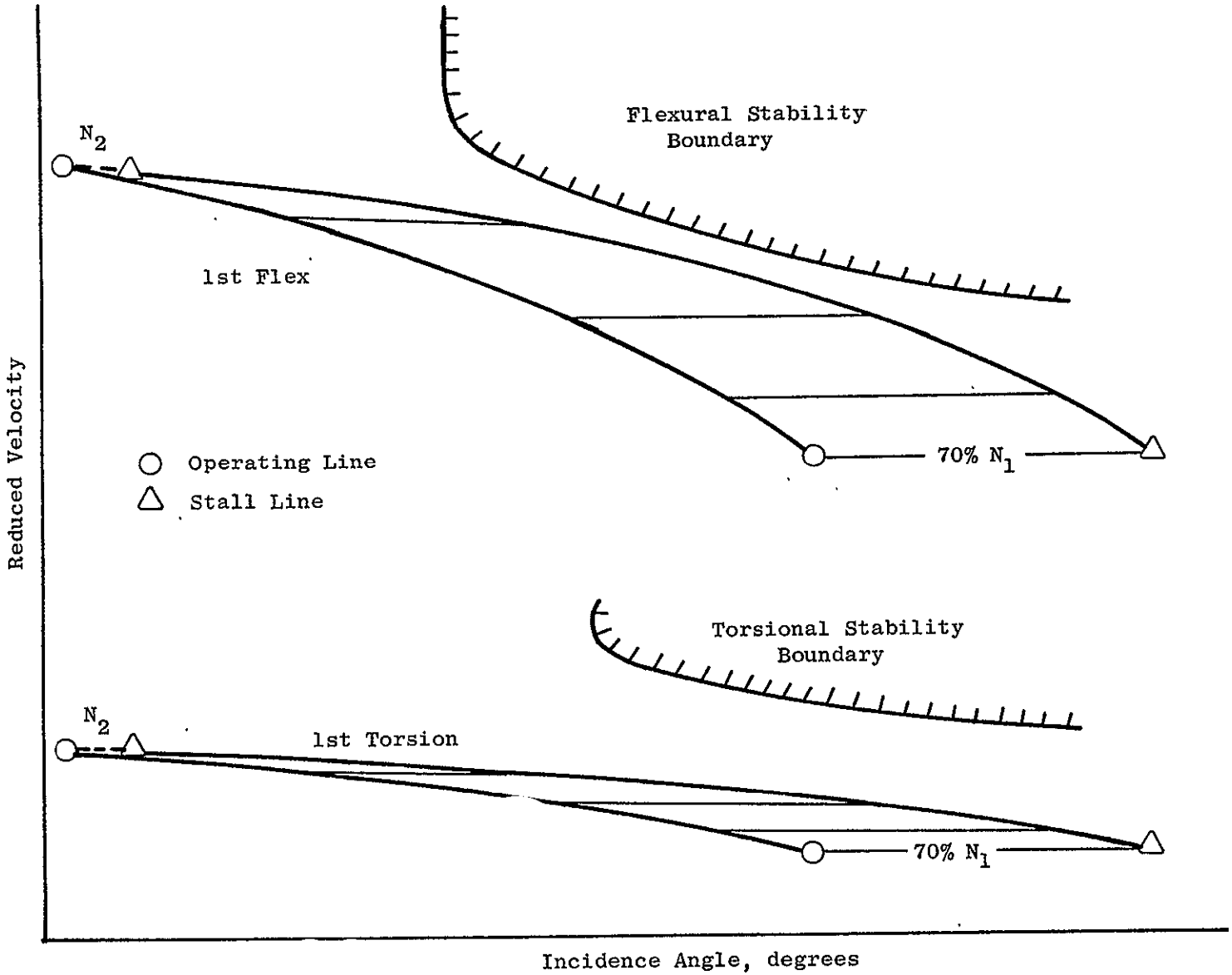

Figure 79. Front Block Fan Component Rotor 1 Stability Plot.

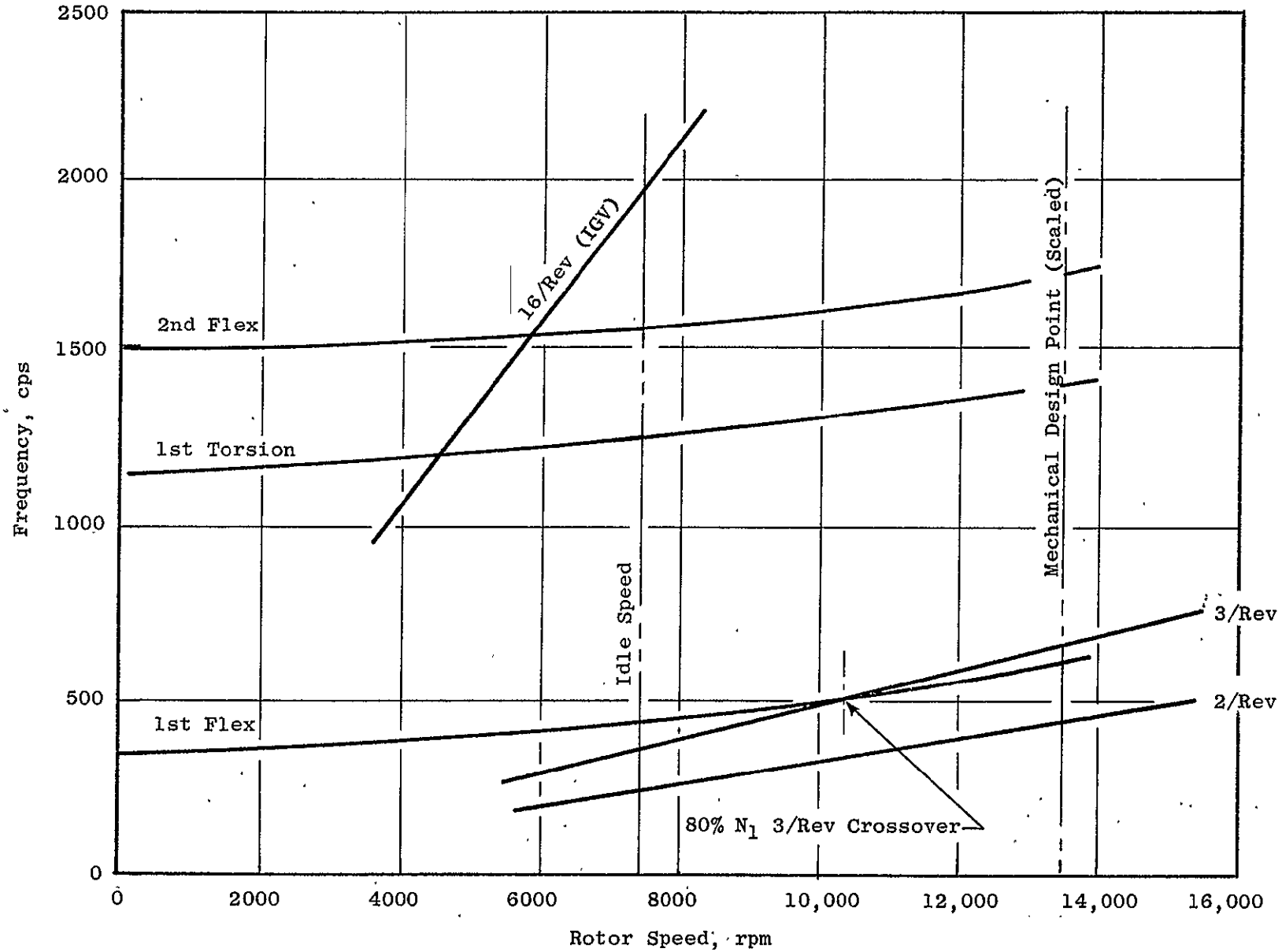

Figure 80. Front Block Fan Component Rotor 2 Campbell Diagram.

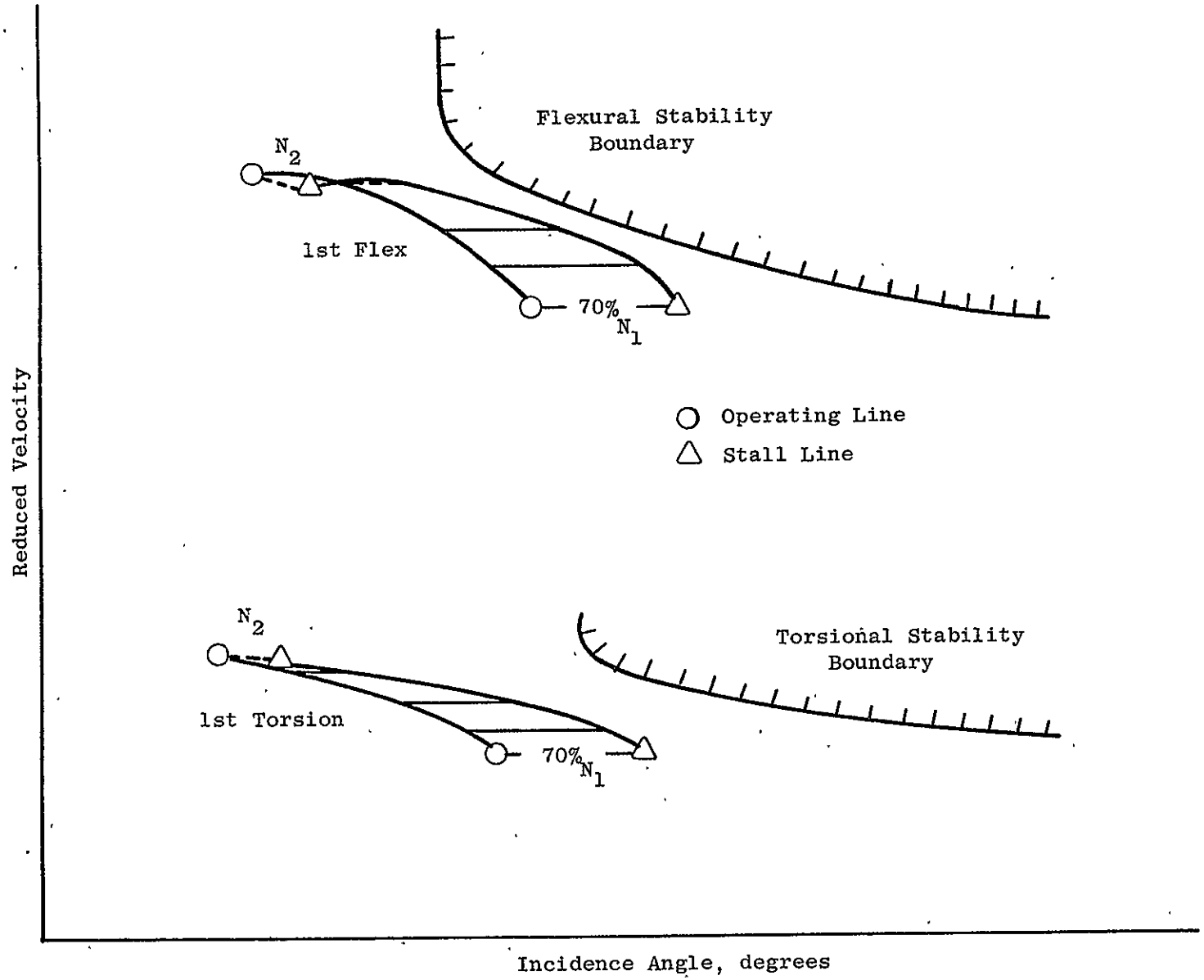

Figure 81. Front Block Fan Component Rotor 2 Stability Plot.

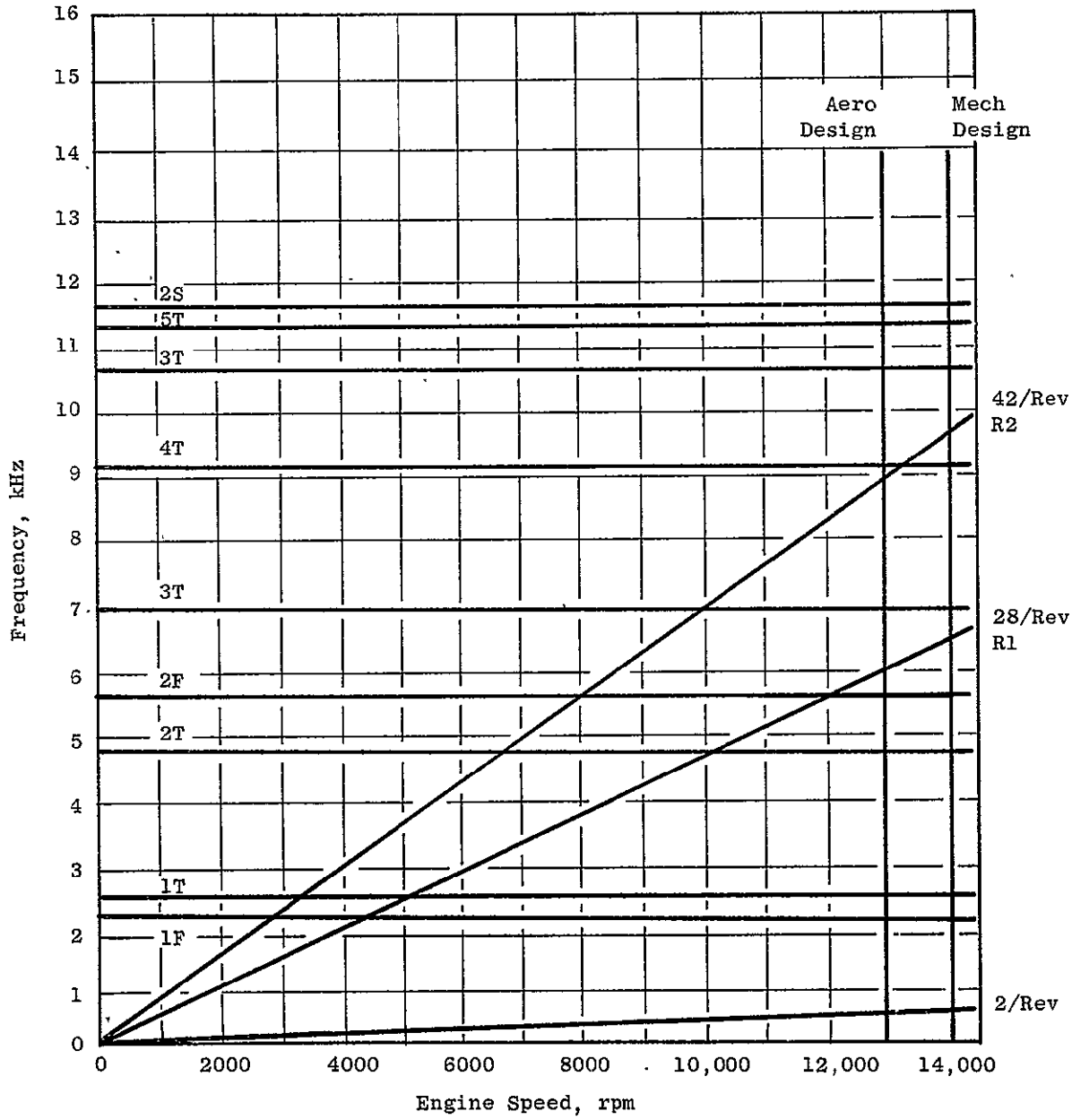
Frequency, kHz
16
15
14
13
12
11
10
9
8
7
6
5
4
3
2
1
0
Aero Design
Mech Design
2S
5T
3T
4T
3T
2F
2T
1T
1F
42/Rev R2
28/Rev R1
2/Rev
0
2000
4000
6000
8000
10,000
12,000
14,000
Engine Speed, rpm

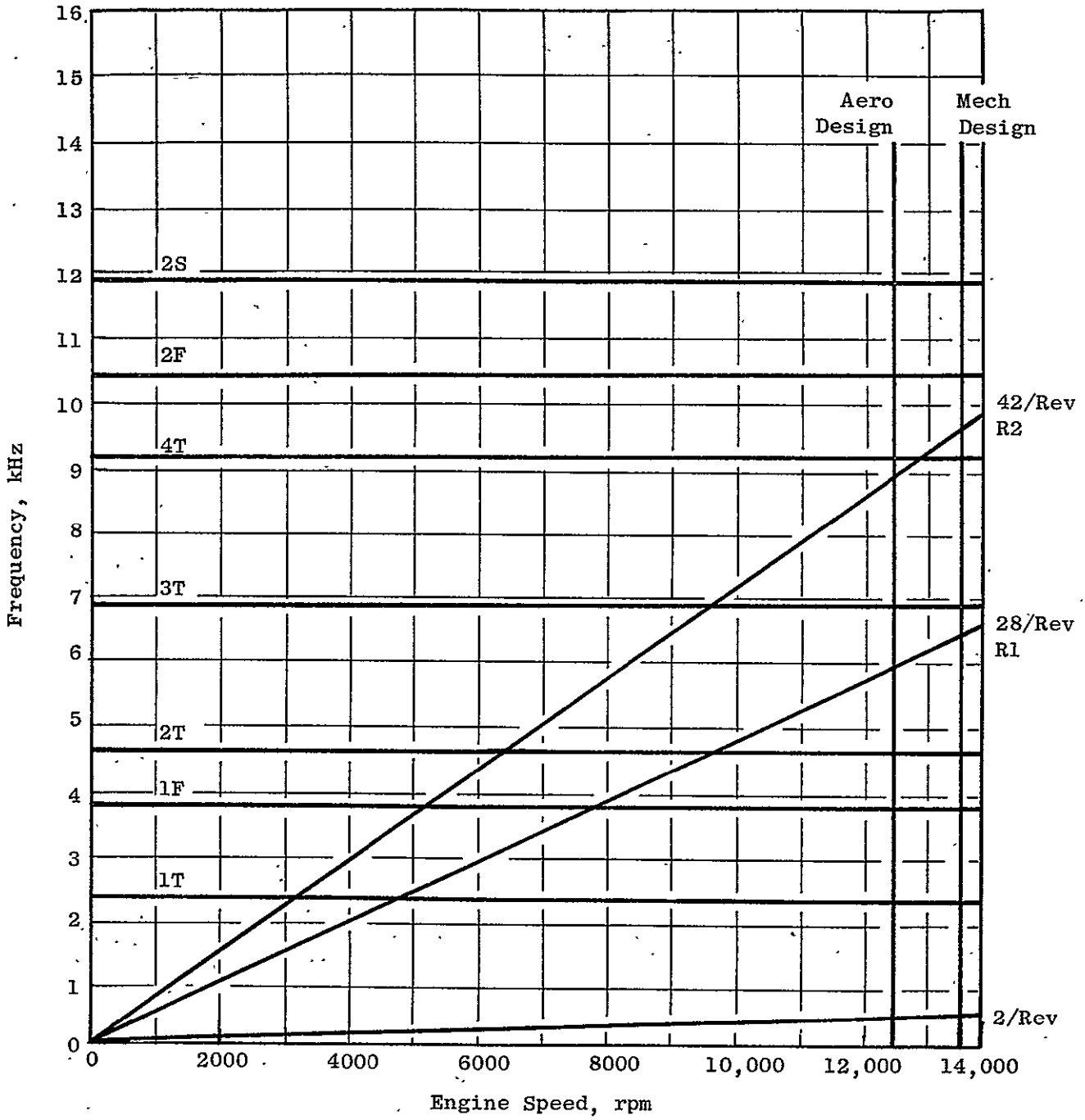

Figure 83. Front Block Fan Component Stator 2 Campbell Diagram.

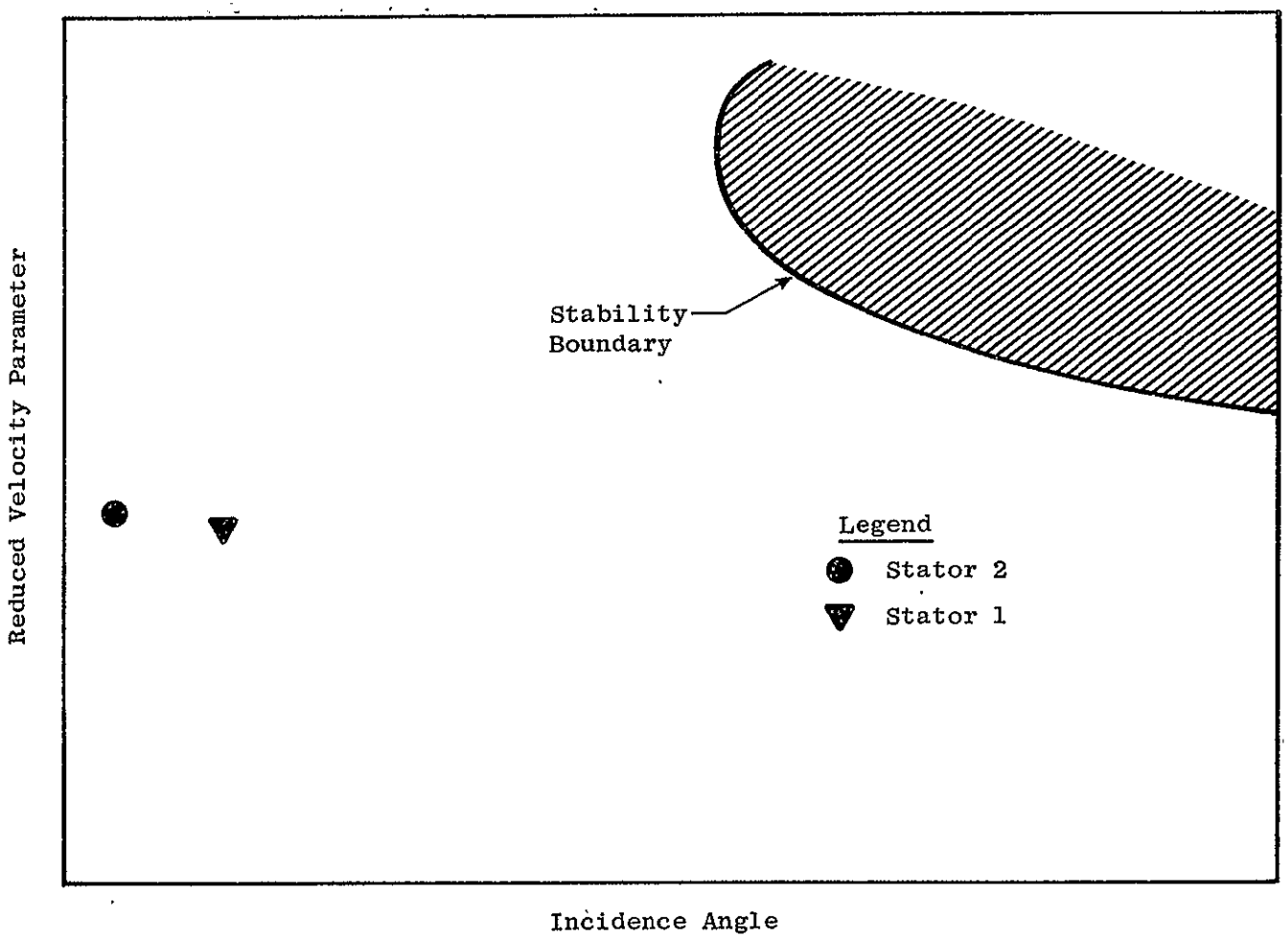

Figure 84. Front Block Fan Component Stator Torsional Stability Plot.

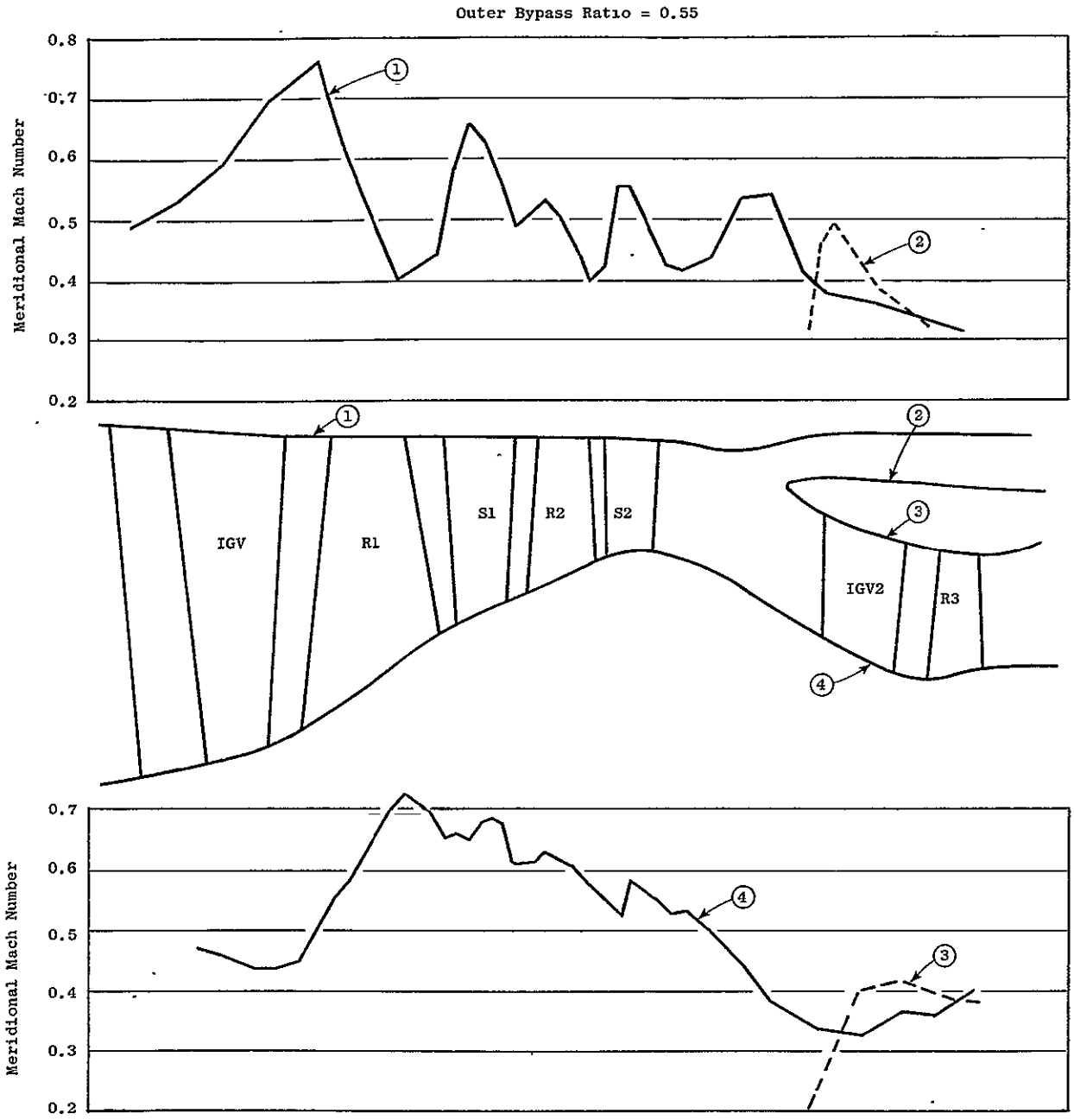

Figure 85. AST Flowpath Wall Meridional Mach Number Distribution - Front Block Fan Design Point.

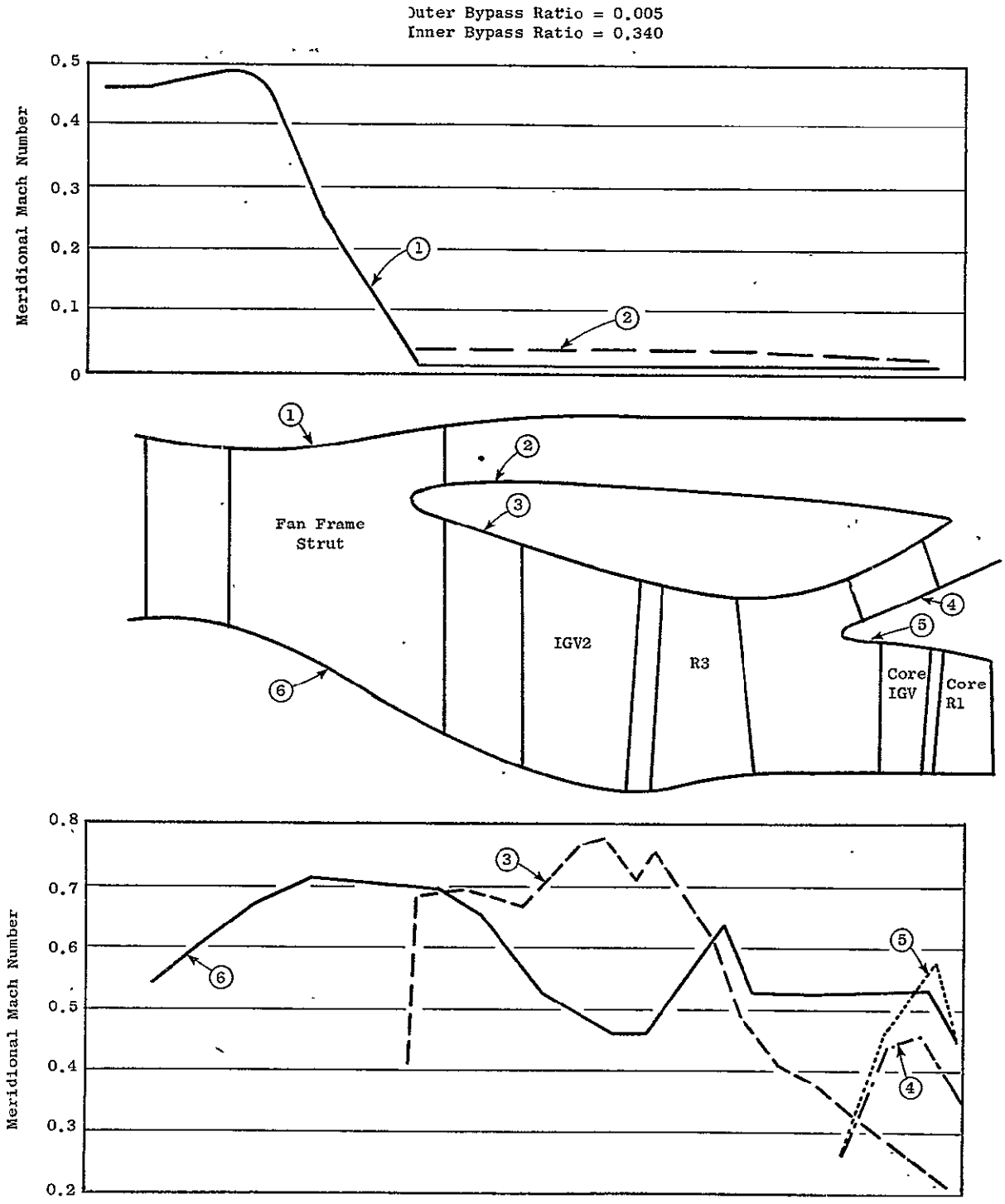

Figure 86. AST Flowpath Wall Meridional Mach Number Distribution - Rear Block Fan Design Point.

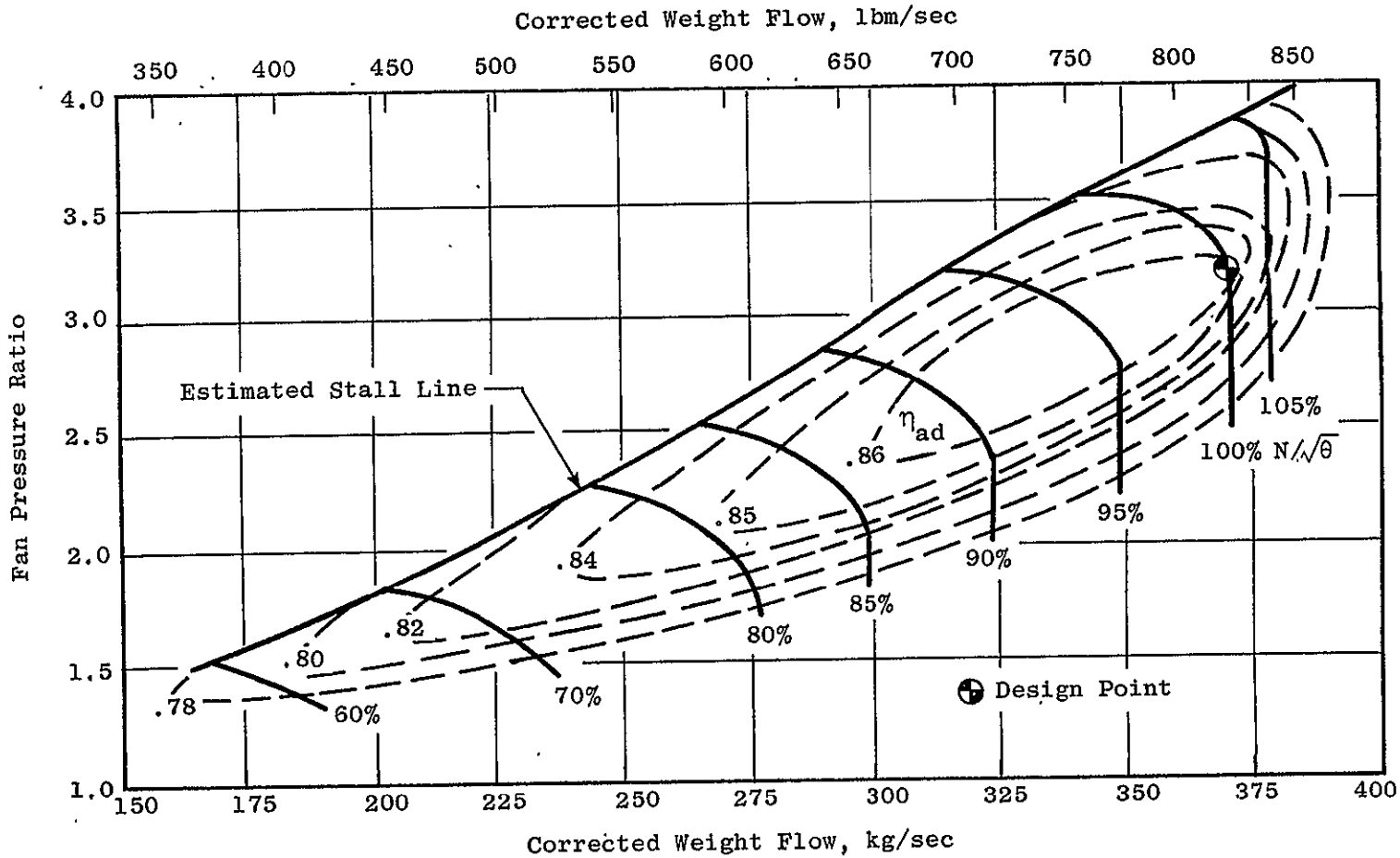

Figure 87. Front Block Fan Performance Map - Design Stator Settings.

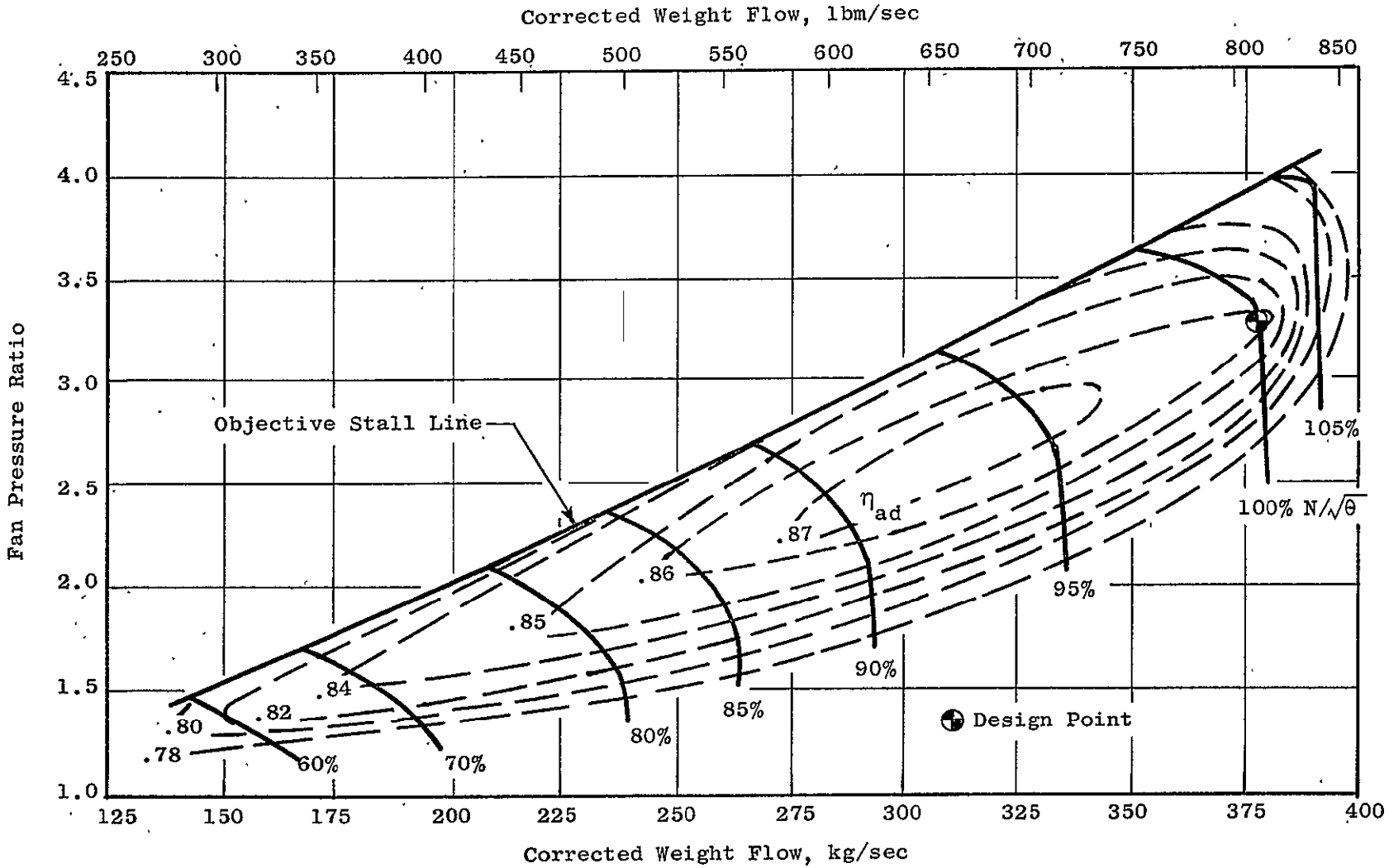

Figure 88. Front Block Fan Performance Map - Variable IGV and Stator 1.

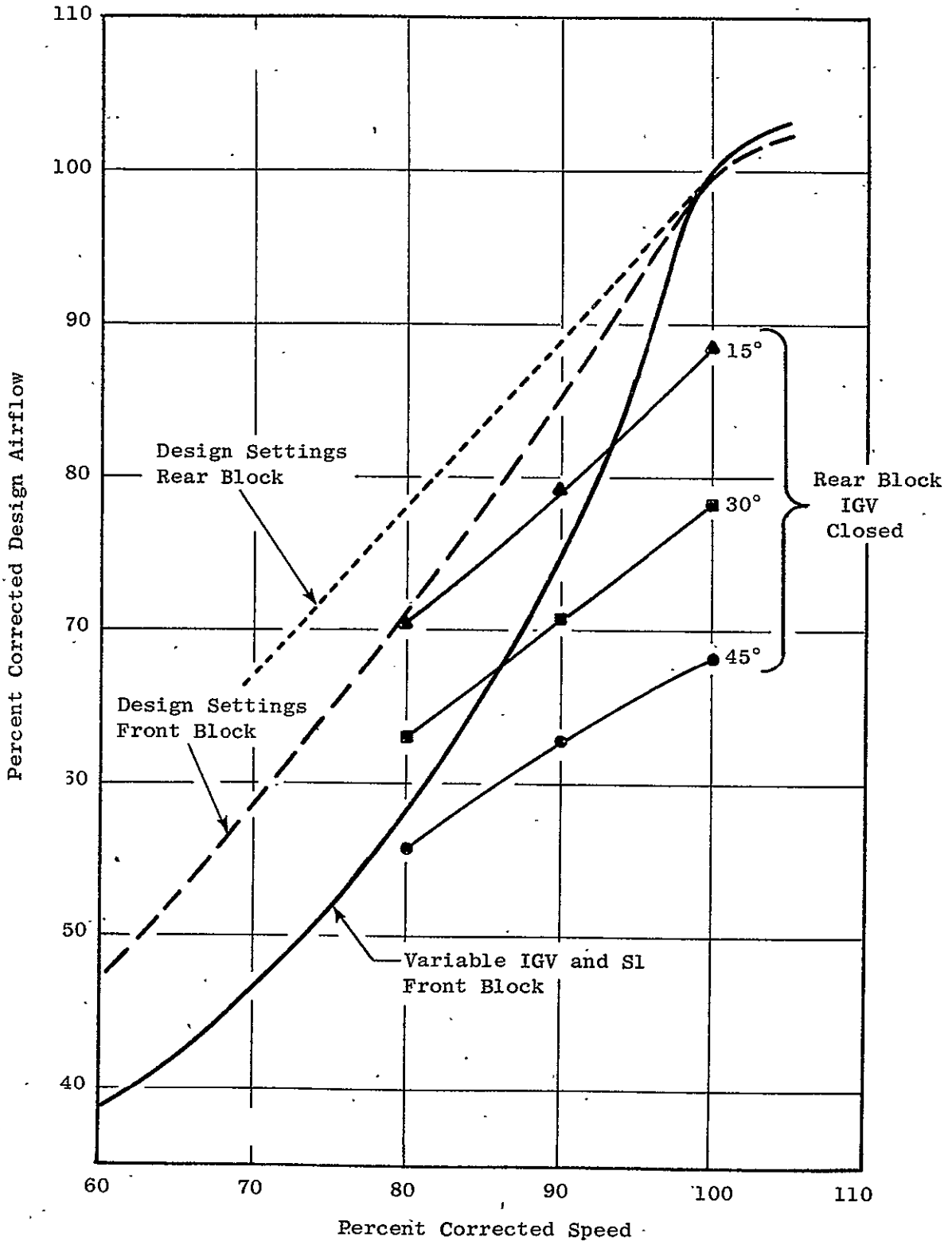

Figure 89. Front and Rear Block Fan Speed - Flow Relationships.

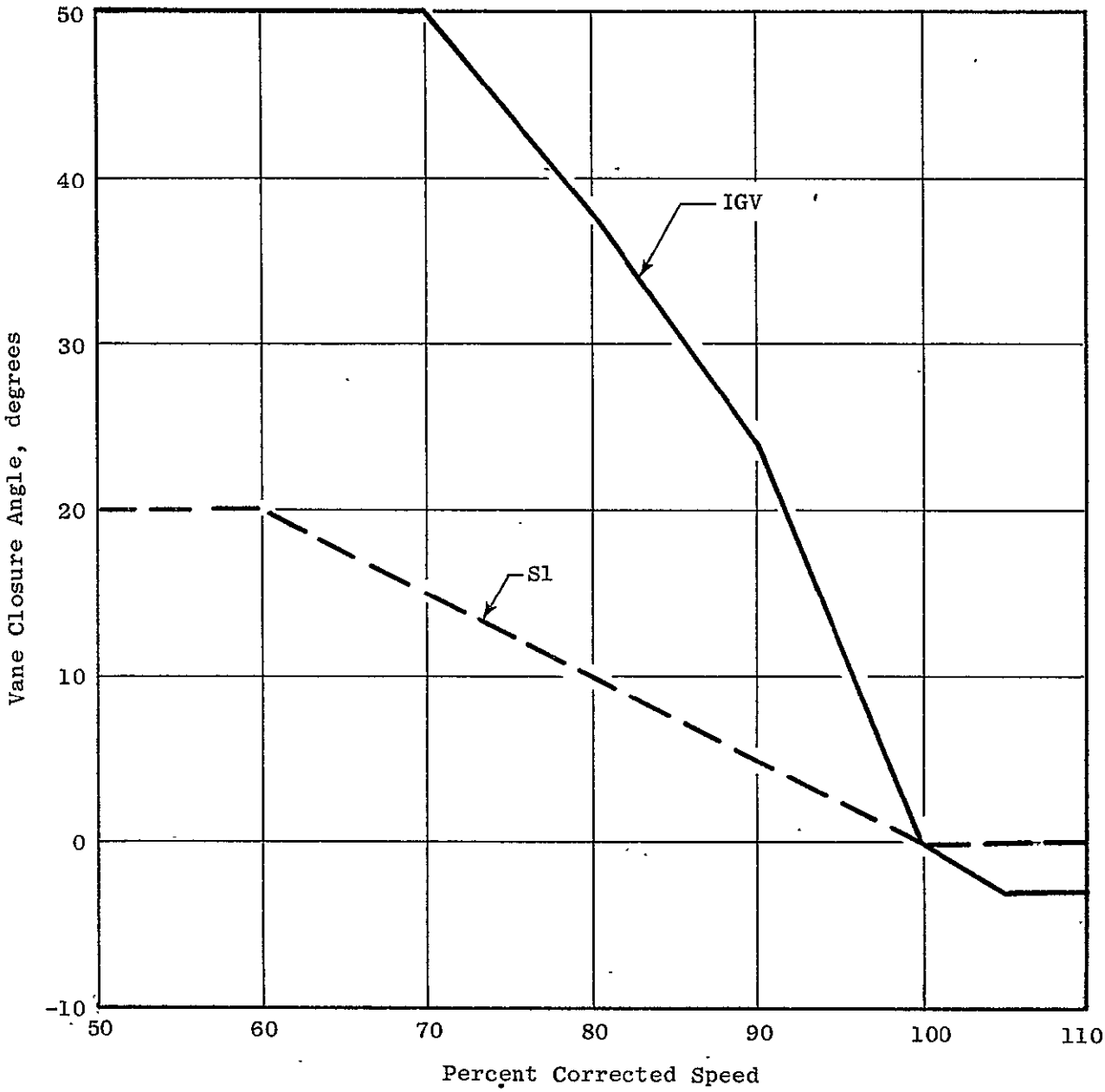

Figure 90. Front Block Fan Stator Schedule.

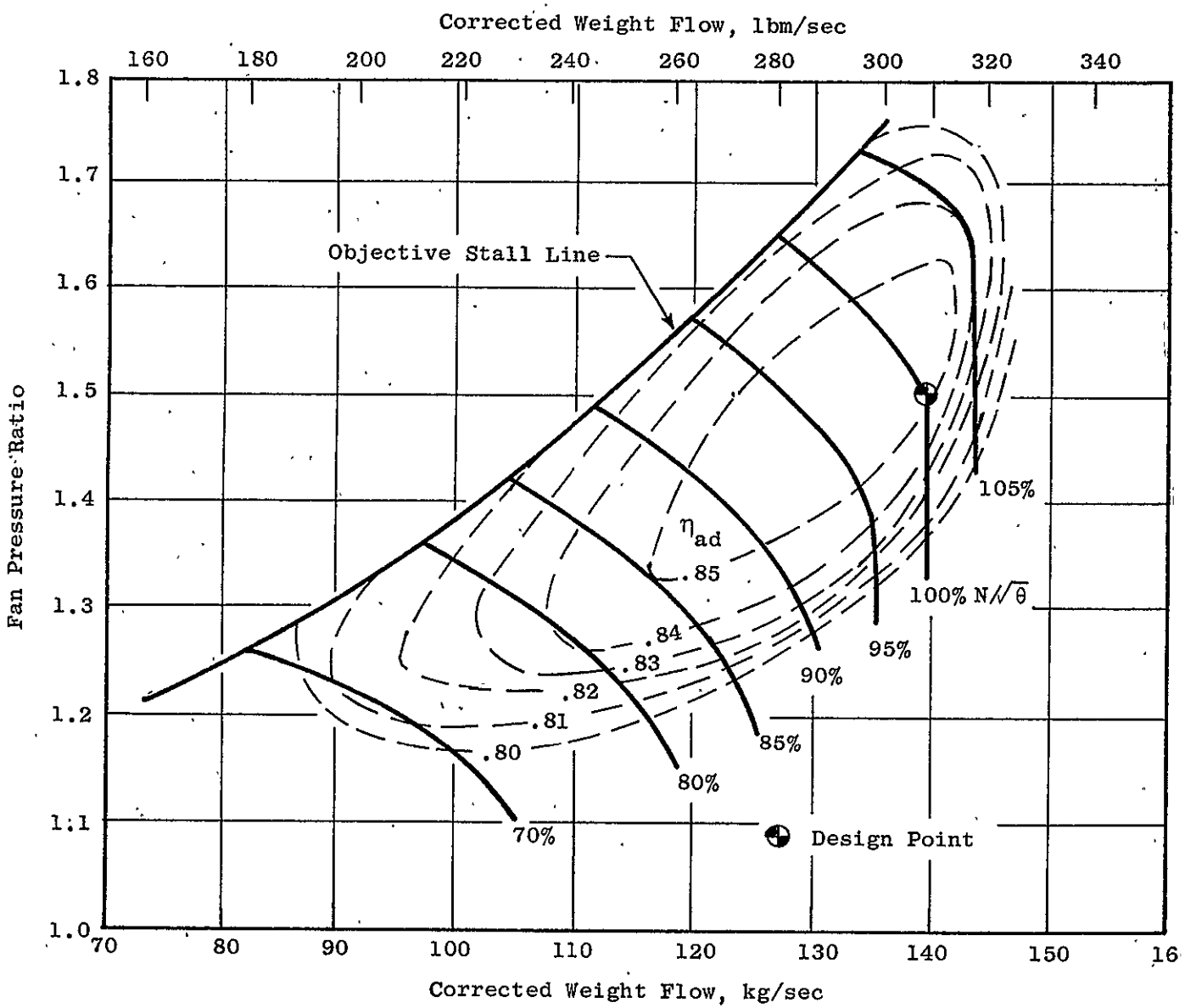

Figure 91. Rear Block Fan Performance Map - Design IGV Settings.

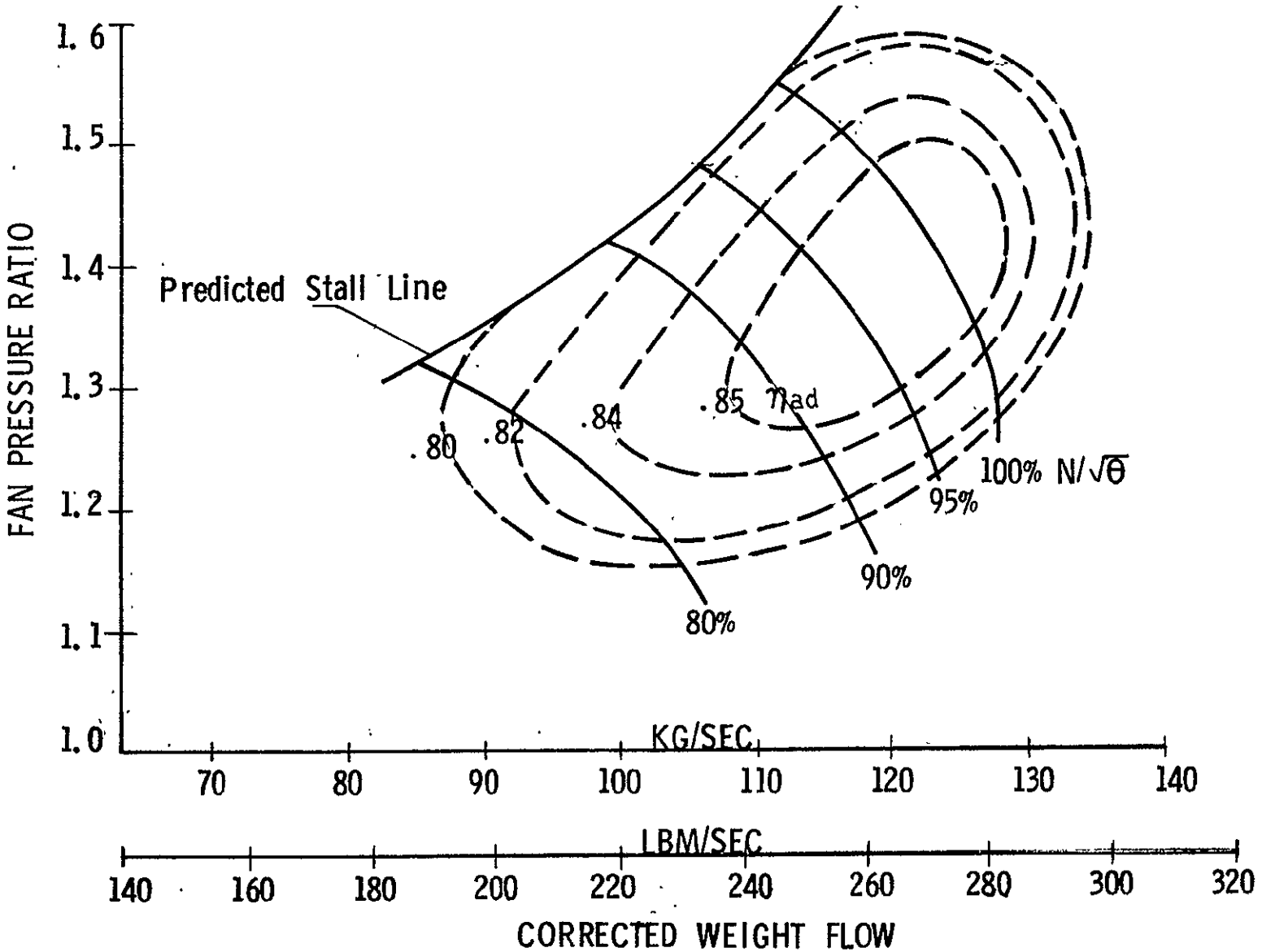

Figure 92. Rear Block Fan Performance Map - IGV Closed 15°.

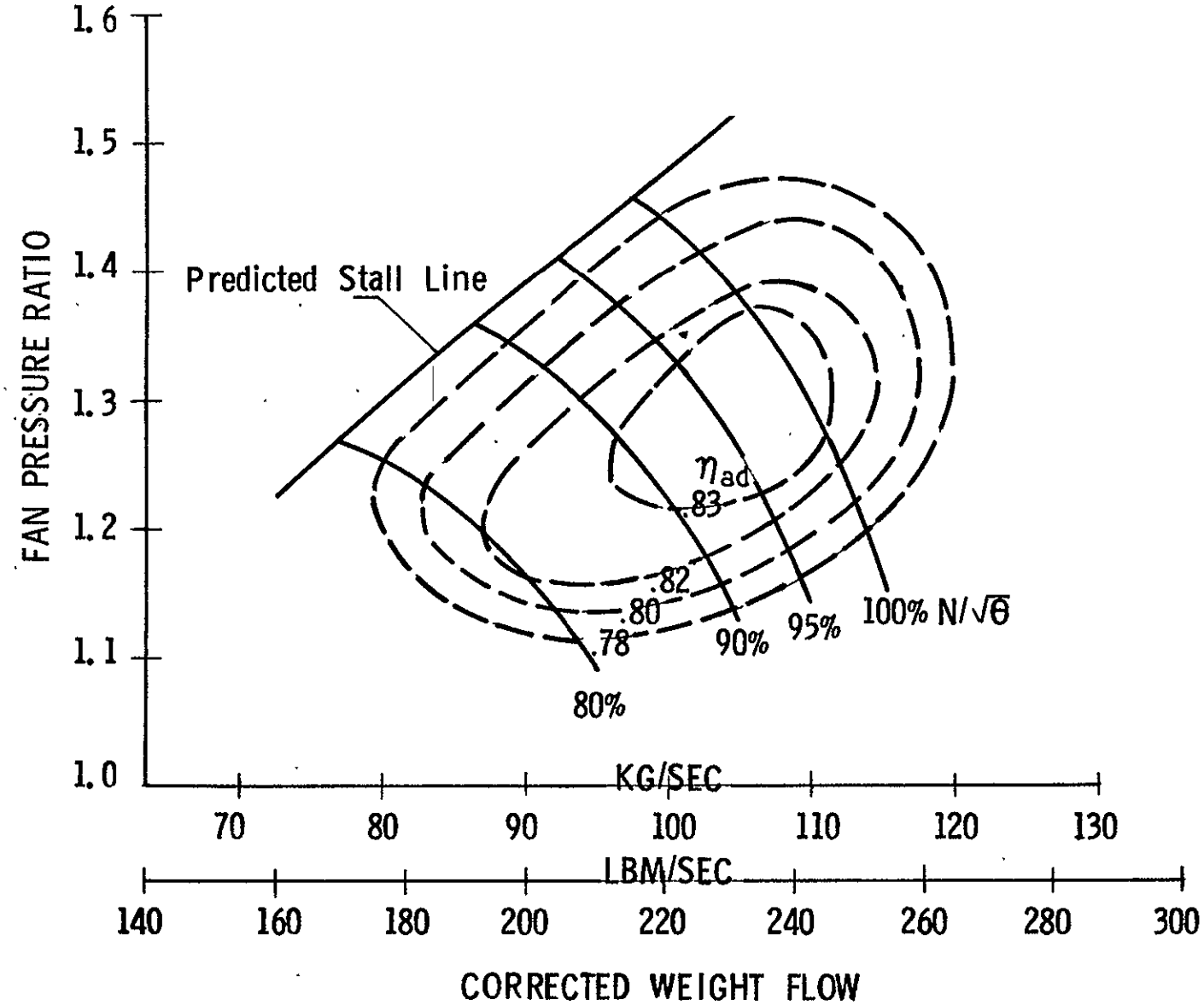

Figure 93. Rear Block Fan Performance Map - IGV Closed 30°.

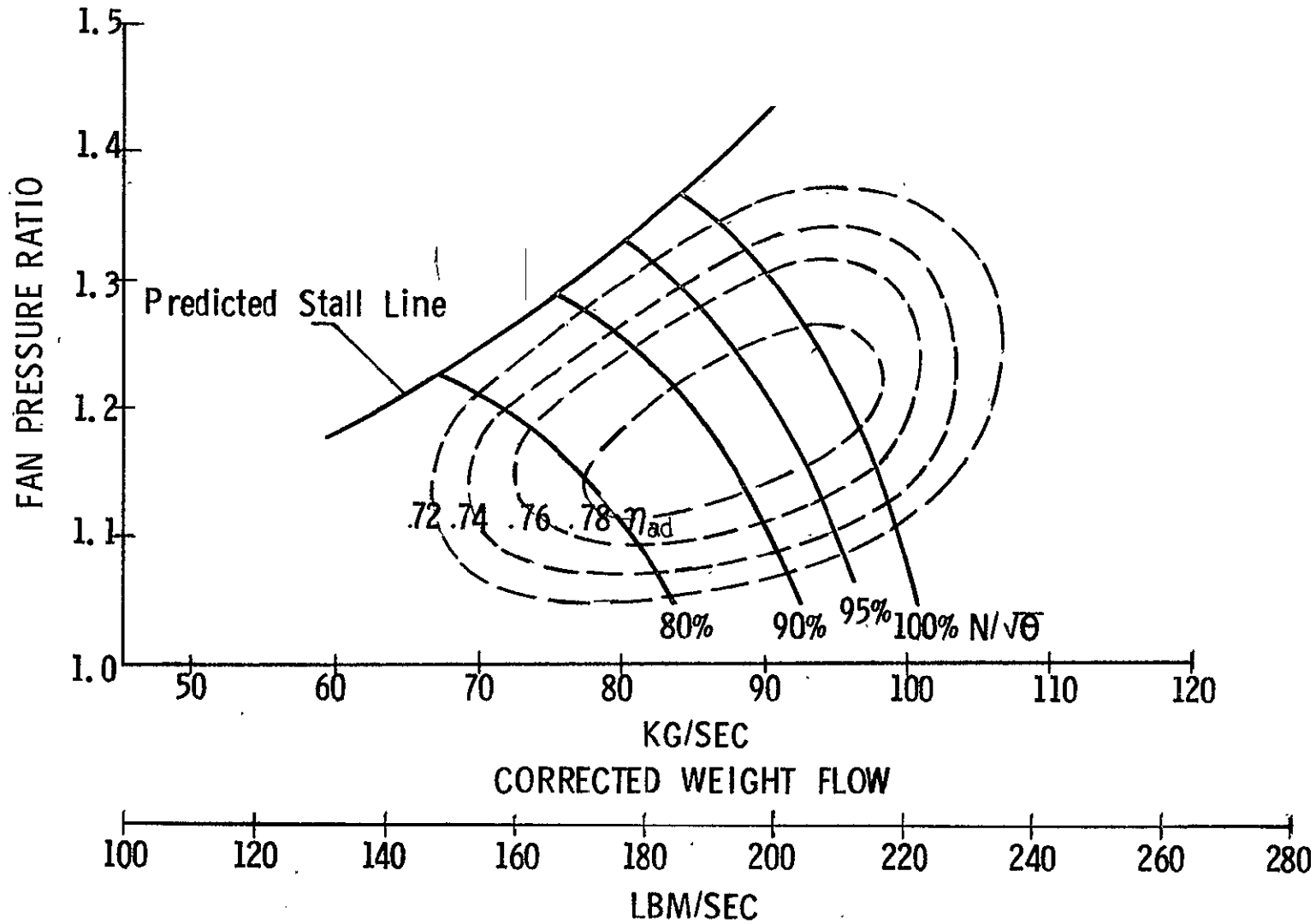

Figure 94. Rear Block Fan Performance Map - IGV Closed 45°.

GENERAL ELECTRIC COMPANY, CONTRACT NAS3-20041

FINAL REPORT, CR-159545

REPORT DISTRIBUTION LIST

1. NASA-Lewis Research Center
   21000 Brookpark Road
   Cleveland, OH 44135
   Attn:

Report Control Office	M.S. 5-5	1
Technical Utilization Office	M.S. 3-19	1
Library	M.S. 60-3	2
Fluid System Components Division	M.S. 5-3	1
Compressor Branch	M.S. 5-9	5
C. L. Ball	M.S. 5-9	1
W. R. Britsch	M.S. 301-2	1
J. E. Dilley	M.S. 500-305	1
C. E. Feiler	M.S. 500-208	1
T. F. Gelder	M.S. 5-9	1
R. D. Hager	M.S. 301-2	1
M. J. Hartmann	M.S. 5-9	1
C. H. Hauser	M.S. 5-9	1
L. J. Herrig	M.S. 5-9	1
A. G. Powers	M.S. 500-307	1
L. Reid	M.S. 5-9	1
W. A. Rostafinski	M.S. 5-9	1
R. S. Ruggeri	M.S. 5-9	1
D. M. Sandercock	M.S. 5-9	1
R. W. Schroeder	M.S. 500-207	1
L. E. Stitt	M.S. 500-307	1
J. B. Whitlow, Jr.	M.S. 500-307	1

2. NASA Scientific and Technical Information Facility
   P. O. Box 8757
   Baltimore/Washington International Airport
   Maryland 21240
   Attn: Accessioning Dept. 25

3. NASA Headquarters
   Washington, D. C. 20546
   Attn: RLC/ 1

4. NASA-Langley Research Center
   Hampton, VA 23665

Attn: E. Boxer	M.S. 249B	1
L. Hasel	M.S. 407	1

5.	U.S. Army Applied Technology Laboratories (AVRADCOM) Director Applied Technology Laboratory Fort Eustis, VA 23604		
	Attn: DAVDL-EU-TA, J. White		1
6.	Headquarters Wright-Patterson AFB, OH 45433		
	Attn: E. E. Bailey, AFAPL/DO		1
	R. P. Carmichael ASD/XRHI		1
	S. Kobelak AFAPL/TBP		1
	A. J. Wennerstrom AFAPL/TBX		1
7.	Naval Air Systems Command NASAIR/52022 Technical Support Branch Washington, D. C. 20362		
	Attn: R. A. Retta		1
8.	U. S. Navy Ship/Engineering Center Code 6141 Washington, D. C. 20362		
	Attn; G. L. Graves		1
9.	Naval Air Propulsion Test Center Trenton, NJ 08628		
	Attn: V. Labosky	PE-7	1
	J. Pichtelberger	PE-7	1
	P. Piscopo	PE-42	1
10.	Pratt & Whitney Aircraft Government Products Division P. O. Box 2691 West Palm Beach, FL 33402		
	Attn: W. R. Alley		1
	J. Brent		1
	R. E. Davis		1
	J. A. Fligg		1
	B. A. Jones		1
	R. W. Rockenbach		1
	H. D. Stetson		1
11.	Pratt & Whitney Aircraft 400 Main Street East Hartford, CT 06108		
	Attn: W. M. Foley (UTRC)		1
	T. J. Gillespie	E2H	1
	A. Mikolajczak	Adm. Bldg. 1	1
	N. T. Monsarrat	E2H	1
	A. Pfeffer	E2H	1
	A. W. Stubner	E2H	1
	H. D. Weingold	E2H	1
	Library (Comm. Prod. Div.)		1
	Library (UTRC)		1

12.	Detroit Diesel Allison Division, GMC Department 8894, Plant 8 P. O. Box 894 Indianapolis, IN 46206		
	Attn: R. F. Alverson	U-28	1
	J. L. Dettner	U-28	1
	G. E. Holbrook	T-22	1
	P. Tramm	U-27	1
	Library	S-5	1
13.	Northern Research and Engineering 219 Vassar Street Cambridge, MA 02139		
	Attn: K. Ginwala		1
14.	General Electric Company Flight Propulsion Division Cincinnati, OH 45215		
	Attn: J. F. Klapproth	K-221	1
	C. C. Koch	H-43	1
	J. W. McBride	E-198	1
	Marlen Miller	K-69	1
	J. R. Osani	H-9	1
	D. E. Parker	H-43	1
	D. Prince	H-48	1
	L. H. Smith	H-43	1
	J. B. Taylor	J-40	1
	Technical Information Center	N-32	1
15.	General Electric Company 1000 Western Avenue Lynn, MA 01910		
	Attn: D. P. Edkins	M.D. 24048	1
	F. F. Ehrich	M.D. 24505	1
	L. H. King	M. D. 240GF	1
	R. E. Neitzel	M. D. 24502	1
16.	Curtiss-Wright Corporation Wright Aeronautical Wood-Ridge, NJ 07075		
	Attn: R. Cole		1
	S. Lombardo		1
17.	AiResearch Manufacturing Company P. O. Box 5217 Phoenix, AZ 85010		
	Attn: J. Dodge		1
	J. R. Erwin		1
	G. L. Perrone		1
	D. Seyler		1
	J. Switzer		1

18. AiResearch Manufacturing Company
2525 West 190th Street
Torrance, CA 90509

Attn: R. Carmody		1
R. Jackson		1
L. W. Pearson		1
Library		1

19. Union Carbide Corporation
Nuclear Division
Oak Ridge Gaseous Diffusion Plant
P. O. Box P
Oak Ridge, TN 37830

Attn: J. L. Petty, K1401	M. S. 385	1

20. AVCO Corporation
Lycoming Division
550 South Main Street
Stratford, CT 06497

Attn: C. Kuintzle		1
Library		1

21. Teledyne, CAE
1330 Laskey Road
Toledo, OH 43612

Attn: Eli H. Benstein		1
Howard C. Walch		1

22. Solar
2200 Pacific Highway
San Diego, CA 92138

Attn: P. A. Pitt	A-5	1
J. Watkins	C-5	1

23. Goodyear Atomic Corporation
Box 628
Piketon, OH 45661

Attn: C. O. Langebrake		1

24. Hamilton Standard Division of
United Technologies Corporation
Windsor Locks, CT 06096

Attn: Mr. Carl Rohrback, Chief, Aerodynamics & Hydrodynamics	M.S. 1A-3-6	1

25. Westinghouse Electric Corporation
Combustion Turbine System Division
Lester, PA 19113

Attn: S. M. DeCorso	M.S. A703	1

26. Williams Research Corporation
P. O. Box 95
Walled Lake, MI 48088

Attn: R. A. Horn, Jr.		1

27. Eaton Research Center
P. O. Box 766
Southfield, MI 48037
Attn: Librarian — 1

28. Chrysler Corporation
Research Office
Department 9510
P. O. Box 1118
Detroit, MI 48288
Attn: Ronald Pampreen CIMS 418-37-18 — 1

29. Elliott Company
Jeannette, PA 15644
Attn: John W. Schlirf
Vice President of Engineering — 1

30. Caterpillar Tractor Company
Research Dept., Technical Center, Bldg. F
Peoria, IL 61629
Attn: J. Wiggins — 1

31. BMAD
Boeing Aeorspace Company
P. O. Box 3999
Seattle, WA 98124
Attn: W. C. Swan M.S. 40-51 — 1
A. D. Welliver M.S. 41-52 — 1

32. Douglas Aircraft Company
3855 Lakewood Blvd.
Long Beach, CA 90801
Attn: Dr. Albert C. Munson-3557 — 1

33. Lockheed Missile and Space Company
P. O. Box 504
Sunnyvale, CA 94088
Attn: Technical Information Center
Dept. 52-50, Bldg. 106 — 1

34. California Institute of Technology
Pasadena, CA 91125
Attn: Professor Duncan Rannie 204-45 — 1
Dr. Frank Marble 204-45

35. Iowa State University of Science
and Technology
Ames, IA 50010
Attn: Professor G. K. Serovy
Dept. of Mechanical Engineering — 1

36. Massachusetts Institute of Technology
Cambridge, MA 02139
Attn: D. J. L. Kerrebrock 1
Dr. J. McCune 1

37. University of Notre Dame
Notre Dame, IN 46556
Attn: Engineering Library 1

38. Penn State University
Department of Aerospace Engineering
233 Hammond Building
University Park, PA 16802
Attn: Prof. B. Lakshminarayana 1

39. Texas A & M University
Department of Mechanical Engineering
College Station, TX 77843
Attn; Dr. Meherwan P. Boyce 1